1-1-2016

Synthesis, Characterization, And Properties Of Peroxo-Based Oxygen-Rich Compounds For Potential Use As Greener High Energy Density Materials

Nipuni-Dhanesha Horadugoda Gamage
Wayne State University,

SYNTHESIS, CHARACTERIZATION, AND PROPERTIES OF PEROXO-BASED OXYGEN-RICH COMPOUNDS FOR POTENTIAL USE AS GREENER HIGH ENERGY DENSITY MATERIALS

by

NIPUNI-DHANESHA HORADUGODA GAMAGE

DISSERTATION

Submitted to the Graduate School

of Wayne State University,

Detroit, Michigan

in partial fulfillment of the requirements

for the degree of

DOCTOR OF PHILOSOPHY

2015

MAJOR: CHEMISTRY (Inorganic)

Approved By:

_____

Advisor Date

_____

_____

_____

_____

DEDICATION

To my parents, husband, and son

The people who have always supported me, helped me to rise up whenever I fell, and encouraged and inspired me to accomplish my goals.

ACKNOWLEDGMENTS

I would like to express my sincere gratitude to Professor Charles H. Winter for taking me into Winter lab, which was similar to a second home for me throughout the phD program. His guidance and support as my advisor at Wayne State University allowed me to progress rapidly and successfully. I have obtained numerous synthetic, technical, writing, and presentation skills that are invaluable for my future career while I was in Winter lab. I am also indebted to Professor Charles H. Winter for the confidence that he built in me to push forward by encouraging me all throughout.

I am extremely grateful for the wonderful collaboration we had with Prof. Thomas M. Klapötke, Ludwig-Maximilians University, Munich, Germany. The syntheses and standard sensitivity measurements carried out by Benedikt Stiasny and the energetic performance calculations carried out by Dr. Jörg Stierstorfer have completed the research study of peroxo-based compounds for my PhD. I greatly appreciate their hard work and time spent on research, discussions via e-mail, and preparation of manuscripts.

I am grateful to my committee members, Prof. James H. Rigby, Dr. Stanislav Groysman, and Dr. Charles L. Dezelah, for their valuable comments and suggestions on my dissertation. I thank Dr. Stanislav Groysman also for allowing me to use the IR spectrometer in his lab.

It was a great pleasure to work with the crystallography expert Dr. Philip D. Martin as he was extremely nice to me whenever I brought down a crystal to place in the diffractometer. I am grateful for all the X-ray crystal structures he solved and for his assistance with cif files in the preparation of manuscripts. I would also like to thank Dr.

Bashar Ksebati and Dr. Yuriy Danylyuk for assisting me with NMR and mass spectrometry, respectively. I am thankful to Nestor Ocampo for his support on software or hardware issues. I appreciate the assistance of the science stores and the non-academic staff members in various ways throughout the PhD program.

I would like to pay my gratitude to the past and present Winter lab members who were there while I was in the PhD program for the friendly working environment. I was happy to get involved in all the long chemistry discussions we had, especially with Joseph P. Klesko. Groysman, Brock, and Verani lab members were also always willing to assist me whenever I was in need and I am sincerely grateful for all of their support and friendship.

I am extremely fortunate to have two wonderful parents who have dedicated their life for me and my siblings and I am unable to express my gratitude in words for all they have done for me. I am what I am today because of my loving parents. My husband, G. H. Layan Savithra has been the man in my life who protected, cared for, and supported me for more than a decade. The B.S. special degree program in chemistry of University of Colombo was an intense program that brought us together and we were able to push through the hard work ending up as the two top students of our batch. Not only had I learned to love chemistry, but also my path towards PhD in chemistry was opened up because of Layan who was an extremely talented student. I am extremely grateful for all he has done. Last but not least my son, Senuk Y. Savithra is the greatest inspiration I have that keeps me pushing forward no matter what comes in the way.

TABLE OF CONTENTS

LIST OF TABLES

LIST OF FIGURES

LIST OF SCHEMES

LIST OF ABBREVIATIONS

ABBREVIATION	LONG FORM
HEDM	High Energy Density Material
IS	Impact Sensitivity
FS	Friction Sensitivity
TNT	Trinitrotoluene
RDX	Cyclotrimethylenetrinitramine
PETN	Pentaerythritol tetranitrate
HMX	Cyclotetramethylenetetrainitramine
CL-20	Hexanitrohexaazaisowurtzitane
ONC	Octanitrocubane
LA	Lead azide
LS	Lead Styphnate
MF	Mercury Fulminate
ESDS	Electrostatic Discharge Sensitivity
V_{Det}	Detonation Velocity
P_{Det}	Detonation Pressure
N	Number of Moles of Gas Released Per Gram of Explosive
M	Average Mass of Gas
Q_{Det}	Heat of Explosion
ρ_0	Loading Density
ρ	Crystalline Density
Ω	Oxygen Balance

ABBREVIATION	**LONG FORM**
MW	Molecular Weight
BAM	Bundesanstalt für Materialforschung
V_0	Detonation Volume
TATP	Triacetone Triperoxide
DADP	Diacetone Diperoxide
MEKP	Methyl Ethyl Ketone Peroxide
HMTD	Hexamethylene Triperoxide Diamine
R	Alkyl Group
OSHA	Occupational Safety & Health Administration
GHS	Globally Harmonized System of Classification and Labeling of Chemicals
$\Delta_f H°$	Heat of Formation
T_{Dec}	Decomposition Temperature
O:C	Oxygen:Carbon
TATB	2,4,6-Triamino-1,3,5-trinitrobenzene
TGA	Thermogravimetric Ananlysis
DTA	Differential Thermal Analysis
V	Volume of Unit Cell
Z	Number of Formula Units
T	Temperature
λ	Wave Length
ρ_{calc}	Calculated Crystalline Density
μ	Absorption Coefficient

ABBREVIATION	**LONG FORM**
VdW	Sum of the van der Waals radii
$\Delta_{Ex}U°$	Energy of Detonation
α_v	Thermal Expansion Coefficient
TITNB	1,3,5-Triiodo-2,4,6-trinitrobenzene

CHAPTER 1

Introduction

1.1 High Energy Density Materials (HEDMs)

HEDMs rapidly release energy through an exothermic process upon initiation by shock, friction, heat, or electrostatic discharge. The energy release is often associated with a total volume expansion due to high volumes of hot gases evolved. HEDMs are important components of rocket propellants, missile propellants, air-bag inflators, fireworks, and as explosives in quarrying, tunneling, mining, demolition, and military applications.[1] The development of HEDMs began with the discovery of black powder in about 220 BC in China, which was widespread at the end of the 13th century as a military explosive.[2] Black powder consists of charcoal (15%) and sulfur (10%) as fuels and potassium nitrate (75%) as the oxidant.[3] The first HEDM to have the fuel and the oxidant combined into a single molecule was nitroglycerin (Figure 1), which was discovered in 1846 by Ascanio Sobrero.[4] This discovery of nitroglycerin has lead to the modern HEDMs with high oxygen and nitrogen contents. High energy density materials can be placed into three main categories based on their different properties: low explosives, high explosives, and tertiary explosives.

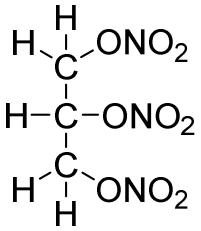

Figure 1. Structure of nitroglycerin.

1.1.1 Low Explosives

Low explosives are materials that deflagrate due to material decomposition at subsonic rates (few cm/s up to 400 m/s).[5] They are usually mixtures of a combustible material like charcoal, sulfur, metallic species (Mg, Cr, Al, and Ti), red phosphorus, silicon, and boron and an oxidant like KNO_3, NH_4NO_3, NH_4ClO_4, and $KClO_4$.[2] Low explosives are mainly used as propellants and pyrotechnics. Propellants provide the thrust required for rockets, missiles, and engines. Pyrotechnics are employed to produce heat, light, color, smoke, sound, or a combination of these effects. Examples of pyrotechnics are signal flares, fireworks, smoke-munitions, matches, and air-bag inflators.

1.1.2 High Explosives

High explosives are materials that can detonate due to material decomposition at supersonic rates, creating a supersonic shock wave with a velocity of 3,500–10,100 m/s.[6] They are usually single component materials that are either inorganic compounds, organic molecules, or polymers. There are two main subclasses of high explosives based on their sensitivity to impact and friction: primary and secondary explosives.

1.1.2.1 Primary Explosives

Primary explosives are high in sensitivity to impact and friction stimuli (impact sensitivity (IS): ≤ 4 J and friction sensitivity (FS): ≤ 10 N).[2] They have lower detonation velocities in the range of 3,500–5,500 m/s with respect to the secondary explosives.[6] The common primary explosives are inorganic compounds: lead azide (LA), lead styphnate (LS), and mercury fulminate (MF) shown in Figure 2.

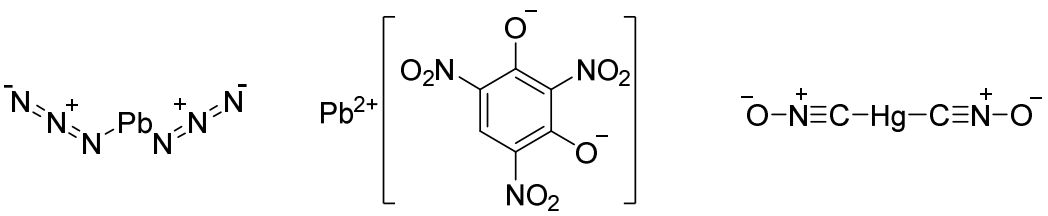

Figure 2. Common primary explosives.

Table 1 includes sensitivities and detonation velocities of these common primary explosives.[6b,7] LA, LS, and MF are all extremely sensitive to impact and friction stimuli and have low detonation velocities. They are mainly employed as initiating substances or primaries in blasting and percussion caps.[8] A major disadvantage of their use is that expensive and time consuming clean up procedures have to be carried out in shooting ranges due to bio-hazardous heavy metal residues resulting from the detonations.[9]

Table 1. Energetic properties of common primary explosives.[6b,7]

Compound	IS (J)	FS (N)	Electrostatic Discharge Sensitivity (ESDS, mJ)	Detonation Velocity (V_{Det}, m/s)
LA	2.5–4	0.1	4.7	5300
LS	2.5–5	0.1	0.2	5200
MF	0.2–2	6.5–7.5	0.51–0.62	4250

1.1.2.2 Secondary Explosives

Secondary explosives are low in sensitivity to impact and friction stimuli (IS: ≥ 4 J and FS: ≥ 50 N).[2] They have higher detonation velocities in the range of 5,500–10,100 m/s with respect to primary explosives.[6] The common secondary explosives are organic compounds that contain nitro functional groups (Figure 3). The nitro group is a relatively

unstable functional group and provides nitrogen and oxygen to form gaseous decomposition products.

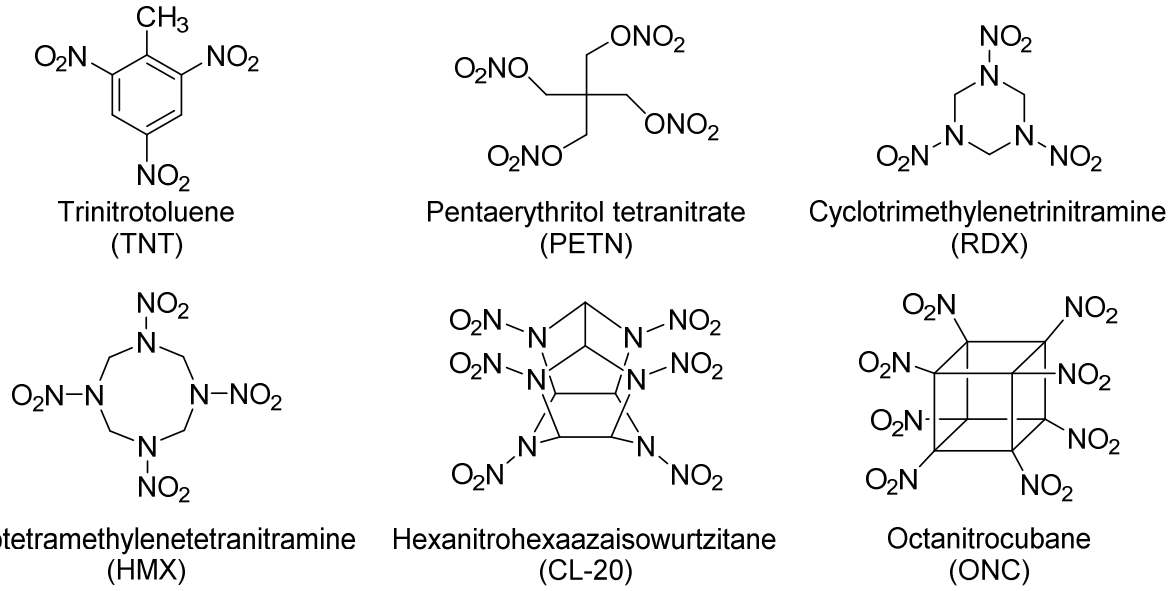

Figure 3. Common secondary explosives.

Table 2 includes sensitivities and detonation velocities of common secondary explosives.[1e,6b,10] These low sensitivity and high power secondary explosives are mainly used in large scale demolition tasks in both civil and military applications.

Table 2. Energetic properties of common secondary explosives.[1e,6b,10]

Compound	IS (J)	FS (N)	ESDS (J)	V_{Det} (m/s)
TNT	15	353	0.57	6,900
PETN	3–4.2	80	0.65–0.115	7,720
RDX	7.4	120	0.15	8,750
HMX	7.4	120	0.21	9,100
CL-20	4	54	low	9,500
ONC	low	low	low	10,100

1.1.3 Tertiary Explosives

Tertiary explosives are highly insensitive to impact and friction. Thus, a detonation from a secondary explosive material is required to initiate tertiary explosives. They are primarily used due to the low material costs and safety in handling. Tertiary explosives are mainly employed in mining and construction work. Ammonium nitrate fuel oil (ANFO) is an example of a tertiary explosive. It consists of NH_4NO_3 (94%) as the oxidizer and petroleum oil (6%) as the fuel and has a detonation velocity of 3,300 m/s.[11]

1.2 Deflagration and Detonation

Deflagration and detonation are the two main processes that cause energy to be released from HEDMs. Deflagration is the main process by which energy is released from low explosive propellants and pyrotechnics. Detonation is the main process by which energy is released from high and tertiary explosives in large scale demolition tasks.

1.2.1 Deflagration Process

Deflagration is a regular self-propagating combustion process that does not require an external oxygen source, which differentiates it from pure combustion. Deflagration occurs at subsonic rates (few cm/s up to 400 m/s) due to heat transfer (via a thermal wave) in the material.[5] The rates of deflagration can be increased by addition of inorganic salts like ferrocene derivatives, which act as deflagration catalysts.[12] Partial confinement or obstacles in the heat transfer path of the materials may lead to acceleration of the flame front to supersonic speeds and a transition from deflagration to detonation.[2]

1.2.2 Detonation Process

Detonation is a much more rapid process (ps–μS)[13] than deflagration and occurs at supersonic rates due to a supersonic shock wave (3,500–10,100 m/s).[6] The shock waves can compress the material, heat it, and induce explosive decompositions in a stepwise material decomposition process (Figure 4).[14] Initially, when a physical stimulus is provided on a bulk material via a shock, impact, friction, or electrostatic spark, shears or cracks appear in the crystalline lattice. Then, physico-chemical responses arise in defect hot spots where energy is concentrated and converted to heat. This heat causes various chemical reactions and molecular degradations until atoms are produced. Temperatures generated in HEDMs may reach up to 2,000–5,000 °C.[13] Finally, due to atom recombinations, stable gaseous products are formed that are released to the environment. This causes a large volume expansion that could be about 10,000–15,000 times the original volume of a HEDM.[13]

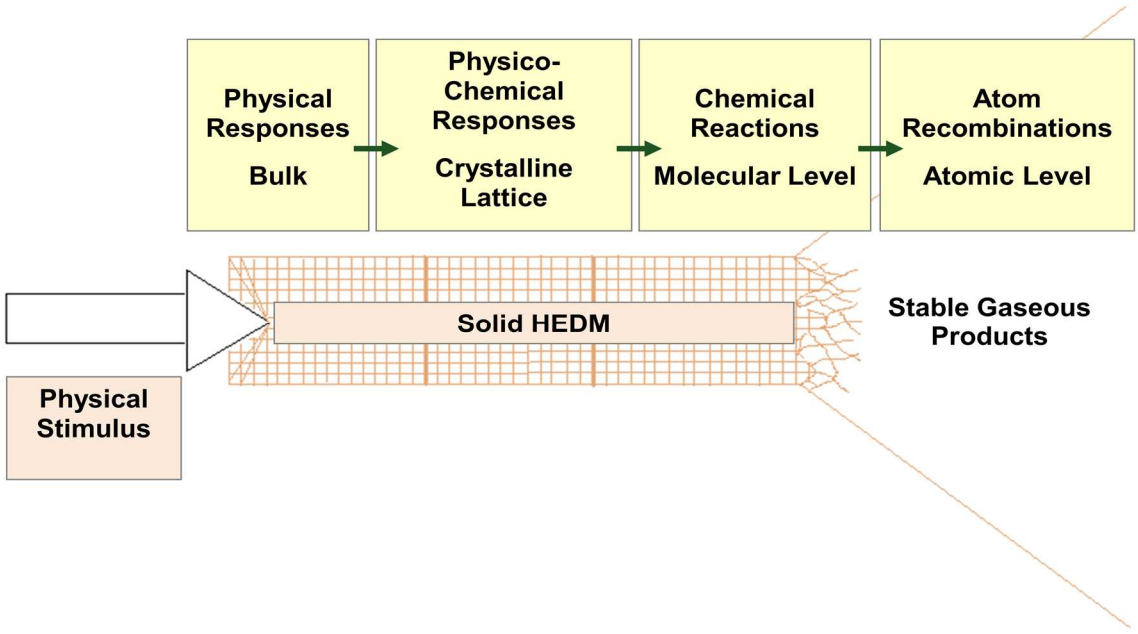

Figure 4. Detonation as a stepwise material decomposition process.[14]

1.3 Design of HEDMs

The design of HEDMs is aimed towards achieving three main goals: (i) a better performance, (ii) lower sensitivities for safety, and (iii) lower toxicity.[2] The main performance criteria are detonation velocity (V_{Det}, m/s), detonation pressure (P_{Det}, kbar), and heat of explosion (Q_{Det}, kJ/kg). There are many important properties that are considered in the design of HEDMs.[2,15]

- ❖ High crystalline densities (≥ 1.8 g/cm^3)
- ❖ High oxygen and nitrogen contents
- ❖ Optimal sensitivities
- ❖ High thermal stabilities (≥ 150 °C)
- ❖ Compatibility with chemicals and moisture
- ❖ Economical synthetic procedures
- ❖ Absence of heavy metals or perchlorate (ClO_4^-)

1.3.1 High Crystalline Densities

A high crystalline density (≥ 1.8 g/cm^3) is important to obtain a high V_{Det} and P_{Det} for a better energetic performance, and is a key parameter that is considered in designing energetic materials.[16] Compounds with highly symmetrical packing modes and some zwitterionic compounds are known to have better energetic performances due to increased crystalline densities.[17] Based on the Kamlet and Jacobs empirical relationships of Equations 1 and 2, loading density (ρ_0, g/cm^3) can be related to V_{Det} (m/s) and P_{Det} (kbar), respectively;

$$V_{Det} = 10^3 A\Phi^{1/2}(1 + B\rho_0) \quad (1)$$

$$P_{Det} = K\rho_0^2\Phi \quad (2)$$

$$A = 1.01,\ B = 1.30,\ K = 15.88$$

$$\Phi = NM^{1/2}Q_{Det}^{1/2}$$

where N is the number of moles of gas released per gram of explosive (mol/g), M is the average mass of gas (g/mol), and Q_{Det} is the heat of explosion (Cal/g). [2]

Equation 1 can be rearranged to Equation 3, which explicitly shows a linear relationship between V_{Det} and ρ_0.

$$V_{Det} = 10^3 A\Phi^{1/2}B\rho_o + 10^3 A\Phi^{1/2} \quad (3)$$

y = m x + c

Based on Equation 2, P_{Det} is proportional to ρ_0^2. Thus, increasing ρ_0 increases both V_{Det} and P_{Det} or the overall performance. The ρ_0 is higher when the crystalline density (ρ) is higher and the maximum theoretical ρ_0 for a particular substance is its crystalline density. Thus, for a better detonation performance, compounds with higher crystalline densities need to be obtained.

1.3.2 High Oxygen and Nitrogen Contents

Increasing the oxygen and nitrogen contents has been a popular strategy used to increase the endothermicity or energy stored in molecules that could be released in decompositions.[18] The release of an N_2 molecule from a compound with nitrogen-nitrogen single and/or double bonds releases a large amount of energy (227 kcal/mol) and thus, many high nitrogen compounds are synthesized as HEDMs.[19] A higher

oxygen content is important for a more complete combustion process where more energy can be released. The degree to which an explosive can be oxidized is given by the oxygen balance (Ω).[20] It can be defined as the weight percentage of oxygen after the complete oxidation of all the other elements on the molecule. For a simple organic molecule with the formula of $C_xH_yO_zN_a$, Ω is given by Equation 4;

$$\Omega = \frac{-1600}{MW}(2x + y/2 - z) \qquad (4)$$

where MW is the molecular weight of the compound and C and H are considered to be completely oxidized into CO_2 and H_2O. Nitrogen is not included in Equation 4 since it is released as gaseous N_2. More terms need to be included in the presence of S (oxidized to SO_2) and/or metals (oxidized to metal oxides). Based on equation 4, Ω can be either positive, zero, or negative. If Ω is equal to zero, the molecule is referred to as an oxygen balanced molecule. The more positive oxygen balance values are preferred since they render more energetic compounds. Increasing the oxygen balance increases the Q_{Det} and Q_{Det} reaches the maximum when Ω is zero.[1e] Although it is desirable to increase the oxygen and nitrogen contents, high oxygen and nitrogen contents result in extremely sensitive compounds with high impact and friction sensitivities.[21] A common remedy has been to blend the organic compounds with oxygen rich inorganic compounds like NH_4NO_3, NH_4ClO_4, KNO_3, and $KClO_4$. Still, more research is carried on to obtain organic HEDMs with high oxygen and nitrogen contents that can be safely handled since rapid self-sustained molecular level combustion is preferred over combustion of physical mixtures.

1.3.3 Optimal Sensitivities

Optimal sensitivities of HEDMs are important for effectiveness in the applications and for safety in handling, storage, and transport. Primary explosives are more sensitive to stimuli than secondary explosives. Impact sensitivities of common primary explosives are in the range of 0.2–5 J while friction sensitivities are in the range of 0.1–10 N.[6b] For safety in handling and transport, impact and friction sensitivity values should ideally be ≥ 3 J and ≥ 10 N, respectively. Secondary explosives should ideally be less sensitive than PETN (IS: 3–4.2 J and FS: 80 N).[6b] Electrostatic discharge sensitivity values of HEDMs should be > 25 mJ, even for laboratory use, since the human body can produce sparks of ~20 mJ.[2] It is an extremely challenging process to gain highly energetic molecules with low sensitivities for impact and friction stimuli.

1.3.4 High Thermal Stabilities

Higher decomposition temperatures provide high thermal stabilities and are important for heat resistant energetic materials.[1a,22] For HEDM applications thermal stabilities should be ≥ 150 °C.[2] Even though a high thermal stability is valuable, it is hard to find compounds with large energy contents that are thermally stable. Energetic compounds require at least sufficient kinetic stabilities to avoid accidents during handling. Thermally stable HEDMs are synthesized by strengthening intra- and intermolecular interactions, especially employing hydrogen bonding interactions and forming energetic salts.[16,22]

1.3.5 Compatibility with Chemicals and Moisture

In most of HEDM applications, energetic formulations are formed with binders, plasticizers, other HEDMs, oxidants, etc.[23] Thus, chemical compatibility is important to

retain the detonation performances within the formulations. Inorganic compounds are more susceptible to damage due to moisture, which is highly disadvantageous for long-term storage. Organic compounds and polymeric materials are more resistant to moisture due to low water solubility. Often mixtures of inorganic and organic/polymeric materials are used to avoid loss of explosive power due to water damage.

1.3.6 Economical Synthetic Procedures

The ease of syntheses and scale up, low cost, and the availability of bulk starting materials render economical synthetic procedures. They are important for wide applicability of HEDMs. Many research efforts are carried out to improve the syntheses of high performing HEDMs.[24]

1.3.7 Absence of Heavy Metals or Perchlorate (ClO_4^-)

The common primary explosives LA, LS, and MF contain heavy metals that cause heavy metal poisoning. Many organs such as kidneys, heart, and intestines as well as the skeletal, reproductive, and nervous systems in the human body can be adversely affected by heavy metal poisoning. Extensive use of NH_4ClO_4 as an oxidant over decades has resulted in it leaching into ground water, causing groundwater plumes.[25] Accumulation of NH_4ClO_4 in ground water causes human exposure to ClO_4^- ions. The ClO_4^- ions are similar in size to I^- ions, resulting in a competitive inhibition of iodine uptake in the thyroid gland and disruption of numerous metabolic pathways.[26] Thus, there is a need for greener HEDMs. Numerous research efforts have been dedicated to find replacements for the inorganic primary explosive LA and the tertiary explosive NH_4ClO_4.[27]

1.4 Sensitivity and Energetic Performance Tests and Calculations

1.4.1 Sensitivity Assessments

1.4.1.1 Preliminary Qualitative Sensitivity Tests

Preliminary qualitative sensitivity tests are the Bunsen burner flame test, hammer impact test, sand paper friction test, and Tesla coil electrostatic discharge test as shown in Figure 5. Sudden, large, and bright flames in the flame tests, loud noises in the hammer and sand paper tests, and sudden appearances of flames in the Tesla coil tests are considered to be positive responses of sensitive and energetic compounds.

Flame Test

Hammer Test

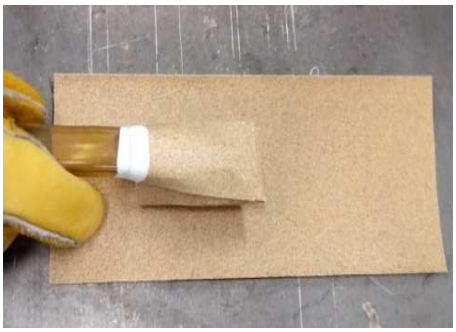

Sand Paper Test

Tesla Coil Test

Figure 5. Preliminary qualitative sensitivity tests.

1.4.1.2 Standard Quantitative Sensitivity Tests

Impact and friction sensitivities of HEDMs are quantified using internationally accepted standard methods. Thus, these sensitivities obtained can be compared with the sensitivities of the other HEDMs in literature. Still, there could be variations based on the country and the various standardizations employed. Electrostatic discharge sensitivity data are obtained with different instruments and modes using various standardizations. These electrostatic discharge sensitivity measurements also depend on numerous environmental conditions like humidity, temperature, and pressure, which causes a high variability of the data obtained.[2] Hence, the electrostatic discharge sensitivity data are generally not comparable with what is available in literature. Impact, friction, and electrostatic discharge sensitivity data are classified based on the "UN Recommendations on the Transport of Dangerous Goods".[28]

1.4.1.2.1 Impact Tests

Impact sensitivity tests can be carried out according to STANAG 4489[29] modified instructions[30] using a BAM (Bundesanstalt für Materialforschung) drop hammer.[31] A HEDM is placed in the sample holder and a series of increasing weights can be dropped from a fixed height or a fixed weight can be dropped from varying heights. A test is considered positive when a distinguishable sound (~160 dB) is heard. A compound is declared as sensitive when one out of six tests is obtained as positive.

1.4.1.2.2 Friction Tests

Friction sensitivity tests can be carried out according to STANAG 4487[32] modified instructions[33] using a BAM friction tester. A line of a HEDM is laid on a ceramic plate and a ceramic peg is kept on it. Then, the ceramic plate is moved so that the ceramic

peg is exerting a frictional force on the sample. The force exerted on the sample is varied by using weights and distances of the weight. A test is considered positive when a detonation is observed. Sensitivity is obtained when one out of six tests is positive.

1.4.1.2.3 Electrostatic Discharge Tests

Compounds can be tested for sensitivity towards electrostatic discharge using an electrostatic spark tester according to STANAG 4515 instructions.[34] These measurements can vary based on the instrument, methods, physical properties of the sample, and environmental conditions. Basically, a HEDM is incorporated in a sample holder and a charge is exerted through an electrode. The test is considered to be positive when a physical change or a detonation is observed or a sound is heard after the electricity interacted with the HEDM.

1.4.2 Energetic Performance Tests and Calculations

Energetic performances of HEDMs are assessed by using parameters V_{Det}, P_{Det}, Q_{Det}, and detonation volume (V_0). Determination of these energetic parameters requires restricted Cheetah-code or Explo5 calculations.[6b] The heat of formation ($\Delta_f H°$) values of HEDMs required for energetic performance calculations are either obtained by theoretical calculations using a Gaussian software or experimentally using bomb calorimetry.[2] Various energetic performance and sensitivity tests can be experimentally performed using detonation chambers.[2] These detonation chambers are made of thick steel walls and are able to dissipate the energy from the detonation shock wave to confine the explosions.[6b]

1.5 Peroxo-Based Oxygen-Rich Compounds for Use as Greener HEDMs

Organic peroxo-based compounds have been categorized as a class of greener HEDMs with CO_2 and/or CO, H_2O, and O_2 as the main decomposition products. The availability, ease, and low cost of syntheses are advantageous properties of peroxo-based compounds. Hydrogen peroxide (H_2O_2), the simplest peroxide, has been employed as a greener liquid rocket propellant.[35] Triacetone triperoxide (TATP), diacetone diperoxide (DADP), hexamethylene triperoxide diamine (HMTD), and methyl ethyl ketone peroxide (MEKP) are the only well-characterized examples of organic peroxo-based HEDMs (Figure 6).[35,36]

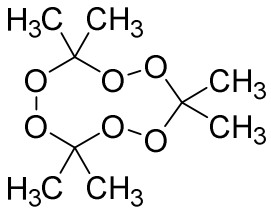

Triacetone triperoxide
(TATP)

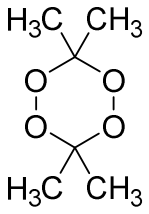

Diacetone diperoxide
(DADP)

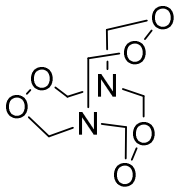

Hexamethylene triperoxide diamine
(HMTD)

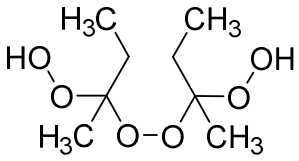

Methyl ethyl ketone peroxide
(MEKP)

Figure 6. Well-characterized peroxo-based oxygen-rich explosives.

TATP, DADP, HMTD, and MEKP are known to be extremely sensitive to impact and friction that cause difficulties in handling,[35,36] which has hindered the progress of

research in this field and their practical use in civil or military HEDM applications. Unfortunately, they have been employed in multiple terrorist attacks due to the ease of synthesis using widely available starting materials. Thus, TATP, DADP, HMTD, and MEKP are referred to as "peroxo-based homemade explosives."[36f] To ensure safety, a large body of research efforts has been dedicated to discover new detection methods for these non-nitrogen-containing peroxo-based explosives.[37] The maximum possible oxygen contents that can be safely incorporated onto peroxo-based compounds, their energetic properties, and paths to gear towards safer less sensitive peroxo-based compounds need to be systematically studied to understand and reach beyond the boundaries set by the few well-characterized peroxo-based explosives.

1.5.1 Properties and Applications of Peroxo-Based Compounds

Organic peroxo-based compounds contain one or more weak O–O bonds and are derivatives of HOOH, where one or both hydrogens are substituted with a group that contains carbon. Benzoyl peroxide (Figure 7) was the first organic peroxide synthesized by B. C. Brodie in 1858.[38] In early 20th century, benzoyl peroxide was found to be an efficient bleaching agent and industrial use of peroxides was initiated.

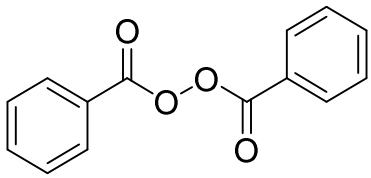

Figure 7. Benzoyl peroxide.

During the Second World War, peroxides were employed as polymerization initiators with the demand for synthetic rubber and plastics.[39] Currently, many organic

peroxides have been synthesized and isolated that are classified based on their structures to different sub-classes. The main peroxo-based sub-classes are hydroperoxides, dialkyl peroxides, ozonides, peroxy acids, peroxy esters, diacyl peroxides, and peroxy dicarbonates (Figure 8).

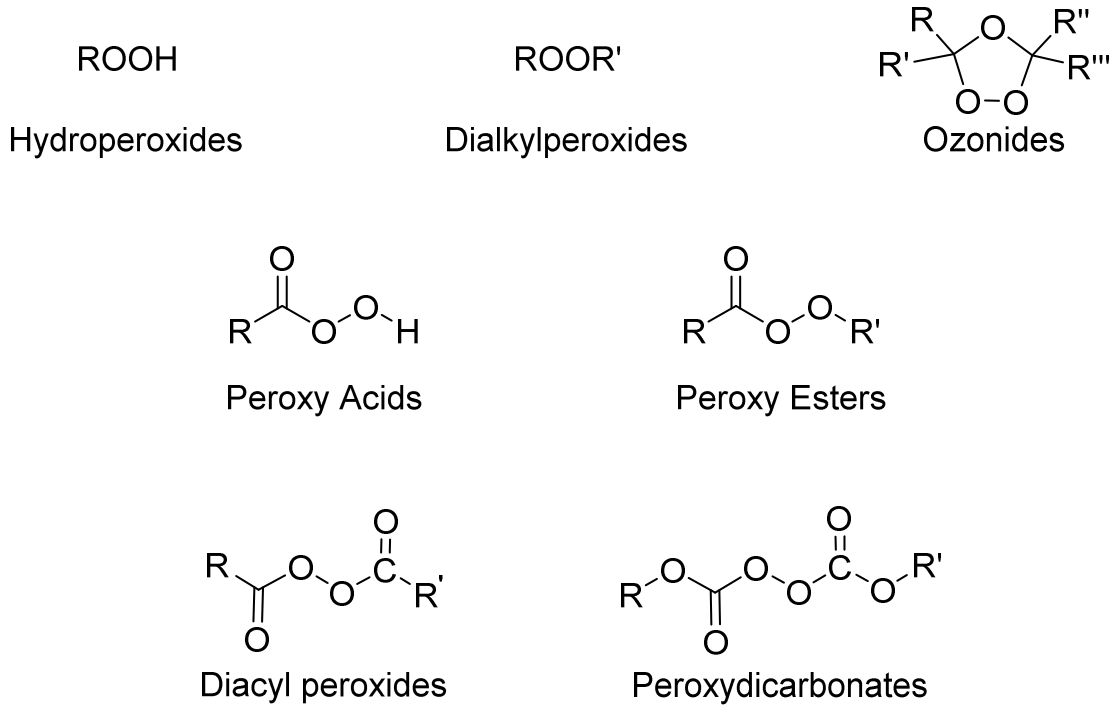

Figure 8. Peroxide subclasses based on structure.

The O–O bond dissociation energy of peroxides is relatively low and is in the range of 45–50 kcal/mol.[40] Due to this low O–O bond dissociation energy, peroxo-based compounds tend to be highly reactive and are known to be thermally and photolytically sensitive.[41] They undergo homolysis forming two highly reactive radical species (Equation 5). Peroxo-based compounds are also able to undergo oxidation, reduction, heterolysis, hydrolysis, and rearrangements.[39,42]

$$ROOR \xrightarrow{\Delta/h\nu} 2RO^{\cdot} \quad (5)$$

Since organic peroxides burn rapidly and are sensitive to impact and friction, they are placed into the hazard classification class 5.2 by the occupational safety & health administration (OSHA) according to UN recommendations on the transport of dangerous goods.[43a] The hazard pictogram for organic peroxides from the globally harmonized system of classification and labeling of chemicals (GHS) is shown in Figure 9.[43b,c]

Figure 9. GHS hazard pictogram for organic peroxides.[43c]

Peroxides are involved in many biological processes: development of rancidity in fats, oxidative damage on proteins, sugars, enzymes, and DNA, and oxidation of lipids in association with oxygenase enzymes.[39,44] Lipid peroxidation has been related to pathological conditions such as cancer and aging.[44] They are also involved in atmospheric and stratospheric chemistry.[45]

There are many applications for peroxo-based compounds based on the ability to produce reactive radical species and undergo oxidation and reduction. They are widely used as polymerization initiators,[46] curing and vulcanizing agents,[47] cross-linking agents,[48] bleaching and disinfecting agents,[49] oxidizing/reducing agents,[39] and have been used in syntheses of organic compounds[50] for decades. Radical species produced by oxygen-rich peroxo-based compounds can initiate subsequent radical chain reactions promptly releasing gaseous decomposition products and large contents of energy, causing detonation responses, which renders them suitable as HEDMs. Based on the high impact friction sensitivities, peroxo-based compounds TATP, DADP, MEKP, and HMTD have been categorized as primary explosives.[35,36]

1.5.2 Hydrogen Peroxide (H_2O_2)

H_2O_2 was first discovered in 1818 by L. J. Thénrad as a product of the reaction between nitric acid and barium peroxide (BaO_2).[51] Pure hydrogen peroxide is a light blue liquid, but it is commonly available as colorless aqueous solutions. For general use, aqueous 3–6% by weight of H_2O_2 solutions are available. Concentrations up to 50% by weight of H_2O_2 can be commercially obtained. When the concentration is > 70% by weight of H_2O_2, aqueous solutions are considered explosive. H_2O_2 is currently mainly produced by the anthraquinone oxidation process, which employs an anthraquinone derivative (2-ethylanthraquinone or 2-amylanthraquinone), H_2, and atmospheric oxygen.[51] H_2O_2 has a wide variety of applications. It is important in biology, medicine, pulp and paper bleaching, cosmetics, detergents, disinfectants, wastewater treatment, textile industry, electronics industry, chemical synthesis, and as a liquid rocket propellant.[52]

The density of pure H_2O_2 (1.448 g/cm^3) is greater than H_2O (1.000 g/cm^3) and along with the high positive oxygen balance (47%) it is an attractive candidate as a HEDM.[35] The decomposition rate of H_2O_2 into H_2O and O_2 is low at room temperature, but at elevated temperatures it rapidly decomposes, causing an explosive response (especially at > 70% by weight concentrations). Decomposition of H_2O_2 is catalyzed by strong acids, strong bases, metals such as copper and silver, metal salts, and light. Due to the greener decomposition products, it is a preferred propellant over HNO_3 and N_2O_4.[35] H_2O_2 was first used in the World War II as a rocket propellant and a fuel for underwater torpedoes. The reported detonation velocities of H_2O_2 are in the range of 5,500–6,000 m/s and it is a moderately powerful HEDM.[53] H_2O_2 has also been mixed with other fuels like methanol, ethanol, and glycerol and has obtained detonation velocities that are as high as 6,700 m/s.[53] One of the challenges of using H_2O_2 as a rocket propellant is to develop effective long-lived catalytic beds for a reliable performance. Currently, silver, alkali metals, and manganese oxides are employed in these catalytic beds.[54] An insensitive H_2O_2-based HEDM formulation was prepared using cellulose and 83 wt.% H_2O_2.[53]

1.5.3 Highly Energetic Organic Peroxo-Based Compounds

Generally, low molecular weight organic peroxides are considered to be potentially explosive compounds. Common solvents like ether, tetrahydrofuran, and 2-propanol and over 200 organic and inorganic compounds have been categorized as “peroxide forming chemicals.”[39] Upon exposure of peroxide forming chemicals to atmospheric oxygen, peroxides are formed either spontaneously or when concentrated and may result in formation of shock and friction sensitive polymeric peroxides. Thus,

safety precautions need to be taken in their use. TATP, DADP, HMTD, and MEKP are the well-characterized organic peroxo-based primary explosives.

1.5.3.1 TATP

TATP was first synthesized by R. Wolffenstein in 1895 by the uncatalyzed reaction of acetone and 50 wt.% H_2O_2 solution. The reaction was kept for four weeks to obtain TATP as a solid precipitate in a low yield (27%).[55] Sulfuric acid was then used initially in large quantities, and later in catalytic amounts.[56] The current synthesis of TATP is shown in Scheme 1.[35] The yield of TATP was found to depend on the reaction temperature, molar ratio of acid to H_2O_2/acetone, concentration of reactants, and reaction time.[57a] DADP is the major byproduct in the syntheses of TATP. TATP is the major form at room temperature in mild acidic conditions.[57]

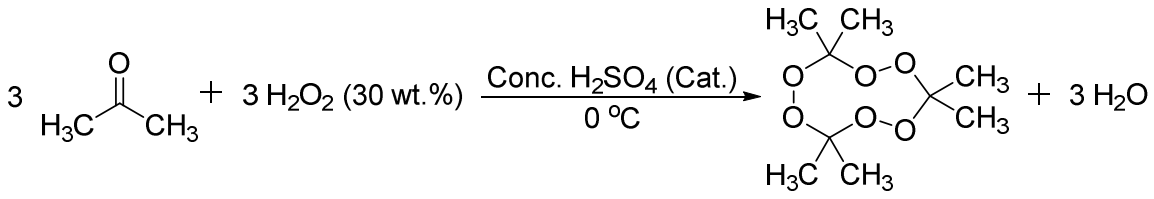

Scheme 1. Current synthesis of TATP.

The trimeric structure of TATP was proposed by R. Wolffenstein but it was confirmed only after obtaining a crystal structure by P. Groth.[58] TATP has a “twisted boat chair” conformation in the crystal structure.[59] There are molecular stacks with no C–H···O interactions in between, and only weak H···H intermolecular contacts of 2.4 Å hold the molecular stacks together.[59] Thus, there is no extensive hydrogen-bonded network to stabilize TATP, which may be one of the reasons for the high sensitivities to impact and friction. There is no ring strain in the structure and the O–O bond lengths 1.470(2) Å are similar to H_2O_2 (1.474 Å).[28] Denkamp et. al. reported that two conformers

of TATP with D_3 and C_2 symmetry exist at room temperature.[60] Later, six different polymorphic crystals were obtained by varying the acid catalyst used in the synthesis and the solvent used in re-crystallization.[61]

The sensitivities and energetic properties of TATP are given in Table 3. TATP is extremely sensitive to impact and friction stimuli and is categorized as a primary explosive. In early 20th century, TATP was used as a primary explosive in place of toxic mercury fulminate in detonators and as a mixture with NH_4NO_3.

Table 3. Sensitivities and energetic properties of TATP.[6b, 35,64,65]

Property	TATP
IS (J)	0.3
FS (N)	0.1
ESDS (J)	0.0056
ρ (g/cm^3)	1.272
Decomposition temperature (T_{Dec}, °C)	150–160
$\Delta_f H°$ (kJ/mol)	–583.8±44
V_{Det} (m/s)	5,300
Calculated V_{Det} (m/s)	6,168
Q_{Det} (kJ/kg)	–2,745
V_0 (L/kg)	855

Unfortunately, TATP is a highly volatile compound and 66% of mass is lost in two weeks at room temperature,[62] which is a highly disadvantageous property for long-term storage. Due to the high sensitivities and low stability, TATP is not currently employed in civil or military applications, but it has been used in multiple terrorist attacks. There have

been some attempts to reduce the high sensitivities of TATP using different strategies without much success.[63]

The decomposition products of TATP were studied by Oxley, who discovered acetone and CO_2 were the main decomposition products while multiple organic compounds were also observed.[66] Dubnikova has proposed that the explosive decomposition of TATP is primarily an energy-neutral entropic explosion where one molecule of solid TATP is decomposed to four gaseous molecules including three acetone molecules and one ozone molecule based on X-ray crystallography and electronic structure calculations.[59] Sinditskii has calculated and experimentally measured the heat of explosion and has described the decomposition of TATP as an exothermic process with acetone and CO_2 as the main decomposition products.[65]

1.5.3.2 DADP

DADP was first synthesized in 1900 by Baeyer and Villiger. It is usually obtained in the synthesis of TATP as a byproduct. Synthesis of pure DADP is carried out by *p*-toluenesulfonic acid-catalyzed isomerization of TATP or by slow addition of H_2O_2 to a mixture of acetone and methanesulfonic acid catalyst at –5 °C (Scheme 2).[59] DADP is more volatile than TATP in the temperature range of 15–50 °C and it is a highly disadvantage property for long-term storage.[59,67]

A chair conformation is adopted by DADP in the solid state and the O–O bond lengths (1.471 Å) are similar to TATP and H_2O_2.[35] The crystalline density of DADP (1.331 g/cm^3) is higher than that of TATP (1.272 g/cm^3).[59] There are intralayer C–H···O interactions formed by all four oxygen atoms of the ring in the crystal structure, which can stabilize the O–O bonds with respect to TATP, resulting in lower sensitivities than

TATP.[52] In between the molecular stacks of DADP, only weak hydrophobic contacts are present from the methyl groups.[59,67]

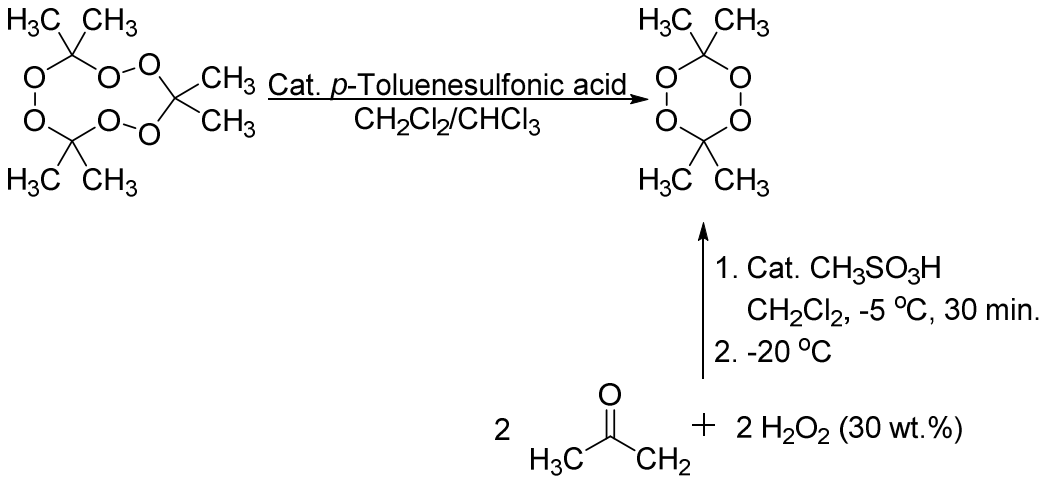

Scheme 2. Synthesis of pure DADP.

The sensitivities and energetic properties of DADP are given in Table 4. It is also a highly sensitive primary explosive but the sensitivities are less than TATP. Recently, co-crystallization was reported as a method to use complex solid state characteristics to influence the stabilities and sensitivities of peroxo-based co-crystals of DADP.[68] Specifically, the stabilization achieved by I···O close contacts in the crystalline lattice was proposed as the cause for the reduced sensitivity of DADP.[68]

The calculated detonation performance is higher than TATP primarily due to the higher crystalline density, but it is experimentally reported to be less explosive than TATP. [35,64] Usually, TATP and DADP are tested as mixtures and the detonation velocity of pure DADP has not yet been reported.

Table 4. Sensitivities and energetic properties of DADP.[6b, 35,64,65]

Property	DADP
IS (J)	1.4
FS (N)	2.99
ESDS (J)	0.026
ρ (g/cm^3)	1.331
T_{Dec} (°C)	165
$\Delta_f H°$ (kJ/mol)	–355.1±51
V_{Det} (m/s)	less than TATP
Calculated V_{Det} (m/s)	6,773
Q_{Det} (kJ/kg)	–2,837
V_0 (L/kg)	713

The decomposition kinetics of DADP were studied in the temperature range of 130–250 °C and is first-order with respect to DADP with acetone as the major organic product.[35] DADP is the less preferred acetone peroxide for HEDM applications due to the lower performance, higher volatility, and lower thermal stability than TATP. The energetic performances of some DADP derivatives with nitro groups have been recently calculated and impressive theoretical performances were observed.[69]

1.5.3.3 HMTD

HMTD was first synthesized by L. Legler in 1885 by the acid catalyzed reaction of hexamine and H_2O_2 (Scheme 3).[70] The two nitrogen atoms of HMTD are bridged by three O–O bonds. HMTD is the known peroxo-based explosive with the highest

oxygen:carbon (O:C) ratio, which is 1:1. It also contains two nitrogen atoms that increase the overall energy content of the molecule.

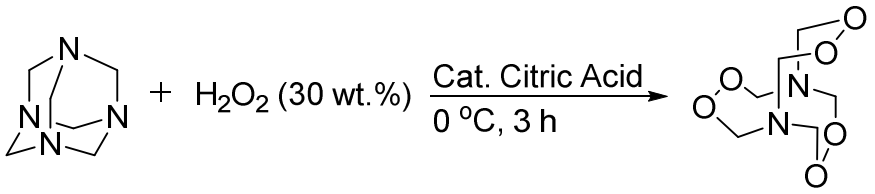

Scheme 3. Synthesis of HMTD.

The X-ray crystal structure was obtained by Schaefer,[71] which confirmed the bond connectivity. Nitrogen atoms are on a threefold axis and have a surprising planar geometry.[35] The crystal structure is a 50:50 racemic mixture of the left-handed and right-handed enantiomers.[72] There is a considerable ring strain in HMTD, unlike TATP or DADP.[35] The O–O bond lengths of HMTD are 1.456(8) Å and are shorter than TATP, DADP, and H_2O_2.[71] The crystalline density of HMTD (1.597 g/cm^3) is higher than TATP (1.272 g/cm^3).[35] Intermolecular interactions are not well defined due to the disorder in the crystal structure of HMTD.

The sensitivities and the measured and calculated energetic properties of HMTD are given in Table 5. It is a highly sensitive peroxide primary explosive with a moderate detonation velocity. The sensitivities can be reduced using it wet, as HMTD is not hygroscopic.[35] Due to slow decomposition at room temperature it is not suitable for long-term storage.[73] There is a considerable discrepancy between the calculated and observed detonation velocities. HMTD is another explosive that is extensively used by terrorists due to the ease of synthesis from widely available starting materials.

Table 5. Sensitivities and energetic properties of HMTD.[6b,7,35,64,73]

Property	HMTD
IS (J)	0.6
FS (N)	0.1
ESDS (J)	0.0088
ρ (g/cm^3)	1.597
T_{Dec} (°C)	150
$\Delta_f H°$ (kJ/kg)	–1731
V_{Det} (m/s)	4,500
Calculated V_{Det} (m/s)	7,777
Q_{Det} (kJ/kg)	–5,080
V_0 (L/kg)	813

The decomposition of HMTD has been studied by Oxley and the decomposition products were found to vary with the temperature. The major gaseous product was CO_2 below 150 °C and Me_3N, H_2O, and NH_3 were also observed.[73] At temperatures above 160 °C, the major gaseous product was CO while HCN and MeOH have also been observed.

1.5.3.4 MEKP

MEKP is a colorless oil that consists of a mixture of products. It is synthesized by the acid catalyzed reaction of 2-butanone and H_2O_2 (Scheme 4).[74] Milas et al. has successfully separated and characterized the components in the MEKP mixture.[74a] The major compound in the mixture is the linear dimer, 2-hydroperoxy-2-((2-hydroperoxybutan-2-yl)peroxy)butane (45%) shown in Scheme 4.[74a] The other products

include a cyclic trimer (25%), monomer (10%), and acyclic oligomers with 3 (12%), 4 (5%), 5 (2%), and 6 (1%) repeating units.[74a] The product mixture can be varied by changing the experimental conditions. Dilute solutions (30–60%) of MEKP have been employed as polymerization initiators, cross-linking agents, and curing agents in polymer industry.

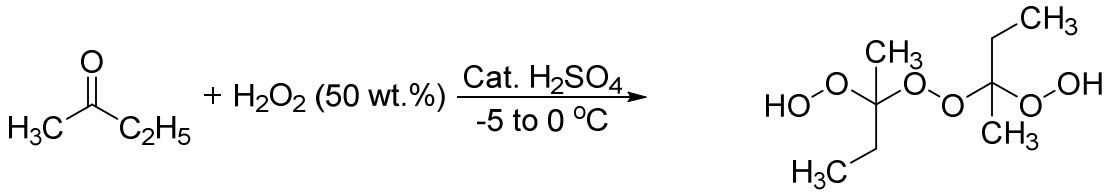

2-Hydroperoxy-2-((2-hydroperoxybutan-2-yl)peroxy)butane (45%)

Scheme 4. Synthesis of MEKP.

The sensitivities and the calculated energetic properties of MEKP are given in Table 6. It is a less studied explosive with respect to the other peroxide explosives TATP, DADP, and HMTD. MEKP is known to be highly sensitive but it is relatively less sensitive than TATP and has a moderate detonation performance. It has also been used in terrorist attacks due to the ease of synthesis from widely available starting materials.

The decomposition of MEKP begins at low temperatures such as 30–32 °C. MEKP becomes explosive around 110 °C.[75] It has been the cause for many explosive accidents in industry.[35,75]

Table 6. Sensitivities and calculated energetic properties of MEKP.[35]

Property	MEKP
IS (J)	High
FS (N)	High
ESDS (J)	High
ρ (g/cm^3)	1.17
T_{Dec} (°C)	75
$\Delta_f H°$ (kJ/mol)	–372.4
V_{Det} (m/s)	5,200
Calculated V_{Det} (m/s)	6,191
Q_{Det} (kJ/kg)	–4,933
V_0 (L/kg)	991

1.5.4 Development of Peroxo-Based HEDMs

The development of peroxo-based HEDMs needs to aim towards achieving two main goals: (i) a better energetic performance and (ii) lower sensitivities. A better energetic performance can be obtained by increasing the oxygen and nitrogen contents and increasing the crystalline densities. Lower sensitivities are challenging to obtain for peroxo-based compounds due to the presence of weak O–O bonds, which are also referred to as highly labile "trigger bonds" that render the peroxo-based compounds highly sensitive to impact and friction.[76] Thus, strategies to stabilize these trigger bonds with the use of intra- and intermolecular interactions in the crystalline lattices need to be considered along with the general strategies to stabilize compounds towards impact, friction, and electrostatic discharge sensitivities.

1.5.4.1 Towards Better Performing Peroxo-Based HEDMs

Increasing the oxygen and nitrogen content of peroxo-based compounds needs to be systematically carried out since high oxygen and nitrogen contents may render unsafe highly sensitive compounds. The highest O:C ratio obtained for peroxo-based compounds is 4:1.[77] There are a few peroxo-based compounds with 2:1 O:C ratios as well.[78] These peroxo-based compounds with high O:C ratios are shown in Figure 10.

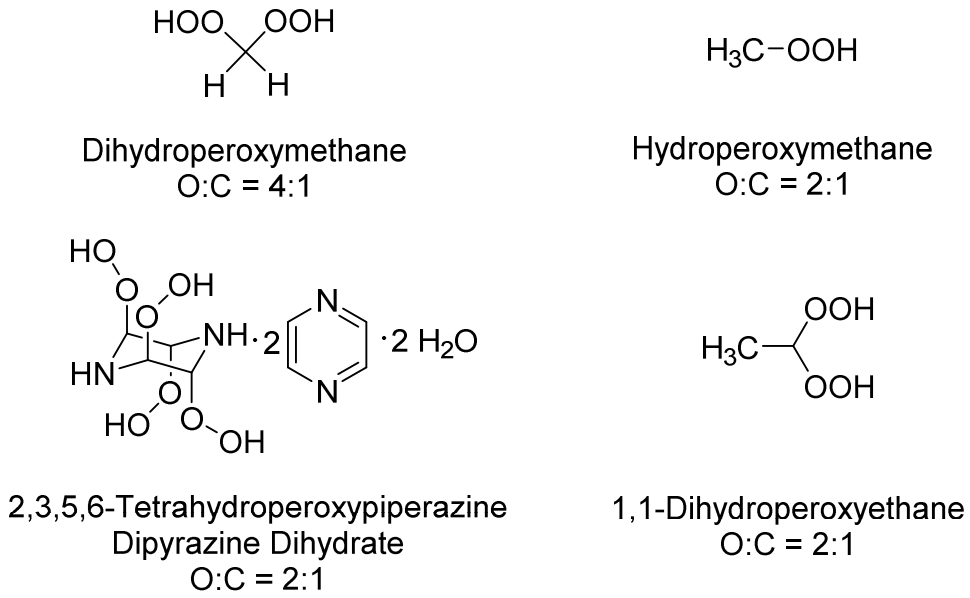

Figure 10. Peroxo-based compounds with high O:C ratios.

Dihydroperoxymethane, with a 4:1 O:C ratio, is explosive when concentrated, and it has only been detected as one of the products of ozonolysis of ethene.[77] Hydroperoxymethane is employed as an oxidant in organic reactions and it is known as a highly unstable compound that is not useful for HEDM applications.[78a] 2,3,5,6-Tetrahydroperoxypiperazine has only been isolated as a disolvate dihydrate, and thus, it is unsuitable for use as a HEDM.[78b] 1,1-Dihydroperoxyethane is an oil, referred to as

“remarkably stable” by Hamann et al. since it is stable at room temperature for a few days, and at –20 °C for several weeks.[78c] Unfortunately, sensitivities and the energetic properties of 1,1-dihydroperoxyethane have not been studied. The maximum peroxy oxygen content that can be safely incorporated onto peroxo-based compounds for their practical use is yet to be discovered.

Addition of nitrogen also increases the endothermicity and the detonation performance. Nitro groups or nitrogen rich heterocycles can be used to increase the nitrogen content of peroxo-based compounds. Nitro groups have been employed from the beginning of HEDM syntheses.[4] Several nitrogen-rich heterocyclic compounds are currently popular as HEDMs.[79] These new nitrogen-rich peroxo-based compounds can be potentially useful HEDMs, but unfortunately, they might result in less greener materials due to the release of nitrogen oxides to the environment.

The crystalline densities can be increased by increasing the crystal packing efficiency, cocrystallization, using zwitterionic forms, and incorporating halogens or nitro groups.[2,17,68] Since peroxo-based compounds have not been systematically studied as HEDMs no attempts have been made to synthesize compounds with high crystalline densities.

1.5.4.2 Towards Low-Sensitivity Peroxo-Based HEDMs

The causes of impact, friction, and electrostatic discharge sensitivities have not been clearly identified yet. Compounds with high oxygen contents like nitroglycerin and lower molecular weight peroxo-based compounds have been reported as highly sensitive compounds to impact and friction.[4,76,80] The oxygen balance needs to be as high as possible for a more complete oxidation, but safety is important for practical use.

Thus, there is a limit for the maximum oxygen content that can be safely incorporated onto peroxo-based compounds. Increasing the nitrogen content using nitro groups or nitrogen rich heterocycles have been carried out without increasing the impact and friction sensitivities as much as increasing the oxygen content.[2,79] Thus, it is safer to increase the endothermicity by using both oxygen and nitrogen.

Crystalline defects and voids create hot spots in the crystalline lattice where the physical energy is transferred to the material, generating shock waves.[14] Thus, crystals with more defects or lower quality crystals are more susceptible for initiation by impact, friction, and electrostatic discharge. The extremely high sensitivities of the known peroxo-based explosives are due to the weak O–O trigger bonds that are not sufficiently stabilized in the crystalline lattice with strong intra- or intermolecular interactions.[76] Most HEDMs lack hydrogen bond donor groups and thus, they lack strong hydrogen bonding interactions. One advantageous feature of peroxo-based compounds such as hydroperoxides and peroxy acids is that they can form strong intra- and/or intermolecular hydrogen bonds, increasing the stability and reducing the sensitivities. Intramolecular hydrogen bonds are shown to be stronger than intermolecular hydrogen bonds.[81] 2,4,6-Triamino-1,3,5-trinitrobenzene (TATB, Figure 11) is one of the least sensitive compounds due to the presence of strong intramolecular hydrogen bonds between the alternating amino and nitro groups as well as intermolecular hydrogen bonds.[82] Oxygen-rich HEDMs can also have O···O and H···H interactions in the solid state that can stabilize the trigger bonds by 3–16 kJ/mol.[83] The stabilizing effect of multiple O···O interactions are cumulative in the solid state, which can assist in reducing the sensitivities of peroxo-based compounds. Recently, cocrystallization has been

shown as an efficient method to reduce the sensitivities of DADP by employing stabilizing I···O close contacts.[68b]

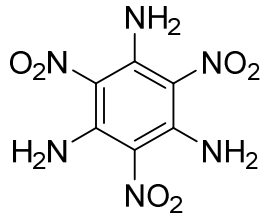

2,4,6-Triamino-1,3,5-trinitrobenzene
(TATB)

Figure 11. Structure of TATB.

The presence of large π-systems and π–π stacking facilitated by intermolecular hydrogen bonds are described as important causes to reduce sensitivities.[84] Crystals that contain face-to-face π–π stacking provide the most insensitive compounds.[84] The use of π–π stacking interactions to gain less sensitive aromatic peroxo-based compounds could be a useful strategy. The presence of slip planes in the crystal structures where the stacked molecular layers can move with respect to one another can efficiently dissipate energy, rendering low sensitivity compounds.[81] Face-to-face π–π stacking provides the least steric hindrance for the sliding movement and thus, results in low impact sensitivities. However, to form face-to-face π–π stacking interactions, electron rich and electron poor aromatic rings are required. This can be only achieved by cocrystallization of aromatic peroxo-based compounds.

Unfortunately, only a little is understood about how these solid state characteristics affect the physical properties of the compounds and the predictability of the resultant properties is low. Also, multiple factors may simultaneously contribute to

the overall sensitivities and thus, it becomes a challenging process to control the final outcomes.

1.5.5 Peroxo-Based Sub-Classes for HEDM Design

Ozonides are the most reactive sub-class of organic peroxides, which are intermediates of ozonolysis reactions but are rarely isolated due to their low stability.[85] Thus, ozonides are hardly suitable candidates for the applications as HEDMs due to difficulty in handling. Most diacyl peroxides and peroxydicarbonates are unstable at room temperature and hence, they are also less useful for HEDMs.[39] Dialkyl peroxides, hydroperoxides, peroxy esters, and peroxy acids are the more thermally stable sub-classes of peroxo-based compounds suitable for HEDM applications.[39] Dialkyl peroxides and peroxy esters are used as radical initiators in industry.[86,87] Hydroperoxides are mainly used as oxidizing or reducing agents and for syntheses of other peroxides.[39] Peroxy acids are powerful oxidizing agents and are used for epoxidation reactions in both academia and in industry. Peroxy acids or peroxy acid precursors are also used as bleaching agents, disinfectants, and fungicides.[39]

tert-Butyl hydroperoxide is readily available as a synthetic reagent, which is cheap and widely used as an oxidant. It is stable and fairly safe in 30–80% solutions of long chain hydrocarbons (nonane or decane) or as aqueous solutions. Thus, *tert*-butyl hydroperoxide can be efficiently used to synthesize *tert*-butyl peroxides and *tert*-butyl peroxy esters in place of dialkyl peroxides and peroxy esters, respectively. Hydrogen peroxide required for the synthesis of hydroperoxides and peroxy acids is also a cheap oxidant sold as 30–50 wt.% aqueous solutions. Thus, the categories of peroxo-based

compounds that can be conveniently used for HEDM design are *tert*-butyl peroxides, *tert*-butyl peroxy esters, hydroperoxides and peroxy acids (Figure 12).

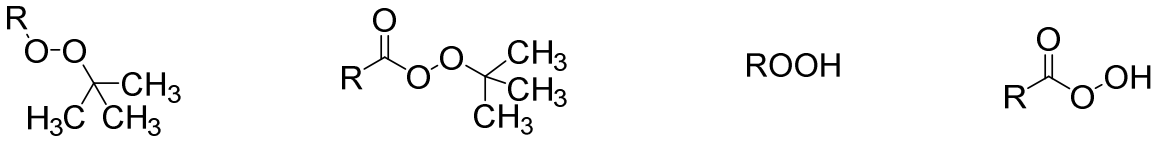

tert-Butyl peroxides *tert*-Butyl peroxy esters Hydroperoxides Peroxy acids

Figure 12. Categories of peroxo-based compounds for HEDM design.

Sensitivities and energetic properties of *tert*-butyl peroxides, *tert*-butyl peroxy esters, hydroperoxides, and peroxy acids need to be assessed. These properties could be related to the structural, physical, and chemical properties to understand more about their function. Then, low-sensitivity, high-performing peroxo-based oxygen-rich compounds could be developed for potential use as greener HEDMs.

1.5.6 Limitations of Peroxo-Based Compounds

There are multiple limitations in need of consideration for peroxo-based compounds. Peroxo-based compounds with high peroxy O:C ratios are known to be extremely sensitive to impact and friction. The known peroxide explosives TATP, DADP, MEKP, and HMTD have low oxygen balance values (Table 7), but they are highly sensitive compounds owing to the instability of the weak O–O trigger bonds. The high sensitivities that result with high peroxy oxygen contents limits the amount of oxygen and hence, the energy content that can be safely incorporated into peroxo-based compounds. An alternative way to incorporate more oxygen atoms to increase the oxygen balance is the use of more stable functional groups like nitro and hydroxyl groups.

Table 7. Oxygen balance values of peroxo-based explosives.

Compound	Ω (%)
TATP	–151
DADP	–151
HMTD	–92
MEKP (dimer)	–145

One of the major limitations of most of the peroxo-based compounds is the low thermal stabilities. This is highly disadvantageous when HEDM applications are considered. Unfortunately, it is an inherent property of peroxo-based compounds to be thermally sensitive due to the weak and highly labile O–O bonds.[39] Through more careful synthetic manipulations, more thermally stable peroxy acids need to be obtained for use as HEDMs.

Peroxo-based compounds are usually incompatible with most acids, bases, metals, metal salts, and dust particles. Since HEDMs need to be prepared as formulations combining different chemical species, it is a highly disadvantageous property of peroxo-based compounds. The known peroxide explosives TATP, DADP, MEKP, and HMTD have been studied in various formulations,[63] but more research needs to be carried out to find appropriate formulations to obtain reliable detonation responses from peroxo-based compounds.

1.6 Thesis Problem

One of the main aspects of HEDM design is to explore greener alternatives for widely used HEDMs that produce toxic byproducts. Primary explosives LA, LS, and MF contain heavy metals that cause heavy metal poisoning. NH_4ClO_4 is an energetic oxidant widely used in propellant and explosive formulations. Leaching of it into groundwater has resulted in accumulation and hence, in human exposure to ClO_4^- ion. The size similarity of ClO_4^- ion to iodide ion results in a competition in the thyroid gland, which causes disruptions of many metabolic pathways and even thyroid cancer. Many research efforts are currently carried out to find replacements for the toxic primary explosives and NH_4ClO_4 with little success. Thus, there is a need for greener HEDMs.

Peroxo-based oxygen-rich compounds are proposed as a potential new class of greener HEDMs due to the evolution of CO_2 and/or CO, H_2O, and O_2 as the main decomposition products. Currently, TATP, DADP, MEKP, and HMTD are the only well-studied highly energetic peroxides, but due to their high impact and friction sensitivities handling of these compounds has been hazardous. Thus, they have not found practical applications both as civilian or military HEDMs and the progress of research in this field has been hindered. Unfortunately, TATP, DADP, MEKP, and HMTD have been used in multiple terrorist attacks. For practical use as HEDMs, high impact and friction sensitivities of peroxo-based compounds need to be reduced. Further, improvements in detonation performances, thermal stabilities, and chemical compatibilities of the new peroxo-based compounds are important for their use as HEDMs.

The peroxo-based compounds need to be systematically studied to explore the maximum possible oxygen contents that can be safely incorporated onto peroxo-based

compounds, their sensitivities and energetic properties, and paths to gear towards safer less sensitive peroxo-based compounds for practical use as greener HEDMs. A complete sensitivity and energetic property study of peroxo-based compounds can ensure safety in numerous current applications as well as assist in gaining insights about developing peroxo-based oxygen-rich compounds with better performances for potential applications as greener HEDMs.

CHAPTER 2

Synthesis, Characterization, and Study of the Sensitivities and Energetic Properties of *tert*-Butyl Peroxides

2.1 Introduction

2.1.1 Dialkyl Peroxides

tert-Butyl peroxides are one of the common categories of peroxo-based compounds that belong to the main peroxide sub-class of dialkyl peroxides. Dialkyl peroxides have the basic R_1OOR_2 formula, where the R_1 and R_2 groups can be the same or different primary, secondary, or tertiary alkyl groups. Synthesis of dialkyl peroxides is carried out with hydroperoxides (using aldehydes, ketones, and alkyl halides), hydrogen peroxide (using alkyl halides), and sodium peroxide (using alkyl halides).[39,86] Dialkyl peroxides are fairly thermally stable compounds. The 10 h half life temperatures range from 110–135 °C for acyclic peroxides and approach 200 °C for five- to six-membered cyclic peroxides.[39] The O–O bond in dialkyl peroxides is thermally and photolytically cleaved into alkoxy radicals more easily with respect to the hydroperoxides, which can be attributed to the relatively higher stability of the two alkoxy radicals produced. Thus, they are commonly employed as cross-linking agents and radical initiators in industry.[86]

TATP and DADP are two well-known highly energetic dialkyl peroxides.[35,36] Sensitivities and energetic properties of TATP and DADP have been discussed in Chapter 1. Low molecular weight dialkyl peroxides are often reported to be shock sensitive whereby the sensitivity decreases with increased molecular weight.[86] High temperature distillations should be avoided with low molecular weight dialkyl peroxides

for safety reasons. Polymeric alkyl peroxides are reported as highly sensitive to impact and friction stimuli and explosive at elevated temperatures.[88]

2.1.2 *tert*-Butyl Peroxides

A wide variety of *tert*-butyl peroxides have been reported in literature.[89] They are common due to the wide availability of the cheap and stable synthetic reagent required for their syntheses, *tert*-butyl hydroperoxide. They are primarily used as cross-linking agents, polymerization initiators, and reagents in various organic syntheses.[86,90] Generally, they are stable carbon-rich compounds that can be handled safely. Di-*tert*-butyl peroxide is the only *tert*-butyl peroxide that has been considered as a potential fuel (Figure 13).

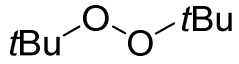

Figure 13. Di-*tert*-butyl peroxide.

Di-*tert*-butyl peroxide was tested as a fuel in an internal combustion engine under anaerobic conditions due to its ability to undergo a thermal explosion.[91] It has also been used as a polymerization initiator.[92a] The thermal decomposition of di-*tert*-butyl peroxide has been studied to assess its hazardous nature to ensure safety.[92]

In this chapter, the synthesis, characterization, and the energetic properties of a series of *tert*-butyl peroxides **1**–**15** (Figure 14) are described. The *tert*-butyl peroxides synthesized in this study have O:C ratios in the range of 0.22–0.36. The ring strain of *tert*-butyl peroxides was varied using 5–7 membered rings and a bicyclopentane ring

system (**11** and **13**). Preliminary qualitative sensitivity tests were performed to observe their sensitivities to flame, impact, friction, and electrostatic discharge stimuli.

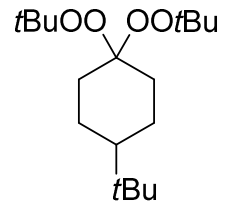

1, 58%
O:C = 2:9 = 0.22

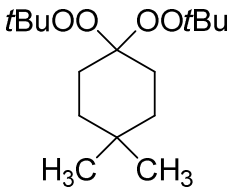

2, 18%, Oil
O:C = 1:4 = 0.25

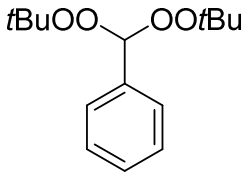

3, 35%, Oil
O:C = 4:15 = 0.27

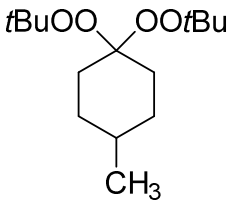

4, 45%, Oil
O:C = 4:15 = 0.27

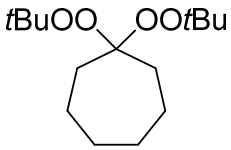

5, 23%
O:C = 4:15 = 0.27

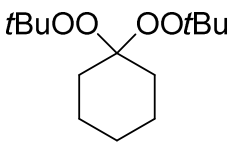

6, 38%, Oil
O:C = 4:15 = 0.29

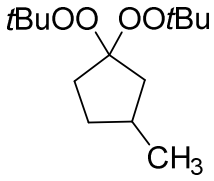

7, 30%, Oil
O:C = 2:7 = 0.29

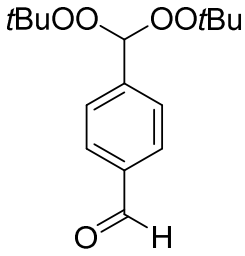

8, 19%
O:C = 1:3 = 0.31

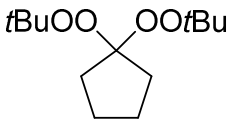

9, 29%, Oil
O:C = 4:13 = 0.31

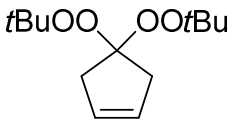

10, 30%, Oil
O:C = 4:13 = 0.31

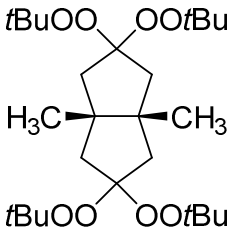

11, 10%
O:C = 4:13 = 0.31

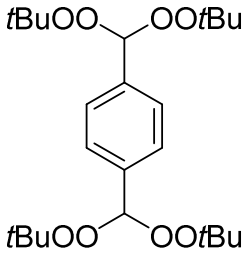

12, 10%
O:C = 1:3 = 0.33

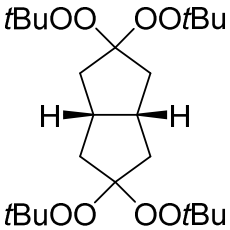

13, 19%
O:C = 1:3 = 0.33

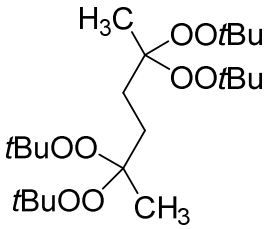

14, 20%, Oil
O:C = 4:11 = 0.36

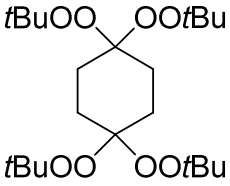

15, 29%
O:C = 4:11 = 0.36

Figure 14. The series of *tert*-butyl peroxides **1**–**15**.

2.2 Results and Discussion

tert-Butyl peroxides **1**–**15** were synthesized to observe the effects of the increased oxygen content and ring strain on their energetic properties. Based on the synthetic design, carbon-rich safe *tert*-butyl peroxides were initially synthesized and then, more oxygen-rich compounds were obtained. Strain in the cyclic compounds increase in the order: cyclohexane (0.1 kcal/mol) < cycloheptane (6.2 kcal/mol) ≤ cyclopentane (6.2 kcal/mol).[93] Since the energetic calculations require crystalline densities, only solid compounds can be energetically characterized in our study. Cyclopentane ring-based *tert*-butyl peroxides **7**, **9**, and **10** were oils, and thus, the solid *tert*-butyl peroxides **11** and **13** were synthesized to observe the effects of the ring strain. Compounds **11** and **13** have a highly strained (12.0 kcal/mol) octahydropentalene ring system.[94] Aromatic compounds **3**, **8**, and **12** were synthesized to observe the effects of π-interactions on the stabilities and sensitivities of *tert*-butyl peroxides.

2.2.1 Synthetic Aspects

Caution: Oxygen-rich organic peroxo-based compounds are potentially explosive and require handling with care. Reactions and other manipulations were performed in a fume hood behind a blast shield. Personal safety gear was used whenever necessary: a face shield, leather gloves, and a leather apron. Interactions with strong acids, metals, metal salts, or easily oxidizable species were avoided to prevent hazardous decomposition reactions. All reactions were performed on small scales (≤ 500 mg) and at room temperature.

The syntheses of *tert*-butyl peroxides were carried out based on a published general procedure for geminal *tert*-butyl peroxides from aldehydes and ketones

(Scheme 1).[95] Compounds **1** and **3** were synthesized based on the exact published procedures.[95] Iodine was the preferred catalyst due to the low cost, safety, and high efficiency observed in the reactions.[95] CH_3CN was able to dissolve iodine, *tert*-butyl hydroperoxide, and the starting material aldehydes and ketones allowing reactions to proceed effectively.

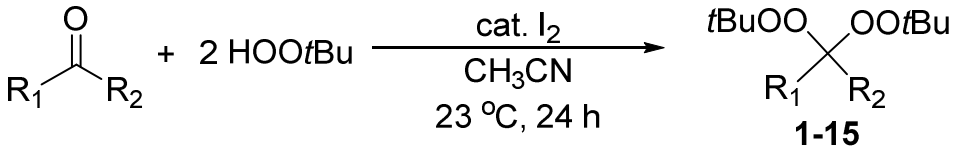

Scheme 5. Synthesis of *tert*-butyl peroxides.

Briefly, a solution of I_2 in CH_3CN was treated with tBuOOH in decane while the reaction was kept stirring at room temperature (23 °C). Then, the aldehyde or ketone was added and the reaction was stirred at room temperature (23 °C) for 24 h. Afterwards, the reaction was concentrated under reduced pressure and the product was purified by silica gel column chromatography. During the synthesis of different *tert*-butyl peroxides, slight variations of the general procedure in the reaction scale, equivalents of *t*BuOOH per ketone/aldehyde group, reaction time, volume of CH_3CN, and the chromatography mobile phase were required to obtain better yields.

tert-Butyl peroxides **1**–**15** were obtained in low to moderate yields (Figure 14). Compounds **2**, **7**, and **10**–**15** are new *tert*-butyl peroxides obtained in this study. *tert*-Butyl peroxides **2**–**4**, **6**, **7**, **9**, **10**, and **14** were isolated as colorless oils while **1**, **5**, **8**, **11**–**13** and **15** were isolated as white solids. Compound **8** is the half reacted product of the reaction between terephthalaldehyde and *t*BuOOH while compound **12** is the product of the complete reaction. The solid *tert*-butyl peroxides and the oil **3** were re-crystallized to obtain X-ray quality single crystals either by slow evaporation (**11**, **13**, and **15**) or by

cooling the saturated solutions to –29 °C in the freezer (**1**, **3**, **5**, and **8**). All *tert*-butyl peroxide single crystals obtained were colorless. They were in the forms of thick needles (**1**, **5**, and **15**), cubes (**3**), planar polygons (**8** and **11**) or thin planar needles (**13**). *tert*-Butyl peroxide syntheses using cyclobutanone, benzene-1,3,5-tricarbaldehyde, cyclohexane-1,3,5-trione, and cyclohexane-1,2,3,4,5,6-hexaone were not successful. The highest O:C ratio obtained for the series of *tert*-butyl peroxides was 0.36 for **15**.

tert-Butyl peroxides **1**–**15** were characterized by ^{1}H and ^{13}C NMR spectroscopy, mass spectrometry, melting point analysis, and IR spectroscopy. When possible, X-ray crystal structures were obtained for complete characterization of the corresponding *tert*-butyl peroxides.

2.2.2 Spectroscopy

The ^{13}C NMR peaks of the two carbon atoms connected to the O–O group, the peroxy carbon peak and the quaternary carbon peak of the *tert*-butyl group were used to confirm that a *tert*-butyl peroxide was obtained versus a decomposed *tert*-butoxy alkane. The chemical shift region for the peroxy carbon atoms of *tert*-butyl peroxides in $CDCl_3$ was 107.00–118.52 ppm. The more deshielded chemical shifts were obtained for the strained cyclopentane ring-based *tert*-butyl peroxides **7**, **9**–**11**, and **13**. The quaternary carbon peak of the *tert*-butyl group was in the chemical shift range of 79.08–81.65 ppm. When a *tert*-butyl peroxide was decomposed to a *tert*-butoxy alkane, both the peroxy carbon peak and the quaternary carbon peak of the *tert*-butyl group were shifted to higher field approximately by 10 ppm.

The characteristic IR stretching frequencies of the *tert*-butyl peroxides are medium CH_3 antisymmetric and symmetric stretching modes in the range of 2850–3000 cm^{-1}, medium or strong C–O stretching modes in the range of 1000–1300 cm^{-1}, and weak O–O stretching modes in the range of 800–900 cm^{-1}.[96,97,98] There were multiple medium and strong peaks in the regions of 2850–3000 and 1000–1300 cm^{-1} in the IR spectra of **1**–**15** for CH_3 stretching modes and C–O stretching modes, respectively. The appearance of strong peaks in the range of 800–1000 cm^{-1} in the IR spectra of **1**–**15** were indicating strong coupling of C–O and O–O stretching modes as reported.[96,98]

2.2.3 X-Ray Crystal Structures

X-ray crystal structures were obtained for the *tert*-butyl peroxides **1**, **3**, **5**, **8**, **11**, **13**, and **15**. They were all normal structures without unusual intermolecular interactions. Experimental crystallographic data of **1**, **3**, **5**, **8**, **11**, **13**, and **15** are summarized in Table 8. Perspective views of the crystal structures of **1**, **3**, **5**, **8**, **11**, **13**, and **15** are given in Figures 15–21. Selected bond lengths from the X-ray crystal structures are provided in Table 9. A list of short contacts generated by Mercury 3.5.1 is provided in Table 10.

The O–O bond lengths of the *tert*-butyl peroxides **1**, **3**, **5**, **8**, **11**, **13**, and **15** were in the range of the O–O bond lengths reported for dialkyl peroxides.[99] *tert*-Butyl peroxy groups are bulky, which prevent close packing of the *tert*-butyl peroxide molecules. Thus, low crystalline densities were obtained for the *tert*-butyl peroxides **1**, **3**, **5**, **8**, **11**, **13**, and **15**. Their crystalline densities were in the range of 1.098–1.166 g/cm^3.

Table 8. Experimental crystallographic data of **1**, **3**, **5**, **8**, **11**, **13**, and **15**.

	1	**3**	**5**	**8**	**11**	**13**	**15**
Formula	$C_{18}H_{36}O_4$	$C_{15}H_{24}O_4$	$C_{15}H_{30}O_4$	$C_{15}H_{22}O_4$	$C_{104}H_{200}O_{32}$	$C_{24}H_{46}O_8$	$C_{11}H_{22}O_4$
FW	316.47	268.34	274.39	266.32	1962.63	462.61	218.28
Space group	P 1 2_1/n 1	P 1 2_1/c 1	P 1bar	C 1 c 1	P 1bar	P 1 2_1/n 1	P 1bar
a (Å)	6.1941(3)	14.4700(8)	8.7498(6)	10.0753(13)	14.7212(19)	18.6961(10)	6.0500(3)
b (Å)	35.6020(17)	9.8681(5)	9.8051(7)	14.7595(13)	16.079(2)	6.0942(3)	8.6910(5)
c (Å)	8.7033(4)	11.4505(6)	10.6228(7)	11.1230(11)	26.271(3)	24.4347(13)	13.0548(7)
V (Å^3)	1913.79(16)	1528.86(14)	811.77(10)	1653.7(3)	5752.6(13)	2678.0(2)	643.92(6)
Z	4	4	2	4	2	4	2
T (K)	100(2)	100(2)	100(2)	100(2)	100(2)	100(2)	100(2)
λ (Å)	0.71073	0.71073	0.71073	0.71073	0.71073	0.71073	0.71073
ρ_{calc} (g/cm^3)	1.098	1.166	1.123	1.070	1.133	1.147	1.126
μ (mm^{-1})	0.075	0.083	0.079	0.076	0.082	0.084	0.084
R(F)[a] (%)	3.81	7.77	3.67	3.77	8.80	3.89	4.12
R_w(F)[b] (%)	14.26	21.95	15.13	11.45	24.02	10.56	12.56

[a] $R(F) = \sum \| F_o | - | F_c \| / \sum | F_o |$; [b] $Rw(F) = [\sum w(F_o^2 - F_c^2)^2 / \sum w(F_o^2)^2]^{1/2}$.

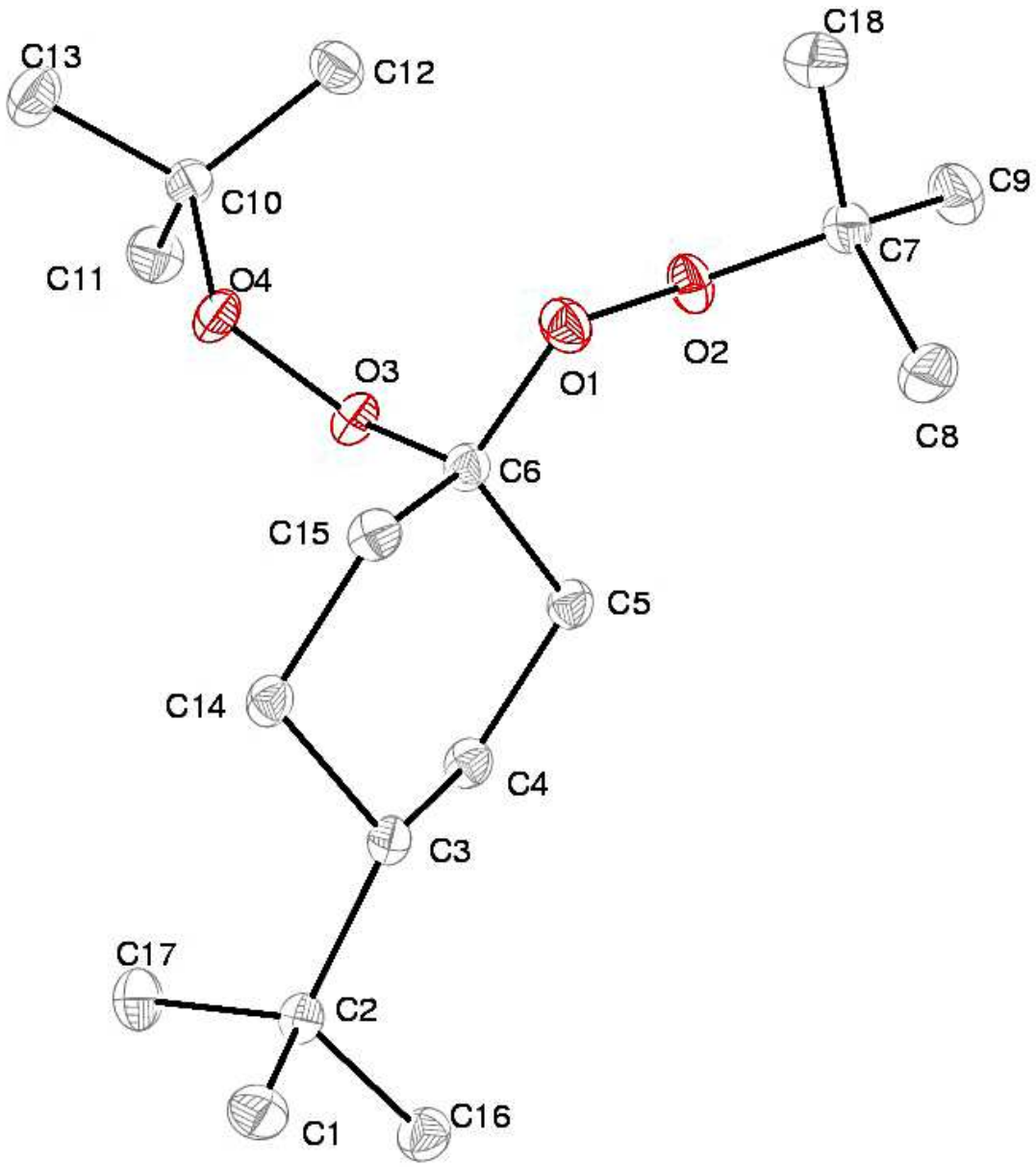

Figure 15. Perspective view of **1** with thermal ellipsoids at the 50% probability level.

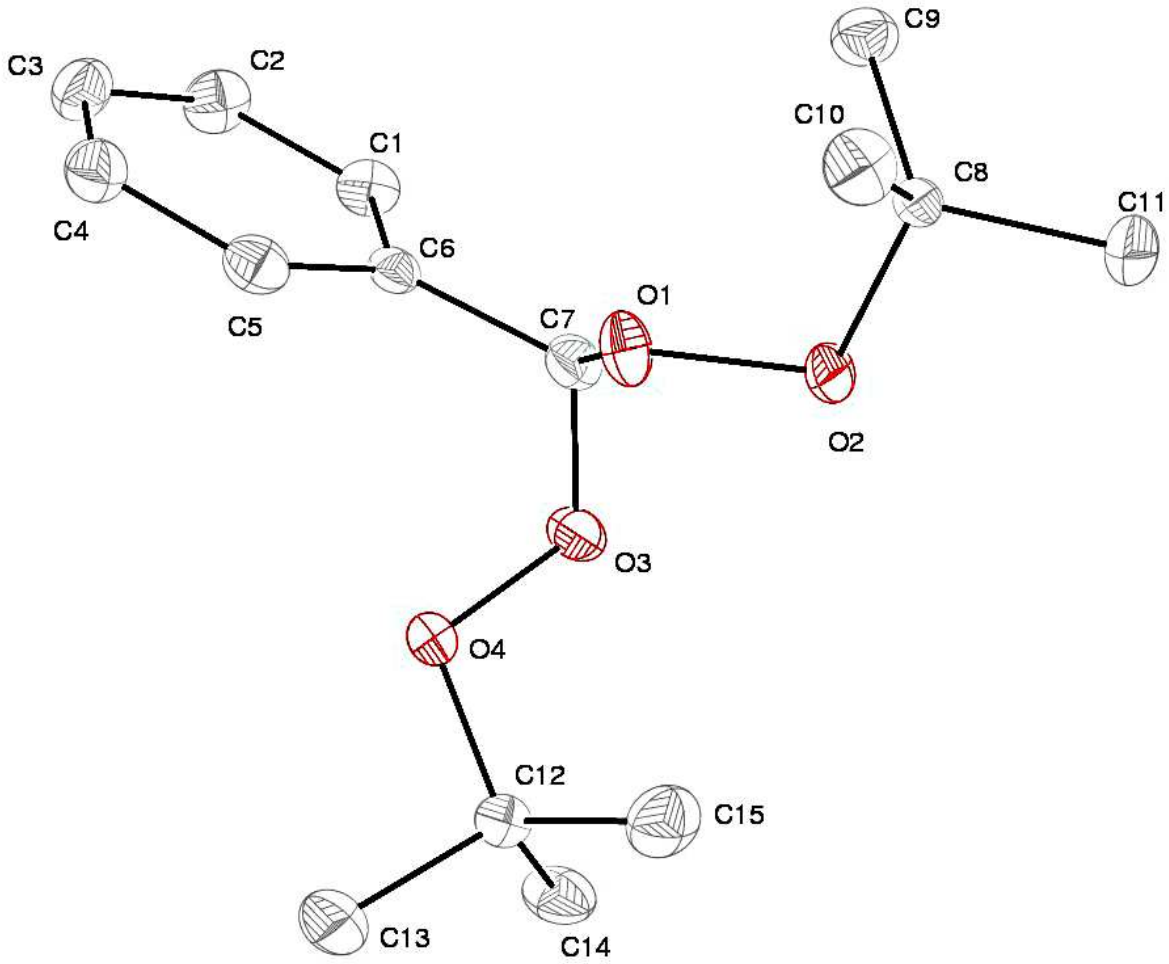

Figure 16. Perspective view of **3** with thermal ellipsoids at the 50% probability level.

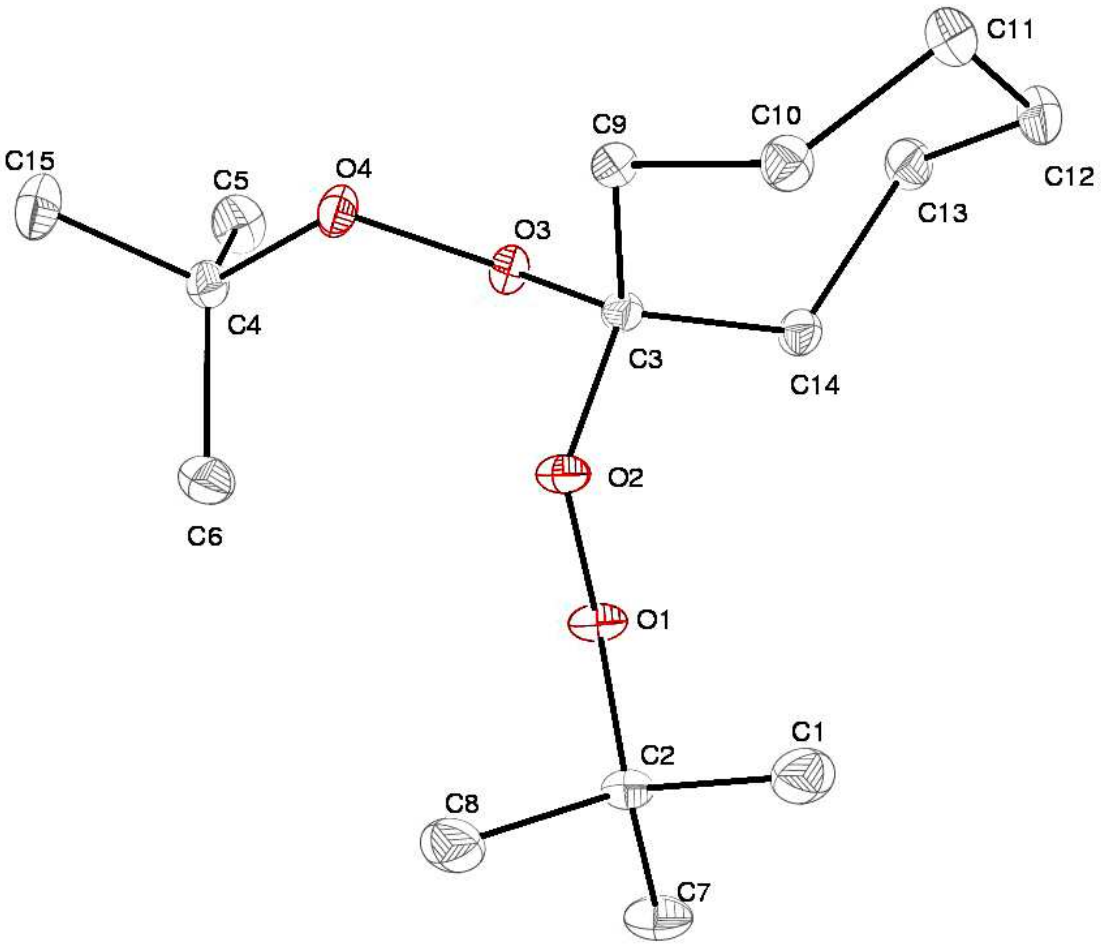

Figure 17. Perspective view of **5** with thermal ellipsoids at the 50% probability level.

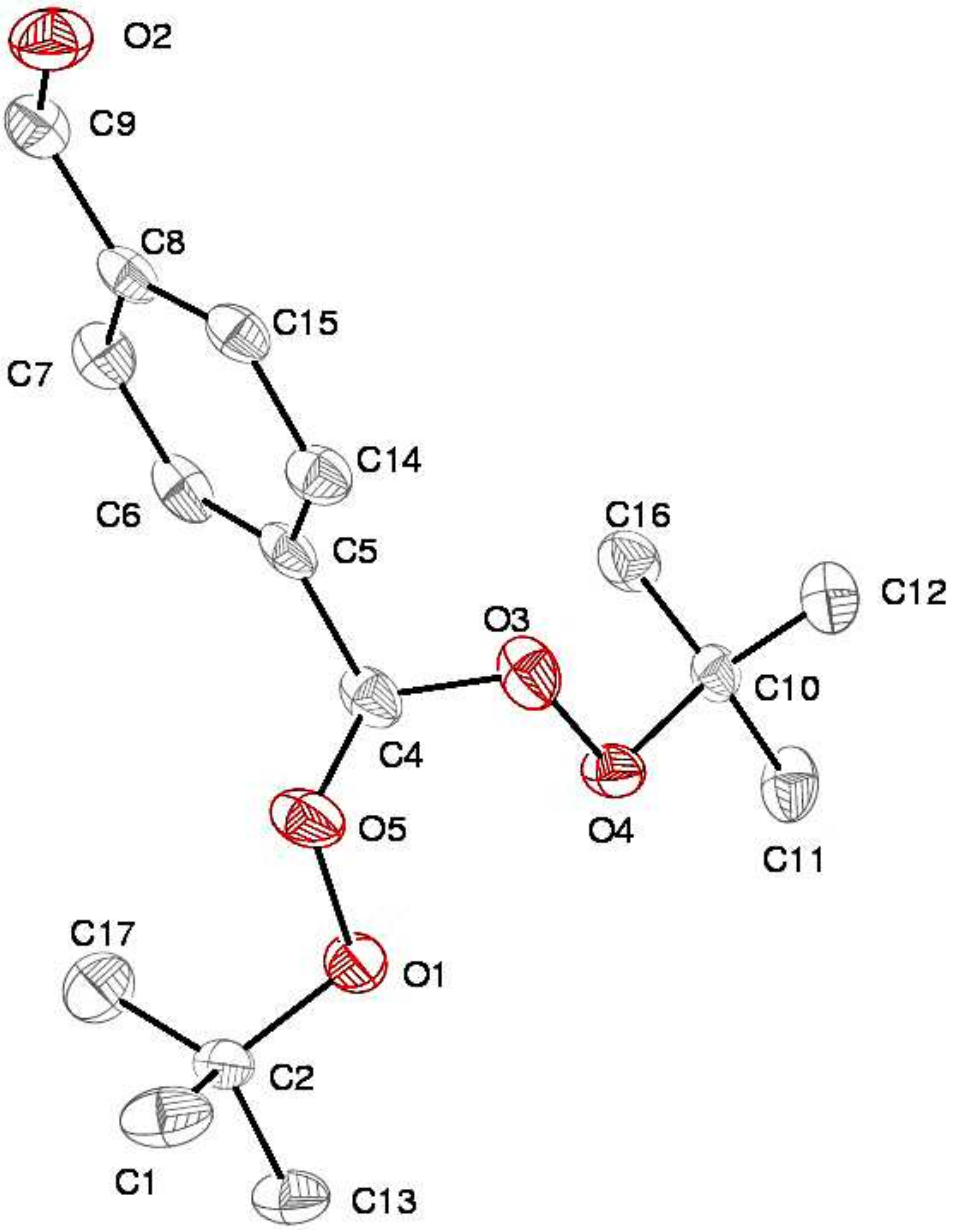

Figure 18. Perspective view of **8** with thermal ellipsoids at the 50% probability level.

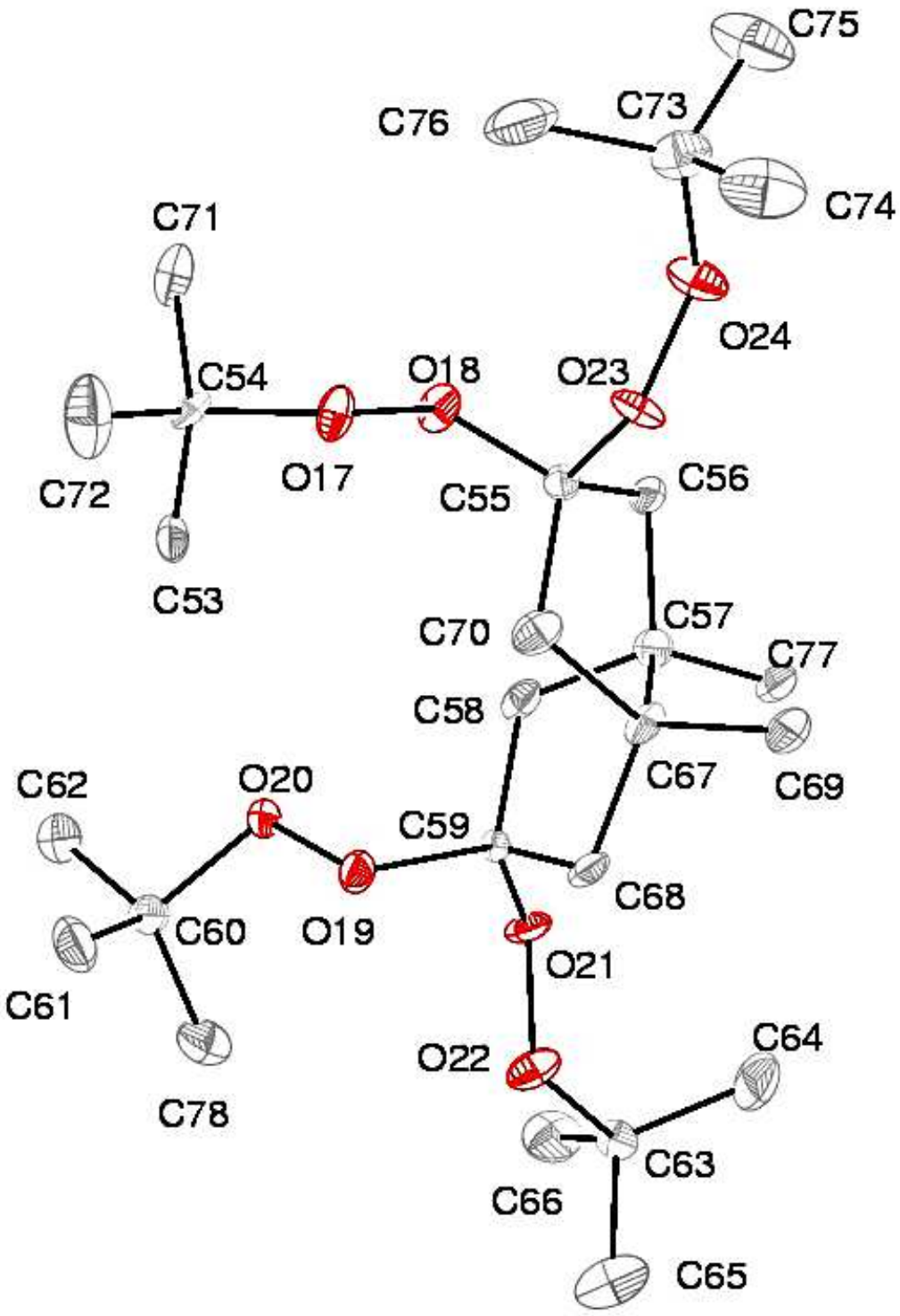

Figure 19. Perspective view of **11** with thermal ellipsoids at the 50% probability level.

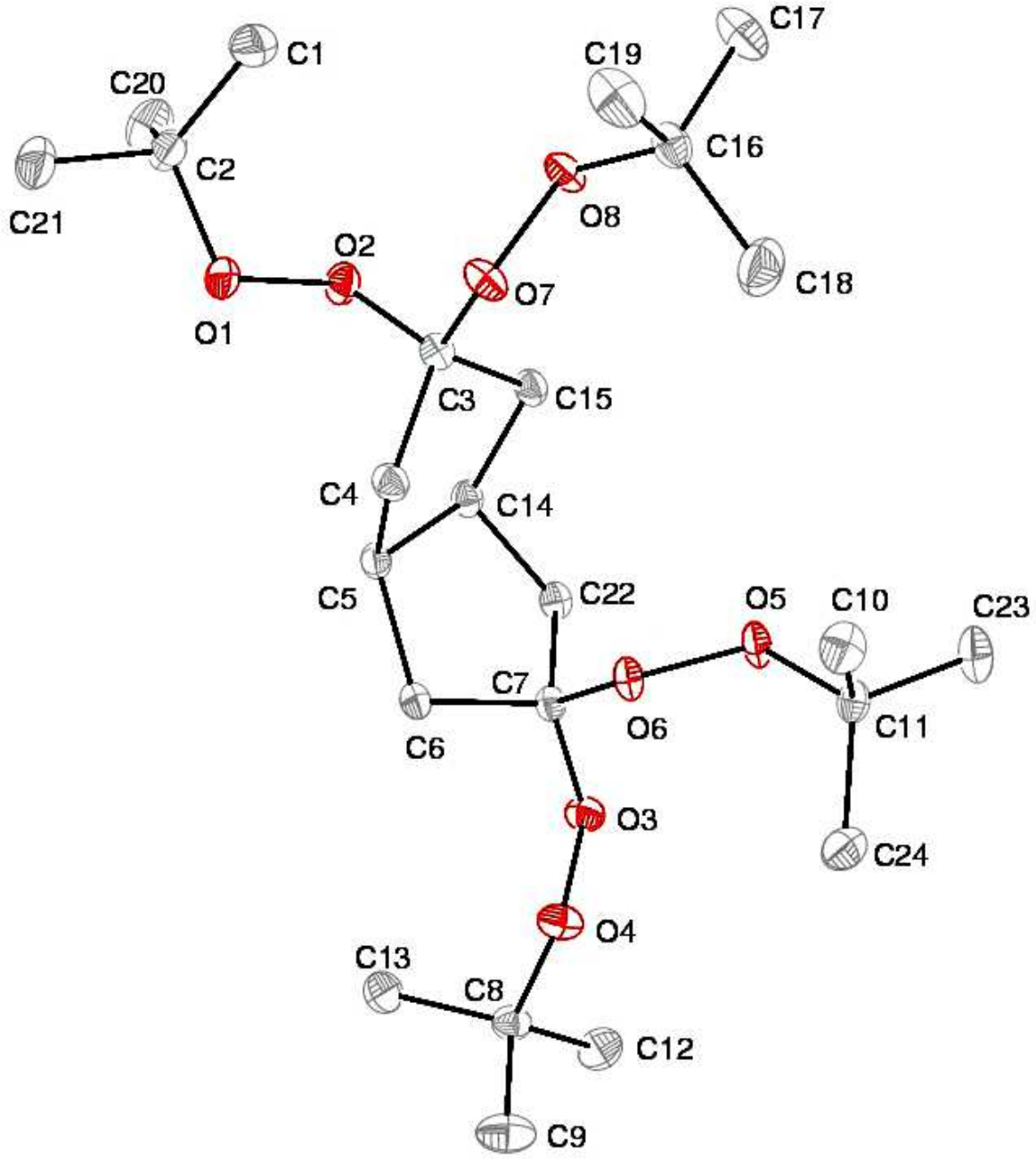

Figure 20. Perspective view of **13** with thermal ellipsoids at the 50% probability level.

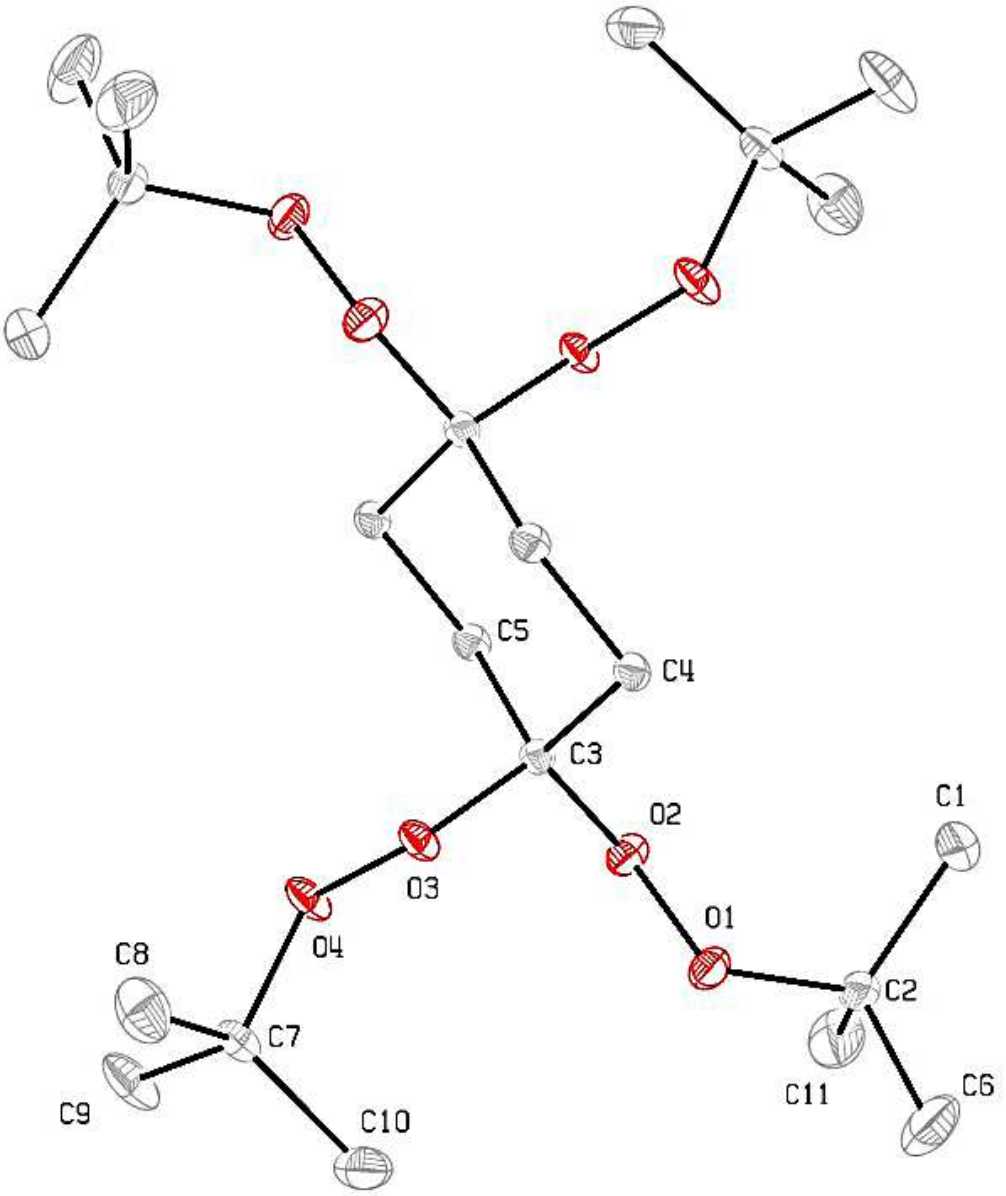

Figure 21. Perspective view of **15** with thermal ellipsoids at the 50% probability level.

Table 9. Selected bond lengths (Å) of **1**, **3**, **5**, **8**, **11**, **13**, and **15**.

Bond	1	3	5	8	11	13	15
O–O	1.4758(7)	1.4631(7)	1.4749(4)	1.481(2)	1.483(6)	1.4777(8)	1.4751(5)
	1.4746(7)	1.4745(6)	1.4742(4)	1.470(2)	1.480(6)	1.4798(8)	1.4758(4)
					1.472(6)	1.4803(8)	
					1.485(6)	1.4786(8)	
C=O				1.213(4)			
C–O	1.4184(9)	1.4024(7)	1.4468(5)	1.444(3)	1.462(8)	1.4479(11)	1.4435(6)
	1.4198(9)	1.4131(7)	1.4192(5)	1.409(3)	1.412(7)	1.4224(10)	1.4140(5)
	1.4483(9)	1.4488(7)	1.4260(5)	1.452(3)	1.476(8)	1.4120(10)	1.4159(5)
	1.4507(9)	1.4572(8)	1.4431(5)	1.411(3)	1.422(7)	1.4505(10)	1.4429(5)
					1.462(8)	1.4464(10)	
					1.416(7)	1.4198(9)	
					1.423(7)	1.4036(10)	
					1.457(7)	1.4447(10)	
C–C (bridge)					1.565(9)	1.5708(11)	

Table 10. The list of short contacts of **1**, **3**, **5**, **8**, **11**, **13**, and **15**.

Compound	Number	Atom 1	Atom 2	Length (Å)	Length-VdW (Å)
1	1	H12	O2	2.678	–0.042
	2	H19	H24	2.385	–0.015
3	1	H14C	H13C	2.34	–0.06
5	1	H22	H22	2.323	–0.077
8	1	H22	O4	2.658	–0.062
	2	C15	H7	2.881	–0.019
	3	H17A	H6	2.4	0
	4	O2	H17	2.586	–0.134
	5	O2	H20	2.466	–0.254
11	1	H27	H137	2.367	–0.033
	2	H34	C53	2.888	–0.012
	3	H34	H120	2.35	–0.05
	4	H88	H126	2.399	–0.001
	5	H97	H113	2.314	–0.086
	6	H51	H169	2.387	–0.013
	7	H184	H190	2.394	–0.006
	8	H186	H186	2.307	–0.093
13	1	O7	H14	2.699	–0.021
	2	C6	H35	2.843	–0.057
	3	H8	H43	2.327	–0.073
	4	C10	H12	2.878	–0.022
	5	H36	C13	2.759	–0.141
	6	H10	H33	2.322	–0.078
	7	H34	H34	2.179	–0.221
15	1	C4	H21	2.768	–0.132
	2	H20	O4	2.642	–0.078

The X-ray crystal structures of *tert*-butyl peroxides **1**, **3**, **5**, **8**, **11**, **13**, and **15** lack strong hydrogen bonds. Their intermolecular interactions are mainly weak C–H···O hydrogen bonds, C···H and H···H contacts, and π-interactions of **3** and **8** (Table 10). The strengths of C–H···O interactions are in the range of 5–10 kJ/mol.[100] These weak C–H···O interactions (H···O: 2.466–2.699 Å) are present in **1**, **8**, **13**, and **15**. Based on the theoretical calculations by Platts, the strengths of C···H interactions can be up to 35 kJ/mol.[101] There are C···H interactions (2.759–2.888 Å) in the crystal structures of *tert*-butyl peroxides **13** and **15**. Short H···H contacts (2.179–2.4 Å) are the most common type of intermolecular interactions that are present in all of the X-ray crystal structures of **1**, **3**, **5**, **8**, **11**, **13**, and **15**. They can exert stabilization energies up to 10 kcal/mol.[102] The X-ray crystal structures of **3** and **8** contain π–π and C–H···π interactions, respectively. The calculated intermolecular interaction energies of π-interactions are in the range of 1.48–2.48 kcal/mol.[103] The highest crystalline density was obtained with the aromatic *tert*-butyl peroxide **3**, which may be due to the presence of π–π interactions.

2.2.4 Thermal Stability

Thermal stabilities of *tert*-butyl peroxides were assessed using thermogravimetry (TGA/DTA). Representative TGA/DTA curves for **1** and **15** are shown in Figure 22 and Figure 23, respectively. The decomposition temperatures (T_{Dec}) of *tert*-butyl peroxides **1**–**15** are provided in Table 11. Decomposition temperatures of *tert*-butyl peroxides were in the range of 110–140 °C. They are fairly thermally stable peroxo-based compounds.

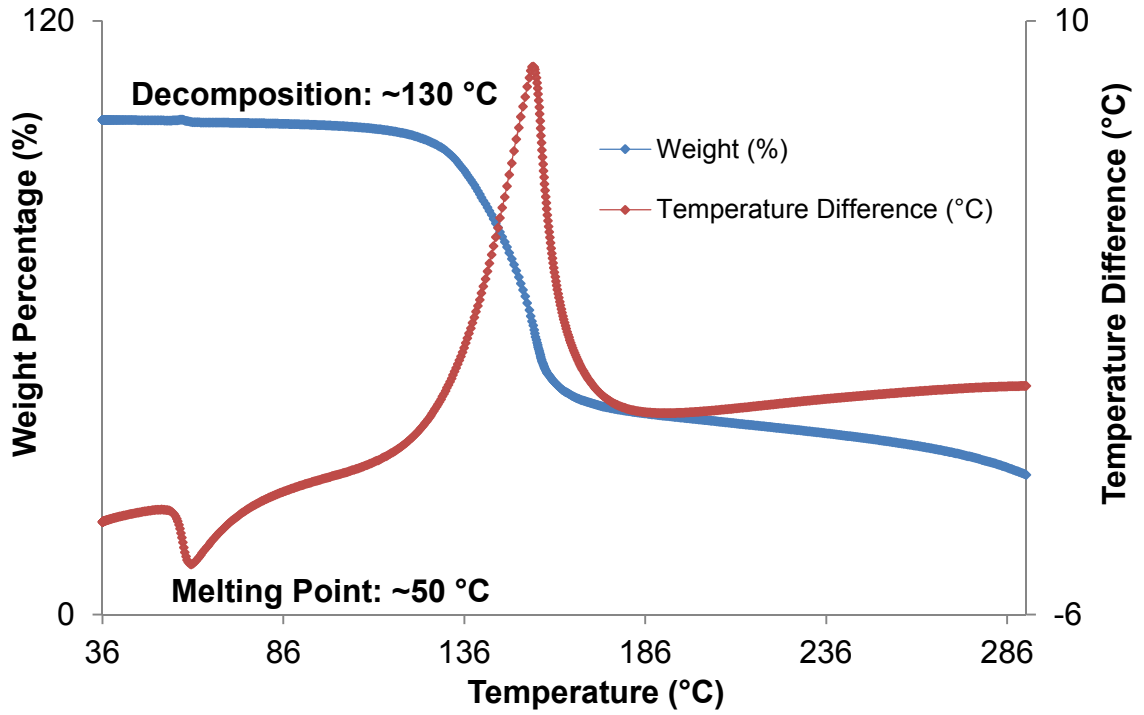

Figure 22. Representative TGA (blue) and DTA (red) curves for **1**.

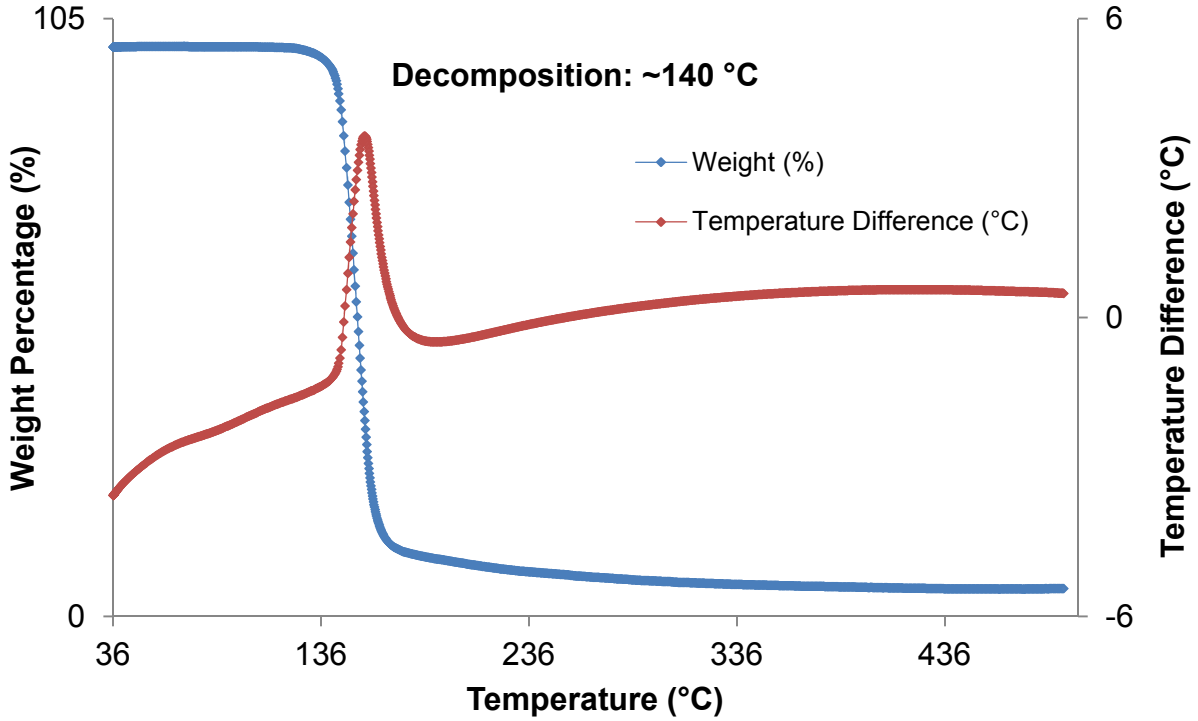

Figure 23. Representative TGA (blue) and DTA (red) curves for **15**.

Table 11. Decomposition temperatures of **1**–**15**.

Compound	T_{Dec} (°C)
1	130
2	110
3	135
4	120
5	110
6	110
7	105
8	140
9	120
10	120
11	110
12	140
13	120
14	125
15	140

The most thermally stable *tert*-butyl peroxides were the aromatic *tert*-butyl peroxides **3**, **8**, **12**, and **15**. The higher thermal stability of aromatic *tert*-butyl peroxides might be due to the presence of conjugated rings and π-interactions. The thermal stabilities of *tert*-butyl peroxides **1**–**15** are still low for most HEDM applications, which require the decomposition temperatures to be ≥ 150 °C.[2]

2.2.5 Preliminary Qualitative Sensitivity Tests

All *tert*-butyl peroxides **1**–**15** deflagrated upon burning in a Bunsen burner flame, indicating slow material decomposition kinetics. There were only slight variations in the flame responses with the increasing oxygen content and ring strain. Compounds **7**, **9**–**11**, and **13**–**15** produced large, bright yellow flames and were more sensitive and energetic than the rest of the *tert*-butyl peroxides. Cyclopentane ring-based peroxides **7**, **9**, and **10** were all relatively high in sensitivity and the most sensitive rapid flame responses were observed with **11** and **13** that contain the strained octahydropentalene rings. The higher sensitivities of **7**, **9**–**11**, and **13**–**15** can be attributed to the higher oxygen content and ring strain. The aromatic *tert*-butyl peroxides **3**, **8**, and **11** were the lowest in sensitivity based on their slow flame responses.

tert-Butyl peroxides **1**–**15** were also not sensitive to impact, friction, or electrostatic spark based on the absence of responses in hammer impact tests, sand paper friction tests, and Tesla coil electrostatic spark tests. Thus, *tert*-butyl peroxides **1**–**15** can be described as peroxo-based compounds that are safe to handle. No further standard sensitivity measurements or energetic calculations were performed since the low energetic performances of *tert*-butyl peroxides **1**–**15** were inadequate for their development as HEDMs.

2.3 Conclusions

tert-Butyl peroxides **1**–**15** were synthesized and fully characterized to study their sensitivities as well as their energetic properties. X-ray crystal structures were obtained for **1**, **3**, **5**, **8**, **11**, **13**, and **15** to confirm the bond connectivity. Their crystalline densities are low for HEDM applications and are in the range of 1.098–1.166 g/cm^3. Compounds

1–**15** are fairly thermally stable compounds with decomposition temperatures in the range of 110–140 °C, which are still low for most HEDM applications. All of the *tert*-butyl peroxides deflagrated upon burning due to their slow decomposition kinetics. Slightly higher sensitivities were observed with increasing oxygen content and ring strain of **1**–**15**. They were also not sensitive to impact, friction, or electrostatic spark based on the preliminary sensitivity tests. Hence, *tert*-butyl peroxides **1**–**15** are fairly safe peroxo-based compounds to handle. These low sensitivities of *tert*-butyl peroxides are advantageous for their use in industry as polymerization initiators.

2.4 Experimental Section

General Considerations: All the reactions for the synthesis of organic peroxides were carried out under ambient conditions (room temperature and non-inert atmosphere). Chemicals were purchased from Sigma-Aldrich, Acros Organics, EMD, or Alfa Aesar and were used without further purifications. ACS grade solvents from EMD and Fisher Scientific were used for the reactions, purifications, and re-crystallizations as obtained. Petroleum ether used in the synthetic protocols was with a boiling point range of 35–60 °C. A solution of 5.5 M tBuOOH in decane (Sigma-Aldrich) was used for the synthesis of the *tert*-butylperoxides. Synthesis of *tert*-butyl peroxides were carried out based on a published general procedure.[95] Compounds **1** and **3** were synthesized based on published procedures.[95]

Silica gel 60, 230–400 mesh (EMD Chemicals) was used to perform silica gel column chromatography.[104] ASTM TLC plates precoated with silica gel 60 F_{254} (250 μm layer thickness) were used for thin-layer chromatography (TLC). TLC spots were observed using a UV lamp and/ or a potassium permanganate solution (3 g $KMnO_4$, 20

g K_2CO_3, 5 mL 5% w/v aqueous NaOH, 300 mL H_2O), which was used as a stain and charring the $KMnO_4$ stained TLC plates by a heat gun was carried out to visualize the spots.

^1H and $^{13}C\{^1H\}$ NMR spectra were obtained from the Varian Mercury-400 (400 MHz and 101 MHz) NMR spectrometer or MR 400 (400 MHz and 101 MHz) NMR spectrometer, in $CDCl_3$ as indicated and were referenced to the residual proton and carbon resonances of $CDCl_3$: ^1H: δ 7.27, ^{13}C: δ 77.23. High-resolution mass spectra were obtained on an electrospray time-of-flight high-resolution Waters Micromass LCT Premier XE mass spectrometer. Infrared spectra were obtained from a Shimadzu MIRacle 10 IRAffinity-1 single reflection ATR accessory. Melting points were determined on an Electrothermal IA 9300 melting point apparatus and are uncorrected. The decomposition characteristics of organic hydroperoxides and *tert*-butylperoxides were studied by TGA and DTA, which were carried out with an SDT-2960 TGA/DTA instrument at a heating rate of 10 °C min^{-1}.

Qualitative Sensitivity Tests: Sensitivity to heat, impact and an electrostatic discharge, were determined to study the effectiveness of the organic peroxides as peroxo-based oxygen-rich high energy dense oxidizers by (i) Burning about 3–5 mg of the compound in the Bunsen burner flame; (ii) Striking 3–5 mg of the compound on a metal plate with a hammer; and (iii) Providing 3–5 mg of the compound on a metal plate with an electrostatic discharge using an Electro Technic BD 10 tesla coil (120 V, 0.35 A).

General Procedure for the Preparation of *tert*-Butylperoxides: A solution of I_2 (0.025 g, 0.100 mmol, 0.1 equivalents per ketone/aldehyde group) in CH_3CN (1–1.5 mL)

was treated with 5.5 M tBuOOH in decane (0.36 mL, 2.0 mmol, 2 equivalents per ketone/aldehyde group) while the reaction was stirred at room temperature (23 °C). Afterwards, the ketone/aldehyde starting material (1 mmol of monoketone/monoaldehyde compound or 0.5 mmol of diketone/dialdehyde compound) was added and the reaction was stirred at room temperature (23 °C) for 24 h. Then, the reaction was concentrated under reduced pressure and the product was purified by silica gel column chromatography with 19:1 petroleum ether:diethyl ether.

Preparation of 4-(*tert*-butyl)-1,1-bis(*tert*-butylperoxy)cyclohexane (1). Compound **1** was prepared in 58% yield as a white solid by a literature procedure[95] starting from 4-(*tert*-butyl)cyclohexan-1-one: mp 49–51 °C (lit[95] 49.5–50.5 °C); IR (ν cm^{-1}): 2968 (s), 2935 (s), 2866 (m), 1652 (m), 1559 (m), 1364 (s), 1248 (m), 1191 (s), 1123 (m), 1061 (s), 975 (m), 934 (s), 880 (s), 828 (w), 752 (m); ^{1}H NMR (400 MHz, $CDCl_3$, 23 °C, δ): 2.34–2.26 (broad d, 2H, *J* = 12.0 Hz), 1.64–1.57 (broad d, 2H, *J* = 12.4 Hz), 1.44–1.20 (m, 4H), 1.28 (s, 9H, C*H*$_3$), 1.24 (s, 9H, C*H*$_3$), 1.09–0.92 (m, 1H, C*H*), 0.86 (s, 9H, C*H*$_3$); ^{13}C{^{1}H} NMR (101 MHz, $CDCl_3$, 23 °C, ppm): 107.00 (peroxy *C*), 79.31 (*C*), 79.11 (*C*), 47.66 (*C*H), 32.59 (*C*), 31.16 (*C*H$_2$), 27.84 (*C*H$_3$), 27.10 (*C*H$_3$), 26.95 (*C*H$_3$), 23.67 (*C*H$_2$); ESI-HRMS: calcd for $[C_{18}H_{36}O_4Na]^+$ 339.2511; found 339.2695. Long, thick, colorless, needle-like single crystals were grown by crystallization from petroleum ether at –29 °C.

Preparation of 1,1-bis(*tert*-butylperoxy)-4,4-dimethylcyclohexane (2). 4,4-Dimethylcyclohexanone was treated with *t*BuOOH based on the general procedure on a 3 times larger scale to obtain 0.153 g (18%) of **2** as a colorless oil. IR (ν cm^{-1}): 2975 (m), 2951(m), 2928 (m), 2868 (w), 1452 (m), 1362 (s), 1270 (m), 1241 (m), 1200 (s),

1178 (s), 1062 (s), 1029 (m), 949 (s), 880 (s); ^{1}H NMR (400 MHz, $CDCl_3$, 23 °C, δ): 1.82 (t, 4H, C*H*$_2$), 1.34 (t, 4H, C*H*$_2$), 1.26 (s, 18H, C*H*$_3$), 0.92 (s, 6H, C*H*$_3$); ^{13}C{^{1}H} NMR (101 MHz, $CDCl_3$, 23 °C, ppm): 107.24 (peroxy *C*), 79.20 (*C*), 35.71(*C*H_2), 29.94 (*C*), 28.32 (*C*H_3), 27.06 (*C*H_2), 27.01 (*C*H_3); ESI-HRMS: calcd for $[C_{16}H_{32}O_4Na]^+$ 311.2198; found 311.2548.

Preparation of (bis(*tert*-butylperoxy)methyl)benzene (3). Compound **3** was prepared in 35% yield as a colorless oil by a literature procedure[95] starting from benzaldehyde: IR (ν cm^{-1}): 3038 (w), 2979 (m), 2933(w), 1648 (w), 1453 (m), 1364 (s), 1304 (w), 1244 (w), 1200 (s), 1086 (w), 1044 (m), 1002 (s), 918 (w), 900 (m), 875 (s), 755 (s), 697 (s); ^{1}H NMR (400 MHz, $CDCl_3$, 23 °C, δ): 7.52–7.43 (m, 2H, C*H*), 7.42–7.34 (m, 3H, C*H*), 6.21 (s, 1H, C*H*), 1.30 (s, 18H, C*H*$_3$); ^{13}C{^{1}H} NMR (101 MHz, $CDCl_3$, 23 °C, ppm): 134.87 (*C*), 129.16(*C*H), 128.26 (*C*H), 127.33 (*C*H), 108.57 (peroxy *C*H), 81.12 (*C*), 26.56 (*C*H_3); ESI-HRMS: calcd for $[C_{15}H_{24}O_4Na]^+$ 291.1572; found 291.1805. Colorless cube-like single crystals were grown by crystallization from hexane at –29 °C.

Preparation of 1,1-bis(*tert*-butylperoxy)-4-methylcyclohexane (4). 4-Methylcyclohexanone was treated with *t*BuOOH based on the general procedure on a 4 times larger scale to obtain 0.490 g (45%) of a colorless oil. IR (ν cm^{-1}): 2977 (m), 2951(m), 2932 (m), 2861 (w), 1452 (m), 1363 (s), 1249 (m), 1198 (s), 1155 (m), 1098 (m), 1047 (m), 1014 (m), 977 (s), 883 (s), 761 (w); ^{1}H NMR (400 MHz, $CDCl_3$, 23 °C, δ): 2.21 (d of m, 1H, *J* = 14.4 Hz, C*H*), 1.59–1.52 (m, 2H), 1.47–1.35 (m, 4H), 1.27 (s, 9H, C*H*$_3$), 1.23 (s, 9H, C*H*$_3$), 1.25–1.16 (m, 2H), 0.90 (d, 3H, *J* = 6.8 Hz, C*H*$_3$); ^{13}C{^{1}H} NMR (101 MHz, $CDCl_3$, 23 °C, ppm): 107.11 (peroxy *C*), 79.33 (*C*), 79.08 (*C*), 32.05 (*C*H),

31.26 (*C*H_2), 30.55 (*C*H_2), 27.08 (*C*H_3), 26.93 (*C*H_3), 21.96 (*C*H_3); ESI-HRMS: calcd for $[C_{15}H_{30}O_4Na]^+$ 297.2042; found 297.2276.

Preparation of 1,1-bis(*tert*-butylperoxy)cycloheptane (5). Cycloheptanone was treated with *t*BuOOH based on the general procedure on a 4 times larger scale and the product was purified by silica gel column chromatography with hexanes and then 30:1 hexanes:ethyl acetate to obtain 0.249 g (23%) of **5** as a white solid: mp 25–27 °C (lit[105] 25–27 °C); IR (ν cm^{-1}): 2977 (m), 2927(m), 2859 (m), 1457 (m), 1386 (w), 1363 (s), 1243 (m), 1196 (s), 1170 (m), 1111 (w), 1011 (s), 960 (w), 912 (m), 881 (s), 793 (w), 760 (w); ^{1}H NMR (400 MHz, $CDCl_3$, 23 °C, δ): 1.95–1.88 (m, 4H), 1.53 (s, 8H, C*H*$_2$), 1.24 (s, 18H, C*H*$_3$); ^{13}C{^{1}H} NMR (101 MHz, $CDCl_3$, 23 °C, ppm): 112.60 (peroxy *C*), 79.35 (*C*), 34.18 (*C*H_2), 30.98 (*C*H_2), 26.90 (*C*H_3), 23.34 (*C*H_2); ESI-HRMS: calcd for $[C_{15}H_{30}O_4Na]^+$ 297.2042; found 297.2231. Colorless, thick, needle-like single crystals were grown in hexanes at –29 °C.

Preparation of 1,1-bis(*tert*-butylperoxy)cyclohexane (6). Cyclohexanone was treated with *t*BuOOH based on the general procedure on a 5 times larger scale to obtain 0.491 g (38%) of **6** as a colorless oil. IR (ν cm^{-1}): 2977 (m), 2937(m), 2861 (w), 1449 (m), 1362 (s), 1238 (m), 1198 (s), 1152 (m), 1090 (m) 1065 (s), 1029 (w), 942 (s), 886 (s), 852 (w), 838 (w), 755 (w); ^{1}H NMR (400 MHz, $CDCl_3$, 23 °C, δ): 1.82–1.73 (m, 4H), 1.58–1.49 (m, 4H), 1.45–1.37 (m, 2H), 1.25 (s, 18H, C*H*$_3$); ^{13}C{^{1}H} NMR (101 MHz, $CDCl_3$, 23 °C, ppm): 107.11 (peroxy *C*), 79.13 (*C*), 31.04 (*C*H_2), 26.99 (*C*H_3), 25.92 (*C*H_2), 22.92 (*C*H_2).

Preparation of 1,1-bis(*tert*-butylperoxy)-3-methylcyclopentane (7). 3-Methylcyclopentanone was treated with *t*BuOOH based on the general procedure on a

3 times larger scale and the product was purified by silica gel column chromatography with hexanes and then 30:1 hexanes:ethyl acetate to obtain 0.234 g (30%) of **7** as a colorless oil. IR (ν cm^{-1}): 2977 (m), 2956 (m), 2931 (m), 2870 (m), 1457 (m), 1385 (w), 1363 (s), 1310 (w), 1241 (m), 1188 (s), 1149 (m), 1084 (w), 1022 (w), 977 (m), 928 (m), 868 (m), 760 (m); ^{1}H NMR (400 MHz, $CDCl_3$, 23 °C, δ): 2.24–2.16 (m, 1H), 2.14–2.02 (m, 2H), 1.99–1.88 (m, 1H), 1.85–1.72 (m, 1H), 1.54–1.45 (m, 1H), 1.263 (s, 9H, C*H*$_3$), 1.259 (s, 9H, C*H*$_3$), 1.34–1.08 (m, 1H), 1.00 (d, 3H, *J* = 6.8 Hz, C*H*$_3$); ^{13}C{^{1}H} NMR (101 MHz, $CDCl_3$, 23 °C, ppm): 118.23 (peroxy *C*), 79.63 (*C*), 79.60 (*C*), 42.29 (*C*H$_2$), 33.69 (*C*H$_2$), 33.42 (*C*H), 33.27 (*C*H$_2$), 26.96 (*C*H$_3$), 26.94 (*C*H$_3$), 20.07 (*C*H$_3$).

Preparation of 4-(bis(*tert*-butylperoxy)methyl)benzaldehyde (8). Terephthalaldehyde was treated with *t*BuOOH based on the general procedure on a 6 times larger scale and the product was purified by silica gel column chromatography with 24:1 hexanes:ethyl acetate to obtain 0.167 g (19%) of **8** as a white solid: mp 45–47 °C; IR (ν cm^{-1}): 3026 (w), 2982 (m), 2931(m), 2866 (w), 1721 (s), 1697 (m), 1662 (w), 1612 (w), 1416 (w), 1366 (m), 1261 (m), 1192 (s), 1171 (m), 1062 (s), 1101 (m), 955 (s), 913 (m), 854 (s), 805 (m), 774 (s); ^{1}H NMR (400 MHz, $CDCl_3$, 23 °C, δ): 10.04 (s, 1H, C*H*), 7.89 (d, 2H, *J* = 8.4 Hz, C*H*), 7.63 (d, 2H, *J* = 8.4 Hz, C*H*), 6.22 (s, 1H, C*H*), 1.28 (s, 18H, C*H*$_3$); ^{13}C{^{1}H} NMR (101 MHz, $CDCl_3$, 23 °C, ppm): 192.12 (*C*), 141.11 (*C*), 136.83 (*C*), 129.78 (*C*H), 128.20 (*C*H), 107.56 (peroxy *C*), 81.65 (*C*), 26.64 (*C*H$_3$); ESI-HRMS: calcd for $[C_{16}H_{24}O_5Na]^+$ 319.1521; found 319.1453. Thin, colorless, plate-like single crystals were grown by crystallization from petroleum ether at –29 °C.

Preparation of 1,1-bis(*tert*-butylperoxy)cyclopentane (9). Cyclopentanone was treated with *t*BuOOH based on the general procedure on a 2 times larger scale to

obtain 0.142 g (29%) of **9** as a colorless oil. IR (ν cm^{-1}): 2977 (m), 2934 (m), 2872 (w), 1363 (m), 1185 (s), 1079 (m), 1017 (w), 975 (m), 866 (m), 758 (w); ^{1}H NMR (400 MHz, $CDCl_3$, 23 °C, δ): 1.98–1.92 (m, 4H, C*H*$_2$); 1.69–1.64 (m, 4H, C*H*$_2$), 1.26 (s, 18H, C*H*$_3$); $^{13}C\{^{1}H\}$ NMR (101 MHz, $CDCl_3$, 23 °C, ppm): 118.50 (peroxy *C*), 79.64 (*C*), 33.82 (*C*H_2), 26.94 (*C*H_3), 24.76 (*C*H_2).

Preparation of 4,4-bis(*tert*-butylperoxy)cyclopent-1-ene (10). 3-Cyclopenten-1-one was treated with *t*BuOOH based on the general procedure on a 3 times larger scale to obtain 0.217 g (30%) of **10** as a colorless oil. IR (ν cm^{-1}): 3065 (w), 2977 (m), 2929 (m), 2869 (w), 1620 (w), 1455 (w), 1364 (m), 1311 (m), 1235 (m), 1193 (s), 1074 (s), 1037 (m), 958 (m), 867 (s), 783 (w), 759 (w); ^{1}H NMR (400 MHz, $CDCl_3$, 23 °C, δ): 5.60 (s, 2H, C*H*), 2.70 (S, 4H, C*H*$_2$), 1.251 (s, 18H, C*H*$_3$); $^{13}C\{^{1}H\}$ NMR (101 MHz, $CDCl_3$, 23 °C, ppm): 127.74 (*C*H), 117.29 (peroxy *C*), 79.89 (*C*), 40.22 (*C*H_2), 26.84 (*C*H_3); ESI-HRMS: calcd for $[C_{13}H_{24}O_4 + H]^+$ 245.1753; found 245.1754.

Preparation of 2,2,5,5-tetrakis(*tert*-butylperoxy)-*cis*-3,6-dimethyloctahydropentalene (11). *cis*-1,5-Dimethylbicyclo[3.3.0]octane-3,7-dione was treated with *t*BuOOH based on the general procedure on a 6 times larger scale and the product was purified by silica gel column chromatography with 30:1 hexanes:ethyl acetate to obtain 0.098 g (10%) of **11** as a white solid: mp 88–90 °C; IR (ν cm^{-1}): 2972 (m), 2929 (m), 2868 (w), 1735 (w), 1454 (m), 1386 (w), 1362 (s), 1282 (w), 1192 (s), 1153 (m), 1126 (m), 1081 (w), 1036 (s), 979 (m), 946 (w), 884 (s), 860 (s), 817 (w), 761 (m); ^{1}H NMR (400 MHz, $CDCl_3$, 23 °C, δ): 2.28 (d, 4H, *J* = 14.8 Hz), 1.93 (d, 4H, *J* = 14.8 Hz), 1.27 (s, 36H, C*H*$_3$), 1.00 (s, 6H, C*H*$_3$); $^{13}C\{^{1}H\}$ NMR (101 MHz, $CDCl_3$, 23 °C, δ ppm): 116.35 (peroxy *C*), 79.35 (*C*), 79.30 (*C*), 49.72 (*C*), 46.20 (*C*H_2), 27.13 (*C*H_3),

27.10 (*C*CH_3), 22.29 (*C*CH_3); ESI-HRMS: calcd for $[C_{26}H_{50}O_8Na]^+$ 513.3403; found 513.3382. Colorless, polygonal single crystals were grown by slow evaporation in toluene.

Preparation of 1,4-bis(bis(*tert*-butylperoxy)methyl)benzene (12). Terephthalaldehyde was treated with *t*BuOOH based on the general procedure on a 6 times larger scale using 4 equivalents of *t*BuOOH per ketone/aldehyde group and the product was purified by silica gel column chromatography with 24:1 hexanes: ethyl acetate to obtain 0.134 g (10%) of **12** as a white solid: mp 61–63 °C; IR (ν cm^{-1}): 2978 (m), 2931(m), 2870 (w), 1651 (w), 1457 (w), 1363 (m), 1243 (w), 1200 (s), 1093 (w), 1042 (m), 999 (s), 915 (w), 879 (m), 860 (m), 825 (m), 756 (w); ^{1}H NMR (400 MHz, $CDCl_3$, 23 °C, δ): 7.45 (s, 4H, C*H*), 6.18 (s, 2H, C*H*), 1.28 (s, 36H, C*H*$_3$); ^{13}C{^{1}H} NMR (101 MHz, $CDCl_3$, 23 °C, ppm): 135.69 (*C*), 127.35 (*C*H), 108.37 (peroxy *C*H), 81.44 (*C*), 26.66 (*C*CH_3); ESI-HRMS: calcd for $[C_{24}H_{42}O_8Na]^+$ 481.2777; found 481.2690.

Preparation of 2,2,5,5-tetrakis(*tert*-butylperoxy)octahydropentalene (13). *cis*-Bicyclo[3.3.0]octane-3,7-dione was treated with *t*BuOOH based on the general procedure on a 4 times larger scale to obtain 0.183 g (19%) of **13** as a white solid: mp 119–122 °C; IR (ν cm^{-1}): 2981 (m), 2930 (m), 2874 (w), 1651 (m), 1363 (s), 1306 (m), 1243 (m), 1194 (s), 1132 (s), 1085 (m), 1044 (m), 1000 (m), 971 (w), 893 (m), 877 (s), 829 (w), 762 (w); ^{1}H NMR (400 MHz, $CDCl_3$, 23 °C, δ): 2.69–2.56 (m, 2H, C*H*), 1.90 (d of d, 4H, *J* = 13.6 Hz, *J* = 8.4 Hz), 1.90 (d of d, 4H, *J* = 13.8 Hz, *J* = 6.0 Hz), 1.26 (s, 18H, C*H*$_3$), 1.25 (s, 18H, C*H*$_3$); ^{13}C{^{1}H} NMR (101 MHz, $CDCl_3$, 23 °C, ppm): 118.52 (peroxy *C*), 79.71 (*C*), 79.47 (*C*), 39.31 (*C*H), 38.97 (*C*H_2), 27.01 (*C*CH_3), 26.94 (*C*CH_3);

ESI-HRMS: calcd for $[C_{24}H_{46}O_8Na]^+$ 485.3090; found 485.3088. Long, thin, planar, and colorless needle-like single crystals were grown by slow evaporation in toluene.

Preparation of 2,2,5,5-tetrakis(*tert*-butylperoxy)hexane (14). 2,5-Hexanedione was treated with *t*BuOOH based on the general procedure on a 2 times larger scale and the product was purified by silica gel column chromatography with 30:1 hexanes: ethyl acetate to obtain 0.087 g (20%) of **14** as a colorless oil. IR (ν cm^{-1}): 2977 (m), 2933 (m), 2865 (w), 1719 (m), 1454 (m), 1364 (s), 1245 (m), 1196 (s), 1108 (s), 970 (w), 910 (m), 880 (s), 751 (m); ^1H NMR (400 MHz, $CDCl_3$, 23 °C, δ): 2.21–2.03 (m, 4H, C*H*$_2$). 1.52 (s, 6H, C*H*$_3$), 1.22 (s, 36H, C*H*$_3$); $^{13}C\{^1H\}$ NMR (101 MHz, $CDCl_3$, 23 °C, ppm): 112.80 (peroxy C), 79.36 (C), 35.96 (*C*H_2), 26.83 (*C*H_3), 23.42 (*C*H_3); ESI-HRMS: calcd for $[C_{22}H_{46}O_8 + H]^+$ 439.3271; found 439.3551.

Preparation of 1,1,4,4-tetrakis(*tert*-butylperoxy)cyclohexane (15). 1,4-Cyclohexanedione was treated with *t*BuOOH based on the general procedure on a 4 times larger scale to obtain 0.257 g (29%) of **15** as a white solid: mp 137–139 °C; IR (ν cm^{-1}): 2978 (m), 2929 (m), 2867 (w), 1362 (s), 1254 (m), 1196 (s), 1152 (w), 1082 (s), 1024 (w), 1000 (m), 959 (s), 922 (m), 882 (s), 803 (m), 756 (w); ^1H NMR (400 MHz, $CDCl_3$, 23 °C, δ): 1.93 (s, 8H, C*H*$_2$), 1.26 (s, 36H, C*H*$_3$); $^{13}C\{^1H\}$ NMR (101 MHz, $CDCl_3$, 23 °C, ppm): 106.94 (peroxy *C*), 79.43 (*C*), 27.25 (*C*H_2), 26.94 (*C*H_3); Large, thick, colorless, needle-like single crystals were grown by slow evaporation of in petroleum ether.

CHAPTER 3

Synthesis, Characterization, and Study of Surprisingly Highly Energetic and Low Sensitivity *tert*-Butyl Peroxy Esters with Low Oxygen and Nitrogen Contents

3.1 Introduction

tert-Butyl peroxy esters are one of the common categories of peroxo-based compounds. They have been extensively used in industry. *tert*-Butyl peroxy esters belong to the main peroxide sub-class of peroxy esters with a wide range of reactivity.

3.1.1 Peroxy Esters

Peroxy esters have the basic $R_1C(O)OOR_2$ formula where the groups R_1 and R_2 can be the same or different primary, secondary, or tertiary alkyl groups. They are commonly prepared from acid chlorides, anhydrides, and esters by reacting with alkyl hydroperoxides. Peroxy esters are also synthesized by the condensation of carboxylic acids with alkyl hydroperoxides using coupling agents such as dicyclohexylcarbodiimide.[39] The 10 h half life temperatures of peroxy esters are in the range of 65–160 °C.[39,106]

They readily undergo homolytic cleavages thermally or photochemically to produce free radicals as shown by Equation 6, followed by decarboxylation of acyloxy radicals and β-scission of alkoxy radicals.[39] Peroxy esters with tertiary or bulky alkyl peroxy esters tend to decompose into alkyl and alkoxy radicals along with CO_2.[39] Thus, they are most popular as radical initiators for free radical polymerization reactions. Peroxy esters can also undergo radical induced decompositions (Equation 7).[106c]

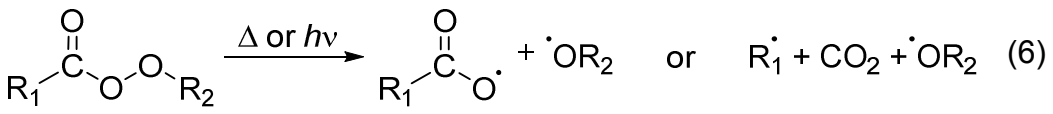

(6)

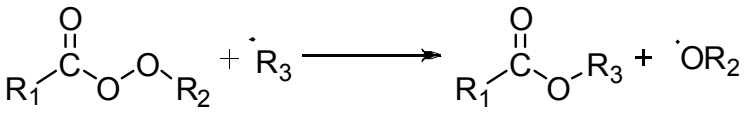

(7)

Low molecular weight peroxy esters can produce violent decompositions at high concentrations and elevated temperatures.[39] Peroxy esters are more easily hydrolyzed into the parent carboxylic acid and alkyl hydroperoxides than the other esters. They can perform oxygen atom or acyl group transfers and are used as oxidizing agents in organic chemistry.[107] Peroxy esters also undergo rearrangement reactions.[108]

3.1.1 *tert*-Butyl Peroxy Esters

tert-Butyl peroxy esters are commonly employed as polymerization initiators in industry and are used as organic synthetic reagents.[39,106,107,109] The availability, low cost, and high stability of *tert*-butyl hydroperoxide has allowed economical syntheses of various *tert*-butyl peroxy esters in industry. Since they are relatively carbon-rich compounds, their energetic properties have not been studied for use as HEDMs. Still, a few low molecular weight *tert*-butyl peroxy esters such as *tert*-butyl peroxy acetate have been reported as shock sensitive compounds, which are potentially explosive.[110]

In this chapter, synthesis, characterization, and the energetic properties of a series of *tert*-butyl peroxy esters **16**–**22** (Figure 24) are described. Compounds **16**–**22** have O:C ratios in the range of 0.38–0.64, which are only slightly greater than that of *tert*-butyl peroxides **1**–**15** in Chapter 1. However, the central cores of *tert*-butyl peroxy esters **16**–**22** contain relatively high oxygen contents (0.75–3.00), when the *tert*-butyl groups on the peripheries are disregarded. Surprisingly, *tert*-butyl peroxy esters **17**–**21** were highly sensitive based on the preliminary flame and Tesla coil tests, even with the low oxygen and nitrogen contents. Thus, standard sensitivity tests and energetic

calculations were performed. Compounds **16**–**22** are the first peroxy esters to be completely energetically characterized to gain insights about their energetic properties.

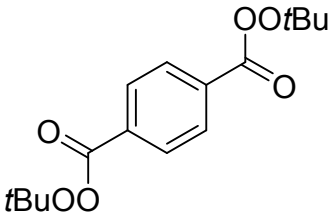

16, 75%
O:C = 3:8 = 0.38
O:C (core) = 3:4 = 0.75

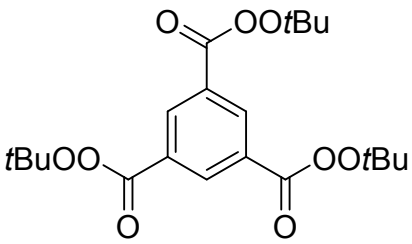

17, 77%
O:C = 3:7 = 0.43
O:C (core) = 1:1 = 1.00

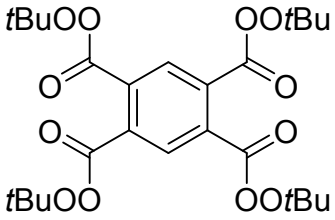

18, 42%
O:C = 6:13 = 0.46
O:C (core) = 6:5 = 1.20

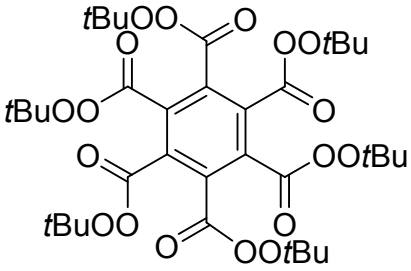

19, 36%
O:C = 1:2 = 0.50
O:C (core) = 3:2 = 1.50

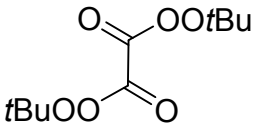

20, 45%
O:C = 3:5 = 0.60
O:C (core) = 3:1 = 3.00

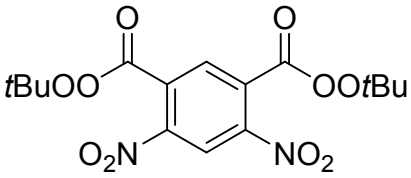

21, 74%
O:C = 5:8 = 0.62
O:C (core) = 5:4 = 1.25

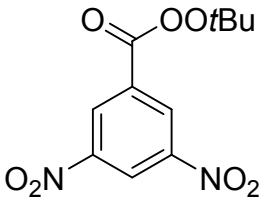

22, 60%
O:C = 7:11= 0.64
O:C (core) = 1:1 = 1.00

Figure 24. The series of *tert*-butyl peroxy esters **16**–**22**.

3.2 Results and Discussion

Aromatic *tert*-butyl peroxy esters **16**–**19**, **21**, and **22** were synthesized in this study since the aromatic *tert*-butyl peroxides **3**, **8**, and **12** of Chapter 1 were more thermally stable and lower in sensitivity with respect to the non-aromatic *tert*-butyl peroxides. Additionally, π-interactions of aromatic *tert*-butyl peroxy esters may allow high crystalline densities. Increasing the number of *tert*-butyl peroxy ester groups on the aromatic rings increases the oxygen content of the *tert*-butyl peroxy esters **16**–**19**. Compounds **21** and **22** each contain two nitro groups that have been widely used in HEDMs due to their ability to increase the energy content without excessively increasing the sensitivities. Compound **20** is a non-aromatic low molecular weight *tert*-butyl peroxy ester with a high oxygen content in the central core.

3.2.1 Synthetic Aspects

Caution: Organic peroxo-based compounds are potentially explosive and require handling with care. Reactions and other manipulations were performed in a fume hood behind a blast shield. Personal protective equipment was used whenever necessary: a face shield, leather gloves, and a leather apron. Interactions with strong acids, metals, metal salts, or easily oxidizable species were avoided to prevent hazardous decomposition reactions. All reactions were performed on small scales (≤ 350 mg) and at or below room temperature.

Aromatic peroxy esters (**16**–**19**, **21**, and **22**) were synthesized by treating the corresponding benzoyl chlorides with *tert*-butyl hydroperoxide in the presence of pyridine as a base (Scheme 6). Briefly, to a solution of anhydrous pyridine and *t*BuOOH in decane that was kept at –4 °C, a solution of the corresponding benzoyl chloride in

anhydrous pentane, CH_2Cl_2, or Et_2O was added dropwise. Then, the reaction was stirred for 0.2–2.0 h and was allowed to warm up to 23 °C. Compounds **16**, **18**, **19**, **21**, and **22** were purified by silica gel column chromatography, but **17** was obtained pure without chromatography. The corresponding benzoyl chlorides for the syntheses of **18**, **19**, and **21** were synthesized prior to the peroxy ester synthesis due to the moisture sensitivity using published procedures.[111] Compound **21** was a four step synthesis starting from 2,4-dimethyl-1-nitrobenzene. Compound **20** was synthesized similar to the aromatic peroxy esters, based on modified published procedures,[112] starting from oxalyl chloride, and was isolated by a crystallization procedure.

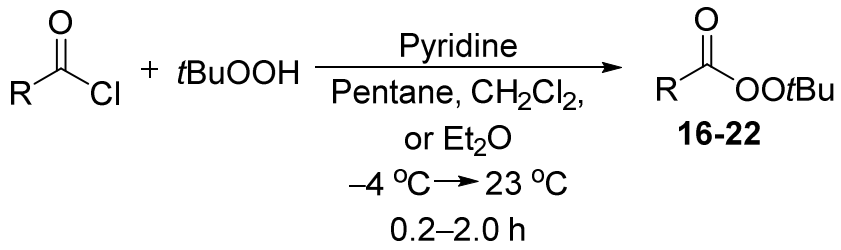

Scheme 6. Synthesis of *tert*-butyl peroxy esters.

tert-Butyl peroxy esters **16**–**22** were obtained in moderate to high yields and were all isolated as white solids. Compounds **19** and **22** are new compounds obtained in this study. X-ray quality single crystals of *tert*-butyl peroxy esters **16**–**22** were grown by slow evaporation (**16**–**18**, **21**, and **22**) or cooling the saturated solutions at –29 °C in the freezer (**19** and **20**). Compounds **16**–**22** all resulted in colorless crystals. They were in forms of planar squares (**16**), thin long plates (**17**), thick hexagons (**18**), thick polygons (**19** and **22**), and thick needles (**20** and **21**). *tert*-Butyl peroxy esters **16**–**22** were characterized by ^{1}H and ^{13}C NMR spectroscopy, mass spectrometry, melting point

analysis, IR spectroscopy, and elemental analysis. X-ray crystal structures were obtained for complete characterization of all of the *tert*-butyl peroxy esters **16**–**22**.

3.2.2 Spectroscopy

^{1}H NMR spectra of **16**–**22** consist of deshielded methyl proton peaks in the chemical shift range of δ 1.36–1.47. The methyl peak of **18** was obtained as a multiplet, which might be due to spatial interactions of the protons or different isomers present in solution. In the ^{13}C NMR spectra, the quaternary carbon peaks of *tert*-butyl groups were present in the chemical shift range of 84.62–86.18 ppm. These quaternary carbon peaks of *tert*-butyl groups were more deshielded than the corresponding quaternary carbon peaks of *tert*-butyl peroxides due to the presence of the carbonyl group. The carbonyl carbon peaks in the ^{13}C NMR spectra were in the chemical shift range of 160.64–163.68 ppm for the aromatic *tert*-butyl peroxy esters **16**–**19**, **21**, and **22**. However, a carbonyl carbon peak was not observed for **20** with 2 s of delay time (d1). When the delay time was increased to 5 s, a peak was observed at 154.36 ppm, which might be from the carbonyl carbons of **20**.

The characteristic IR stretching frequencies of the *tert*-butyl peroxy esters are medium CH_3 antisymmetric and symmetric stretching modes in the range of 2850–3000 cm^{-1}, strong C=O stretching modes in the range of 1700–1820 cm^{-1}, medium or strong C–O stretching modes in the range of 1000–1300 cm^{-1}, and weak O–O stretching modes in the range of 800–900 cm^{-1}.[96,97] In the IR spectra of **16**–**22**, there were medium to weak CH_3 antisymmetric and symmetric stretching modes in the range of 2870–2984 cm^{-1}. Strong C=O stretching modes were present in the range of 1753–1805 cm^{-1} and the highest C=O stretching mode (1805 cm^{-1}) was observed in **20**. The

C=O stretching frequencies increase from **16**–**19** indicating that C=O bonds become stronger with more *tert*-butyl peroxy ester groups on the phenyl ring. Two different C=O stretching frequencies were observed for **18** (1759 and 1771 cm^{-1}) and **22** (1761 and 1749 cm^{-1}). There were multiple strong peaks within the frequency range of 1000–1300 cm^{-1} and medium to weak peaks in the frequency range of 800–900 cm^{-1} for the stretching modes of C–O and O–O, respectively.

3.2.3 X-Ray Crystal Structures

X-ray crystal structures were obtained for all of the *tert*-butyl peroxy esters **16**–**22**. Compound **19** was crystallized as an adduct of hexane (**19**·hexane). In the X-ray crystal structure of **19**·hexane, the hexane molecule was disordered. However, the disorder of hexane did not influence the chemistry of **19**. The X-ray crystal structures were normal without unusual intermolecular interactions. Experimental crystallographic data are summarized in Table 12. Perspective views of the crystal structures are given in the Figures 25–31. Selected bond lengths from the structures are provided in Tables 13 and 14. Short contact lists generated by Mercury 3.5.1 software are provided in Tables 15, 16, and 17.

The O–O bond lengths of the *tert*-butyl peroxy esters **16**–**22** (Table 12) were in the range of the O–O bond lengths reported for peroxy esters.[99] Low crystalline densities were obtained for the *tert*-butyl peroxy esters **16**–**22** due to the bulky *tert*-butyl peroxy groups. Their crystalline densities were in the range of 1.161–1.487 g/cm^3.

Table 12. Experimental crystallographic data of **16**–**18**, **19**·hexane, and **20**–**22**.

	16	**17**	**18**	**19**·hexane	**20**	**21**	**22**
Formula	$C_{16}H_{22}O_6$	$C_{21}H_{30}O_9$	$C_{26}H_{38}O_{12}$	$C_{42}H_{68}O_{18}$	$C_{40}H_{72}O_{24}$	$C_{16}H_{20}N_2O_{10}$	$C_{11}H_{12}N_2O_7$
FW	310.33	426.45	542.56	860.96	936.97	400.34	284.23
Space group	P 1 2_1/c 1	P 1bar	C 1 2/c 1	C 1 c 1	P 1bar	P 1 2_1/c 1	P 1bar
a (Å)	17.5862(13)	5.9235(4)	27.942(2)	22.1254(16)	10.4787(4)	15.0401(9)	5.8362(4)
b (Å)	9.3966(7)	12.4414(7)	7.9924(5)	19.4588(16)	14.5660(6)	5.7008(3)	10.2950(7)
c (Å)	9.9604(7)	16.3240(10)	29.958(2)	11.4416(9)	16.5368(7)	21.6710(13)	10.8250(7)
V (Å^3)	1642.2(2)	1158.37(13)	5938.8(7)	4926.0(7)	2524.06(18)	1857.58(19)	634.81(7)
Z	4	2	8	4	2	4	2
T (K)	100(2)	100(2)	100(2)	100(2)	100(2)	100(2)	100(2)
λ (Å)	0.71073	0.71073	0.71073	0.71073	0.71073	0.71073	0.71073
ρ_{calc} (g/cm^3)	1.255	1.223	1.214	1.161	1.233	1.431	1.487
μ (mm^{-1})	0.096	0.095	0.096	0.090	0.102	0.121	0.126
R(F)[a] (%)	6.12	4.00	4.46	4.67	3.54	3.62	3.83
R_w(F)[b] (%)	18.23	11.58	14.62	13.24	7.91	12.72	11.45

[a] $R(F) = \sum \| F_o | - | F_c \| / \sum | F_o |$; [b] $Rw(F) = [\sum w(F_o^2 - F_c^2)^2 / \sum w(F_o^2)^2]^{1/2}$

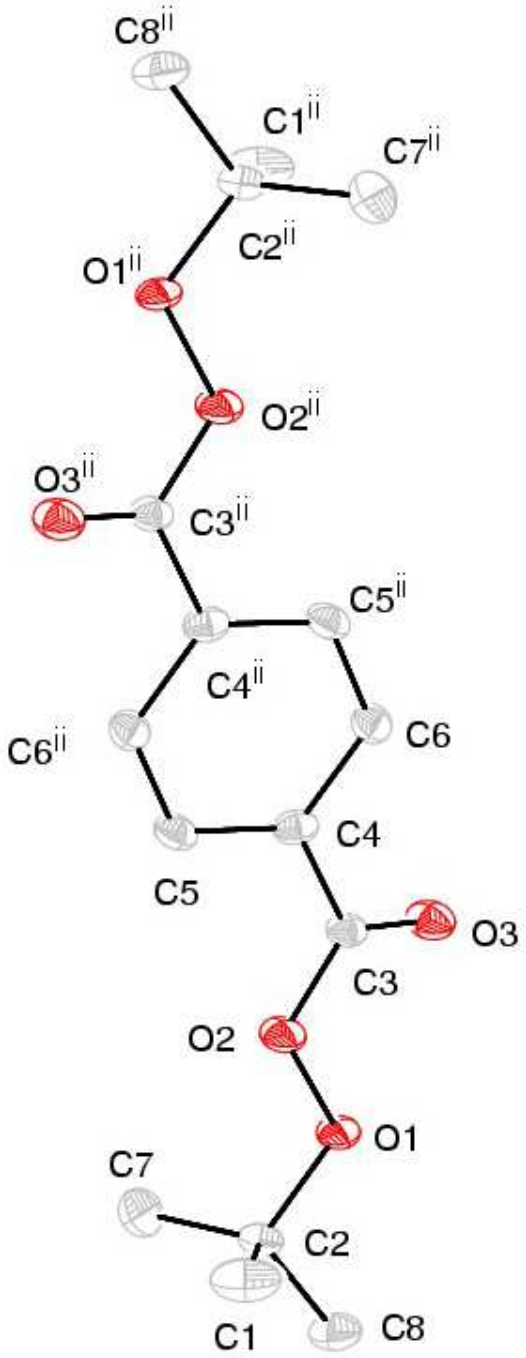

Figure 25. Perspective view of **16** with thermal ellipsoids at the 50% probability level.

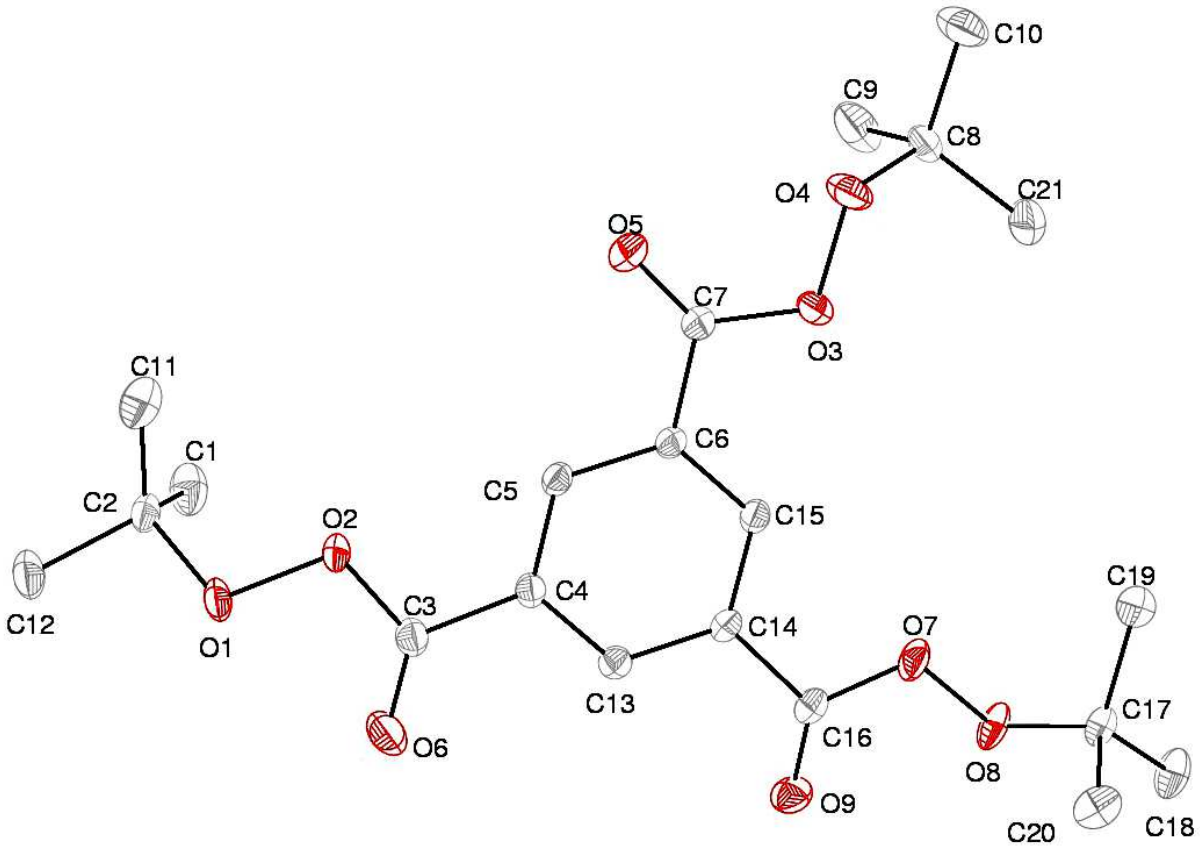

Figure 26. Perspective view of **17** with thermal ellipsoids at the 50% probability level.

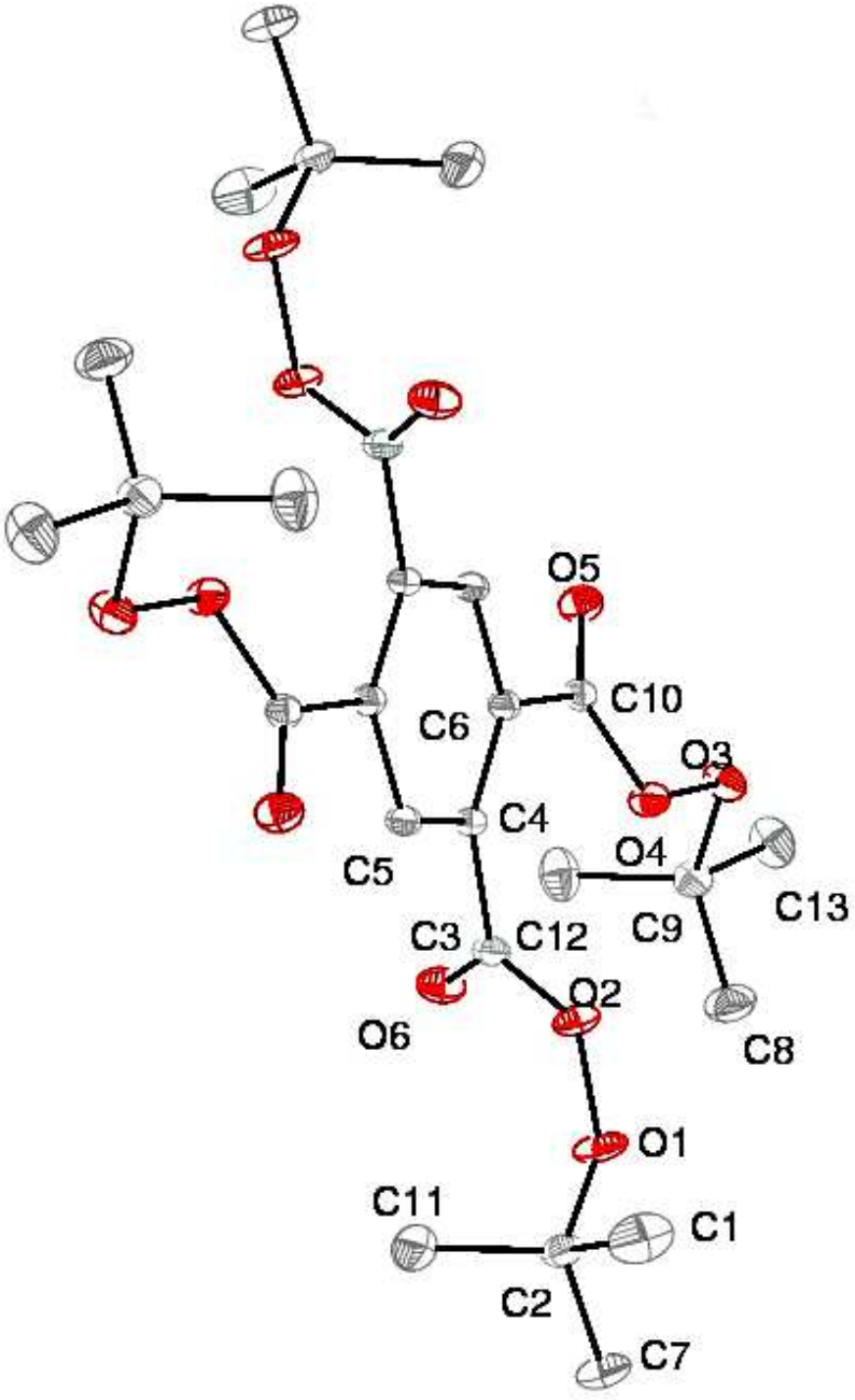

Figure 27. Perspective view of **18** with thermal ellipsoids at the 50% probability level.

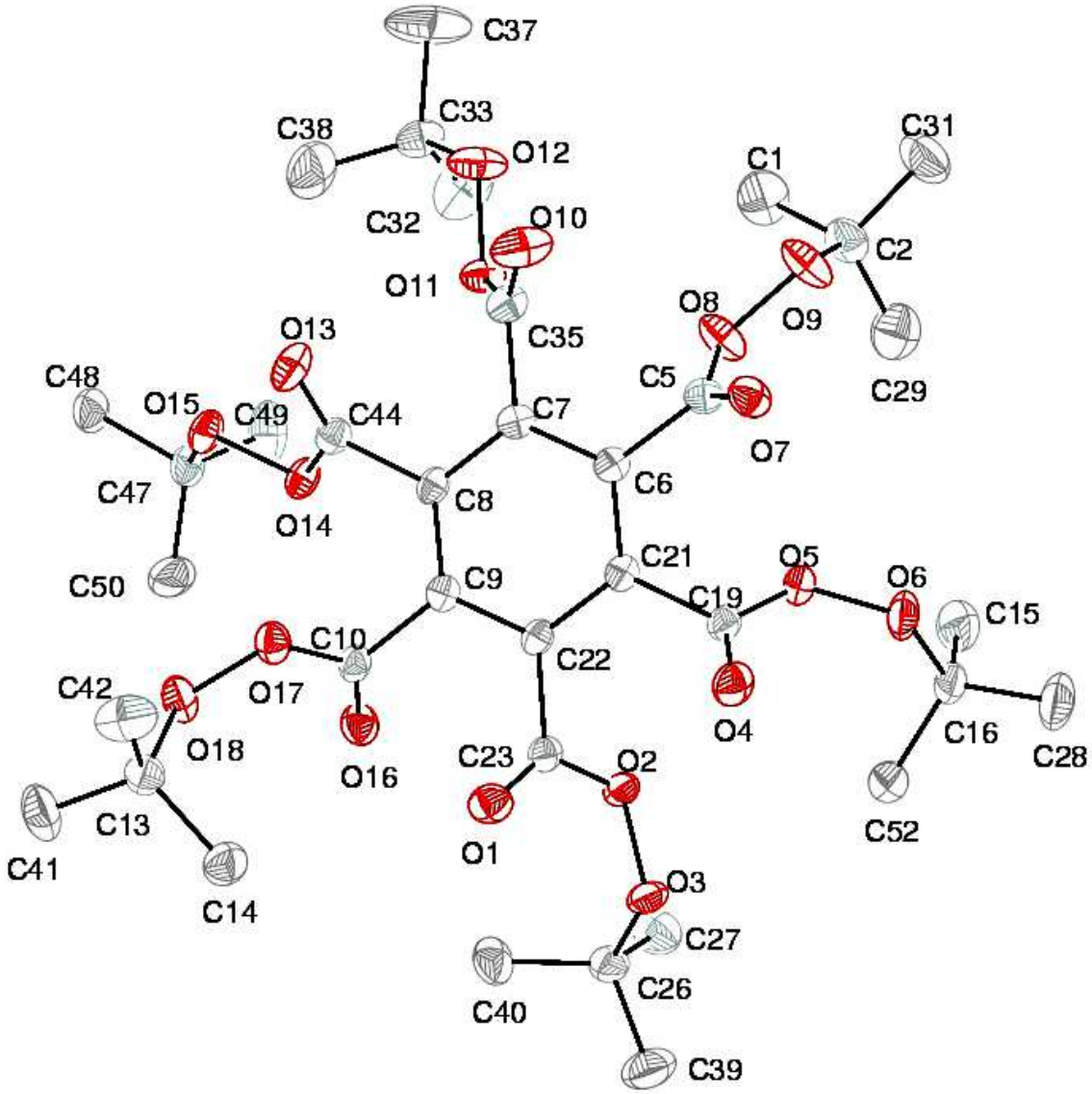

Figure 28. Perspective view of **19**·hexane with thermal ellipsoids at the 50% probability level.

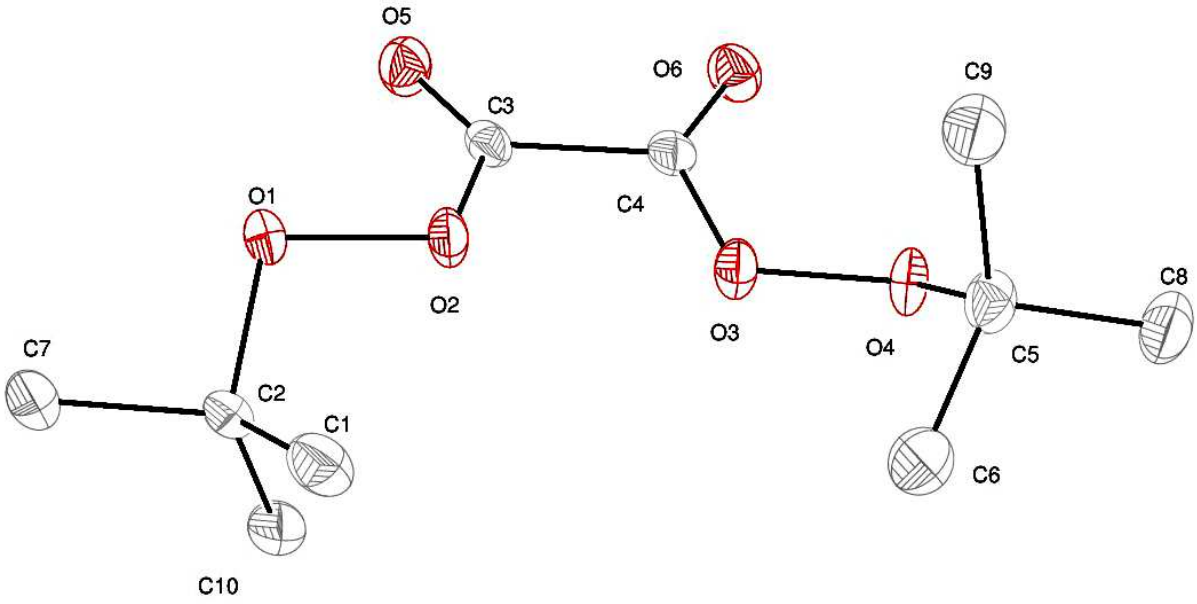

Figure 29. Perspective view of **20** with thermal ellipsoids at the 50% probability level.

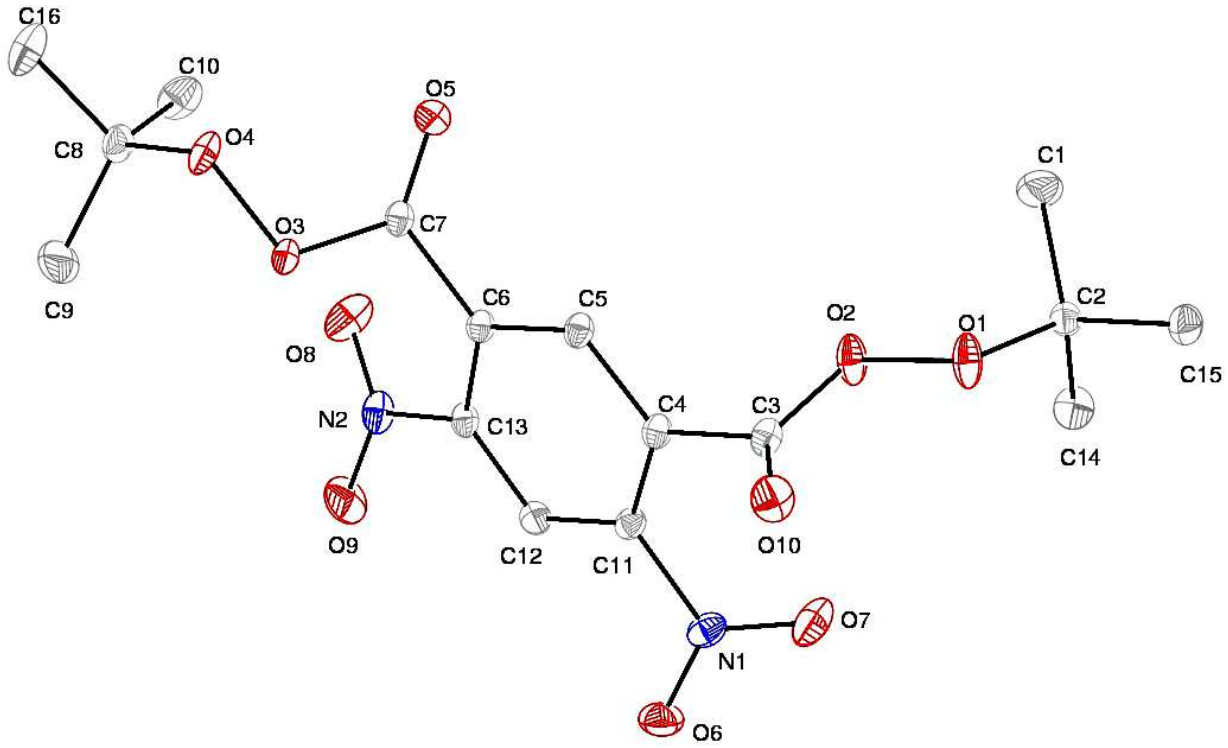

Figure 30. Perspective view of **21** with thermal ellipsoids at the 50% probability level.

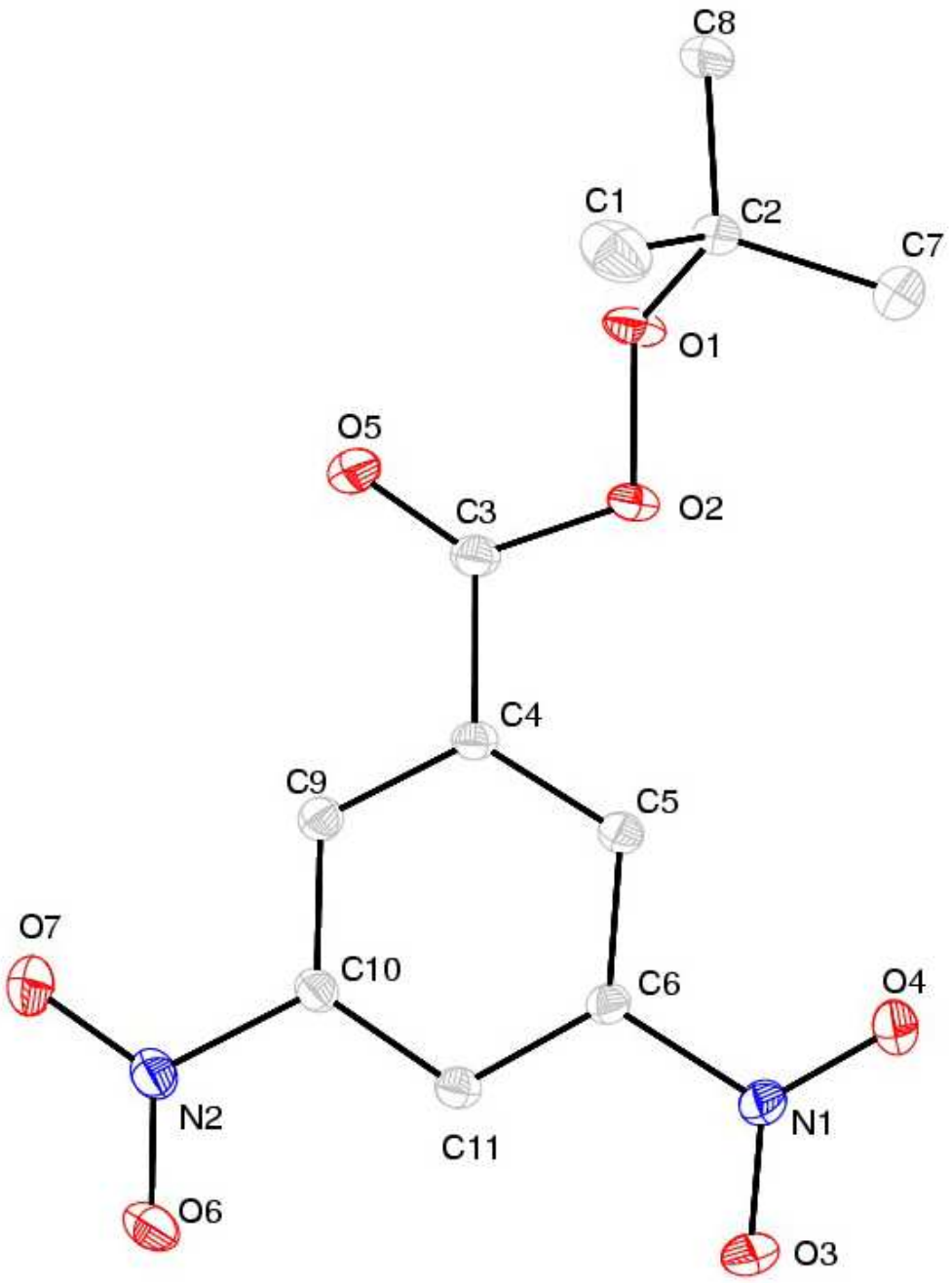

Figure 31. Perspective view of **21** with thermal ellipsoids at the 50% probability level.

Table 13. The O–O, C=O, and N–O bond lengths (Å) of **16**–**18**, **19**·hexane, and **20**–**22**.

Bond	16	17	18	19·hexane	20	21	22
O–O	1.466(3)	1.4655(8)	1.4667(9)	1.467(3)	1.4737(17)	1.4693(7)	1.4594(7)
		1.4599(8)	1.4649(9)	1.462(3)	1.4723(18)	1.4642(7)	
		1.4636(8)		1.468(3)			
				1.477(3)			
				1.476(3)			
				1.468(3)			
C=O	1.199(4)	1.1983(10)	1.1948(11)	1.185(4)	1.194(2)	1.1932(10)	1.1971(9)
		1.1938(10)	1.2000(11)	1.185(4)	1.186(2)	1.1908(9)	
		1.1986(10)		1.187(4)			
				1.192(4)			
				1.206(4)			
				1.189(4)			
N–O						1.2268(10)	1.2228(8)
						1.2249(9)	1.2273(8)
						1.2246(10)	1.2268(8)
						1.2219(10)	1.2206(9)

Table 14. The C(O)–O, C–O, and C–N bond lengths (Å) of **16**–**18**, **19**·hexane, and **20**–**22**.

Bond	16	17	18	19·hexane	20	21	22
C(O)–O	1.355(4)	1.3556(10)	1.3564(12)	1.356(4)	1.338(2)	1.3408(9)	1.3592(8)
		1.3548(9)	1.3552(10)	1.353(4)	1.347(2)	1.3559(8)	
		1.3579(10)		1.337(4)			
				1.348(4)			
				1.331(4)			
				1.359(4)			
C–O	1.458(4)	1.4580(10)	1.4624(11)	1.465(4)	1.473(2)	1.4538(9)	1.4610(9)
		1.4630(10)	1.4608(11)	1.470(4)	1.476(2)	1.4615(9)	
		1.4634(10)		1.456(4)			
				1.447(4)			
				1.446(4)			
				1.472(4)			
C–N						1.4688(9)	1.4732(9)
						1.4698(9)	1.4722(9)

Table 15. The list of short contacts of **16**, **17**, **18**, and **19**·hexane.

Compound	Number	Atom 1	Atom 2	Length (Å)	Length-VdW (Å)
16	1	O3	H9	2.626	–0.094
	2	O1	H20	2.693	–0.027
	3	H1	H12	2.334	–0.066
	4	O4	H21	2.685	–0.035
	5	C14	C15	3.365	–0.035
17	1	O8	C6	3.092	–0.128
	2	O9	C4	3.124	–0.096
	3	C3	H5	2.768	–0.132
	4	C16	C5	3.197	–0.203
	5	H28	O6	2.611	–0.109
	6	O5	H9	2.604	–0.116
18	1	O3	H38	2.679	–0.041
	2	O5	C21	2.953	–0.267
	3	C6	O12	3.053	–0.167
	4	C10	O12	2.98	–0.24
	5	C5	O10	3.199	–0.021
	6	C5	O12	3.107	–0.113
	7	H4	O10	2.461	–0.259
	8	H9	O10	2.591	–0.129
	9	O5	H29	2.537	–0.183
	10	O5	H31	2.584	–0.136
	11	H6	O7	2.662	–0.058
	12	O4	O6	2.982	–0.058
	13	O8	O10	2.911	–0.129
19·hexane	1	H1	O10	2.634	–0.086
	2	H32C	O10	2.674	–0.046
	3	H27A	O1	2.642	–0.078
	4	H34	O1	2.376	–0.344
	5	O16	H43	2.678	–0.042
	6	H13	H51	2.304	–0.096
	7	H64	H21	2.399	–0.001
	8	H66	H45	2.371	–0.029
	9	H6	O13	2.494	–0.226
	10	H62	O13	2.514	–0.206
	11	O4	H53	2.522	–0.198
	12	O11	O13	3.001	–0.039
	13	O5	O7	3.008	–0.032
	14	O4	O2	2.999	–0.041

Table 16. The list of short contacts of **20**.

Compound	Number	Atom 1	Atom 2	Length (Å)	Length-VdW (Å)
20	1	O3	C4	3.137	–0.083
	2	O4	C3	3.124	–0.096
	3	O4	C4	3.184	–0.036
	4	O5	H8	2.693	–0.027
	5	O1	C22	3.106	–0.114
	6	O1	C23	3.098	–0.122
	7	O2	C23	3.185	–0.035
	8	H1	O18	2.559	–0.161
	9	C3	O16	3.065	–0.155
	10	C3	O17	3.122	–0.098
	11	C4	O17	3.186	–0.034
	12	H3	O25	2.543	–0.177
	13	H10	O24	2.672	–0.048
	14	O6	H62	2.572	–0.148
	15	O9	C14	3.142	–0.078
	16	O10	C13	3.129	–0.091
	17	O10	C14	3.19	–0.03
	18	O13	H31	2.699	–0.021
	19	H33	O18	2.669	–0.051
	20	O11	H51	2.578	–0.142
	21	H24	O19	2.547	–0.173
	22	O7	C32	3.113	–0.107
	23	O7	C33	3.099	–0.121
	24	O8	C33	3.187	–0.033
	25	H41C	O24	2.563	–0.157
	26	C13	O22	3.064	–0.156
	27	C13	O23	3.123	–0.097
	28	C14	O23	3.184	–0.036
	29	O14	C22	3.093	–0.127
	30	O14	C23	3.148	–0.072
	31	O15	C22	3.118	–0.102
	32	O19	H36	2.678	–0.042
	33	O20	C32	3.088	–0.132
	34	O20	C33	3.149	–0.071
	35	O21	C32	3.113	–0.107
	36	H57	O25	2.681	–0.039

Table 17. The list of short contacts of **21** and **22**.

Compound	Number	Atom 1	Atom 2	Length (Å)	Length-VdW (Å)
21	1	O7	H1	2.655	–0.065
	2	C11	O5	3.044	–0.176
	3	C12	O5	3.155	–0.065
	4	O9	H14	2.506	–0.214
	5	O6	N1	2.923	–0.147
	6	O6	C11	3.072	–0.148
	7	O7	C12	3.215	–0.005
	8	C14	O8	3.148	–0.072
	9	O1	C5	3.207	–0.013
	10	O10	C3	3.175	–0.045
	11	O10	H4	2.566	–0.154
	12	C3	C3	3.392	–0.008
	13	O5	H13	2.574	–0.146
	14	O3	O8	2.843	–0.197
	15	O7	O10	2.985	–0.055
22	1	C9	O3	3.152	–0.068
	2	C9	N1	3.175	–0.075
	3	C10	O3	3.201	–0.019
	4	O5	H10	2.555	–0.165
	5	O7	H7	2.43	–0.29
	6	O6	C6	3.207	–0.013
	7	O6	C11	3.179	–0.041
	8	O1	N2	2.977	–0.093
	9	O1	C10	3.129	–0.091
	10	C3	C9	3.219	–0.181
	11	O4	H8	2.519	–0.201
	12	H5	H5	2.386	–0.014
	13	O3	O3	2.927	–0.113
	14	O3	H11	2.492	–0.228

The X-ray crystal structures of **16–22** lack strong hydrogen bonding interactions. All of the aromatic compounds **16–19**, **21**, and **22** contain various π-interactions, C–H···O hydrogen bonds (O···H: 2.430–2.693 Å), and O···O, N···O, C···H, and H···H short contacts that increase the molecular stability (Tables 15–17). The non-aromatic compound **20** contains only C–H···O hydrogen bonds (O···H: 2.543–2.693 Å) and C···O contacts (3.065–3.186 Å). π-Interactions of the aromatic *tert*-butyl peroxy esters include C–H···π (**16** and **19**), C_{π}···O (**17**, **18**, **21**, and **22**), C_{π}···C (**16**, **17**, and **22**), and C_{π}···N (**22**) interactions. Compound **16** contains C–H···π interactions that involve the methyl C–H bonds. There are C–H···π interactions in the crystalline lattice of **19** that involve the C–H bonds of hexane molecules trapped between molecules of **19**. The C_{π}···O, C_{π}···C, and C_{π}···N distances are in the range of 3.044–3.219 Å. They are caused by *tert*-butyl peroxy ester group-aromatic ring interactions of **17** (Figure 31), **18**, and **21**, and both *tert*-butyl peroxy ester group-aromatic ring and nitro group-aromatic ring interactions of **22** (Figure 32). There are two intramolecular O···O contacts (2.843 and 2.985 Å) in the crystal structure of **21** and one intermolecular O···O contact (2.927 Å) in the crystal structure of **22** (Figure 33). N···O short contacts are present in both **21** (2.977 Å) and **22** (2.923 Å). There are C···H short contacts (2.768 Å) in the crystal structure of **17**. Compounds **16**, **19**, and **22** contain H···H short contacts (2.304–2.399 Å).

The intermolecular interactions that involve the O–O bonds and the oxygen atoms of carbonyl groups assist in holding the atoms of the peroxy ester groups together. Also, the additional energy from impact or friction stimuli could be dissipated through the network of short contacts without breaking covalent bonds. Thus, these numerous stabilization interactions could lead to lower sensitivity materials. The number

of bulky *tert*-butyl peroxy ester groups increases from **16–19**, and thus, the O–O bonds become more hindered from the surrounding molecules. Compound **16** contains C–H···O hydrogen bonds that involve one oxygen atom of each of the two O–O bonds. In the crystal structure of **17**, one of the *tert*-butyl peroxy ester groups interacts with the aromatic ring of a neighboring molecule via C_{π}···O interactions and molecular stacks are formed. The O–O bonds of the two other *tert*-butyl peroxy ester groups of **17** are not involved in intermolecular interactions although oxygen atoms of their carbonyl groups form O···H–C interactions. All four O–O bonds of **18** are involved in forming intermolecular interactions. Two *tert*-butyl peroxy ester groups of **18** have multiple C_{π}···O interactions with two neighboring aromatic rings, forming stacks. The other two *tert*-butyl peroxy ester groups of **18** contain C–H···O hydrogen bonding interactions that involve one oxygen atom of each of the O–O bonds. Compound **19** contains six *tert*-butyl peroxy ester groups and none of the O–O bonds are involved in intermolecular interactions due to the crowding of the *tert*-butyl groups, which can lead to high sensitivities. However, all of the oxygen atoms of the carbonyl groups form O···H–C interactions. In the X-ray crystal structures of **21** and **22**, there are additional stabilizing interactions in the crystalline lattice from the nitro groups. There are C_{π}···O and N···O intermolecular interactions and an intramolecular O···O contact (**21**) that are involved in reducing the high activity of O–O bonds in the crystalline lattice. The oxygen atoms of the carbonyl groups of **21** and **22** form C_{π}···O, C···O, and C–H···O interactions and one intramolecular O···O contact (**21**).

The non-aromatic *tert*-butyl peroxy ester **20** contain multiple C···O contacts that involve only one of the two O–O bonds. There are multiple C–H···O interactions that

involve the oxygen atoms of the carbonyl groups. Still, there are large voids (4.912 and 7.651 Å) among the molecules of **20** in the crystalline lattice (Figure 34) that can increase the sensitivities of **20**.

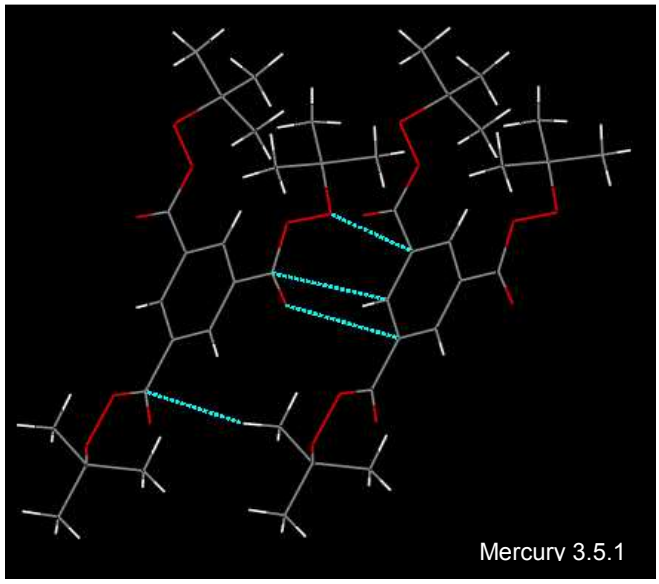

Figure 32. *tert*-Butyl peroxy ester group-aromatic ring interactions (blue) of **17**.

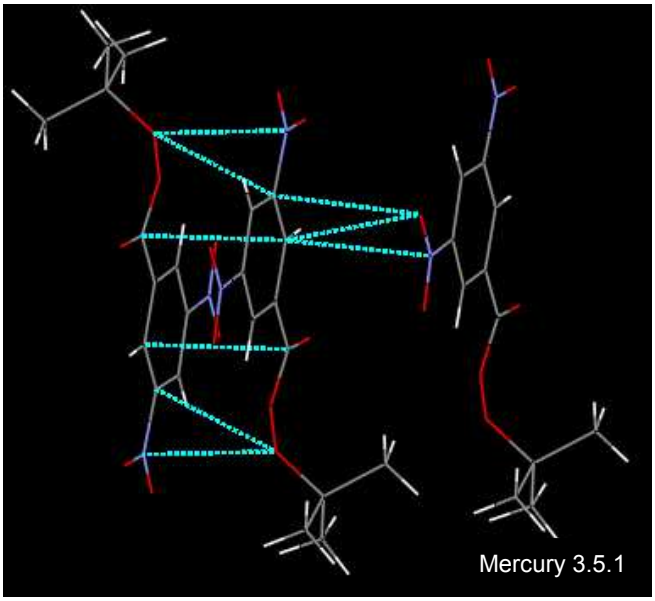

Figure 33. *tert*-Butyl peroxy ester group-aromatic ring and nitro group-aromatic ring interactions (blue) of **22**.

Figure 34. Intra- and intermolecular O···O contacts (blue) of **21** (left) and **22** (right).

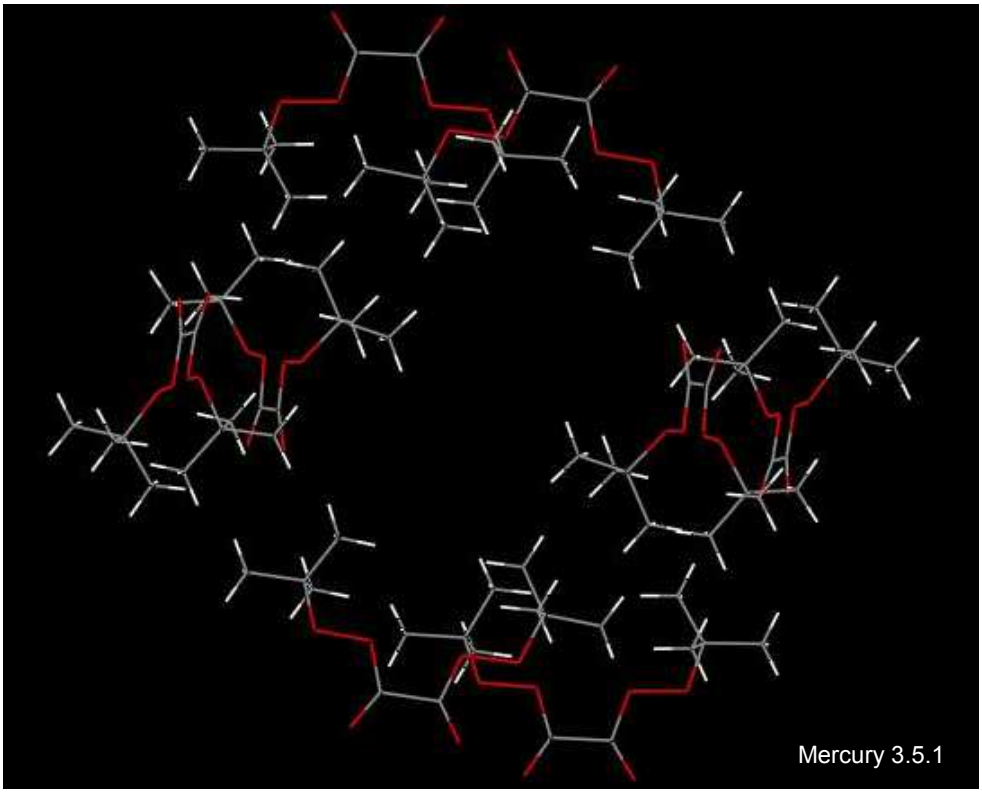

Figure 35. Large voids (4.912 and 7.651 Å) among the molecules of **20**.

3.2.4 Thermal Stability

Thermal stabilities of *tert*-butyl peroxy esters **16**–**22** were assessed using thermogravimetry (TGA/DTA). The decomposition temperatures (T_{Dec}) were obtained from the thermograms of **16**–**22**. CBS-4M electronic enthalpies were calculated using the Gaussian09 software to obtain heats of formation values ($\Delta_f H°$) by our collaborators from the Klapötke lab.[113] The T_{Dec} and $\Delta_f H°$ values are provided in Table 18.

Table 18. Decomposition temperatures and heats of formation values of **16**–**22**.

Compound	T_{Dec} (°C)	$\Delta_f H°$ (kJ/mol)
16	122	–820.7
17	123	–1211.3
18	123	–1584.7
19	86	< –1584.7[a]
20	53	–811.4
21	95	–790.0
22	121	–436.9

[a]Estimated value based on the trend of **16**–**18**.

Except for **20**, the rest of the aromatic *tert*-butyl peroxy esters **16**–**19**, **21**, and **22** are fairly thermally stable compounds with T_{Dec} values ranging from 86–123 °C (Table 18). Compound **20** has a very low T_{Dec} making it unsuitable for HEDM applications. The $\Delta_f H°$ values are all exothermic ranging from –1584.7 to –436.9 kJ/mol and relatively more positive heats of formation values were obtained for nitro-substituted aromatic compounds **21** and **22**. More positive $\Delta_f H°$ values are desirable for HEDMs since they render more energetic molecules. The $\Delta_f H°$ values decrease with the increasing number of *tert*-butyl peroxy ester groups on the phenyl rings from **16**–**18,** which indicates that

increasing the number of *tert*-butyl peroxy ester groups result in less energetic molecules. Unfortunately, the $\Delta_f H°$ calculation of **19** was not possible due to software issues with this compound. However, based on the decreasing trend of heats of formation values from **16**–**19**, the heat of formation value for compound **19** should be below –1584.7 kJ/mol.

3.2.5 Preliminary Qualitative Sensitivity Tests

Sensitivities of *tert*-butyl peroxy esters **16**–**22** were studied using the flame, hammer, sand paper, and electrostatic discharge (Tesla coil) tests. Surprisingly, **17**–**21** were sensitive and energetic compounds based on the flame and Tesla coil tests (Table 19) regardless of the low oxygen and nitrogen contents. No responses were observed for **16**–**22** in the hammer impact and sand paper friction tests.

Table 19. Flame and Tesla coil test results for **16**–**22**.

Compound	Flame Test Response	Tesla coil test response
16	Bright flame	No response
17	Sudden, bright flame with smoke and soot	Flame popped out
18	Sudden, bright flame with smoke and soot	No response
19	Sudden, large, bright flame with smoke	Flame popped out
20	Sudden, large, bright flame	Flame popped out
21	Sudden, large, bright flame with soot	Flame popped out
22	Bright flame	No response

Based on the preliminary sensitivity tests, an O:C ratio of 0.43 (**17**) was sufficient to provide observable sensitivity responses. The high sensitivities of **17**–**21** may be a result of high oxygen contents in the cores of these molecules. Since the carbon content

is high, smoke and/or soot were observed in the flame tests of **17**–**19** and **21**, indicating that they were not completely oxidized. Compound **20** was the most sensitive *tert*-butyl peroxy ester in the study and provided the most sensitive test responses. The sensitivities of **19** were the highest from aromatic *tert*-butyl peroxy esters **16**–**19**, which can be attributed to the O–O trigger bonds that are not involved in any intermolecular interactions in the crystal structure. Compound **22** was not high in sensitivity based on the preliminary sensitivity tests. The low sensitivity of **22** can be attributed to the additional stabilizing intermolecular interactions in the crystalline lattice due to the presence of nitro groups with only one *tert*-butyl peroxy ester group.

3.2.6 Standard Sensitivity Tests

Impact, friction, and electrostatic discharge sensitivities of **16**–**22** were determined with a BAM drop hammer, BAM friction tester, and an electrostatic spark sensitivity tester using standard experimental methods by our collaborators in the Klapötke lab.[29–34] Table 20 includes the impact, friction, and electrostatic discharge sensitivities of **16**–**22**. Based on the "UN Recommendations on the Transport of Dangerous Goods",[28] **16** is "less sensitive", **17**, **18**, and **22** are "sensitive", and **19**–**21** are "very sensitive" towards impact. Compounds **16** and **22** are "less sensitive", **17** and **21** are "sensitive", **18** is "very sensitive", **19** should be "very sensitive", and **20** is "extremely sensitive" towards friction. The peroxy esters **16**–**22** are much lower in sensitivity than TATP, DADP, HMTD, and MEKP (Tables 3–6).

The aromatic peroxy esters **17**–**19**, **21**, and **22** show low sensitivities to both impact and friction. These sensitivities are among the lowest reported impact and friction sensitivities for peroxo-based compounds. The impact and friction sensitivities increase

with the number of *tert*-butyl peroxy ester groups from **16**–**18**. Thus, although the sensitivity measurements were not obtained due to the difficulty in scaling up, the impact and friction sensitivities of **19** can be predicted to be greater than **18**. The high sensitivities of **19** were also observed in preliminary sensitivity tests. The non-aromatic peroxy ester **20** shows the highest sensitivities towards impact, friction, and electrostatic discharge. Large voids in the crystal structure of **20** might be the cause of these high sensitivities. The aromatic *tert*-butyl peroxy esters **16**–**19**, **21**, and **22** show electrostatic discharge sensitivity values that are higher than the electrical discharges that can be created by the human body (≤ 0.02 J)[2] and they can be safely handled. Unfortunately, the electrostatic discharge sensitivity of **20** is too high for practical use.

Table 20. Impact, friction, and electrostatic discharge sensitivities of **16**–**22**.

Compound	IS (J)	FS (N)	ESDS (J)
16	40	360	0.7
17	20	240	0.5
18	2	60	0.7
19	< 2[a]	< 60[a]	0.1
20	1	< 5	0.015
21	5	96	0.4
22	10	360	0.5

[a]Estimated values based on the trends of compounds **16**–**18**.

3.2.7 Energetic Performance Calculations

The energetic properties of **16**–**22** were calculated using the EXPLO5 V6.02 software (Table 21) by our collaborators in the Klapötke lab.[114] These calculated V_{Det} and P_{Det} values of **16**–**22** are in the range of 4896–6003 m/s and 60–118 kbar,

respectively. They are moderate to high detonation performances, which are useful for HEDMs.

The moderate V_{Det} values of **16**–**18** can be attributed to the high negative oxygen balance values in the range of –190.75 to –173.98 and the low crystalline densities 1.214–1.255 g/cm^3. These calculated V_{Det} values decrease with the increasing number of *tert*-butyl peroxy ester groups on the phenyl rings from **16**–**18**. The reduction of crystalline density from **16**–**18** has caused the detonation velocities to decrease, although the O:C ratio increases from 0.43–0.50 for **16**–**18**. Thus, we can predict the detonation velocity of **19** with a lower crystalline density to be < 4896 m/s.

The calculated detonation velocities of **20**–**22** are in the range of 5361–6003 m/s, which are greater than the detonation velocities of the known peroxide explosives TATP, DADP, HMTD, and MEKP (4,511–5,300 m/s). The non-aromatic compound **20** has larger values for total energy of detonation ($\Delta_{Ex}U$) and V_0 than **16**–**18,** and thus, a higher detonation velocity was observed than **16**–**18** with similar crystalline densities. The highest detonation velocities were obtained with the nitro-substituted aromatic peroxy esters **21** and **22** with the highest crystalline densities (1.431 and 1.487 g/cm^3). These impressively high detonation velocities (5764 and 6003 m/s) are surprising with the low oxygen and nitrogen contents of the *tert*-butyl peroxy esters **21** and **22**.

Table 21. Calculated energetic properties of **16**–**22**.

Property	16	17	18	19	20	21	22
Formula	$C_{16}H_{22}O_6$	$C_{21}H_{30}O_9$	$C_{26}H_{38}O_{12}$	$C_{36}H_{54}O_{18}$	$C_{10}H_{18}O_6$	$C_{11}H_{12}N_2O_7$	$C_{11}H_{12}N_2O_7$
FW (g/mol)	310.28	390.48	542.57	774.33	234.28	400.34	284.06
Ω[a] (%)	–190.75	–180.08	–173.98	–167.37	–157.10	–127.89	–118.21
ρ[b] (g/cm^3)	1.255	1.223	1.214	1.161	1.233	1.431	1.487
ρ[c] (g/cm^3)	1.231	1.200	1.192	1.140[d]	1.210	1.205	1.460
EXPLO5 V6.02							
$\Delta_{Ex}U°$ (kJ/kg)	–2589	–2726	–2836	< –2836[e]	–3124	–3950	–4099
P_{Det} (kbar)	63	60	61	< 60[e]	75	104	118
V_{Det} (m/s)	5083	4906	4896	< 4896[e]	5361	5764	6003
V_o (L/kg)	707	731	745	> 745[e]	836	699	670

[a]Oxygen balance for oxidation of carbon to CO_2
[b]Crystalline density at 100 K
[c]Crystalline densities at 298 K (for energetic calculations)
$\rho_{298K} = \rho_T / [1 + \alpha_v (298 - T)]$ (T = 100 K, ρ_T = Desnsity at 100 K, α_v = 1.5 x 10^{-4} K^{-1})
[d]Solvent free estimated crystalline density at 298 K (for energetic calculations)
[e]Estimated values based on the trends of **16**–**18**

3.3 Conclusions

tert-Butyl peroxy esters **16**–**22** were synthesized in moderate to high yields and were completely characterized. Sensitivities and energetic performances of **16**–**22** were studied for their use as HEDMs. *tert*-Butyl peroxy esters **16**–**22** are all surprisingly energetic even though the oxygen and nitrogen contents are low. This might be a result of the instability with the high O:C ratios in the central cores of these molecules (0.75–3.00). *tert*-Butyl peroxy esters **16**–**22** have moderate to high detonation velocities, which are useful for HEDM applications.

The aromatic *tert*-butyl peroxy esters **16**–**18**, **21**, and **22** are much lower in impact and friction sensitivities with respect to the extremely sensitive known peroxo-based explosives TATP, DADP, MEKP, and HMTD. These aromatic peroxy esters **18**, **21**, and **22** show the lowest reported impact and friction sensitivities for peroxo-based compounds to date. Thus, they can be safely handled in industry. Compounds **16**–**19** could potentially be good initiators of radical polymerization due to the ability to provide higher concentrations of radicals than *tert*-butyl benzoperoxoate, which is currently employed as a radical initiator. Compound **19** is the first reported aryl hexaperoxy ester of mellitic acid. It could potentially be an excellent initiator of radical polymerization with the ability to provide the highest concentration of radicals. Compound **20** has the highest core O:C ratio (3.00), but based on the thermal stability and sensitivity measurements, it is evident that **20** is a thermally unstable and highly sensitive compound that is not useful for HEDM applications.

The calculated detonation velocities of compounds **20**–**22** (5361–6003 m/s) surpass the detonation velocities of the known peroxide explosives TATP, DADP, MEKP, and HMTD (4,511–5,300 m/s). The highest detonation velocities were obtained for the nitro-substituted aromatic *tert*-butyl peroxy esters **21** and **22** due to their high crystalline densities. With their very low impact and friction sensitivities, they could be useful as secondary explosives. Compounds **21** and **22** are among the first highly energetic and low sensitivity peroxo-based compounds that can be categorized as secondary HEDMs.

3.4 Experimental Section

General Considerations: All manipulations during the reactions and filtrations through Celite on coarse glass frits were carried out under an argon atmosphere using either Schlenk line or glove box techniques. Diethyl ether was distilled in the presence of sodium benzophenone ketyl. Hexane was distilled in the presence of P_2O_5. Dichloromethane was distilled in the presence of calcium hydride. Chemicals were purchased from Sigma-Aldrich, Acros Organics, or Alfa Aesar and were used without further purification. ACS grade solvents were obtained from EMD and Fisher Scientific. Petroleum ether used in the synthetic protocols had a boiling point range of 35–60 °C.

Synthesis of benzene-1,2,4,5-tetracarbonyl tetrachloride (for the synthesis of **18**) was carried out using a published procedure.[111a] Synthesis of benzene-1,2,3,4,5,6-hexacarbonyl hexachloride was carried out using a slightly modified published procedure.[111b] Instead of the 24 h reaction time in the published procedure, a reaction time of 7 h was sufficient for the completion of the reaction

(for complete dissolution of 4.9 g of mellitic acid in thionyl chloride). Compound **20** was synthesized by a procedure based on published procedures.[112] Syntheses of 1,5-dimethyl-2,4-dinitrobenzene, 4,6-dinitroisophthalic acid, and 4,6-dinitroisophthaloyl dichloride (for the synthesis of **21**) were carried out using the published procedures.[111c]

Silica gel 60, 230–400 mesh (EMD Chemicals) was used to perform silica gel column chromatography.[104] ASTM TLC plates precoated with silica gel 60 F_{254} (250 μm thickness) were used for thin-layer chromatography (TLC). TLC spots were observed using a UV lamp and/or a potassium permanganate solution as a stain (3 g $KMnO_4$, 20 g K_2CO_3, 5 mL 5% w/v aqueous NaOH, 300 mL H_2O). The spots on the stained TLC plates were visualized after heating with a heat gun.

^1H and $^{13}C\{^1H\}$ NMR spectra were obtained at 400 MHz and 101 MHz, respectively, in $CDCl_3$ and CD_3OD as indicated and were referenced to the residual proton and carbon resonances of the solvent ($CDCl_3$: ^1H δ 7.27, ^{13}C 77.23; CD_3OD: ^1H δ 3.31, ^{13}C 49.00). Mass spectra were obtained on an electrospray time-of-flight high-resolution Waters Micromass LCT Premier XE mass spectrometer. Infrared spectra were obtained from a Shimadzu MIRacle 10 IRAffinity-1 equipped with a single reflection ATR accessory. Melting points were determined on an Electrothermal IA 9300 melting point apparatus and are uncorrected. Thermogravimetric (TGA/DTA) measurements to determine the decomposition temperatures of compounds **16–22** were performed at a heating rate of 5 °C min^{-1} with an OZM Research DTA 552-Ex instrument.

Qualitative Sensitivity Tests: Qualitative sensitivity tests include burning about 3-5 mg of the compound in the Bunsen burner flame, striking 3-5 mg of the compound on a metal plate with a hammer, and passing an electrostatic discharge through 3-5 mg of the compound on a metal plate using an Electro Technic BD 10 Tesla coil (120 V, 0.35 A).

Quantitative Sensitivity Tests: Quantitative sensitivity Tests include BAM drop hammer[31] impact tests carried out according to STANAG 4489[29] modified instructions[30] using approximately 0.4 mL of the compound, Friction tests with a BAM friction tester carried out according to STANAG 4487[32] modified instructions[33] using approximately 5 mg of the compound, and electrostatic spark tests with an ESD 2010 EN, OZM Electric Spark Tester according to STANAG 4515[34] instructions using 0.1 mL of the compound performed by the Klapötke group.

Preparation of Di-*tert*-butyl benzene-1,4-bis(carboperoxoate) (16). To a solution of anhydrous pyridine (0.13 mL, 3.0 mmol) and 5.5 M tBuOOH in decane (0.60 mL, 3.0 mmol) in a 100 mL Schlenk flask, which was kept at –4 °C (ice-water-salt bath), a solution of terephthaloyl chloride (0.305 g, 1.50 mmol) in anhydrous pentane (25 mL) was added dropwise with a cannula over a period of 15 min. Then, the reaction was stirred for about 15 min at –4 °C. Afterwards, the reaction was allowed to warm up to room temperature (23 °C) and was filtered through a 1.5 cm pad of Celite on a coarse glass frit. Then, the solvent was removed under reduced pressure to obtain 0.350 g (75%) of crude **16** as a white solid. Recrystallization in 1:1 hexanes:dichloromethane by slow evaporation resulted in 0.280 g (60%) of colorless, square-shaped crystals of **16**:

mp 116–118 °C; IR (ν cm^{-1}): 2982 (m), 2935 (w), 2902 (w), 2873 (w), 1753 (s), 1692 (m), 1527 (w), 1501 (w), 1455 (w), 1404 (m), 1387 (w), 1366 (m), 1295 (w), 1263 (m), 1233 (s), 1186 (s), 1117 (w), 1069 (s), 1011(s), 901 (w), 872 (m), 851 (m), 820 (m), 799 (m), 744 (w), 721 (s); ^{1}H NMR (400 MHz, $CDCl_3$, 23 °C, δ): 8.04 (s, 4H, C*H*), 1.42 (s, 18H, C*H*$_3$); ^{13}C{^{1}H} NMR (101 MHz, $CDCl_3$, 23 °C, ppm): 163.56 (*C*), 132.13 (*C*), 129.56 (*C*H), 84.62 (*C*), 26.43 (*C*H$_3$); Anal. Calcd for $C_{16}H_{22}O_6$: C, 61.92; H, 7.15. Found: C, 61.75; H, 7.09. X-ray quality colorless, square-shaped single crystals were grown by slow evaporation in diethyl ether.

Preparation of Tri-*tert*-butyl benzene-1,3,5-tris(carboxyloperoxoate) (17). To a solution of anhydrous pyridine (0.13 mL, 3.0 mmol) and 5.5 M tBuOOH in decane (1.0 mL, 5.0 mmol) in a 100 mL Schlenk flask, which was kept at –4 °C (ice-water-salt bath), a solution of benzene-1,3,5-tricarbonyl trichloride (0.270 g, 1.00 mmol) in anhydrous pentane (10 mL) was added slowly with a cannula over a period of 5 min. Then, the reaction was stirred for about 1 h while allowing it to warm up to 10 °C. Afterwards, the reaction was allowed to warm up to room temperature (23 °C) and it was filtered through a 1.5 cm pad of Celite on a coarse glass frit. Then, the solvent was removed under reduced pressure to obtain 0.328 g (77%) of **17** as a white solid. Recrystallization in 1:1 petroleum ether:diethyl ether by slow evaporation resulted in 0.272 g (64%) of **17** as colorless, thin, long, plate-like single crystals: mp 112–114 °C; IR (ν cm^{-1}): 2980 (m), 2936 (w), 2872 (w), 1753 (s), 1701 (m), 1631 (w), 1526 (m), 1495 (w), 1458 (w), 1391 (m), 1366 (m), 1315 (m), 1260 (m), 1173 (s), 1103 (s), 1022 (w), 922 (m), 881 (m), 845 (s), 802 (m), 764 (m), 719 (s); ^{1}H NMR (400 MHz, CD_3OD, 23 °C, δ): 8.65 (s, 3H, C*H*), 1.43 (s, 27H, C*H*$_3$); ^{13}C{^{1}H} NMR (101 MHz, CD_3OD, 23 °C, ppm): 163.68 (*C*), 134.52

(*C*H), 130.72 (*C*), 85.92 (*C*), 26.37 (*C*H_3); Anal. Calcd for $C_{21}H_{30}O_9$: C, 59.15; H, 7.09. Found: C, 58.90; H, 7.16.

Preparation of Tetra-*tert*-butyl benzene-1,2,4,5-tetrakis(carboxyloperoxoate) (18). To a solution of anhydrous pyridine (0.20 mL, 4.7 mmol) and 5.5 M tBuOOH in decane (1.6 mL, 7.9 mmol) in a 100 mL Schlenk flask, which was kept at –4 °C (ice-water-salt bath), a solution of benzene-1,2,4,5-tetracarbonyl tetrachloride (0.387 g, 1.18 mmol) in distilled dichloromethane (10 mL) was added slowly with a cannula over a period of 5 min. Then, the reaction was stirred for about 1 h while allowing it to warm up to 10 °C. Afterwards, the reaction was allowed to warm up to room temperature (23 °C) and it was filtered through a 1.5 cm pad of Celite on a coarse glass frit. Then, the filtrate was concentrated and the product was purified by silica gel column chromatography with 10:1 dichloromethane:ethyl acetate to obtain 0.269 g (42%) of **18** as a white solid. Recrystallization in 10:1 diethyl ether:tetrahydrofuran by slow evaporation resulted in 0.163 g (25%) of colorless, thick, hexagonal single crystals of **18**: mp 113–115 °C; IR (ν cm^{-1}): 2984 (m), 2934 (w), 2870 (w), 1771 (s), 1759 (s), 1651 (w), 1541 (w), 1366 (m), 1294 (m), 1240 (m), 1209 (m), 1184 (s), 1096 (s), 1061 (s), 1028 (m), 926 (m), 890 (w), 835 (m), 814 (m), 773 (w), 748 (m), 719 (m); ^{1}H NMR (400 MHz, $CDCl_3$, 23 °C, δ): 8.04–8.01 (m, 2H, C*H*), 1.42–1.32 (m, 36H, C*H*$_3$); ^{13}C{^{1}H} NMR (101 MHz, $CDCl_3$, 23 °C, ppm): 162.82 (*C*), 132.52 (*C*), 130.51 (*C*H), 85.29 (*C*), 26.34 (*C*H_3); ESI-HRMS: calcd for $[C_{26}H_{38}O_{12}Na]^+$ 565.2261; found 565.2250. Anal. Calcd for $C_{26}H_{38}O_{12}$: C, 57.56; H, 7.06. Found: C, 57.19; H, 7.07.

Preparation of Hexa-*tert*-butyl benzene-1,2,3,4,5,6-hexakis(carboxyloperoxoate) (19). To a solution of anhydrous pyridine (0.075 mL,

1.75 mmol) and 5.5 M tBuOOH in decane (0.6 mL, 3.0 mmol) in a 100 mL Schlenk flask, which was kept at –4 °C (ice-water-salt bath), a solution of benzene-1,2,3,4,5,6-hexacarbonyl hexachloride (0.113 g, 0.25 mmol) in distilled dichloromethane (10 mL) was slowly added with a cannula. Then, the reaction was stirred for about 2 h while allowing it to warm up to room temperature (23 °C). The reaction was concentrated and the product was purified by silica gel column chromatography with CH_2Cl_2 to obtain 0.070 g (36%) of **19** as a white solid. Recrystallization in 1:1 dichloromethane:hexanes at –29 °C resulted in 0.057 g (29%) of colorless, thick, polygonal single crystals of **19**: mp 85 °C dec. before melting; IR (ν cm^{-1}): 2982 (m), 2932 (w), 2870 (w), 1775 (s), 1462 (w), 1412 (w), 1393 (w), 1368 (m), 1327 (w), 1298 (w), 1263 (w), 1248 (w), 1140 (s), 1109 (m), 1076 (m), 1032(m), 970 (m), 922 (w), 868 (w), 835 (m), 804 (w), 739 (w), 727 (w); ^{1}H NMR (400 MHz, $CDCl_3$, 23 °C, δ): 1.37 (s, 54H, C*H*$_3$); ^{13}C{^{1}H} NMR (101 MHz, $CDCl_3$, 23 °C, ppm): 161.12 (*C*), 133.10 (*C*), 85.69 (*C*), 26.46 (*C*H_3); ESI-HRMS: calcd for $[C_{36}H_{54}O_{18}Na]^+$ 797.3208; found 797.3225.

Preparation of Di-*tert*-butyl ethanebis(peroxoate) (20). To a solution of anhydrous pyridine (0.5 mL, 6 mmol) and 5.5 M tBuOOH in decane (1.10 mL, 6 mmol), which was kept at –4 °C (ice-water-salt bath), a solution of oxalyl chloride (0.25 mL, 3 mmol) in anhydrous pentane (5 mL) was added dropwise with a cannula over a period of 15 min. Since stirring ceased, more anhydrous pentane (5 mL) was added to the reaction. Then, the reaction was allowed to warm up in a water bath for about 10 minutes. Afterwards, it was filtered through a 1.5 cm pad of Celite on a coarse glass frit. This filtrate was cooled to –78 °C for about 15 min. in a dry ice-acetone bath to obtain a fine white crystalline solid that was separated from the solution. The fine white crystals

dissolved at room temperature. Repeated recrystallization in pentane –29 °C was carried out to obtain 0.316 g (45%) of **20** as colorless, thick, long, needle-like single crystals: mp 49–51 °C; IR (ν cm^{-1}): 2984 (m), 2938 (w), 2876 (s), 1805 (s), 1744 (m), 1653 (w), 1466 (w), 1369 (m), 1252 (m), 1204 (s), 1182 (s), 1121 (s), 1034(m), 930 (w), 889 (m), 831 (m), 789 (w), 743 (w); ^{1}H NMR (400 MHz, $CDCl_3$, 23 °C, δ): 1.37 (s, 18H, C*H*$_3$); $^{13}C\{^{1}H\}$ NMR (400 MHz, $CDCl_3$, 23 °C, ppm): 154.36 (*C*, delay time had to be increased to observe this peak; d1 = 5 s), 86.07 (*C*), 26.20 (*C*H_3); Anal. Calcd for $C_{10}H_{18}O_6$: C, 51.27; H, 7.75. Found: C, 51.22; H, 7.70.

Preparation of Di-*tert*-butyl 4,6-dinitrobenzene-1,3-bis(carboperoxoate) (21). To a solution of anhydrous pyridine (0.065 mL, 1.50 mmol) and 5.5 M tBuOOH in decane (0.30 mL, 1.5 mmol) in a 100 mL Schlenk flask, which was kept at –4 °C (ice-water-salt bath), a solution of 4,6-dinitroisophthaloyl dichloride (0.220 g, 0.75 mmol) in distilled dichloromethane (10 mL) was slowly added with a cannula. Then, the reaction was stirred for about 1 h while allowing it to warm up to 10 °C. The reaction was concentrated and the product was purified by silica gel column chromatography with 9:1 hexanes:ethyl acetate to obtain 0.223 g (74%) of **21** as a white solid. Recrystallization in toluene by slow evaporation resulted in 0.195 g (65%) of colorless, thick, needle-like single crystals of **21**: mp 95 °C dec. before melting; IR (ν cm^{-1}): 3117 (w), 3042 (w), 2984 (m), 2936 (w), 2874 (w), 1775 (s), 1697 (w), 1605 (m), 1531 (s), 1474 (w), 1456 (w), 1389 (w), 1368 (m), 1348 (s), 1295 (w), 1312 (w), 1261 (m), 1248 (w), 1200 (m), 1182 (s), 1136 (w), 1011(s), 1078 (m), 1032 (w), 968 (m), 926 (m), 899 (w), 876 (m), 835 (m), 818 (m), 773 (w), 758 (m), 746 (w), 719 (m); ^{1}H NMR (400 MHz, $CDCl_3$, 23 °C, δ): 8.72 (s, 1H, C*H*), 7.98 (s, 1H, C*H*), 1.37 (s, 18H, C*H*$_3$); $^{13}C\{^{1}H\}$ NMR (101 MHz,

$CDCl_3$, 23 °C, ppm): 161.03 (C), 148.43 (C), 132.15 (*CH*), 130.14 (*C*), 120.96 (*C*H), 86.18 (*C*), 26.29 (*C*H_3); Anal. Calcd for $C_{16}H_{20}N_2O_{10}$: C, 48.00; N, 7.00; H, 5.04. Found: C, 47.71; N, 6.97; H, 5.65.

Preparation of *Tert*-butyl 3,5-dinitrobenzoperoxoate (22). To a solution of anhydrous pyridine (0.13 mL, 3.0 mmol) and 5.5 M tBuOOH in decane (0.60 mL, 3.0 mmol) in a 100 mL Schlenk flask, which was kept at –4 °C (ice-water-salt bath), a solution of 3,5-dinitrobenzoyl chloride (0.346 g, 1.50 mmol) in distilled diethyl ether (25 mL) was added slowly with a cannula over a period of 5 min. Then, the reaction was stirred for about 1 h while allowing it to warm up to 10 °C. Afterwards, the reaction was allowed to warm up to room temperature (23 °C) and it was filtered through a 1.5 cm pad of Celite on a coarse glass frit. Then, the solvent was removed under reduced pressure to obtain 0.333 g (78%) of crude **22** as a beige solid. the product was purified by silica gel column chromatography with 20:1 hexanes:ethyl acetate to obtain 0.257 g (60%) of **22** as a white solid: mp 91–93 °C; IR (ν cm^{-1}): 3422 (w), 3110 (w), 2982 (m), 2943 (w), 2880 (w), 1761 (m), 1749 (m), 1694 (w), 1630 (m), 1539 (s), 1491 (m), 1458 (m), 1389 (m), 1366 (m), 1342 (s), 1288 (m), 1252 (m), 1182 (m), 1132 (s), 1072 (m), 1018 (m), 945 (m), 916 (m), 845 (m), 820 (m), 800 (m), 762 (w), 729 (m), 716 (s); ^{1}H NMR (400 MHz, $CDCl_3$, 23 °C, δ): 9.30–9.22 (m, 1H, C*H*), 9.07 (d, 2H, *J* = 1.6 Hz, C*H*), 1.46 (s, 18H, CH_3); $^{13}C\{^1H\}$ NMR (101 MHz, $CDCl_3$, 23 °C, ppm): 160.64 (*C*), 148.98 (*C*), 131.54 (*C*), 129.18 (*C*H), 122.99 (*C*H), 85.74 (*C*), 26.42 (*C*H_3); Anal. Calcd for $C_{11}H_{12}N_2O_7$: C, 46.48; N, 9.86; H, 4.26. Found: C, 46.26; N, 9.57; H, 4.57. Colorless, thick, long single crystals were grown by slow evaporation in toluene.

CHAPTER 4

Synthesis, Characterization, and Study of Oxygen-Rich Geminal Hydroperoxides with Impressive Detonation Performances and Practically Useful Sensitivities

4.1 Introduction

Geminal hydroperoxides (Figure 36) contain two hydroperoxy groups on the same carbon atom. They are a common class of peroxo-based compounds. Geminal hydroperoxides belong to the main peroxide sub-class of hydroperoxides.

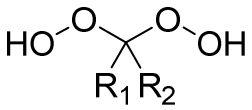

Figure 36. Structure of geminal hydroperoxides.

4.1.1 Hydroperoxides

Hydroperoxides have the basic ROOH formula where the R group can be a primary, secondary or tertiary alkyl group. The pK_a values of the hydroperoxides are lower than corresponding alcohols, which makes hydroperoxides stronger acids than alcohols and water. Ten hour half-life temperatures of dilute solutions of hydroperoxides are in the range of 133–172 °C. Thus, hydroperoxides are considered to be fairly thermally stable.[39]

Syntheses of hydroperoxides can be carried out using hydrogen peroxide and other organic peroxides. Hydrogen peroxide is used to synthesize a variety of different types of hydroperoxides with aldehydes, ketones, acetals, and ketals.[86] The reactions of hydroperoxides can be categorized into two main types: (i) reactions without the

cleavage of the O–O bond where hydroperoxides react with aldehydes, ketones, acyl chlorides, anhydrides, etc. to produce different peroxides, and (ii) reactions with cleavage of the O–O bond where the cleavage of O–O bond can either be heterolytic or homolytic. Hydroperoxides are also capable of undergoing both oxidations and reductions. They are mainly used as oxidizing or reducing agents and polymerization initiators.[86]

tert-Butyl hydroperoxide and cumene hydroperoxide are two common commercially available hydroperoxides that are sold as dilute solutions. *tert*-Butyl hydroperoxide has been reported as an explosion hazard and is known to be shock sensitive at high concentrations.[86] MEKP is a known high explosive mixture of hydroperoxides,[74] and the energetic properties of MEKP were discussed in Chapter 1.

4.1.2 Geminal Hydroperoxides

The interest towards geminal hydroperoxides has increased recently due to their antiparasitic activity.[115] Geminal hydroperoxides are also used as polymerization initiators and synthetic reagents in organic chemistry.[116] A variety of different synthetic methods of geminal hydroperoxides using different catalysts like iodine, Lewis acids, and mineral acids have been reported.[93,117] Yet, these geminal hydroperoxides have not been energetically characterized.

In this chapter, the synthesis, characterization, and the energetic properties of a series of geminal hydroperoxides **23**–**38** (Figure 37) are described. The O:C ratios of these geminal hydroperoxides are in the range of 0.40–1.33, which is higher than the *tert*-butyl peroxides and *tert*-butyl peroxy esters. Ring strain was varied using 5–7 membered rings and a bicyclopentane ring system (**27**, **34**, and **35**). Based on the

preliminary sensitivity tests the geminal hydroperoxides **30**–**38** are highly sensitive and energetic compounds.

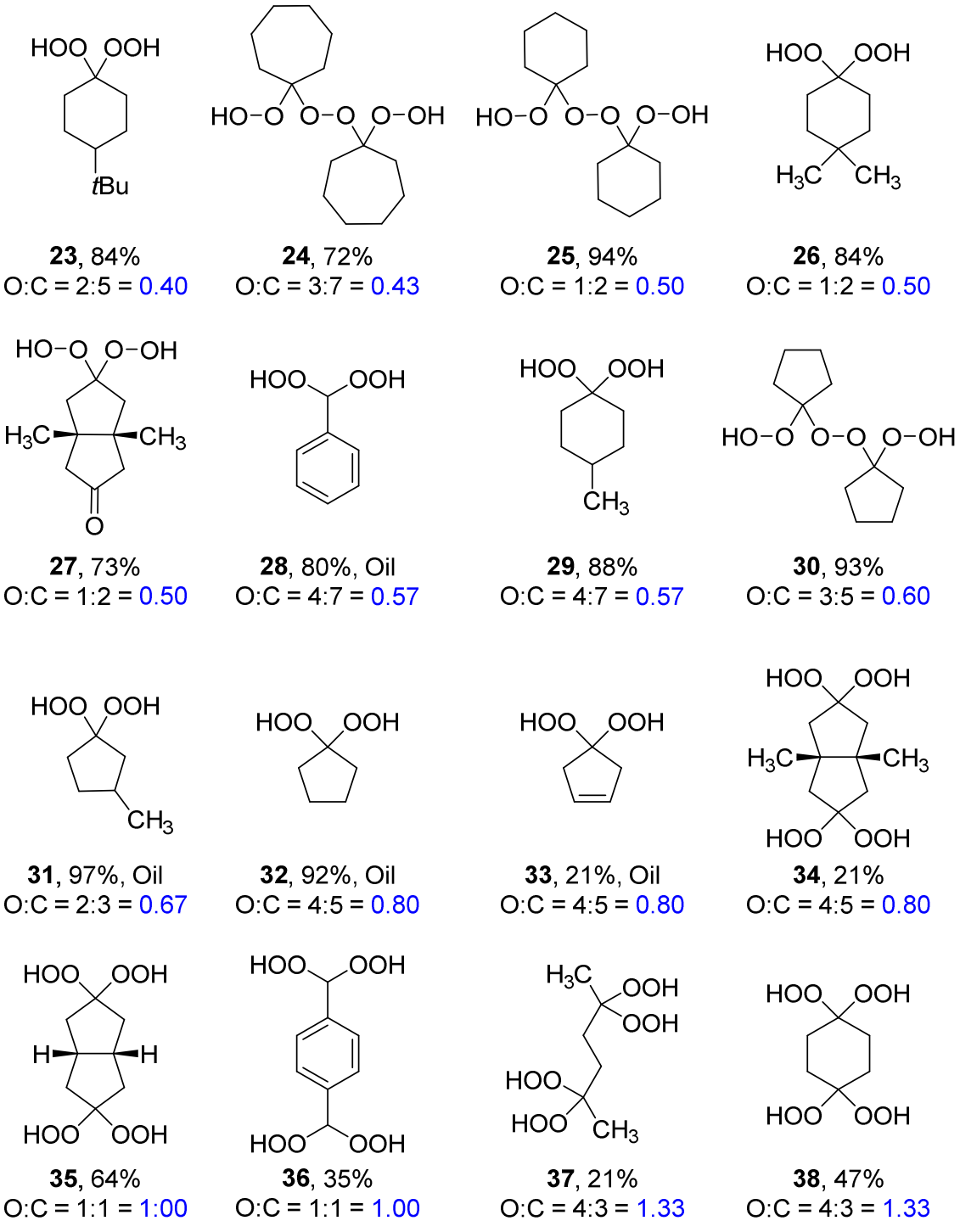

23, 84%
O:C = 2:5 = 0.40

24, 72%
O:C = 3:7 = 0.43

25, 94%
O:C = 1:2 = 0.50

26, 84%
O:C = 1:2 = 0.50

27, 73%
O:C = 1:2 = 0.50

28, 80%, Oil
O:C = 4:7 = 0.57

29, 88%
O:C = 4:7 = 0.57

30, 93%
O:C = 3:5 = 0.60

31, 97%, Oil
O:C = 2:3 = 0.67

32, 92%, Oil
O:C = 4:5 = 0.80

33, 21%, Oil
O:C = 4:5 = 0.80

34, 21%
O:C = 4:5 = 0.80

35, 64%
O:C = 1:1 = 1:00

36, 35%
O:C = 1:1 = 1.00

37, 21%
O:C = 4:3 = 1.33

38, 47%
O:C = 4:3 = 1.33

Figure 37. The series of geminal hydroperoxides **23**–**38**.

We have selected the most sensitive and energetic geminal hydroperoxides **34**–**36**, and **38** and they were completely energetically characterized with the standard sensitivity tests and energetic calculations. Oxygen-rich geminal hydroperoxides with impressive detonation performances and lower sensitivities than the known peroxo-based explosives were obtained in this study for potential use as HEDMs.

4.2 Results and Discussion

Most of the geminal hydroperoxides in this study are the corresponding hydroperoxides of the *tert*-butyl peroxides in Chapter 2. Compounds **23**–**38** were synthesized to observe the effects of the increased oxygen content and ring strain on their energetic performances. Cyclopentane ring-based geminal hydroperoxides **31**–**33** were oils. Since oils are unable to be energetically characterized, the solid *tert*-butyl peroxides **34** and **35** were synthesized to observe the effects of ring strain. Aromatic compounds **28** and **36** were synthesized to observe the effects of π-interactions on the stabilities and sensitivities of geminal hydroperoxides.

4.2.1 Synthetic aspects

Caution: Oxygen-rich organic peroxo-based compounds and high concentrations of aqueous H_2O_2 are potentially explosive and require handling with care. Reactions and other manipulations were performed in a fume hood behind a blast shield. Personal safety equipment was used whenever necessary: a face shield, leather gloves, and a leather apron. Interactions with strong acids, metals, metal salts, or easily oxidizable species were avoided to prevent hazardous decomposition reactions. All reactions were performed on small scales (≤ 350 mg) and at room temperature.

The syntheses of geminal hydroperoxides were carried out based on a published general procedure for geminal hydroperoxides (Scheme 7).[95] Compounds **23**, **28**, **29**, and **32** were synthesized based on the exact published procedures.[95] Compounds **24**, **25**, and **30** were obtained as dimers from recrystallization of the monomer products obtained from the reactions with cycloheptanone, cyclohexanone, and cyclopentanone, respectively, which were performed based on the published preocedures.[95]

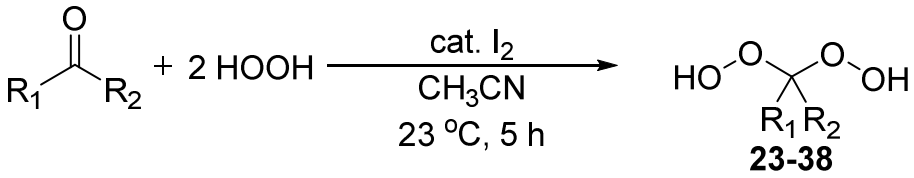

Scheme 7. Synthesis of geminal hydroperoxides.

Briefly, a solution of I_2 in CH_3CN was treated with 30–50 wt.% aqueous H_2O_2 while the reaction was kept stirring at room temperature (23 °C). Then, the aldehyde or ketone was added and the reaction was stirred at room temperature (23 °C) for 5 h. Afterwards, the reaction was concentrated under reduced pressure and the product was purified by silica gel column chromatography. During the syntheses of different geminal hydroperoxides, slight variations of the general procedure in the reaction scale, equivalents of H_2O_2 per ketone/aldehyde group, reaction time, volume of CH_3CN, and the chromatography mobile phase were required to obtain better yields.

Geminal hydroperoxides **23**–**38** were obtained in moderate to high yields (Figure 37). Compounds **26**, **27**, **31**, and **33**–**38** are new geminal hydroperoxides obtained in this study. Geminal hydroperoxides **28** and **31**–**33** were isolated as colorless oils while **23**–**27**, **29**, **30**, and **35**–**38** were isolated as white solids. Compound **34** was a highly viscous and colorless wax-like solid. Compound **27** was the half reacted product of the

reaction between *cis*-1,5-Dimethylbicyclo[3.3.0]octane-3,7-dione and H_2O_2. The solid geminal hydroperoxides were re-crystallized to obtain X-ray quality single crystals either by slow evaporation (**25**, **29**, and **34**), layering (**26**, **27**, and **36**) or cooling the saturated solutions to –29 °C in the freezer (**24** and **30**). All geminal hydroperoxide single crystals obtained were colorless. They were in the forms of needles (**24** and **26**), planar diamonds (**27** and **36**), planar polygons (**25**, **29**, and **30**) or planar hexagons (**34**). Geminal hydroperoxide syntheses using cyclobutanone, benzene-1,3,5-tricarbaldehyde, cyclohexane-1,3,5-trione, and cyclohexane-1,2,3,4,5,6-hexaone based on the same general procedure were not successful. The highest O:C ratio safely obtained for the series of geminal hydroperoxides and for the whole study was 1.33 of **37** and **38**.

Geminal hydroperoxides **23**–**38** were characterized by ^{1}H and ^{13}C NMR spectroscopy, mass spectrometry, melting point analysis, and IR spectroscopy. Elemental analyses were performed for a few selected highly energetic compounds (**34**–**36**, and **38**). When possible, X-ray crystal structures were obtained for complete characterization of the corresponding geminal hydroperoxides.

4.2.2 Spectroscopy

The ^{13}C NMR peak of the carbon atom connected to the O–O group, the peroxy carbon peak, was used to confirm that a hydroperoxide was obtained. The chemical shift region for the peroxy carbons of geminal hydroperoxides **23**–**26**, **28**, **29**, and **36**–**38** in $CDCl_3$ or CD_3OD was 110.08–116.47 ppm. More deshielded chemical shifts were obtained for the strained cyclopentane ring-based geminal hydroperoxides **27** and **30**–**35**, which were in the range of 119.90–127.47 ppm.

The characteristic IR stretching frequencies of the geminal hydroperoxides are medium and broad O–H stretching modes in the range of 3100–3700 cm^{-1},[118] medium or strong C–O stretching modes in the range of 1000–1300 cm^{-1}, and weak O–O stretching modes in the range of 800–900 cm^{-1}.[96,97,98] There were broad and medium peaks in the region of 3067–3460 cm^{-1} for O–H stretching modes. Hydrogen bonding is responsible for the relatively low O–H stretching frequencies. Medium and/or strong peaks were present in the region of 1000–1300 cm^{-1} for C–O stretching modes. There were weak O–O stretching modes as well as strong peaks in the range of 800–1000 cm^{-1} in the IR spectra of **23**–**38**. The strong peaks in the range of 800–1000 cm^{-1} indicate coupling of C–O and O–O stretching modes.[96,98]

4.2.3 X-Ray Crystal Structures

X-ray crystal structures were obtained for the geminal hydroperoxides **24**, **26**, **27**, **29**, **30**, **34**, and **36**. Compound **34** crystallized as an adduct of diethyl ether. The X-ray crystal structure of **34**·diethyl ether was disordered. An X-ray crystal structure of **38**·H_2O was obtained by our collaborators in the Klapötke group. Experimental crystallographic data are summarized in Table 22. Perspective views of the crystal structures are given in Figures 38–44. Selected bond lengths from the X-ray crystal structures are provided in Table 23. Lists of hydrogen bonds and short contacts of **24**, **26**, **27**, **29**, **30**, and **36** generated by Mercury 3.5.1 software are provided in Tables 24–26. The O–O bond lengths of the geminal hydroperoxides were in the range of the O–O bond lengths reported for dialkyl peroxides.[99]

Table 22. Experimental crystallographic data of **24**, **26**, **27**, **29**, **30**, **34**·diethyl ether, and **36**.

	24	**26**	**27**	**29**	**30**	**34**·diethyl ether	**36**
Formula	$C_{14}H_{26}O_6$	$C_8H_{16}O_4$	$C_{10}H_{16}O_5$	$C_{14}H_{28}O_8$	$C_{20}H_{36}O_{12}$	$C_{42}H_{72}O_{27}$	$C_4H_5O_4$
FW	290.35	176.21	216.23	324.36	468.49	1008.99	117.08
Space group	P 2_1 2_1 2_1	P 1 2_1/c 1	P 1 2_1/n 1	P 1bar	P 1 2_1/n 1	P 1 2_1/n 1	P 1 2_1/c 1
a (Å)	7.0415(6)	5.9681(4)	10.0706(13)	5.8158(6)	9.3130(6)	13.2439(8)	9.776(3)
b (Å)	10.7330(9)	29.3919(18)	10.0083(13)	10.8732(11)	12.0164(8)	11.9066(7)	6.0458(16)
c (Å)	20.1622(15)	5.9453(4)	10.6508(14)	13.8557(15)	20.6023(14)	34.029(2)	8.133(2)
V (Å^3)	1523.8(2)	907.58(11)	1020.7(2)	829.22(15)	2252.1(3)	5265.6(6)	471.9(2)
Z	4	4	4	2	4	4	4
T (K)	100(2)	100(2)	100(2)	100(2)	100(2)	100(2)	100(2)
λ (Å)	0.71073	0.71073	0.71073	0.71073	0.71073	0.71073	0.71073
ρ_{calc} (g/cm^3)	1.266	1.290	1.407	1.299	1.382	1.273	1.648
μ (mm^{-1})	0.098	0.102	0.113	0.106	0.114	0.107	0.152
R(F)[a] (%)	3.36	6.23	3.46	3.62	4.39	12.69	3.28
R_w(F)[b] (%)	7.51	17.05	11.13	15.02	15.74	34.40	13.55

[a] $R(F) = \sum \| F_o | - | F_c \| / \sum | F_o |$; [b] $Rw(F) = [\sum w(F_o^2 - F_c^2)^2 / \sum w(F_o^2)^2]^{1/2}$

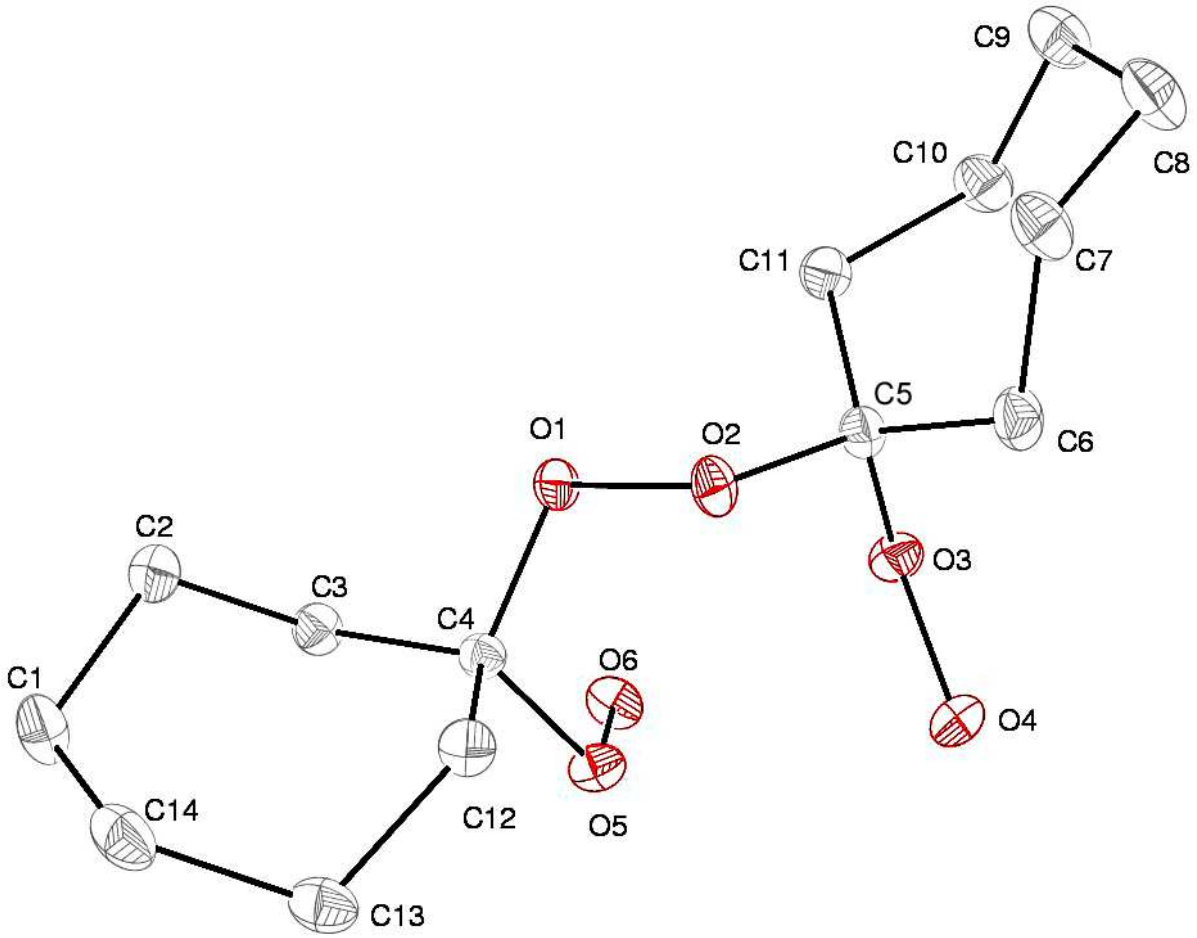

Figure 38. Perspective view of **24** with thermal ellipsoids at the 50% probability level.

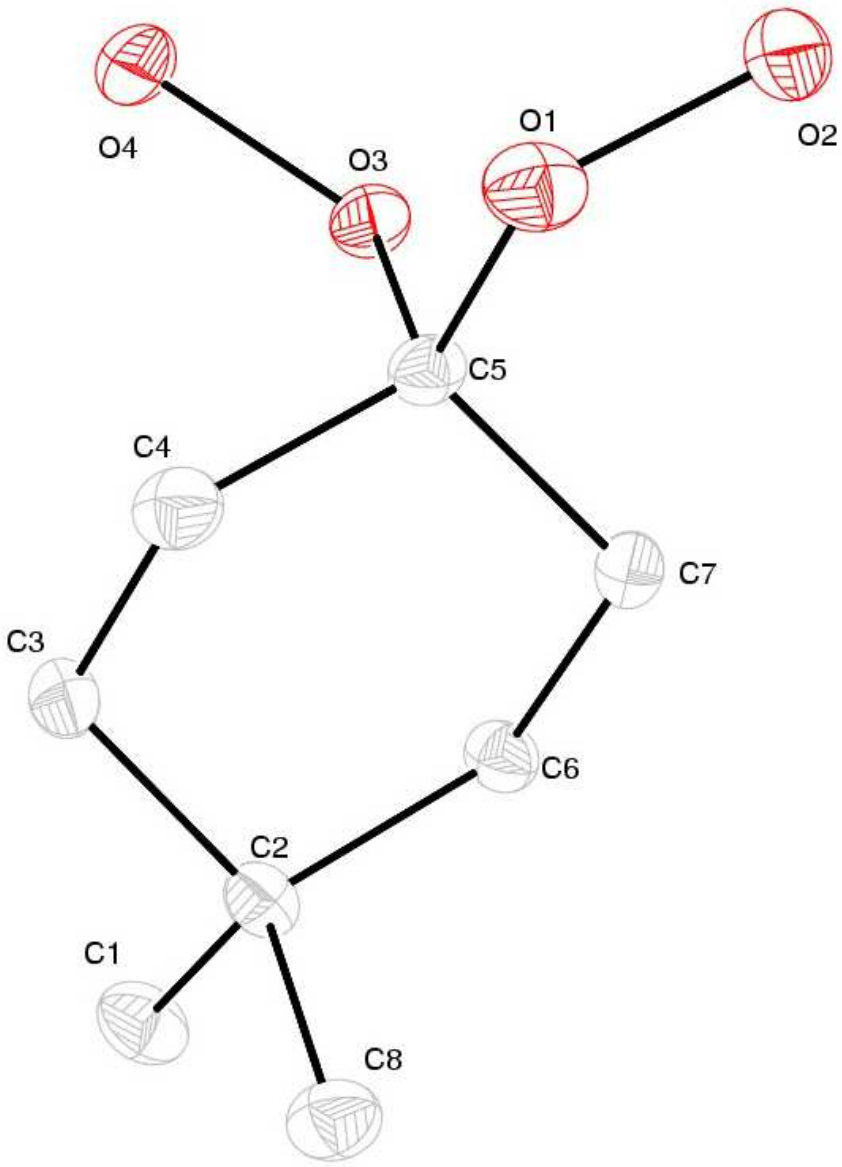

Figure 39. Perspective view of **26** with thermal ellipsoids at the 50% probability level.

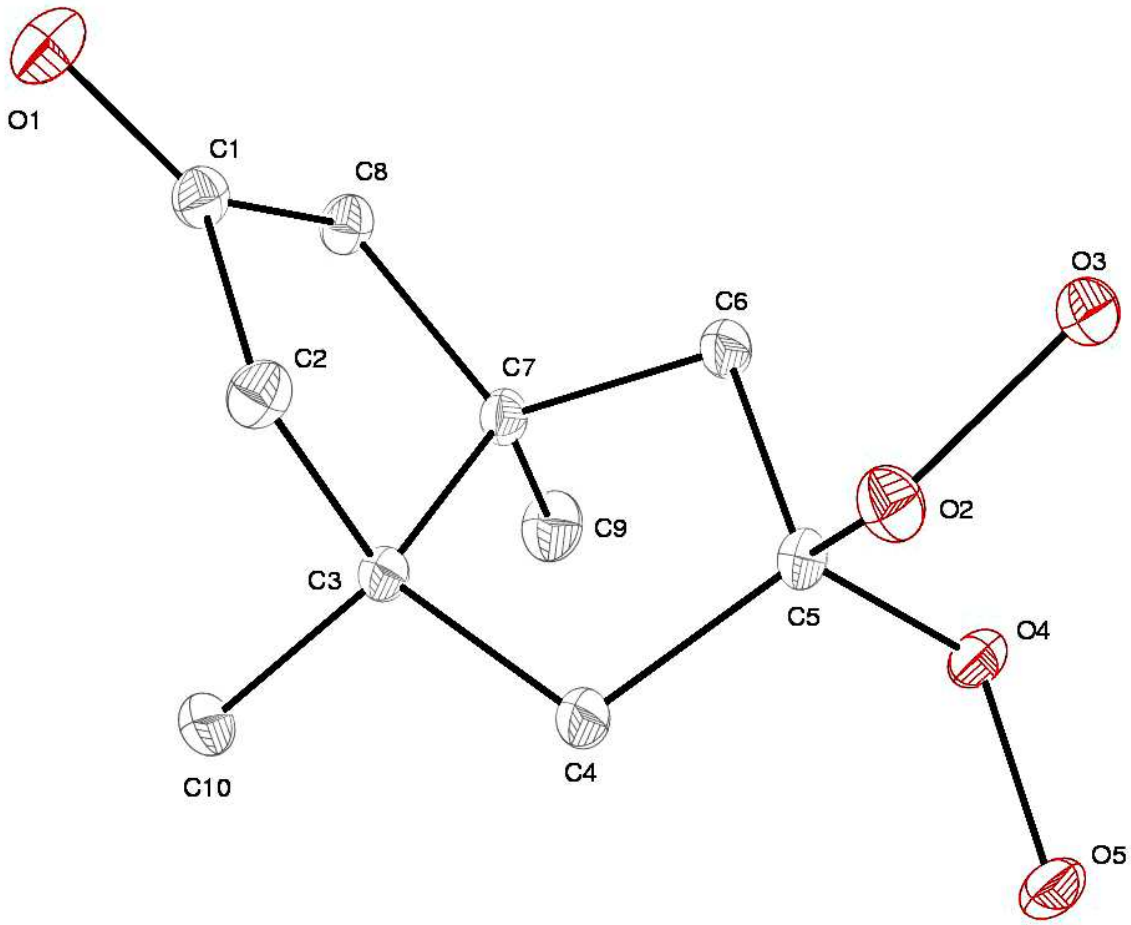

Figure 40. Perspective view of **27** with thermal ellipsoids at the 50% probability level.

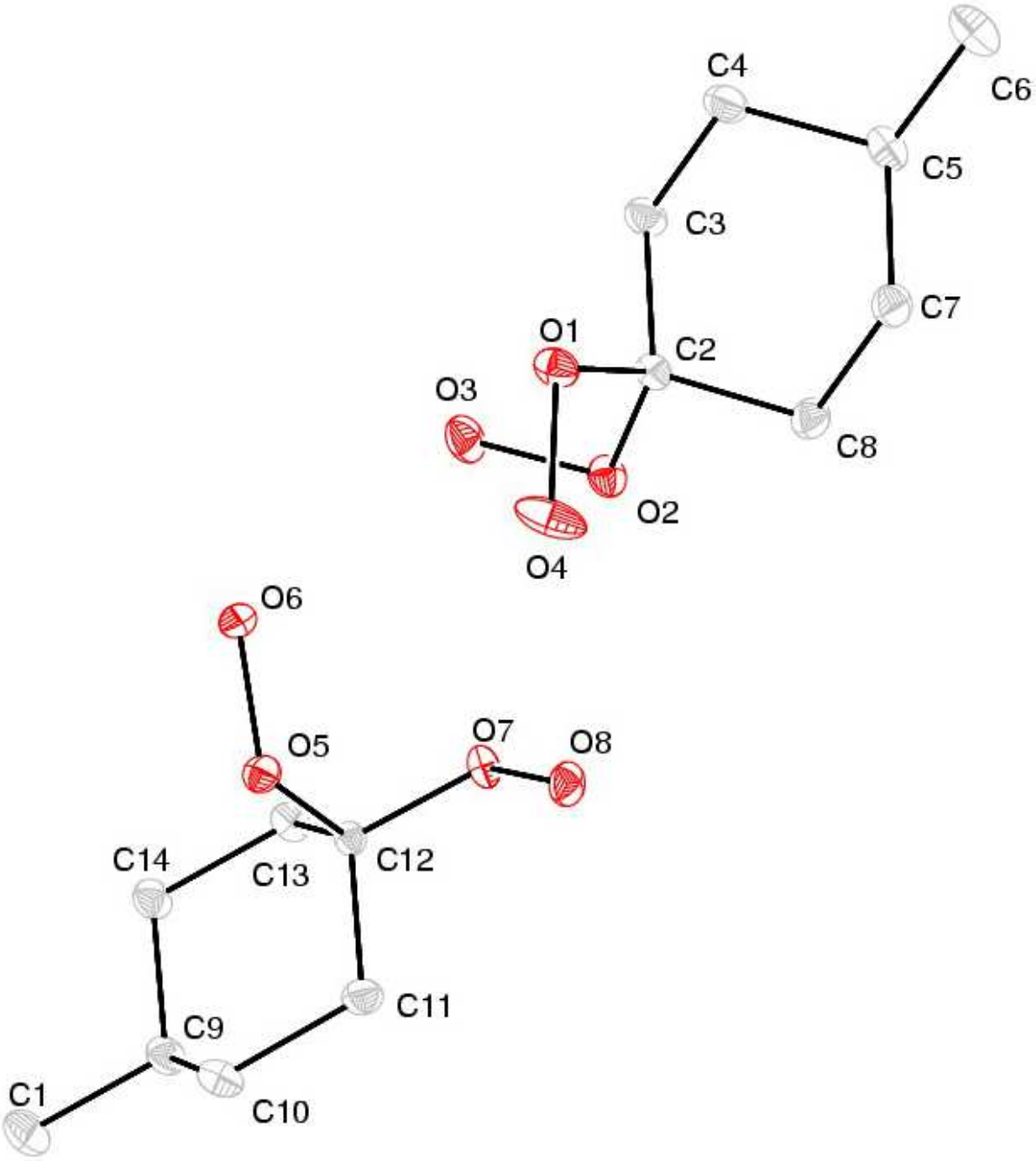

Figure 41. Perspective view of **29** with thermal ellipsoids at the 50% probability level.

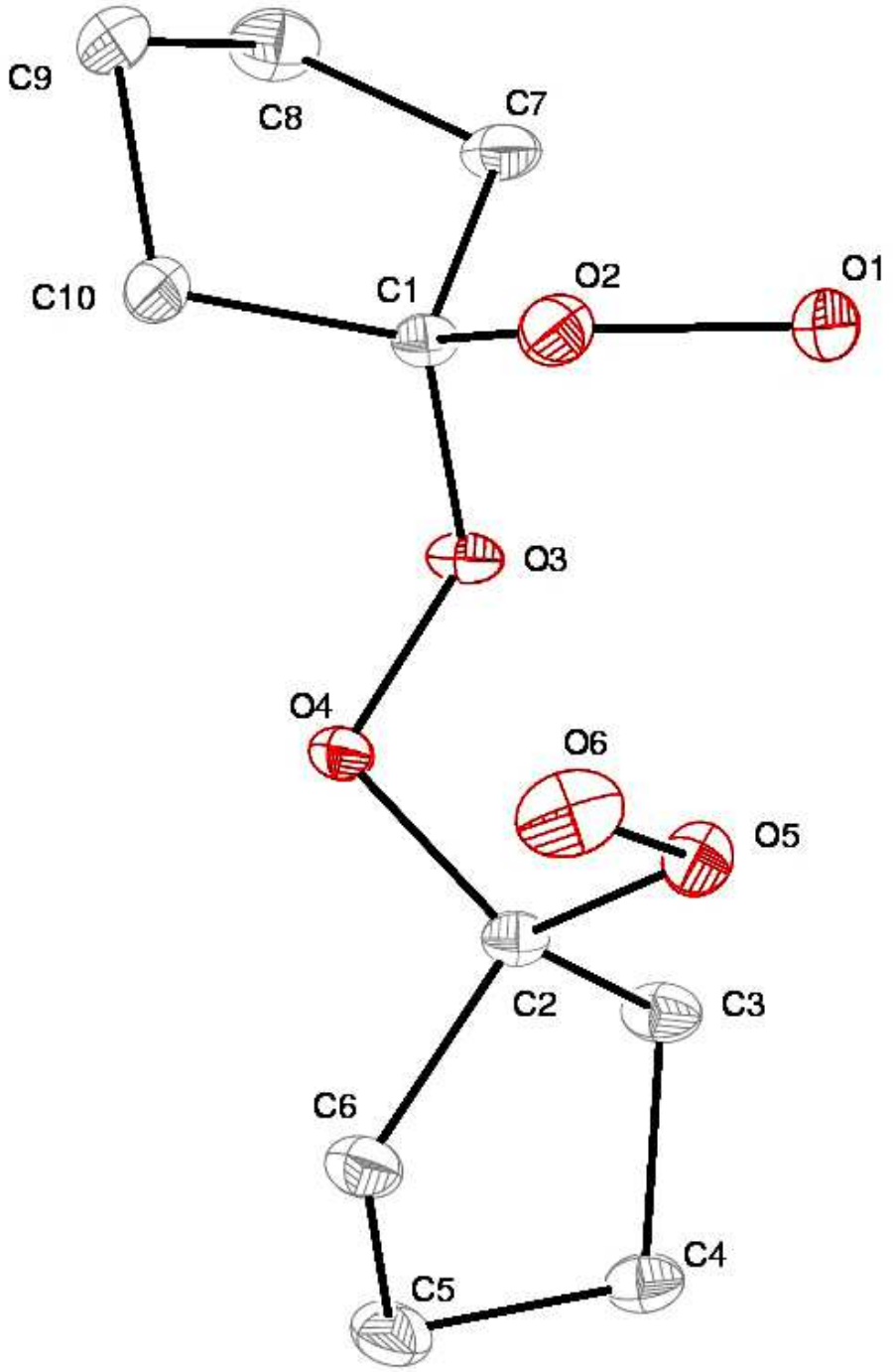

Figure 42. Perspective view of **30** with thermal ellipsoids at the 50% probability level.

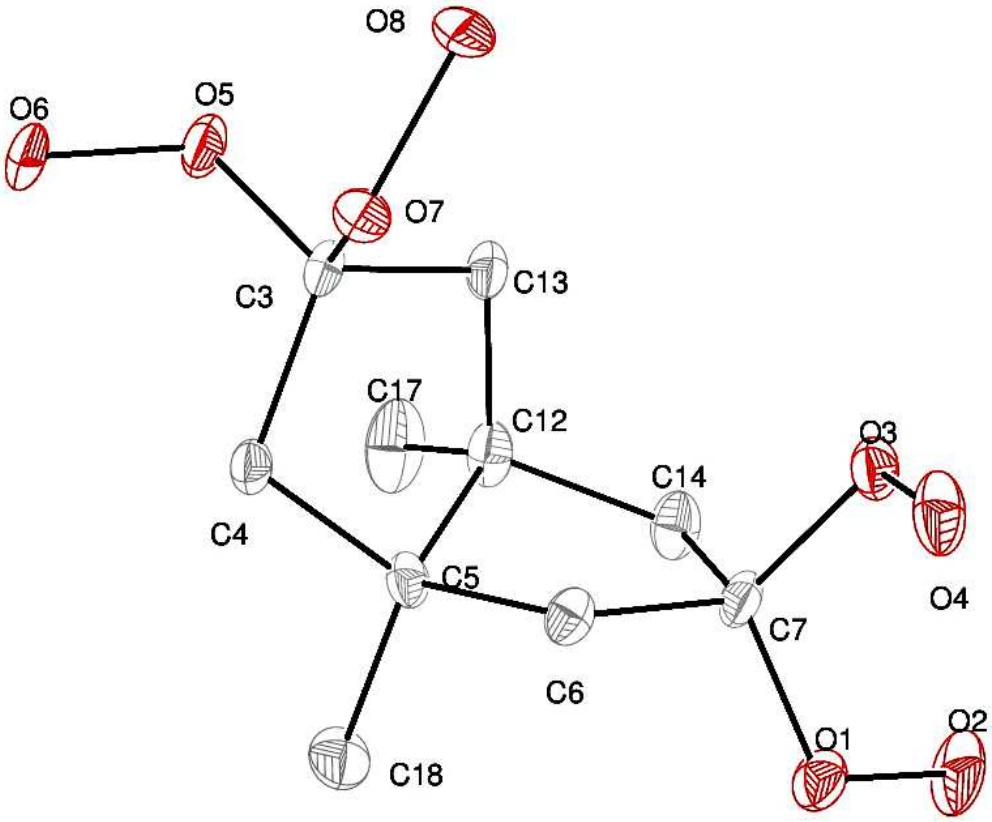

Figure 43. Perspective view of **34**·diethyl ether with thermal ellipsoids at the 50% probability level.

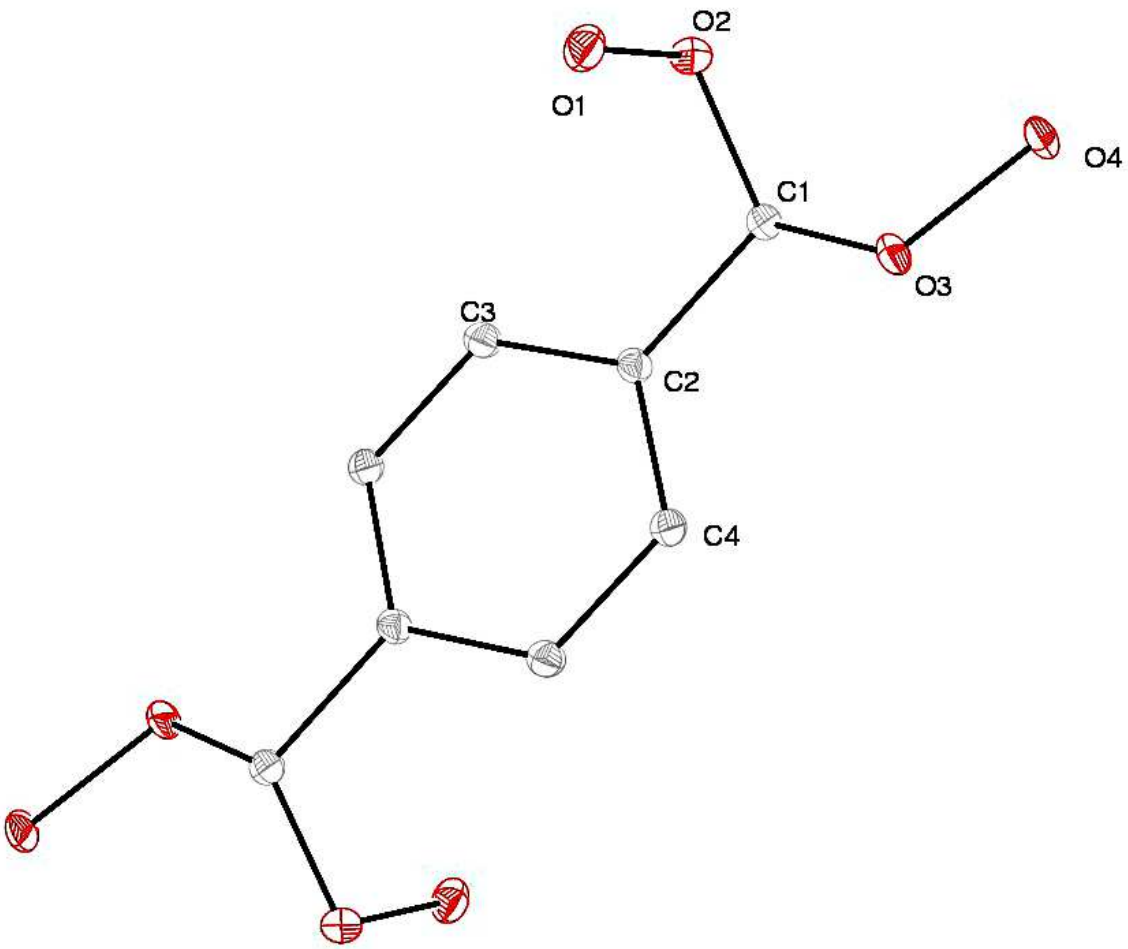

Figure 44. Perspective view of **36** with thermal ellipsoids at the 50% probability level.

Table 23. The selected bond lengths (Å) of **24**, **26**, **27**, **29**, **30**, **34**·diethyl ether, and **36**.

Bond	24	26	27	29	30	34·diethyl ether	36
O–O	1.4865(16)	1.464(2)	1.4657(9)	1.4574(6)	1.4638(9)	1.465(5)	1.4714(7)
	1.4709(19)	1.463(2)	1.4672(9)	1.4652(5)	1.4796(8)	1.465(5)	1.4594(7)
	1.4641(16)			1.4660(5)	1.4636(8)	1.472(5)	
				1.4669(5)		1.469(5)	
C=O			1.2207(11)				
C–O	1.428(2)	1.413(2)	1.4199(11)	1.4198(6)	1.4213(9)	1.423(5)	1.4115(8)
	1.429(2)	1.440(2)	1.4207(11)	1.4153(6)	1.4184(9)	1.418(6)	1.4115(8)
	1.4359(19)			1.4290(5)	1.4193(9)	1.422(5)	
	1.4405(18)			1.4178(6)	1.4155(9)	1.427(5)	
C–C (bridge)			1.5651(12)			1.552(6)	
C–CH_3		1.533(3)	1.5272(12)	1.5260(7)		1.528(6)	
		1.534(3)	1.5283(12)	1.5264(8)		1.530(7)	

Table 24. The list of short contacts of **24**, **26**, and **27**.

Compound	Number	Atom 1	Atom 2	Length (Å)	Length-VdW (Å)
24	1	H13	O4	2.656	–0.064
	2	H16	H1	2.372	–0.028
	3	H2	O4	2.55	–0.17
	4	O6	H5	2.407	–0.313
	5	O6	O5	2.663	–0.377
	6	H17	O5	2.205	–0.515
	7	H11	O6	2.475	–0.245
	8	H22	H3	2.331	–0.069
	9	O3	O6	2.826	–0.214
	10	O4	O5	2.857	–0.183
26	1	O3	O2	2.989	–0.051
	2	H7	O2	2.708	–0.012
	3	H1	O1	2.68	–0.04
	4	H16	O2	2.491	–0.229
	5	O3	H3	2.213	–0.507
	6	O4	O2	2.81	–0.23
	7	O4	H2	1.976	–0.744
	8	O4	H3	2.317	–0.403
27	1	O1	H3	2.557	–0.163
	2	H13	O4	2.652	–0.068
	3	H13	O5	2.691	–0.029
	4	O3	O5	2.804	–0.236
	5	O3	H2	1.915	–0.805
	6	H1	H2	2.278	–0.122
	7	H9	H12	2.298	–0.102
	8	O3	O1	2.69	–0.35
	9	H1	O1	1.822	–0.898
	10	H1	C1	2.792	–0.108
	11	O5	H4	2.522	–0.198

Table 25. The list of short contacts of **29**.

Compound	Number	Atom 1	Atom 2	Length (Å)	Length-VdW (Å)
29	1	H9	O1	2.565	–0.155
	2	O4	O4	2.84	–0.2
	3	O2	O7	2.954	–0.086
	4	O2	H20	2.657	–0.063
	5	O3	O6	2.988	–0.052
	6	H4	O6	2.146	–0.574
	7	H4	O7	2.577	–0.143
	8	O4	O8	2.765	–0.275
	9	O4	H20	1.891	–0.829
	10	H9	H25	2.315	–0.085
	11	O4	O5	2.775	–0.265
	12	H4A	O5	1.953	–0.767
	13	H4A	O6	2.487	–0.233
	14	O2	H24	2.719	–0.001
	15	O3	H24	2.655	–0.065
	16	O3	H22	2.655	–0.065
	17	O7	H18	2.567	–0.153
	18	O8	O6	2.738	–0.302
	19	O8	H18	1.925	–0.795
	20	H20	H18	2.344	–0.056
	21	O7	H24	2.715	–0.005

Table 26. The list of short contacts of **30** and **36**.

Compound	Number	Atom 1	Atom 2	Length (Å)	Length-VdW (Å)
30	1	O1	O11	2.892	-0.148
	2	H1	O11	2.252	-0.468
	3	O5	O7	2.991	-0.049
	4	O5	H19	2.328	-0.392
	5	O5	O11	2.841	-0.199
	6	H13	H26	2.38	-0.02
	7	H2	H26	2.302	-0.098
	8	H10	O8	2.551	-0.169
	9	O6	O9	2.981	-0.059
	10	O6	H28	2.394	-0.326
	11	H36	O12	2.619	-0.101
	12	C20	O12	3.195	-0.025
	13	O1	O5	2.93	-0.11
	14	O2	O6	2.813	-0.227
	15	O7	O11	2.868	-0.172
	16	O8	O12	2.826	-0.214
36	1	O2	O2	2.912	-0.128
	2	O4	O1	2.701	-0.339
	3	O4	H1	1.865	-0.855
	4	H2	H1	2.178	-0.222
	5	H2	O1	1.902	-0.818
	6	O1	H3	2.511	-0.209
	7	O3	H3	2.617	-0.103
	8	H5	C3	2.896	-0.004

Crystalline densities obtained for the geminal hydroperoxides **24**, **26**, **27**, **29**, **30**, **34**·diethyl ether, and **36** in the range of 1.266–1.648 g/cm^3 were higher than the *tert*-butyl peroxides and *tert*-butyl peroxy esters. The crystalline density of **36** (1.648 g/cm^3 at 100 K) was the highest crystalline density obtained for the series of geminal hydroperoxides. It is higher than the densities of all the known peroxo-based explosives and slightly lower than orthorhombic (1.704 g/cm^3 at 123 K) and monoclinic (1.713 g/cm^3 at 100 K) TNT.[119] Since the molecular weights of **36** and TNT are similar (234.18 and 227.14 g/cm^3), **36** packs nearly as efficiently as TNT in the solid state.

X-ray crystal structures of geminal hydroperoxides **24**, **26**, **27**, **29**, **30**, **34**, and **36** have hydrogen bonded networks, unlike *tert*-butyl peroxides and *tert*-butyl peroxy esters. They form stacks or layers held together mainly by intrastack or intralayer hydrogen bonding interactions, respectively (Figures 45 and 46). However, in the crystalline lattice of **24**, the hydrogen bonds are in between the molecular layers. In the rest of the crystal structures, there are multiple short contacts (**27**, **34**, and **36**) or hydrophobic interactions (**26**, **29**, and **30**) in between the stacks or layers. Compound **36** also contains C–H···π interactions (2.896 Å) in between the molecular layers (Figure 47). The presence of stacks or layers allows dissipation of the energy by movement of stacks or layers with respect to each other upon initiation with various stimuli.[81] Still, the presence of a large number of short contacts (**27**, **34**, and **36**), hydrogen bonds (**24**), or π interactions (**36**) between the stacks or layers could restrict the free movement and thus, energy dissipation. Hence, there could be no proper slip planes or stacks that can significantly reduce the sensitivities in the crystal structures of **24**, **27**, **34**, and **36**. There

are only weak hydrophobic interactions between stacks of **26**, **29**, and **30**, which might result in low sensitivities to stimuli.

There are O–H···O and C–H···O hydrogen bonds in all of the X-ray crystal structures of geminal hydroperoxides. Compound **24** and **30** contain two intramolecular O–H···O hydrogen bonds (2.813–2.930 Å). The short contacts present in these crystal structures are O···O, H···H, and C···H contacts that are shorter or at the edge of their van der Waals radii (Tables 24–26).[120] The O···O contacts (2.804–2.991 Å) and H···H (2.178–2.380 Å) contacts are present in all of the crystal structures. There are C···H contacts (2.808–2.817 Å) in the crystal structure of **34**. The oxygen atoms of O–O trigger bonds from the hydroperoxy groups of **24**, **26**, **27**, **29**, **30**, **34**, and **36** are involved in many stabilizing intermolecular interactions that also hold the oxygen atoms in close proximity. They are involved in multiple O–H···O hydrogen bonds and O···O contacts, which can reduce the sensitivities. Figure 48 shows these stabilizing intermolecular interactions of **36**.

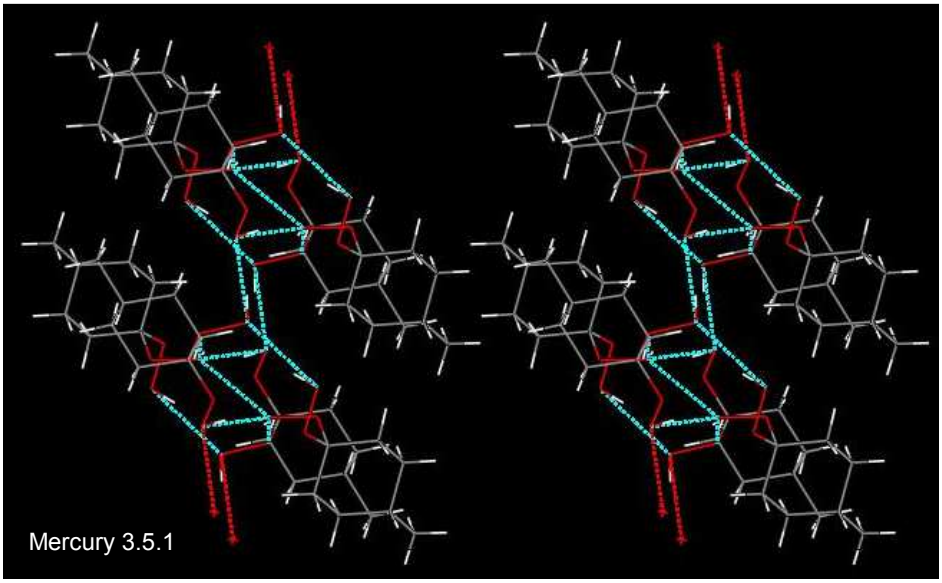

Figure 45. Hydrogen bonded (red and blue) molecular stacks of **29**.

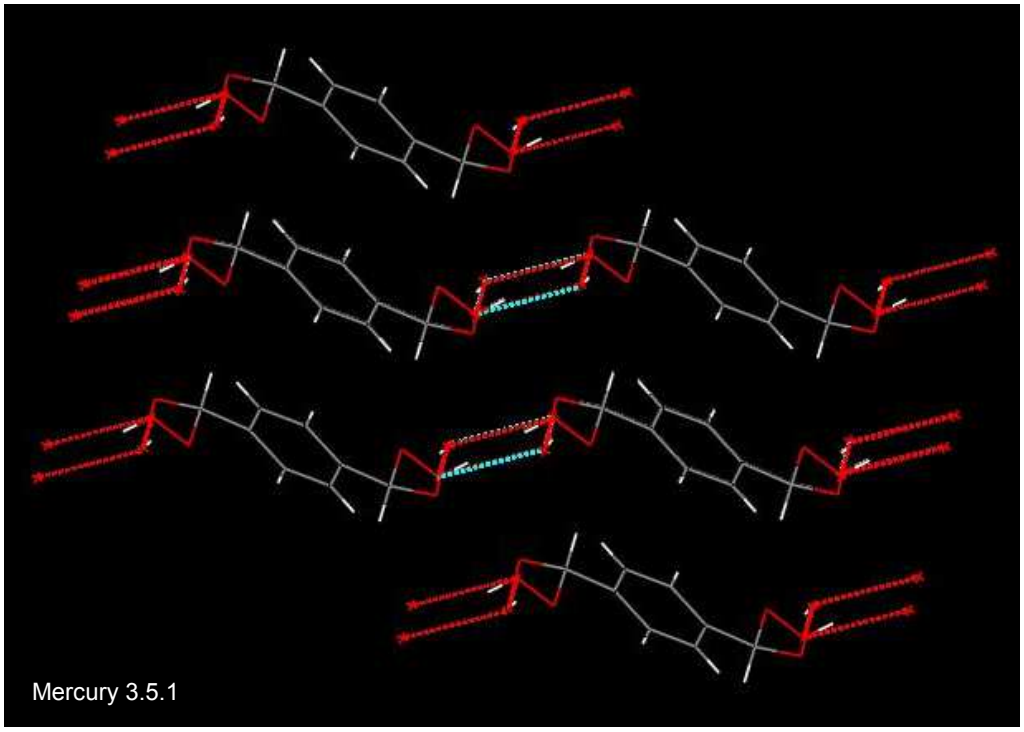

Figure 46. Hydrogen bonded (red and blue) molecular layers of **36**.

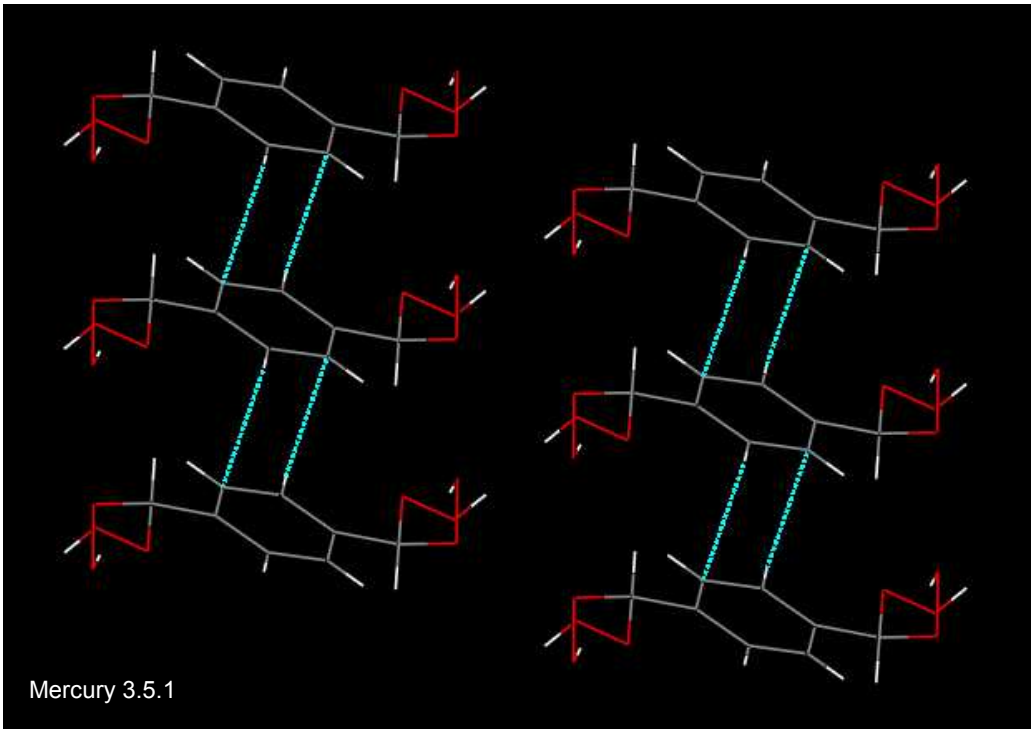

Figure 47. C–H···π interactions (blue) of **36**.

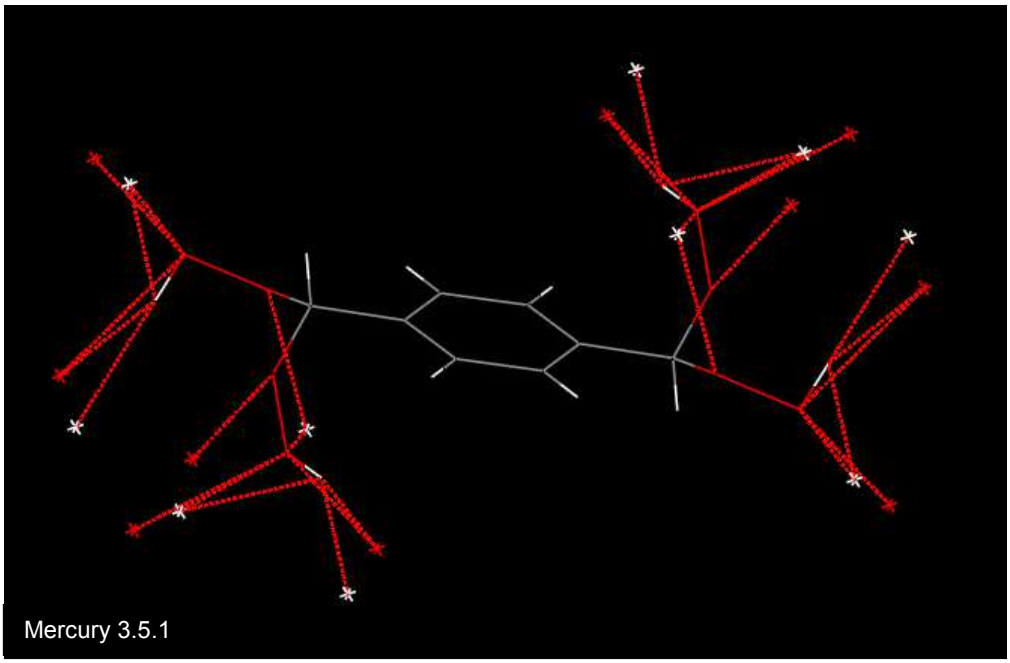

Hydrogen and oxygen atoms of the neighboring molecules are shown by white and red asterisks, respectively.

Figure 48. Intermolecular interactions (red) of the O–O trigger bonds of **36**.

4.2.4 Thermal Stability

Thermal stabilities of geminal hydroperoxides **23**–**38** were assessed using thermogravimetry (TGA/DTA). The decomposition temperatures (T_{Dec}) of **23**–**38** are provided in Table 27. T_{Dec} values of geminal hydroperoxides **23**–**38** were in the range of 70–130 °C. The thermal stabilities of **23** and **33** are too low for HEDM applications. Compounds **24**–**32** and **34**–**38** were fairly thermally stable geminal hydroperoxides. The most thermally stable geminal hydroperoxide was the aromatic geminal hydroperoxide **28** (T_{Dec} = 130 °C). Since most HEDM applications require decomposition temperatures to be ≥ 150 °C,[2] more thermally stable geminal hydroperoxides need to be obtained. High thermal sensitivities of peroxo-based compounds arise from the weak O–O trigger bonds, which is highly disadvantageous for HEDM applications.

Table 27. Decomposition temperatures of **23**–**38**.

Compound	T_{Dec} (°C)
23	80
24	125
25	120
26	110
27	120
28	130
29	115
30	110
31	125
32	90
33	70
34	117
35	100
36	112
37	105
38	117

CBS-4M electronic enthalpies were calculated for the more oxygen-rich geminal hydroperoxides **34**–**36** and **38**. Gaussian09 software package was used to obtain these heats of formation values ($\Delta_f H°$) by our collaborators in the Klapötke lab.[113] The $\Delta_f H°$ values of **34**–**36** and **38** are provided in Table 28.

Table 28. Heats of formation values of **34**–**36** and **38**.

Compound	$\Delta_f H°$ (kJ/mol)
34	–703.6
35	–617.0
36	–418.2
38	–627.1

The $\Delta_f H°$ values of geminal hydroperoxides **34**–**36** and **38** are all negative. They are in the range of –703.6 to –418.2 kJ/mol. The most positive $\Delta_f H°$ value was obtained for **36**, which indicates that it is the most energetic geminal hydroperoxide of **34**–**36** and **38**.

4.2.5 Preliminary Qualitative Sensitivity Tests

Sensitivities of geminal hydroperoxides **23**–**38** were studied using the flame, hammer impact, sand paper friction, and electrostatic discharge (Tesla coil) tests. Although there were no significant variations in the test responses for the series of corresponding *tert*-butyl peroxides **1**–**15** in Chapter 1, sensitivity differences of **23**–**38** were observable in the flame tests. No responses were obtained in the hammer and sand paper tests. Sudden, large, bright flames were obtained for the most sensitive compounds, which are the cyclopentane ring-based peroxides **30**–**33**, the most strained octahydropentalene ring-based peroxides **34** and **33**, and the most oxygen-rich peroxides **36**–**38**. Compound **35** was the most sensitive geminal hydroperoxide, producing a sudden ball of flame with a sound. During the Tesla coil test, **35** produced a sudden bright flame upon providing an electrostatic discharge.

4.2.6 Standard Sensitivity Tests

Impact, friction, and electrostatic discharge sensitivities of the most sensitive and energetic solid geminal hydroperoxides **34**–**36** and **38** (based on the preliminary tests) were determined with a BAM drop hammer, BAM friction tester, and an electrostatic spark sensitivity tester using standard experimental methods by our collaborators in the Klapötke lab.[29–34] Compound **37** was omitted due to the failure to confirm the structure with an X-ray crystal structure. Table 29 includes the impact, friction, and electrostatic discharge sensitivities of **34**–**36** and **38**.

Table 29. Impact, friction, and electrostatic discharge sensitivities of **34**–**36** and **38**.

Compound	IS (J)	FS (N)	ESDS (J)
34	2	5	0.2
35	2	5	0.1
36	3	< 5	0.25
38	< 1	< 5	0.6

Based on the "UN Recommendations on the Transport of Dangerous Goods",[28] **34**–**36** and **38** are "very sensitive" towards impact. Compounds **34**–**36** and **38** are "extremely sensitive" towards friction. Still, the geminal hydroperoxides **34**–**36** are much lower in impact and friction sensitivities than the known peroxo-based explosives TATP, DADP, HMTD, and MEKP (Tables 3–6). Impact sensitivities < 1 J and friction sensitivities < 5 N could not be obtained in this study. Thus, the impact and friction sensitivities of compound **38** are comparable to the known peroxo-based explosives (Tables 3–6). All the geminal hydroperoxides **34**–**36** and **38** show electrostatic discharge sensitivity values that are much higher than the electrical discharges that can be

created by the human body (≤ 0.02 J)[2] and they can be safely handled. Based on the sensitivities of **34**–**36** and **38**, they can be categorized as primary explosives.

The impact and friction sensitivities of **34**–**36** and **38** do not vary much with the nature of the organic framework, since the O–O linkages act as trigger bonds that initiate decomposition upon cleavage. The solid state structures of highly sensitive TATP and DADP lack O–H···O hydrogen bonds and O···O close contacts, and contain only very weak O···H and C···H interactions.[59] Stabilization achieved by I···O close contacts in the crystalline lattice was found to reduce the sensitivities of DADP.[68] Geminal hydroperoxides **34**–**36** and **38** contain many O–H···O hydrogen bonds and O···O contacts that can reduce the high activity of the O–O trigger bonds. Thus, they have lower sensitivities than the known peroxo-based explosives TATP and DADP.

However, they are all still highly sensitive to impact and friction stimuli. High oxygen contents are known to result in highly sensitive compounds.[76,80] Thus, the high sensitivities of **34**–**36** and **38** might be due to the high peroxy O:C ratios that are in the range of 0.8–1.33. Compound **38** with the highest peroxy O:C ratio (1.33) demonstrates the highest impact and friction sensitivities. Although optimum sensitivities for primary explosives were not obtained with **34**–**36** and **38**, they are still practically useful sensitivities for HEDM applications since typical primary energetic materials have impact and friction sensitivities of ≤ 4 J and ≤ 10 N, respectively.[2]

4.2.7 Energetic Performance Calculations

The energetic performances of **34**–**36** and **38** were calculated using the EXPLO5 V6.02 software (Table 30) by our collaborators in the Klapötke lab.[114] These calculated V_{Det} and P_{Det} values of **34**–**36** and **38** are in the range of 6150–7170 m/s and 117–195

kbar, respectively. They are high detonation performances, which are useful for HEDM applications.

Table 30. Calculated energetic properties of **34**–**36** and **38**.

Property	34	35	36	38
Formula	$C_{10}H_{18}O_8$	$C_9H_{16}O_8$	$C_8H_{10}O_8$	$C_6H_{12}O_8$
FW (g/mol)	266.28	252.25	234.18	212.18
Ω[a] (%)	–126.20	–114.18	–88.83	–75.41
ρ[b] (g/cm^3)	1.273	-	1.648	1.602
ρ[c] (g/cm^3)	1.35[d]	1.375 [d]	1.60	1.40 [d]
EXPLO5 V6.02				
$\Delta_{Ex}U°$ (kJ/kg)	–4636	–4875	–5498	–5329
P_{Det} (kbar)	117	126	195	155
V_{Det} (m/s)	6150	6250	7130	6700
V_o (L/kg)	829	831	688	847

[a]Oxygen balance for oxidation of carbon to CO_2
[b]Crystalline density at 100 K
[c]Crystalline densities at 298 K (for energetic calculations)
$\rho_{298K} = \rho_T / [1 + \alpha_v (298 - T)]$ (T = 100 K, ρ_T = Desnsity at 100 K, α_v = 1.5 x 10^{-4} K^{-1})
[d]Solvent free estimated crystalline density at 298 K (for energetic calculations)

The calculated detonation velocities of **34**–**36** and **38** are greater than the detonation velocities of all the known peroxo-based explosives (4,511–5,300 m/s).[6b,35] Compound **36** has the highest crystalline density (1.648 g/cm^3) and also the highest detonation velocity (7130 m/s) of the geminal hydroperoxides **34**–**36** and **38**. The

detonation velocity of **36** is highly impressive for HEDM applications and it surpasses the detonation velocity of TNT (6,900 m/s),[11b] which is a secondary high explosive.

The increase in detonation velocities along the series **34** to **36** is parallel to the increasing O:C ratios and increasing crystalline densities. The high ring strain of the octahydropentalene ring-based geminal hydroperoxides **34** and **35** caused no increase in their detonation performances since the lower crystalline densities have primarily determined the detonation performance. Although the oxygen content is the highest in compound **38**, the crystalline density is lower than **36**. Thus, the detonation performance of **38** is lower than for **36**.

4.3 Conclusions

Geminal hydroperoxides **23**–**38** were synthesized in moderate to high yields and were fully characterized. The O:C ratios of these geminal hydroperoxides are in the range of 0.40–1.33. Sensitivities and energetic performances of **23**–**38** were studied for their use as HEDMs. The sensitivities of **23**–**38** increase with the oxygen content and the ring strain based on the preliminary sensitivity tests.

Compounds **34**–**36** and **38** were the most energetic compounds in the study. Their detonation velocities are in the range of 6150–7170 m/s. These are impressive detonation velocities for their use as HEDMs. The impact and friction sensitivities of **34**–**36** and **38** are high and they can be categorized as primary explosives. However, the sensitivities of **34**–**36** are much lower than the known peroxo-based explosives due to the relatively stabilized O–O trigger bonds with the O–H···O hydrogen bonds and O···O contacts. These sensitivities of **34**–**36** are practically useful although they are higher than the optimum sensitivities for primary explosives. Compound **38** with the

highest O:C ratio (1.33) has impact and friction sensitivities comparable to the known peroxo-based explosives. This indicates that the peroxy O:C ratio that is safe to handle is approximately 1.00. This work demonstrates that through careful manipulation of organic peroxide structures compounds with useful energetic materials properties can be obtained.

4.4 Experimental Section

General Considerations: Syntheses of all organic peroxides were carried out at room temperature under ambient atmosphere. Chemicals were purchased from Sigma-Aldrich, Acros Organics, EMD, or Alfa Aesar and were used without further purification. ACS grade solvents were obtained from EMD and Fisher Scientific. Petroleum ether used in the synthetic protocols was with a boiling point range of 35–60 °C. A 50 wt.% aqueous solution of H_2O_2 purchased from Sigma-Aldrich was used to synthesize the hydroperoxides. Geminal hydroperoxides have been synthesized using a modified published general procedure for geminal hydroperoxides.[95] Compounds **23**, **28**, **29**, and **32** were synthesized based on the exact published procedures.[95] Compounds **24**, **25**, and **30** were obtained as dimers from recrystallization of the products obtained from the reactions with cycloheptanone, cyclohexanone, and cyclopentanone based on the published preocedures.[95]

Silica gel 60, 230–400 mesh (EMD Chemicals) was used to perform silica gel column chromatography.[104] ASTM TLC plates precoated with silica gel 60 F_{254} (250 μm layer thickness) were used for thin-layer chromatography (TLC). TLC spots were observed using a UV lamp and/or a potassium permanganate solution as a stain (3 g

$KMnO_4$, 20 g K_2CO_3, 5 mL 5% w/v aqueous NaOH, 300 mL H_2O). The spots on the stained TLC plates were visualized after heating with a heat gun.

^1H and $^{13}C\{^1H\}$ NMR spectra were obtained from a Varian Mercury 400 (400 MHz and 101 MHz) NMR spectrometer or MR 400 (400 MHz and 101 MHz) NMR spectrometer, in $CDCl_3$ or CD_3OD as indicated, and were referenced to the residual proton and carbon resonances of the solvent ($CDCl_3$: ^1H: δ 7.27, ^{13}C: δ 77.23; CD_3OD: ^1H: δ 3.31, ^{13}C: δ 49.00). Mass spectra were obtained on an electrospray time-of-flight high-resolution Waters Micromass LCT Premier XE mass spectrometer. Infrared spectra were obtained from a Shimadzu MIRacle 10 IRAffinity-1 equipped with a single reflection ATR accessory. Melting points were determined on an Electrothermal IA 9300 melting point apparatus and are uncorrected. Thermogravimetric (TGA/DTA) measurements to determine the decomposition temperatures of **23**–**33** and **37** were performed at a heating rate of 10 °C min^{-1} with an SDT-2960 TGA/DTA instrument. Thermogravimetric (TGA/DTA) measurements of **34**–**36** and **38** were performed at a heating rate of 5 °C min^{-1} with an OZM Research DTA 552-Ex instrument in the Klapötke lab.

Qualitative Sensitivity Tests: Qualitative sensitivities to heat, impact, and electrostatic discharge were determined to assess initial safety issues. Tests included burning about 3-5 mg of the compound in the Bunsen burner flame, striking 3-5 mg of the compound on a metal plate with a hammer, and passing an electrostatic discharge through 3-5 mg of the compound on a metal plate using an Electro Technic BD 10 Tesla coil (120 V, 0.35 A).

Quantitative Sensitivity Tests: Quantitative sensitivity Tests include BAM drop hammer[31] impact tests carried out according to STANAG 4489[29] modified instructions[30] using approximately 0.4 mL of the compound, Friction tests with a BAM friction tester carried out according to STANAG 4487[32] modified instructions[33] using approximately 5 mg of the compound, and electrostatic spark tests with an ESD 2010 EN, OZM Electric Spark Tester according to STANAG 4515[34] instructions using 0.1 mL of the compound performed by the Klapötke group.

General Procedure for the Preparation of Geminal Hydroperoxides: A solution of I_2 (0.025 g, 0.100 mmol, 0.1 equivalents per ketone/aldehyde group) in CH_3CN (3–10 mL) was treated with a 50 wt.% aqueous solution of H_2O_2 (0.23 mL, 4.0 mmol, 4 equivalents per ketone/aldehyde group) while the reaction was stirred at room temperature (23 °C). Afterwards, the ketone/aldehyde starting material (1 mmol of monoketone/monoaldehyde compound or 0.5 mmol of diketone/dialdehyde compound) was added and the reaction was stirred at room temperature (23 °C) for 5 h. Then, the reaction was concentrated under reduced pressure, redissolved in dichloromethane (10 mL), and anhydrous Na_2SO_4 was added to dry the solution. The dichloromethane solution was again concentrated and the product was purified by silica gel column chromatography with 4:1 dichloromethane:ethyl acetate.

Preparation of 4-(*tert*-Butyl)-1,1-dihydroperoxycyclohexane (23). Compound **23** was prepared in 84% yield as a white solid by a literature procedure[95] starting from 4-(*tert*-butyl)cyclohexan-1-one: mp 79–81 °C (lit[95] 79–81 °C); IR (ν cm^{-1}): 3332 (broad, m), 2952 (s), 1440 (w), 1367 (m), 1281 (w), 1254 (w), 1194 (m), 1127 (m), 1061 (s), 958

(m), 931 (m), 909 (m), 869 (w), 819 (w), 790 (w); ^{1}H NMR (400 MHz, $CDCl_3$, 23 °C, δ): 9.09 (s, 1H, OO*H*), 9.07 (s, 1H, OO*H*), 2.40–2.26 (m, 2H), 1.82–1.65 (m, 2H), 1.53–1.41 (m, 2H), 1.32–1.19 (m, 2H), 1.11–1.02 (m, 1H), 0.87 (s, 9H, C*H*$_3$); ^{13}C{^{1}H} NMR (101 MHz, $CDCl_3$, 23 °C, ppm): 111.06 (peroxy *C*), 47.59 (*C*H), 32.50 (*C*), 29.91 (*C*H$_2$), 27.79 (*C*H$_3$), 23.54 (*C*H$_2$). Thin, colorless, needle-like single crystals were grown by recrystallization from diethyl ether at –29 °C.

Preparation of 1,1'-Peroxybis(1-hydroperoxycycloheptane) (24). Cycloheptanone was treated with a 50 wt.% aqueous solution of H_2O_2 based on the general procedure for geminal hydroperoxides to obtain a colorless oil that crystallized into 0.209 g (72%) of **24** as thin, colorless, needle-like single crystals in a solution of 1:1 $CHCl_3$:hexanes at –29 °C: mp 71–73 °C (lit[121] 71–72 °C); IR (ν cm^{-1}): 3424 (broad, m), 2931 (s), 2921 (s), 2853 (m), 1708 (m), 1459 (m), 1353 (m), 1277 (m), 1179 (m), 1030 (s), 1014 (s), 988 (m), 960 (m), 912 (s), 893 (m), 862 (m), 834 (s), 779 (m); ^{1}H NMR (400 MHz, $CDCl_3$, 23 °C, δ): 9.63 (s, 2H, OO*H*), 2.04–1.92 (m, 8H), 1.70–1.52 (m, 16H); ^{13}C{^{1}H} NMR (101 MHz, $CDCl_3$, 23 °C, ppm): 116.47 (peroxy *C*), 33.21 (*C*H$_2$), 30.04 (*C*H$_2$), 22.98 (*C*H$_2$).

Preparation of 1,1'-Peroxybis(1-hydroperoxycyclohexane) (25). Cyclohexanone was treated with a 50 wt.% aqueous solution of H_2O_2 based on the general procedure for geminal hydroperoxides to obtain a white solid that was crystallized by slow evaporation in hexanes to obtain 0.246 g (94%) of **25** as colorless, planar, hexagonal single crystals: mp 79–81 °C (lit[121] 80–81 °C); IR (ν cm^{-1}): 3420 (broad, m), 3389 (w), 2942 (m), 2855 (w), 1713 (m), 1652 (m), 1559 (m), 1452 (m), 1365 (m), 1264 (m), 1155 (m), 1057 (s), 949 (s), 929 (m), 913 (s), 850 (m), 822 (m), 784

(w); ^{1}H NMR (400 MHz, $CDCl_3$, 23 °C, δ): 9.54 (s, 2H, OO*H*), 1.95–1.78 (m, 8H), 1.66–1.39 (m, 12H); $^{13}C\{^{1}H\}$ NMR (101 MHz, $CDCl_3$, 23 °C, ppm): 111.38 (peroxy *C*), 30.20 (*C*H_2), 25.54 (*C*H_2), 22.68 (*C*H_2).

Preparation of 1,1-Dihydroperoxy-4,4-dimethylcyclohexane (26). 4,4-Dimethylcyclohexan-1-one was treated with a 50 wt.% aqueous solution of H_2O_2 based on the general procedure to obtain 0.148 g (84%) of **26** as a white solid: mp 80–82 °C; IR (ν cm^{-1}): 3460 (broad, m), 3418 (broad, m) 2950 (m), 2923(m), 1684 (m), 1652 (m), 1559 (m), 1457 (m), 1361 (m), 1278 (w), 1173 (m), 1038 (s), 933 (s), 890 (m) 851 (m); ^{1}H NMR (400 MHz, $CDCl_3$, 23 °C, δ): 8.66 (broad s, 2H, OO*H*), 1.88 (t, 4H, *J* = 6.4 Hz), 1.39 (t, 4H, *J* = 6.4 Hz), 0.96 (s, 6H, C*H*$_3$); $^{13}C\{^{1}H\}$ NMR (101 MHz, $CDCl_3$, 23 °C, ppm): 111.22 (peroxy *C*), 35.33 (*C*H_2), 30.02 (*C*), 27.99 (*C*H_3), 25.87 (*C*H_2). Colorless, long, needle-like single crystals were grown by layering a solution of **26** in $CHCl_3$ with hexanes.

Preparation of 5,5-Dihydroperoxy-*cis*-3,6-dimethylhexahydropentalen-2(1H)-one (27). *cis*-1,5-Dimethylbicyclo[3.3.0]octane-3,7-dione was treated with a 50 wt.% aqueous solution of H_2O_2 based on the general procedure to obtain 0.158 g (73%) of **27** as a white solid: mp 115–117 °C; IR (ν cm^{-1}): 3362 (broad, m), 3187 (broad, m), 2970 (m), 2879 (w), 1722 (s), 1454 (m), 1431 (m), 1325 (w), 1254 (m), 1225 (m), 1138 (w), 1039 (m), 993 (m), 929 (w), 884 (w), 860 (w), 822 (m); ^{1}H NMR (400 MHz, CD_3OD, 23 °C, δ): OO*H* resonance not observed due to exchange with CD_3OD, 2.47 (d, 4H, *J* = 19.6 Hz), 2.17 (d, 2H, *J* = 20.0 Hz), 2.09 (s, 4H), 1.12 (s, 6H, C*H*$_3$); $^{13}C\{^{1}H\}$ NMR (101 MHz, CD_3OD, 23 °C, ppm): 220.47 (*C*), 119.90 (peroxy *C*), 51.97 (*C*H_2), 48.63 (*C*), 46.54 (*C*H_2), 22.14 (*C*H_3); ESI-HRMS: calcd for $[C_{10}H_{16}O_5Na]^+$ 239.0895; found

239.1043. Colorless, diamond-shaped single crystals were grown by layering a solution of **27** in methanol with hexanes.

Preparation of (Dihydroperoxymethyl)benzene (28). Compound **28** was prepared in 80% yield as a colorless oil by a literature procedure[95] starting from benzaldehyde: IR (ν cm^{-1}): 3424 (broad, m), 3095 (w), 3065(w), 3041 (w), 1659 (w), 1495 (w), 1453 (m), 1342 (m), 1304 (m), 1196 (w), 1086 (w), 1023 (m), 984 (m), 923 (w), 854 (w), 808 (w), 751 (s), 711 (s), 695 (s); ^{1}H NMR (400 MHz, $CDCl_3$, 23 °C, δ): 9.60 (s, 2H, OO*H*), 7.50–7.30 (m, 5H, C*H*), 6.30 (s, 1H, C*H*); $^{13}C\{^{1}H\}$ NMR (101 MHz, $CDCl_3$, 23 °C, ppm): 132.71 (*C*), 129.83 (*C*H), 128.62 (*C*H), 127.17 (*C*H), 110.08 (peroxy *C*H).

Preparation of 1,1-Dihydroperoxy-4-methylcyclohexane (29). Compound **29** was prepared in 88% yield as a white solid by a literature procedure[95] starting from 4-methylcyclohexan-1-one: decomposes around 115 °C (lit[95] mp 135 °C with decomposition); IR (ν cm^{-1}): 3420 (broad, m), 2977 (m), 2962(m), 2944 (m), 2873 (w), 1715 (m), 1651 (m), 1557 (m), 1471 (m), 1324 (w), 1185 (s), 1076 (s), 1013 (w), 971 (s), 829 (s); ^{1}H NMR (400 MHz, $CDCl_3$, 23 °C, δ): 9.16 (broad s, 2H, OO*H*), 2.26–2.16 (m, 2H), 1.72–1.61 (m, 2H), 1.58–1.40 (m, 3H), 1.20 (q of d, 2H, *J* = 11.6, 4.0 Hz), 0.93 (d, 3H, *J* = 6.8 Hz, C*H*$_3$); $^{13}C\{^{1}H\}$ NMR (101 MHz, $CDCl_3$, 23 °C, ppm): 111.38 (peroxy *C*), 31.78 (*C*H), 30.77 (*C*H_2), 29.24 (*C*H_2), 21.60 (*C*H_3). Large, thick, colorless, plate-like single crystals were grown by slow evaporation of a solvent mixture of 1:1:1 hexanes:petroleum ether:diethyl ether.

Preparation of 1,1'-Peroxybis(1-hydroperoxycyclopentane) (30). Cyclopentanone was treated with a 50 wt.% aqueous solution of H_2O_2 based on the

general procedure for geminal hydroperoxides to obtain a colorless oil that crystallized in to 0.218 g (93%) of **30** as colorless, polygonal single crystals in a toluene at –29 °C: mp 60–63 °C (lit[121] 60–63 °C); IR (ν cm^{-1}): 3418 (broad, m), 2949 (m), 2872 (w), 1753 (s), 1730 (s), 1711 (s), 1452 (m), 1435 (m), 1387 (m), 1368 (m), 1325 (m), 1306 (w), 1252 (m), 1186 (s), 1179 (s), 1074 (s), 1059 (s), 1032 (m), 1013 (m), 972 (s), 947 (s), 886 (m), 829 (m), 789 (m), 772 (w); ^{1}H NMR (400 MHz, CD_3OD, 23 °C, δ): OO*H* resonance not observed due to exchange with CD_3OD, 2.02–1.86 (m, 8H), 1.80–1.64 (m, 8H). $^{13}C\{^{1}H\}$ NMR (101 MHz, CD_3OD, 23 °C, ppm): 121.63 (peroxy *C*), 34.37 (*C*H_2), 25.51 (*C*H_2).

Preparation of 1,1-Dihydroperoxy-3-methylcyclopentane (31). 3-Methylcyclopentan-1-one was treated with a 50 wt.% aqueous solution of H_2O_2 based on the general procedure and the product was purified by silica gel column chromatography with 10:1 dichloromethane:ethyl acetate and then 4:1 dichloromethane:ethyl acetate to obtain 0.144 g (97%) of **31** as a colorless oil. IR (ν cm^{-1}): 3406 (broad, m), 2957 (s), 2871 (m), 1458 (m), 1435 (m), 1379 (w), 1312 (m), 1274 (w), 1193 (m), 1150 (m), 1086 (w), 1023 (w), 971 (s), 928 (m), 829 (s); ^{1}H NMR (400 MHz, CD_3OD, 23 °C, δ): 2.16–1.92 (m, 3H), 1.88–1.75 (m, 2H), 1.47–1.19 (m, 2H), 1.99 (d, 3H, J = 6.4, C*H*$_3$); $^{13}C\{^{1}H\}$ NMR (101 MHz, CD_3OD, 23 °C, ppm): 121.66 (peroxy *C*), 42.18 (*C*H_2), 34.19 (*C*H), 33.76 (*C*H_2), 20.02 (*C*H_3). ESI-HRMS: calcd for $C_{14}H_{28}O_4Na$ 283.1885; found 283.1874.

Preparation of 1,1-Dihydroperoxycyclopentane (32). Compound **32** was prepared in 92% yield as a colorless oil by a literature procedure[95] starting from cyclopentanone: IR (ν cm^{-1}): 3389 (broad, m), 2959 (m), 2875 (m), 1708 (m), 1437 (m),

1384 (m), 1327 (m), 1196 (s), 1184 (s), 1075 (s), 969 (s), 868 (m), 828 (s); ^{1}H NMR (400 MHz, $CDCl_3$, 23 °C, ppm): 9.66 (s, 2H, OO*H*), 2.07–1.88 (m, 4H), 1.82–1.65 (m, 4H); $^{13}C\{^{1}H\}$ NMR (101 MHz, $CDCl_3$, 23 °C, ppm): 122.76 (peroxy *C*), 33.31 (*C*H_2), 24.77 (*C*H_2).

Preparation of 4,4-Dihydroperoxycyclopent-1-ene (33). Cyclopent-3-en-1-one was treated with a 50 wt.% aqueous solution of H_2O_2 based on the general procedure on a 3 times larger scale to obtain 0.085 g (21%) of **33** as a colorless viscous oil. IR (ν cm^{-1}): 3401 (broad, m), 3067 (w), 2928 (w), 2840 (w), 1712 (m), 1688 (m), 1651 (w), 1622 (w), 1424 (m), 1397 (m), 1315 (s), 1236 (s), 1189 (w), 1075 (s), 1036 (m), 960 (s), 875 (m), 839 (s), 779 (s); ^{1}H NMR (400 MHz, $CDCl_3$, 23 °C, δ): 9.82 (bs, 2H, OO*H*), 5.63 (S, 2H, C*H*), 1.72 (s, 4H, C*H*$_2$); $^{13}C\{^{1}H\}$ NMR (101 MHz, $CDCl_3$, 23 °C, ppm): 127.47 (*C*H), 121.24 (peroxy *C*), 39.66 (*C*H_2).

Preparation of 2,2,5,5-Tetrahydroperoxy-*cis*-3,6-dimethyloctahydropentalene (34). 3,6-Dimethyltetrahydropentalene-2,5(1H,3H)-dione was treated with a 50 wt.% aqueous solution of H_2O_2 (4.5 equivalents per ketone/aldehyde group) based on the general procedure on a 2 times larger scale and the product was purified by silica gel column chromatography with 20:1 dichloromethane:methanol to obtain 0.061 g (21%) of **34** as a white solid: mp not taken due to explosion hazard; IR (ν, cm^{-1}) 3365 (broad, m), 2965 (m), 2874 (m), 2808 (w), 1688 (w), 1452 (m), 1431 (m), 1380 (m), 1319 (m), 1274 (s), 1225 (m), 1189 (m), 1156 (m), 1125 (m), 1083 (m), 1045 (s), 1001, 993 (m), 982 (m), 945 (m), 901 (m), 866 (m), 826 (s), 798 (m), 732 (w); ^{1}H NMR (400 MHz, CD_3OD, 23 °C, δ) OO*H* resonances not observed due to exchange with CD_3OD, 2.18 (d, 4H, *J* = 14.8 Hz), 1.88 (d, 2H, *J* = 14.8

Hz), 1.01 (s, 6H, C*H*$_3$); ^{13}C{^{1}H} NMR (101 MHz, CD_3OD, 23 °C, ppm): 120.14 (peroxy *C*), 50.55 (C), 46.49 (*C*H_2), 22.27 (*C*H_3); Anal. Calcd for $C_{10}H_{18}O_8$: C, 45.11; H, 6.81. Found: C, 44.90; H, 6.90. Colorless, planar, hexagonal crystals of **34** were grown by slow evaporation from diethyl ether.

Preparation of 2,2,5,5-tetrahydroperoxyoctahydropentalene (35). *cis*-1,5-Dimethylbicyclo[3.3.0]octane-3,7-dione was treated with a 50 wt.% aqueous solution of H_2O_2 (8.5 equivalents per ketone/aldehyde group) based on the general procedure on a 0.4 scale and the reaction mixture was concentrated under reduced pressure to obtain 0.031 g (64%) of **35** as a crude white solid. In an attempt to purify the crude product by silica gel column chromatography with 4:1 dichloromethane:ethyl acetate, an explosion occurred upon solvent removal under reduced pressure: mp not taken due to explosion hazard; ^{1}H NMR (400 MHz, CD_3OD, 23 °C, δ) OO*H* resonances not observed due to exchange with CD_3OD, 2.72–2.56 (m, 2H, C*H*), 2.18 (d of d, 4H, *J* = 14.4, 8.8 Hz), 1.86 (d of d, 4H, *J* = 14.4, 5.6 Hz); ^{13}C{^{1}H} NMR (101 MHz, CD_3OD, 23 °C, ppm): 122.10 (peroxy *C*), 40.54 (*C*H), 39.03 (*C*H_2). Anal. Calcd for $C_8H_{14}O_8$: C, 40.34; H, 5.92. Found: C, 39.98; H, 5.77.

Preparation of 1,4-Bis(dihydroperoxymethyl)benzene (36). Terephthalaldehyde was treated with a 50 wt.% aqueous solution of H_2O_2 based on the general procedure on an 8 times larger scale to obtain 0.328 g (35%) of **36** as a white solid: mp. 108–110 °C; IR (ν, cm^{-1}) 3236 (broad, m), 2944 (w), 2816 (w), 2797 (w), 2762 (w), 2738 (w), 1699 (w), 1683 (w), 1413 (m), 1314 (m), 1201 (w), 1128 (w), 1033 (s), 982 (s), 930 (w), 869 (m), 825 (w), 781 (s), 693 (s); ^{1}H NMR (400 MHz, CD_3OD, 23 °C, δ) OO*H* resonance not observed due to exchange with CD_3OD, 7.45 (s, 4H, C*H*), 6.10

(s, 2H, C*H*); $^{13}C\{^{1}H\}$ NMR (101 MHz, CD_3OD, 23 °C, ppm): 136.78 (*C*), 128.02 (*C*H), 110.73 (peroxy *C*H); Anal. Calcd for $C_8H_{10}O_8$: C, 41.04; H, 4.30. Found: C, 41.02; H, 4.50. Colorless, diamond-shaped single crystals of **36** were grown by layering a solution of compound **36** in 1:1 THF:diethyl ether with hexanes.

Preparation of 2,2,5,5-Tetrahydroperoxyhexane (37). Hexane-2,5-dione was treated with a 50 wt.% aqueous solution of H_2O_2 based on the general procedure on a 2 time larger scale. Then, dichloromethane (10 mL) was added to the reaction mixture and it was concentrated under reduced pressure. The aqueous layer was separated from the dichloromethane layer by decanting it. This aqueous layer was dissolved in methanol and was concentrated under reduced pressure. Then, the product was purified by silica gel column chromatography with 10:1 dichloromethane:methanol to obtain 0.045 g (21%) of **37** as a white solid: mp 121–123 °C; IR (ν cm^{-1}): 3381 (broad, m), 3315 (broad, m), 2955 (w), 2916 (w), 1371 (s), 1293 (m), 1223 (s), 1099 (s), 1071 (s), 889 (m), 855 (m); ^{1}H NMR (400 MHz, CD_3OD, 23 °C, δ): 1.79 (s, 4H, CH_2), 1.33 (s, 6H, CH_3); $^{13}C\{^{1}H\}$ NMR (101 MHz, CD_3OD, 23 °C, ppm): 111.71 (*C*), 28.92 (*C*H_2), 18.37 (*C*H_3).

Preparation of 1,1,4,4-Tetrahydroperoxycyclohexane (38). Cyclohexane-1,4-dione was treated with a 50 wt.% aqueous solution of H_2O_2 based on the general procedure on a 2 times larger scale and the reaction mixture was concentrated under reduced pressure to afforded a crude white precipitate. This precipitate was separated by filtration and was washed with CH_3CN (10 mL) to obtain 0.102 g (47%) of **38** as a white solid: mp not taken due to explosion hazard; IR (ν, cm^{-1}) 3308 (broad, m), 2929 (broad, m), 2627 (w), 2529 (w), 1710 (s), 1407 (s), 1304 (m), 1195 (s), 1174 (s), 1072

(m), 957 (m), 909 (s), 800 (m). Anal. Calcd for $C_6H_{12}O_8$: C, 33.97; H, 5.70. Found: C, 33.61; H, 6.03; ^{1}H NMR (400 MHz, CD_3OD, 23 °C, δ) 10.63 (broad s, 4H, OO*H*), 1.86 (s, 8H, C*H*$_2$); ^{13}C{^{1}H} NMR (101 MHz, CD_3OD, 23 °C, ppm) 109.83 (peroxy *C*), 26.73 (*C*H$_2$). Purification or crystallization of **38** was not carried out due to explosion hazard.

CHAPTER 5

Tuning the Impact and Friction Sensitivities and Energetic Performances of a Series of Well-Characterized Cyclic Hydroperoxy Compounds

5.1 Introduction

5.1.1 Sensitivities and Energetic Performances of Peroxo-Based Compounds

TATP, DADP, HMTD, and MEKP are the only peroxo-based compounds that have been energetically characterized, but these compounds are also known to be extremely sensitive to impact and friction, which hinders their applications as HEDMs.[35,36] For the applications of peroxo-based oxygen-rich compounds as safer HEDMs, the impact and friction sensitivities need to be reduced. Also, the energetic properties of peroxo-based oxygen-rich compounds need to be more systematically studied to understand and improve the low detonation performances of TATP, DADP, HMTD, and MEKP (Tables 3–6).[6b,35,64,65,73]

There have been many attempts to reduce the high sensitivities of the known peroxo-based compounds using different strategies, without much success.[122] Matyáš has used water and WD-40 oil as desensitizing agents to reduce the friction sensitivities of TATP, DADP, and HMTD.[122a] Although a significant reduction of friction sensitivity was observed with about 20 wt.% of water and WD-40 oil,[122a] this could lead to reduced detonation performances as well. Contini has used low-melting paraffin wax as a phlegmatizing agent with TATP and DADP to perform enthalpies of combustion and formation using oxygen bomb calorimetry.[122b] Recently, co-crystallization has been employed to use complex solid state characteristics to influence the density, oxygen balance, and sensitivity of peroxo-based co-crystals of DADP.[68] The presence of

stabilizing I···O interactions in the crystalline lattice of 1,3,5-triiodo-2,4,6-trinitrobenzene (TITNB) and DADP cocrystals has resulted in lower sensitivities of both components.[68b] However, little is understood about how these solid-state interactions affect the physical properties of materials. Also, many different solid-state characteristics may act simultaneously to influence the physical properties. Thus, the predictability and fine tuning capability of impact and friction sensitivities through solid-state interactions are low.

The low detonation performances of TATP, DADP, HMTD, and MEKP have also resulted in avoidance of research development on peroxo-based oxygen-rich compounds to develop HEDMs.[2,35] The difficulty in increasing the oxygen balance without increasing the sensitivities, low crystalline densities, and low thermal and chemical stabilities are the difficult challenges to overcome for better performing peroxo-based HEDMs.[2,35,68]

Herein, we have synthesized a series of cyclic hydroperoxy compounds to study and understand how structural variations can be used to tune the impact and friction sensitivities and the energetic properties of peroxo-based compounds. The structural variations are more convenient to control and the resultant properties are more predictable once the structure and function relationships are understood. The synthesis and study of the properties of stable five- and six-membered cyclic peroxo-based compounds have been popular among the organic research community.[123]

5.1.2 Five- and Six-Membered Cyclic Peroxides

Interest in five- and six-membered cyclic peroxides such as tetroxanes, trioxanes, dioxanes, trioxolanes, and dioxolanes (Figure 49) has been due to their

presence as structural units in natural products and antimicrobial, antiproliferative, and antitumor activities.[123,124] Hydroperoxy dioxolanes have been employed as oxidizing agents.[125] Still, no study has been carried out to discover the energetic properties of these oxygen-rich cyclic peroxides.

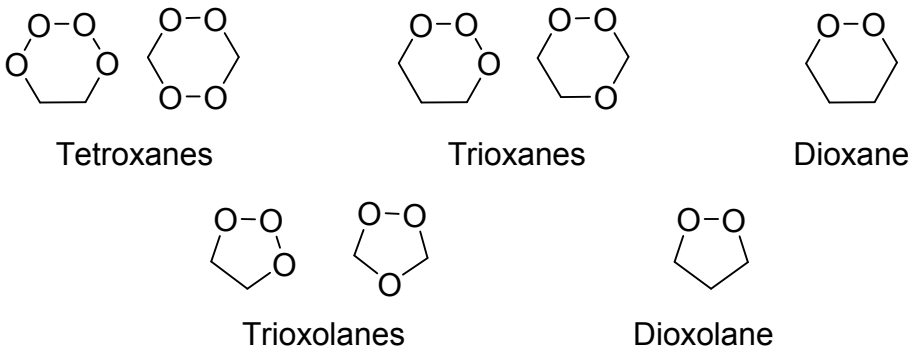

Figure 49. Five- and six-membered cyclic peroxides.

The reactions of β- and γ-diketones with H_2O_2 were studied in detail where structures and properties of oxygen-rich hydroperoxy dioxolanes and dioxanes were further discussed.[126] Milas has reported that the hydroperoxy dioxolanes and dioxanes obtained by the reactions between 2,4-pentanedione and 2,5-hexanedione with H_2O_2 were highly brisant and shock sensitive compounds.[126b,c] In these reactions between the diketones and H_2O_2, cyclic peroxides with hydroxy groups or both hydroxy and peroxy groups were also obtained.[126] The energetic properties of even these highly oxygen-rich cyclic hydroxy and/or hydroperoxy compounds were not studied.

In this Chapter, different β- and γ-diketones were chosen to react with H_2O_2 for the synthesis of a series of oxygen-rich cyclic hydroperoxy compounds. Dihydroperoxy compounds **39**–**43** (Figure 50) and hydroperoxy compounds **44**–**48** (Figure 51) were

obtained for a systematic study of their sensitivities and energetic properties. In the hydroperoxy dioxanol **44** and dioxolanols **45**–**48**, there is a hydroxy group instead of a hydroperoxy group of the dihydroperoxy dioxane **39** and dioxolanes **40**–**43**.

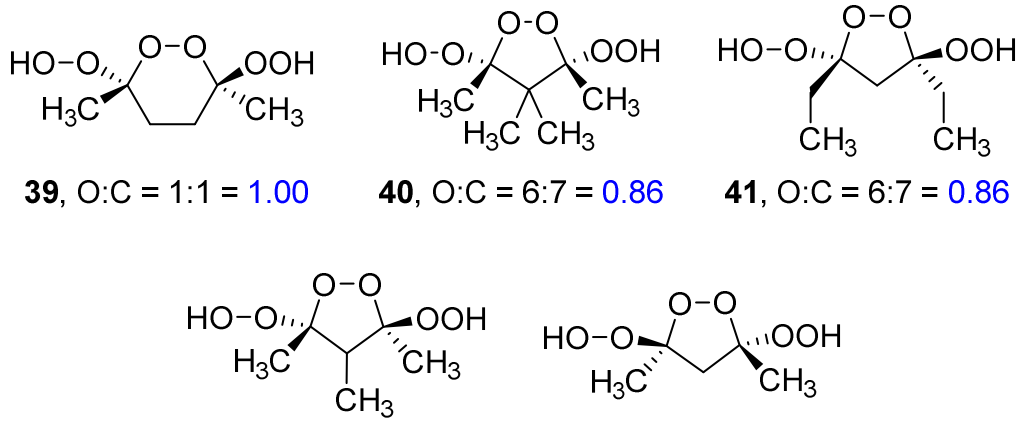

39, O:C = 1:1 = 1.00 **40**, O:C = 6:7 = 0.86 **41**, O:C = 6:7 = 0.86

42, O:C = 1:1 = 1.00 **43**, O:C = 6:5 = 1.20

Figure 50. Dihydroperoxy dioxane **39** and dioxolanes **40**–**43**.

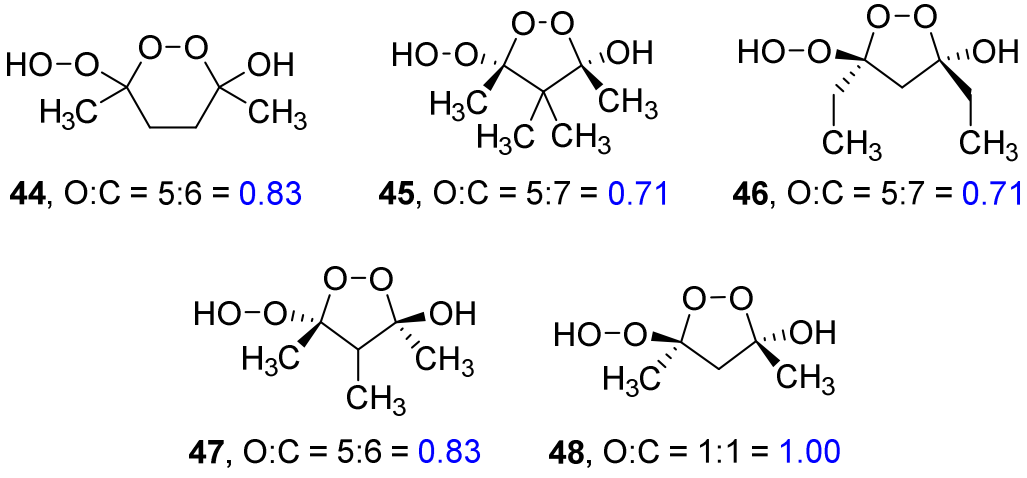

44, O:C = 5:6 = 0.83 **45**, O:C = 5:7 = 0.71 **46**, O:C = 5:7 = 0.71

47, O:C = 5:6 = 0.83 **48**, O:C = 1:1 = 1.00

Figure 51. Hydroperoxy dioxanol **44** and dioxolanols **45**–**48**.

The O:C ratios of these cyclic hydroperoxy compounds were in the range of 0.71–1.20. Dihydroperoxy dioxane **39** and dioxolanes **40**–**43** contain one more oxygen atom than the corresponding hydroperoxy dioxanol **44** and dioxolanols **45**–**48**. All of the solid cyclic hydroperoxy compounds were fully characterized without structural ambiguities with X-ray crystal structures. Their stereochemistry was assigned based on the X-ray crystal structures. The oxygen content, ring strain, and steric strain were varied to observe the effects on their sensitivities and energetic performances. Interestingly, we have discovered that the impact and friction sensitivities and energetic properties of peroxo-based compounds can be tuned through these structural variations.

5.2 Results and Discussion

The dihydroperoxy compounds **39**–**43** and hydroperoxy compounds **44**–**48** all contain relatively high oxygen contents similar to the more oxygen-rich geminal hydroperoxides of Chapter 5. Compounds **43** and **48** are the highest oxygen containing dihydroperoxy and hydroperoxy compounds. The effect of a more stable hydroxy group in place of a hydroperoxy group can be studied by comparison of the energetic properties of the corresponding hydroperoxy and dihydroperoxy compounds. The dihydroperoxy compound pair **39** and **42** and hydroperoxy compound pair **44** and **47** can be used to observe the effects of increased ring strain. The dihydroperoxy compound pair **40** and **41** and hydroperoxy compound pair **45** and **46** can be used to observe the effects of increased steric strain. Compounds **40** and **45** are the only *cis*-compounds obtained in this study. The rest of the dihydroperoxy and hydroperoxy compounds are *trans*.

5.2.1 Synthetic Aspects

Caution: Organic peroxo-based compounds and high concentrations of aqueous H_2O_2 are potentially explosive and require handling with care. Reactions and other manipulations were performed in a fume hood behind a blast shield. Personal safety gear was used whenever necessary: a face shield, leather gloves, and a leather apron. Interactions with strong acids, metals, metal salts, or easily oxidizable species were avoided to prevent hazardous decomposition reactions. All reactions were performed on small scales (≤ 300 mg) and at room temperature.

The two series of cyclic peroxo-based oxygen-rich compounds were synthesized by treating the corresponding diketones with H_2O_2 in the presence of a catalyst at or below room temperature (Scheme 1) and the products (except **39**, **41**, and **43**) were purified by silica gel column chromatography to obtain moderate yields. Compounds **39**, **41**, and **43** were purified by direct re-crystallizations also to obtain moderate yields.

Iodine was used as the catalyst in the syntheses of **39**, **40**, **42**, and **45**–**47** based on a modified published procedure for geminal hydroperoxides.[95] Briefly, a solution of I_2 in CH_3CN and H_2O_2 was treated with the corresponding diketone, and the reaction was stirred at room temperature for 5–24 h. Iodine was the preferred catalyst due to the low cost, safety, and high efficiency observed in the reactions.[95] Compound **39** was purified by re-crystallization in a concentrated solution of methanol at –29 °C while the compounds **40**, **42**, and **45**–**47** were purified by silica gel column chromatography using dichloromethane and/or dichloromethane and ethyl acetate solution mixtures as mobile phases. Compounds **39**, **40**, **42**, and **45**–**47** were all obtained in moderate yields.

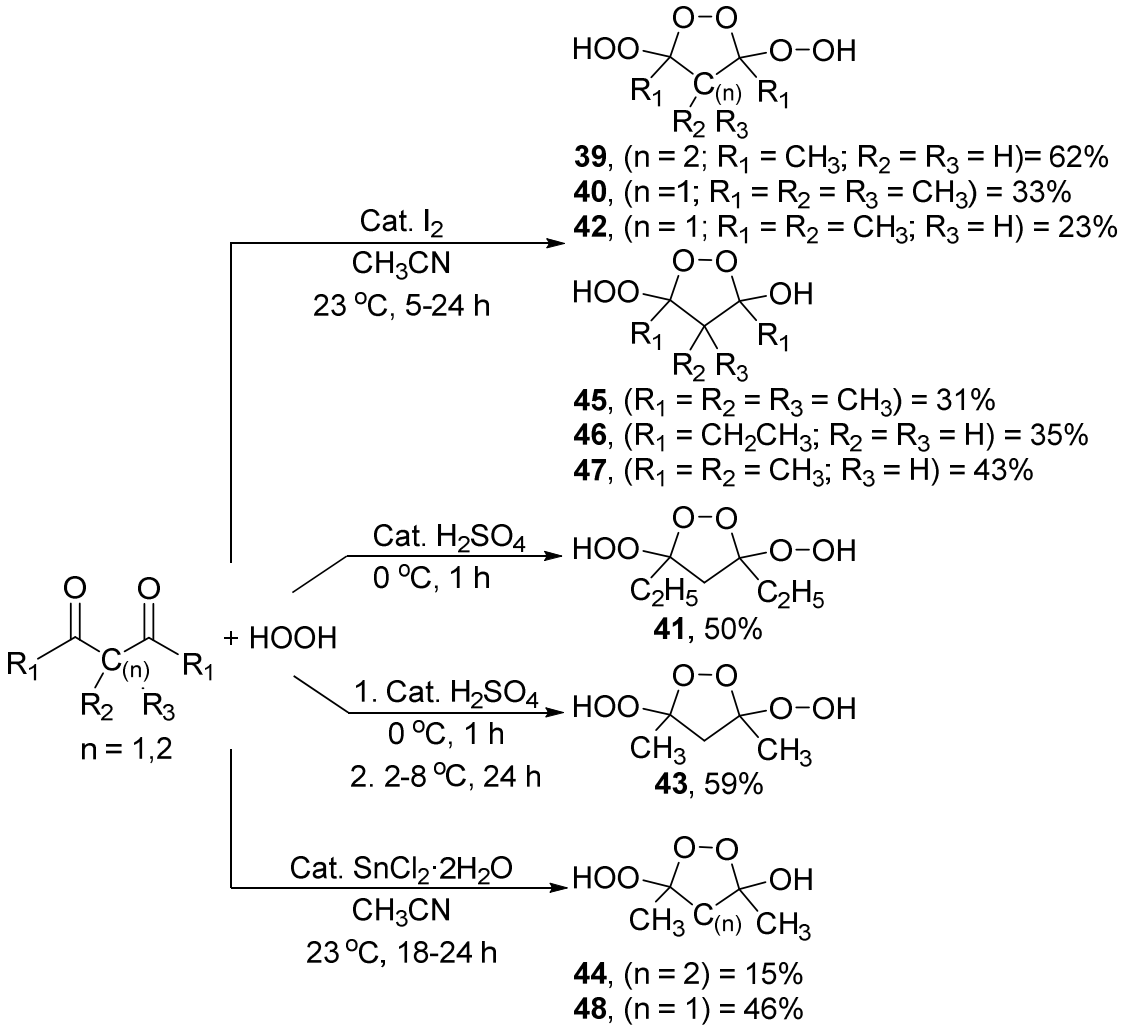

Scheme 8. Synthesis of cyclic dihydroperoxy and hydroperoxy compounds.

Synthesis of **41** was not possible using the iodine-based method, and the corresponding reaction only produced **46**. A solution of H_2O_2 and a catalytic amount of concentrated H_2SO_4 acid was treated with 3,5-heptanedione and the reaction was stirred for 1 h at 0 ˚C to obtain the crude solid of **41**. A low temperature was sufficient with the stronger H_2SO_4 acid catalyst for the reaction to proceed. This synthetic method, which uses concentrated H_2SO_4 acid as the catalyst, was rapid and produced **41** exclusively. Compound **41** was recrystallized by slow evaporation in diethyl ether, and pure **41** was obtained in a moderate yield. Compound **43** was synthesized using a

modified published procedure with the use of a catalytic amount of concentrated H_2SO_4 acid as well.[126c] Briefly, a solution of H_2O_2 and a catalytic amount of concentrated H_2SO_4 acid was treated with 2,4-pentanedione and the reaction was stirred for 1 h, after which it was kept at 2–8 °C for 24 h. No additional solvent was used in these reactions. A longer reaction time was required for the synthesis of **43** with respect to **41**. Purification of **43** was carried out by recrystallization in a solution mixture of 20:1 dichloromethane:ethyl acetate at –29 °C to obtain **43** in a moderate yield. The hydroperoxy analogues **46** and **48** were not obtained in the H_2SO_4 acid-based synthetic methods of **41** and **43**, revealing that the strong acid is able to catalyze the reaction all the way until three H_2O_2 molecules react to provide **41** and **43**.

Since **44** was not obtained during the iodine-based synthetic procedure of **39**, and **48** was not obtained in the concentrated H_2SO_4 acid-based procedure of **43**, the Lewis acid catalyst $SnCl_2{\cdot}2H_2O$ was used as a heterogeneous catalyst in the syntheses of **44** and **48** based on a slightly modified published procedure for **43**.[125a] Briefly, a mixture of the corresponding diketone in CH_3CN and $SnCl_2{\cdot}2H_2O$ was treated with H_2O_2 and the reaction was allowed to stir at room temperature for 18–24 h. Both **44** and **48** were purified by silica gel column chromatography using a 4:1 dichloromethane:ethyl acetate solution mixture as the mobile phase. Compound **44** was only obtained in a low yield, since **39** was still the major product in the Lewis acid $SnCl_2{\cdot}2H_2O$-based procedure. Compound **48** was obtained in a moderate yield.

Compounds **39**–**43** and **45**–**48** were all isolated as solids. Compound **44** was the only compound that was isolated as a colorless oil. The cyclic hydroperoxy compounds **40**–**42** and **44**–**47** were new compounds obtained in this study. X-ray quality single

crystals were obtained by either cooling at –29 °C (**39**, **42**, **43**, **45**, and **47**) or slow evaporation (**40**, **41**, **46**, and **48**) of saturated solutions of the corresponding crude (**39**, **41**, and **43**) or purified (**40**, **42**, and **45**–**48**) compounds. All of the cyclic hydroperoxy compound single crystals obtained were colorless. They were in the forms of plate-like (**39**, **46**), needle-like (**41**), hexagonal (**47**), or polygonal (**40**, **45**, **42**, **43**, and **48**) single crystals.

Attempts to synthesize more oxygen-rich cyclic hydroperoxy compounds using diketones or dialdehydes with fewer carbons either resulted in oils that could be energetically characterized in our study or produced violent reactions. Thus, the highest O:C ratio that was safely achievable was 1.20. All compounds were characterized with ^{1}H and ^{13}C NMR spectroscopy, infrared (IR) spectroscopy, and elemental analyses. Additionally X-ray crystal structures were obtained for all the solid cyclic hydroperoxy compounds **39**–**43** and **45**–**48**.

5.2.2 Spectroscopy

^{1}H and ^{13}C NMR spectra were obtained in CD_3OD solutions and thus, the OOH and OH resonances were not observed due to exchange with CD_3OD. The characteristic hydroperoxy-C and hydroxy-C ^{13}C NMR peaks aided in identification of the dihydroperoxy compounds and hydroperoxy compounds, respectively. ^{13}C NMR chemical shifts of hydroperoxy-Cs were in the range of 107.21–115.93 ppm and were more deshielded than the ^{13}C NMR chemical shifts of hydroxy-Cs, which were in the range of 100.04–108.57 ppm. The differences of ^{1}H and ^{13}C NMR spectra based on the symmetry of the dihydroperoxy compounds versus hydroperoxy compounds was also important to differentiate these compounds, except in the case of **42** and **47**. The fixed

orientation of CH_3 and H groups on the central carbon of compound **42** with respect to the functional groups on the sides with *trans*-stereochemistry changes the environment of the hydroperoxy-C atoms, resulting in different chemical shifts. But this chemical shift difference (1.86 ppm) is smaller than the mean chemical shift difference of hydroperoxy-Cs and hydroxy-Cs (7.29 ppm).

Vibrational spectroscopy was also useful in characterization of the peroxo-based compounds. Compounds **39** and **44** have broad peaks at 3332 cm^{-1} and 3399 cm^{-1} for O–H stretching frequencies, respectively. These frequencies are in the region of hydrogen-bonded O–H stretching frequencies. Also, these values are close to each other and that indicates equal participation in hydrogen bonding. There is a significant difference in the O–H stretching region of the five-membered ring containing dihydroperoxy compounds **40**–**43** and the hydroperoxy compounds **45**–**48**. The dihydroperoxy compounds **40**–**43** each contains only one broader peak for the O–H stretching frequency in the range of 3362–3414 cm^{-1}. In contrast, the hydroperoxy compounds **45**–**48** contain two narrower peaks in the ranges of 3410–3455 cm^{-1} and 3260–3333 cm^{-1}. These frequencies might be corresponding to the two different hydroperoxy and hydroxy group O–H frequencies, respectively. The lower hydroxy group O–H frequencies indicate stronger hydrogen bonding interactions. The other characteristic IR stretching frequencies of the peroxo-based compounds are medium or strong C–O stretching modes in the range of 1000–1300 cm^{-1},[96,97] and weak O–O stretching modes in the range of 800–900 cm^{-1}.[21] Compounds **39**–**43** and **45**–**48** all contain multiple medium and strong peaks in the region of 1000–1300 cm^{-1} for C–O stretching modes. The appearance of strong peaks in the range of 800–1000 cm^{-1} in the

IR spectra of **39**–**43** and **45**–**48** indicate strong coupling of C–O and O–O stretching modes as reported.[96,98]

5.2.3 X-Ray Crystal Structures

X-ray crystal structures were obtained for all of the solid cyclic hydroperoxy compounds **39**–**43** and **45**–**48**. They were all normal structures without unusual interactions. No solvate crystals were obtained for the cyclic dihydroperoxy and hydroperoxy compounds. Experimental crystallographic data of the X-ray crystal structures of **39**–**43** and **45**–**48** are summarized in Tables 31 and 32, respectively. Perspective views of the crystal structures of **39**–**43** and **45**–**48** are given in Figures 52–60. Selected bond lengths and bond angles from the crystal structures of **39**–**43** and **45**–**48** are provided in Tables 33 and 34, respectively. The lists of hydrogen bonds and short contacts of **39**–**43** and **45**–**48** generated from Mercury 3.5.1 software are provided in Tables 35–38.

The O–O bond lengths of the cyclic hydroperoxy compounds **39**–**43** and **45**–**48** (Tables 33 and 34) were in the range of the O–O bond lengths reported for hydroperoxides.[99] The crystalline densities of **39**–**43** are in the range of 1.387–1.469 g/cm^3, while the crystalline densities of **45**–**48** are in the range of 1.328–1.474 g/cm^3. These crystalline densities are higher than that of the *tert*-butyl peroxides and *tert*-butyl peroxy esters, but lower than the geminal hydroperoxides **36** and **38** of Chapter 4. The crystalline densities of **43** and **48** are the highest from the cyclic dihydroperoxy and hydroperoxy compounds, respectively. The crystalline density of **48** is the highest crystalline density obtained for the cyclic hydroperoxy compounds.

Table 31. Experimental crystallographic data of **39**–**43**.

	39	**40**	**41**	**42**	**43**
Formula	$C_5H_{10}O_7$	$C_{14}H_{28}O_{12}$	$C_7H_{14}O_6$	$C_6H_{12}O_6$	$C_5H_{10}O_6$
FW	182.13	388.36	194.18	180.16	166.13
Space group	I -4	P b c a	P 1 2_1/n 1	P b c a	P 1 2_1/n 1
a (Å)	14.0266(7)	12.6452(16)	5.6429(3)	8.1894(6)	5.5729(5)
b (Å)	14.0266(7)	12.5922(15)	17.6201(9)	6.6753(4)	15.4498(12)
c (Å)	8.7135(5)	23.364(3)	9.1491(5)	30.7184(19)	8.7244(7)
V (Å^3)	1714.3(2)	3720.3(8)	909.63(8)	1679.27(19)	751.17(11)
Z	8	8	4	8	4
T (K)	100(2)	100(2)	100(2)	100(2)	100(2)
λ (Å)	0.71073	0.71073	0.71073	0.71073	0.71073
ρ_{calc} (g/cm^3)	1.411	1.387	1.418	1.425	1.469
μ (mm^{-1})	0.136	0.122	0.125	0.129	0.138
R(F)[a] (%)	2.93	3.05	3.80	4.50	6.18
R_w(F)[b] (%)	8.83	8.22	10.93	12.54	23.33

[a] $R(F) = \sum \| |F_o| - |F_c| \| / \sum |F_o|$; [b] $Rw(F) = [\sum w(F_o^2 - F_c^2)^2 / \sum w(F_o^2)^2]^{1/2}$

Table 32. Experimental crystallographic data of **45**–**48**.

	45	**46**	**47**	**48**
Formula	$C_7H_{14}O_5$	$C_7H_{14}O_5$	$C_6H_{12}O_5$	$C_5H_{10}O_5$
FW	178.18	178.18	164.16	150.13
Space group	P 1 2_1/n 1	P b c a	P 1 2_1/n 1	P 1 2_1/n 1
a (Å)	8.811(2)	9.9659(7)	7.6155(5)	8.6193(6)
b (Å)	8.8031(18)	10.7296(7)	11.9510(8)	8.7945(6)
c (Å)	11.281(3)	16.6680(12)	9.3339(6)	9.2016(6)
V (Å^3)	870.4(3)	1782.3(2)	779.08(9)	676.56(8)
Z	4	8	4	4
T (K)	100(2)	100(2)	100(2)	100(2)
λ (Å)	0.71073	0.71073	0.71073	0.71073
ρ_{calc} (g/cm^3)	1.360	1.328	1.400	1.474
μ (mm^{-1})	0.116	0.113	0.123	0.134
R(F)[a] (%)	4.85	3.01	3.57	3.62
R_w(F)[b] (%)	13.71	9.15	9.41	12.61

[a] $R(F) = \sum \| |F_o| - |F_c| \| / \sum |F_o|$; [b] $Rw(F) = [\sum w(F_o^2 - F_c^2)^2 / \sum w(F_o^2)^2]^{1/2}$

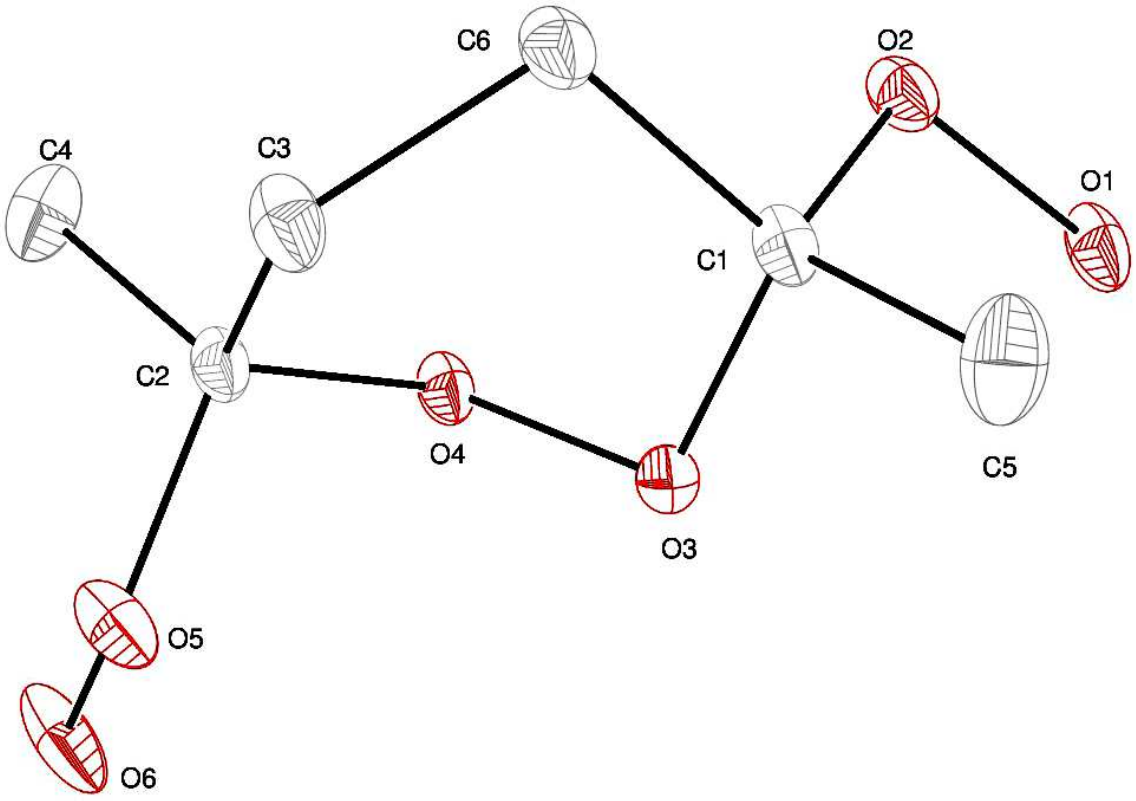

Figure 52. Perspective view of **39** with thermal ellipsoids at the 50% probability level.

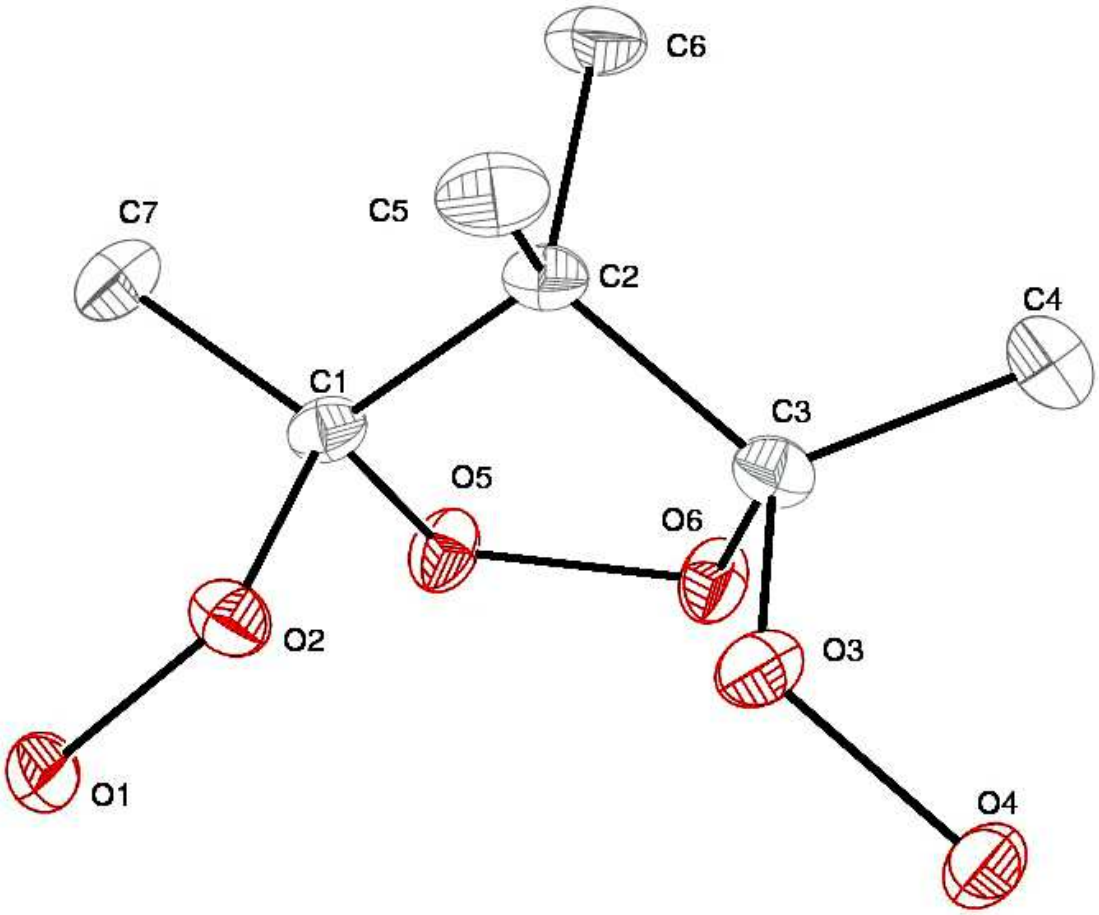

Figure 53. Perspective view of **40** with thermal ellipsoids at the 50% probability level.

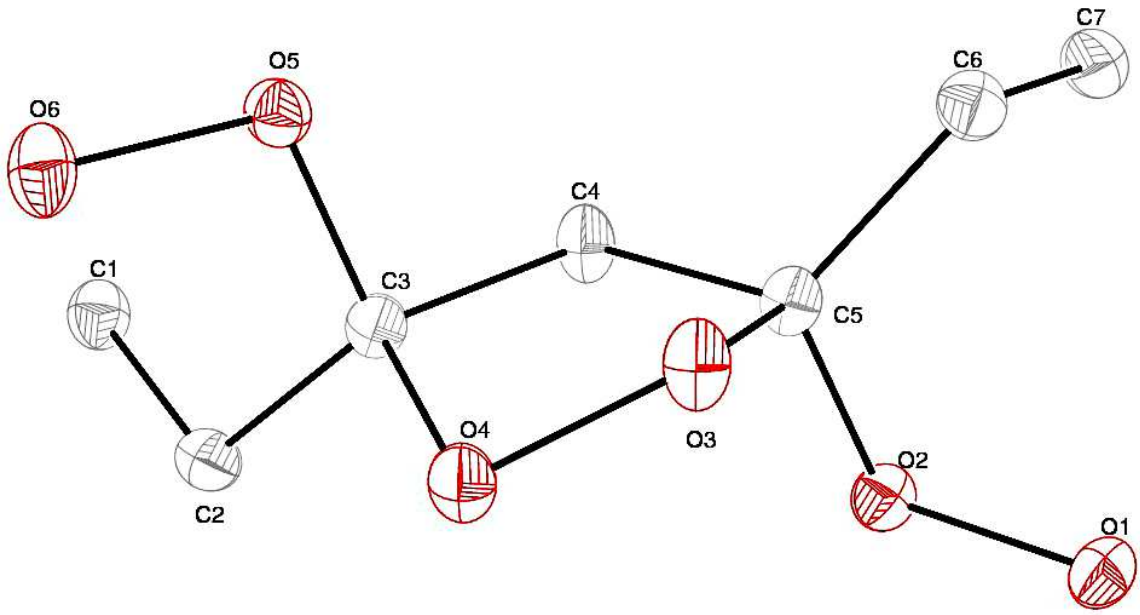

Figure 54. Perspective view of **41** with thermal ellipsoids at the 50% probability level.

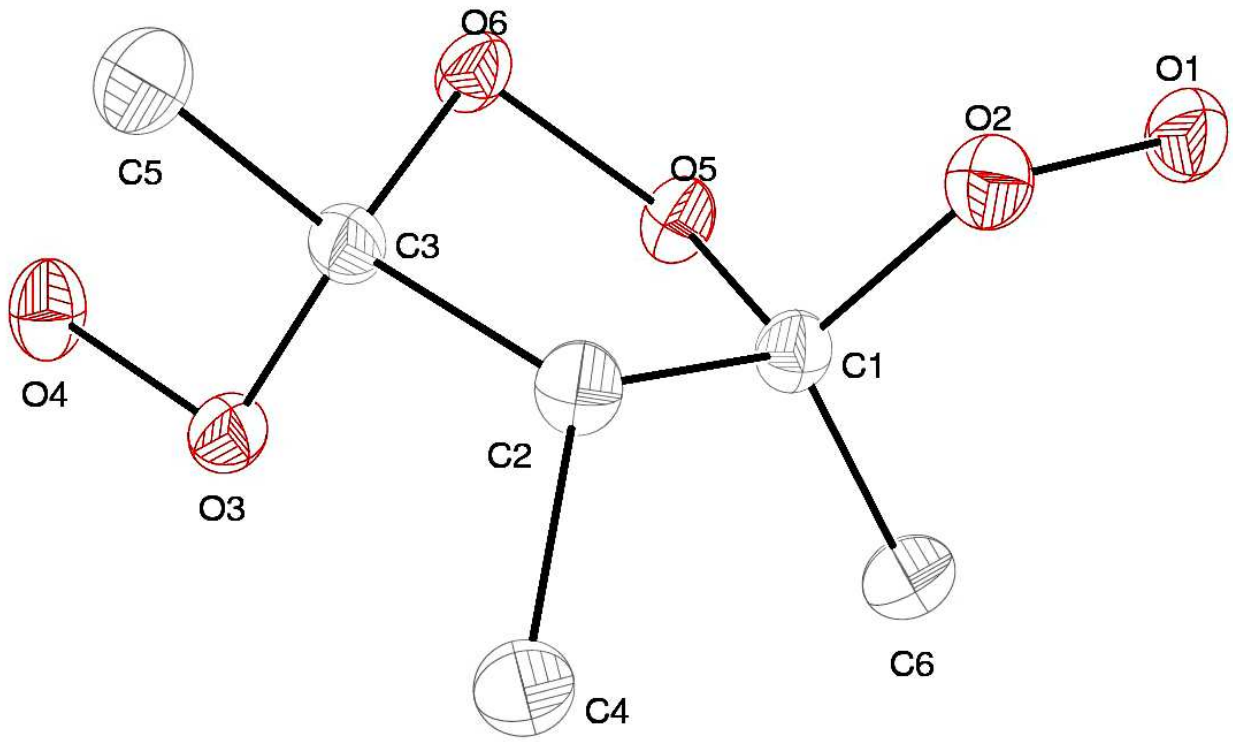

Figure 55. Perspective view of **42** with thermal ellipsoids at the 50% probability level.

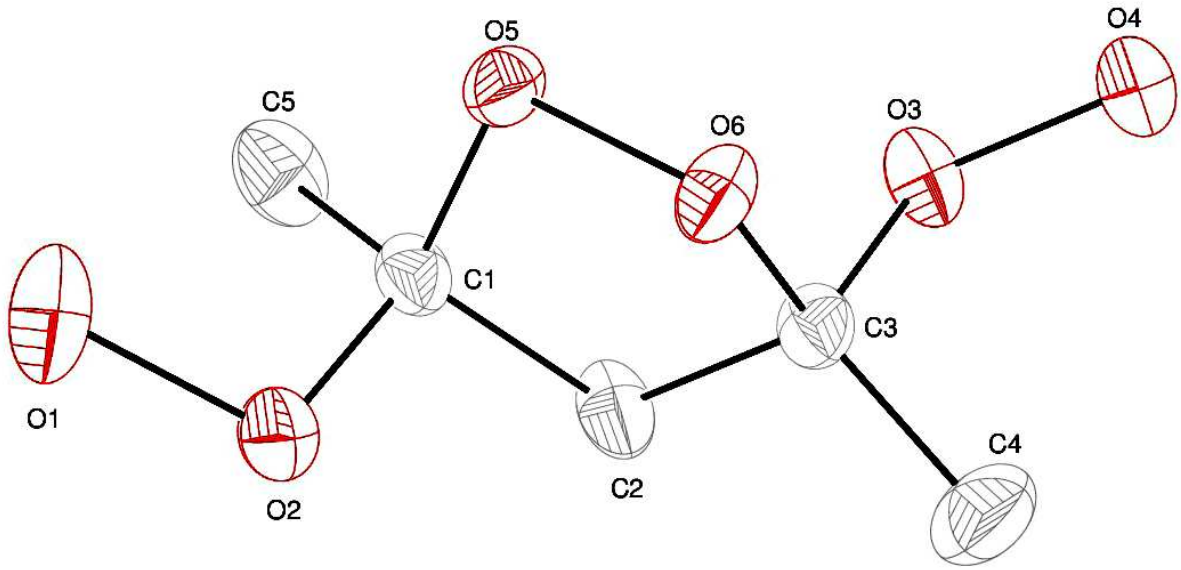

Figure 56. Perspective view of **43** with thermal ellipsoids at the 50% probability level.

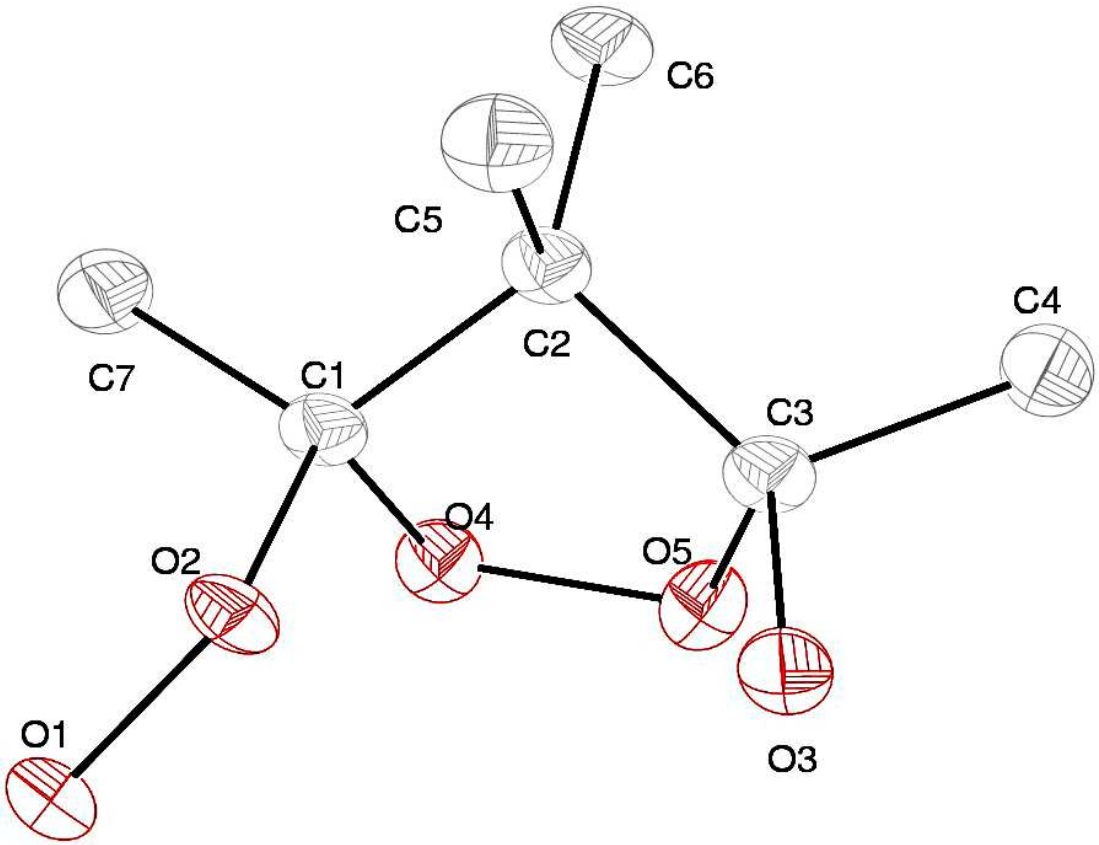

Figure 57. Perspective view of **45** with thermal ellipsoids at the 50% probability level.

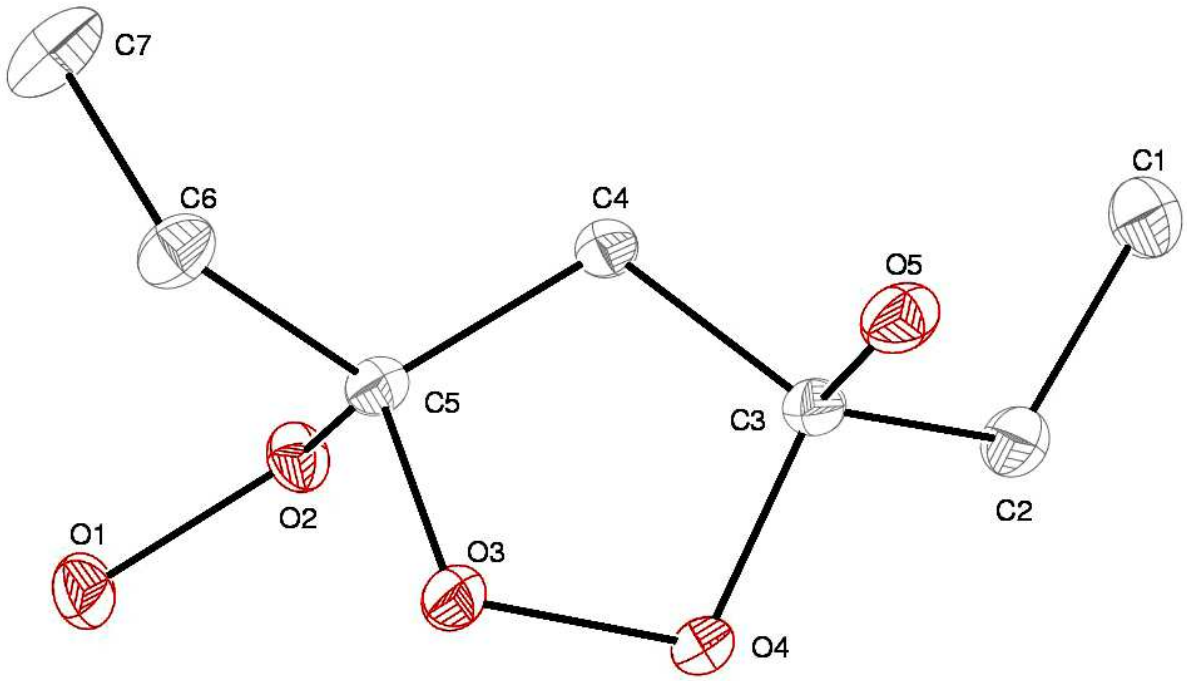

Figure 58. Perspective view of **46** with thermal ellipsoids at the 50% probability level.

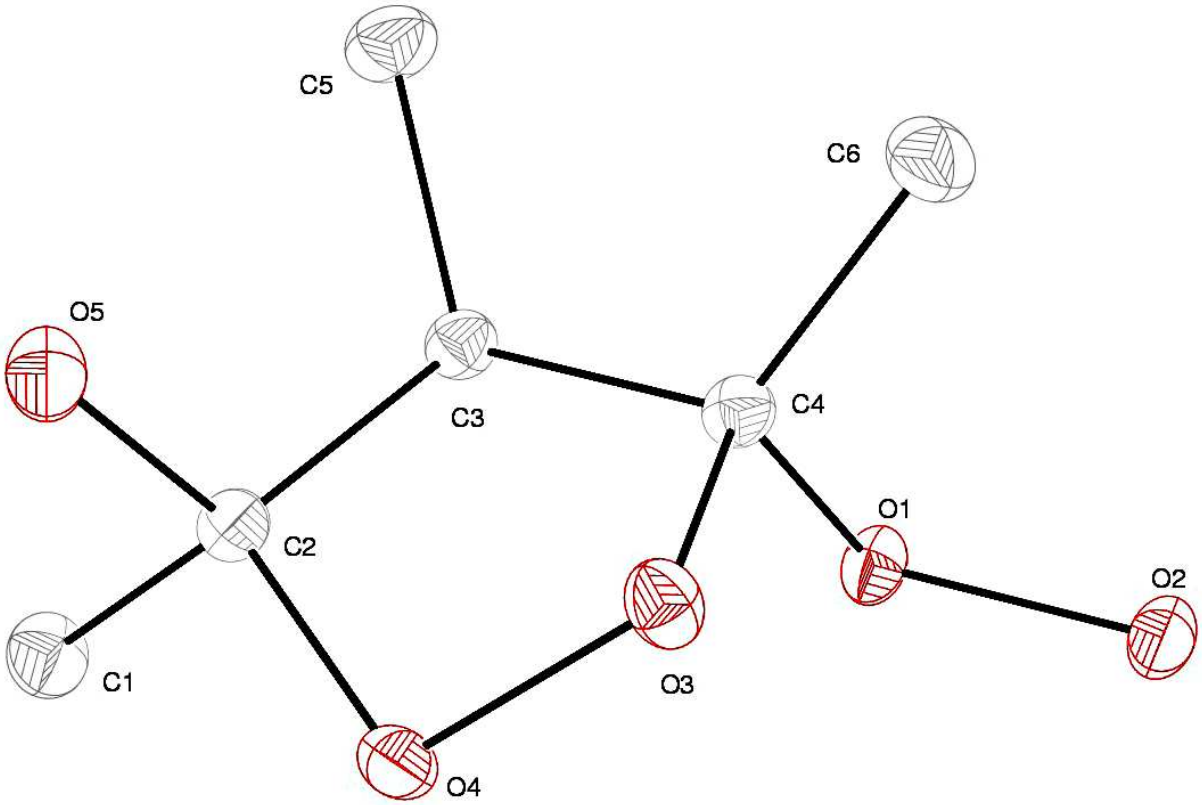

Figure 59. Perspective view of **47** with thermal ellipsoids at the 50% probability level.

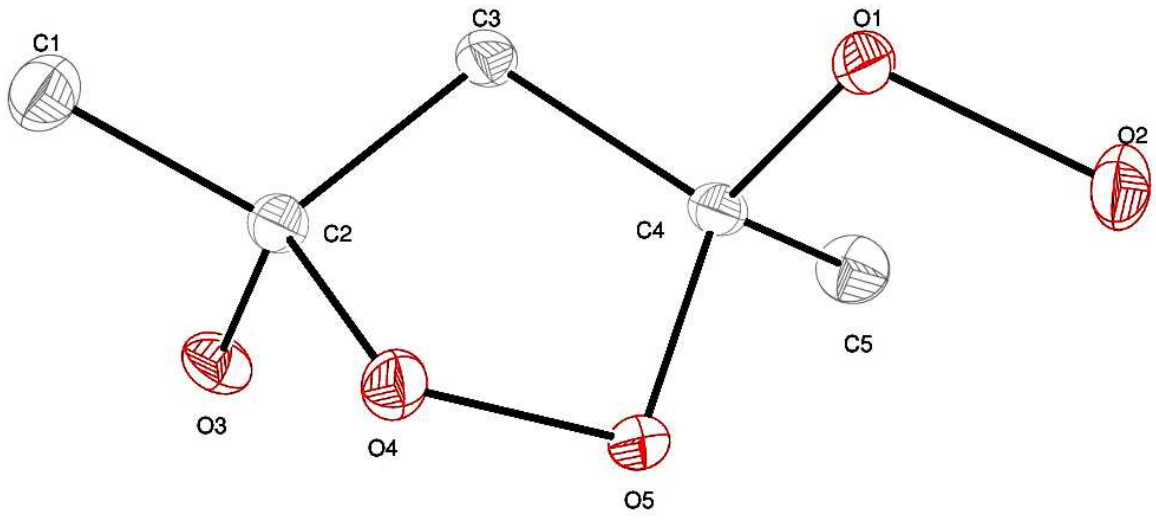

Figure 60. Perspective view of **48** with thermal ellipsoids at the 50% probability level.

Table 33. The selected bond lengths (Å) and angles (°) of **39**–**43**.

Bond/Angle	39	40	41	42	43
O–O	1.4576(8)	1.4647(9)	1.4636(9)	1.464(3)	1.4579(12)
	1.4613(8)	1.4635(9)	1.4764(9)	1.465(2)	1.4596(12)
	1.4607(9)	1.4956(9)	1.4640(8)	1.482(2)	1.4750(10)
C–O	1.4221(9)	1.4344(11)	1.4154(9)	1.442(3)	1.4242(13)
	1.4252(9)	1.4144(10)	1.4278(9)	1.420(3)	1.4197(12)
	1.4259(8)	1.4253(11)	1.4280(9)	1.427(3)	1.4239(13)
	1.4128(9)	1.4243(11)	1.4171(9)	1.417(3)	1.4186(12)
C–CH_3	1.5134(11)	1.5139(13)	1.5188(11)	1.506(4)	1.5133(16)
or	1.5182(12)	1.5292(13)	1.5162(11)	1.510(4)	1.5062(15)
C–CH_2CH_3		1.5351(13)		1.507(4)	
		1.5198(14)			
Angles:					
C_{ring}–O–O_{ring}	107.34(5)	107.77(6)	103.43(5)	104.65(16)	103.59(7)
	106.82(5)	108.32(6)	103.85(5)	103.20(16)	103.59(7)
C_{ring}–C–C_{ring}	108.79(6)	100.32(7)	102.72(6)	101.8(2)	103.64(8)
	109.08(6)				
C_{ring}–C–O_{ring}	110.53(6)	104.93(7)	105.40(6)	106.71(19)	105.12(7)
	110.69(6)	104.40(7)	105.60(6)	104.19(19)	105.18(7)
H_3C–C–OOH	113.45(7)	110.56(8)	113.41(6)	112.7(2)	113.20(8)
or	113.35(7)	111.31(8)	113.38(6)	112.7(2)	112.95(8)
H_3CH_2C–C–OOH					

Table 34. The selected bond lengths (Å) and angles (°) of **45**–**48**.

Bond/Angle	45	46	47	48
O–O	1.4641(17)	1.4636(5)	1.4575(9)	1.4638(6)
	1.4928(19)	1.4706(5)	1.4818(8)	1.4783(6)
C–O	1.4401(19)	1.4381(6)	1.4326(10)	1.4324(7)
	1.406(2)	1.4084(6)	1.4085(10)	1.4240(7)
	1.4241(19)	1.4155(6)	1.4340(10)	1.4155(7)
	1.433(2)	1.4284(5)	1.4243(10)	1.4339(7)
C–CH_3	1.510(3)	1.5199(7)	1.5129(12)	1.5106(8)
or	1.525(2)	1.5196(6)	1.5239(12)	1.5159(8)
C–CH_2CH_3	1.538(2)		1.5129(12)	
	1.512(3)			
Angles:				
C_{ring}–O–O_{ring}	106.85(12)	103.39(3)	102.45(6)	102.62(4)
	107.97(12)	103.94(3)	103.94(6)	104.35(4)
C_{ring}–C–C_{ring}	99.21(14)	103.35(3)	102.82(7)	103.03(4)
C_{ring}–C–O_{ring}	105.05(14)	105.79(3)	103.20(7)	103.08(4)
	104.69(14)	103.30(3)	105.43(7)	105.87(4)
H_3C–C–OOH or H_3CH_2C–C–OOH	111.08(15)	113.86(4)	112.44(7)	110.09(4)
H_3C–C–OH or H_3CH_2C–C–OOH	105.84(14)	112.60(4)	107.65(7)	112.50(5)

Table 35. The list of short contacts of **39** and **40**.

Compound	Number	Atom 1	Atom 2	Length (Å)	Length-VdW (Å)
39	1	O1	O6	2.726	–0.314
	2	O1	H2	1.954	–0.766
	3	H1	H2	2.34	–0.06
	4	O4	H6A	2.679	–0.041
	5	H5	H5	2.387	–0.013
	6	H6A	O6	2.57	–0.15
	7	O1	O4	2.877	–0.163
	8	H1	O4	2.535	–0.185
	9	H1	O6	2.076	–0.644
	10	O3	O6	3.022	–0.018
	11	O4	O6	2.94	–0.1
	12	O4	H2	2.706	–0.014
40	1	O2	H3	2.646	–0.074
	2	H10	O4	2.523	–0.197
	3	O1	O12	2.856	–0.184
	4	H1	O12	1.991	–0.729
	5	O2	O10	2.873	–0.167
	6	O2	H16	2.172	–0.548
	7	O3	O10	2.867	–0.173
	8	O3	H16	2.133	–0.587
	9	O4	O8	2.875	–0.165
	10	O4	O9	2.844	–0.196
	11	H2	O8	2.213	–0.507
	12	H2	O9	2.117	–0.603
	13	H2	H16	2.388	–0.012
	14	O6	O7	2.855	–0.185
	15	O6	H15	2.017	–0.703
	16	O5	H18	2.628	–0.092
	17	H11	O10	2.454	–0.266
	18	O4	C13	3.169	–0.051
	19	O4	H23	2.461	–0.259
	20	O11	H18	2.659	–0.061
	21	O12	H22	2.549	–0.171
	22	H23	O8	2.585	–0.135

Table 36. The list of short contacts of **41**–**43**.

Compound	Number	Atom 1	Atom 2	Length (Å)	Length-VdW (Å)
41	1	O4	H8	2.711	–0.009
	2	O6	C1	3.199	–0.021
	3	O6	O2	2.788	–0.252
	4	H4	O1	2.462	–0.258
	5	H4	O2	1.919	–0.801
	6	O1	O5	2.783	–0.257
	7	H3	O5	1.932	–0.788
	8	H3	O6	2.413	–0.307
42	1	C4	O5	3.188	–0.032
	2	H3	O6	2.656	–0.064
	3	H5	O5	2.683	–0.037
	4	H11	O1	2.61	–0.11
	5	O4	H9	2.679	–0.041
	6	O2	O1	2.868	–0.172
	7	O2	H1	2.001	–0.719
	8	C1	H1	2.883	–0.017
	9	H6	O6	2.585	–0.135
	10	H5	O2	2.669	–0.051
	11	O3	O4	2.915	–0.125
	12	O3	H2	2.039	–0.681
	13	O4	H2	2.692	–0.028
	14	H4	O3	2.698	–0.022
	15	H4	O5	2.701	–0.019
	16	O1	H10	2.71	–0.01
43	1	O1	O3	2.73	–0.31
	2	H1	O3	1.752	–0.968
	3	H1	O4	2.306	–0.414
	4	H1	C3	2.9	0
	5	O4	O2	2.727	–0.313
	6	H2	O1	2.285	–0.435
	7	H2	O2	1.707	–1.013
	8	H2	C1	2.825	–0.075

Table 37. The list of short contacts of **45** and **46**.

Compound	Number	Atom 1	Atom 2	Length (Å)	Length-VdW (Å)
45	1	O3	H9	2.606	–0.114
	2	O1	H10	2.615	–0.105
	3	O1	O3	2.746	–0.294
	4	O1	H5	2.71	–0.01
	5	H1	O3	1.885	–0.835
	6	H1	H2	2.398	–0.002
	7	H1	C3	2.733	–0.167
	8	H1	H5	2.356	–0.044
	9	O4	H11	2.72	0
	10	O5	H11	2.599	–0.121
	11	H6	O4	2.631	–0.089
	12	O2	O3	2.732	–0.308
46	1	O1	H9	2.652	–0.068
	2	O4	O5	2.799	–0.241
	3	O4	H3	1.994	–0.726
	4	O2	O5	2.762	–0.278
	5	H2	O5	1.941	–0.779
	6	O3	H8	2.61	–0.11

Table 38. The list of short contacts of **47** and **48**.

Compound	Number	Atom 1	Atom 2	Length (Å)	Length-VdW (Å)
47	1	O2	O5	2.722	–0.318
	2	H2	O5	1.875	–0.845
	3	H2	H3	2.394	–0.006
	4	O3	H4	2.696	–0.024
	5	O2	H11	2.6	–0.12
	6	C5	H8	2.88	–0.02
	7	H8	H8	2.382	–0.018
	8	O1	O5	2.837	–0.203
	9	O1	H3	2.047	–0.673
	10	O1	H7	2.708	–0.012
	11	O1	H10	2.549	–0.171
	12	O2	H7	2.661	–0.059
	13	H9	O3	2.51	–0.21
	14	H1	O2	2.7	–0.02
48	1	O3	O1	2.904	–0.136
	2	H3	O1	2.033	–0.687
	3	O5	H10	2.562	–0.158
	4	H1	O1	2.667	–0.053
	5	H8	O2	2.675	–0.045
	6	O1	H7	2.719	–0.001
	7	O3	O2	2.733	–0.307
	8	O3	H2	1.823	–0.897
	9	H9	O4	2.636	–0.084
	10	H9	O5	2.712	–0.008
	11	C2	H2	2.875	–0.025
	12	H5	H2	2.373	–0.027

The X-ray crystal structures of the cyclic hydroperoxy compounds **39**, **41**–**43**, and **46**–**48** all have the more stable *trans*-geometry, which has lower torsional strain than the *cis*-geometry. However, **40** and **45** are both of *cis*-geometry according to the X-ray crystal structures. The *cis*-geometry of **40** and **45** minimizes the overall torsional strain by increasing the distance between the bulky methyl and –OOH groups, although the –OOH groups are eclipsed. The angle strain is the lowest in **39** where the bond angles are close to the tetrahedral angle of 109.5°. The X-ray crystal structures of **40** and **45** have C_{ring}–C–C_{ring} bond angles 100.32(7) and 99.21(14)° that are significantly smaller than the tetrahedral angle of 109.5°. This might be due to the presence of two methyl groups on the corresponding central carbon that need to be as far apart as possible to reduce the torsional strain. Thus, **40** and **45** are highly strained molecules with both torsional and angle strain.

The X-ray crystal structures of **39**–**43** and **45**–**48** all contain a variety of intermolecular interactions. They are O–H···O and C–H···O hydrogen bonds and O···O, O···H, H···H, C···H, and C···O short contacts (Tables 35–38). There is no significant difference between the molecular packing of the dihydroperoxy compounds **39**–**43** and the hydroperoxy compounds **45**–**48**. However, the hydroperoxy compounds **45**–**48** lack one O–O trigger bond with respect to the dihydroperoxy compounds **39**–**43**, which can result in reduced impact and friction sensitivities.

The O–H···O hydrogen bond distances are in the range of 2.610–2.915 Å and are present in all the X-ray crystal structures of **39**–**43** and **45**–**48**. These are hydrogen bonds of moderate strength (4–14 kcal/mol).[127] There is an intramolecular O–H···O hydrogen bond (2.732 Å) in the crystal structure of **45** (Figure 61). Except for **43**, weak

C–H···O hydrogen bonds (< 4 kcal/mol)[127] are also common for the crystal structures of **39**–**42** and **45**–**48**. The O···H distances of the C–H···O hydrogen bonds are in the range of 2.454–2.720 Å.

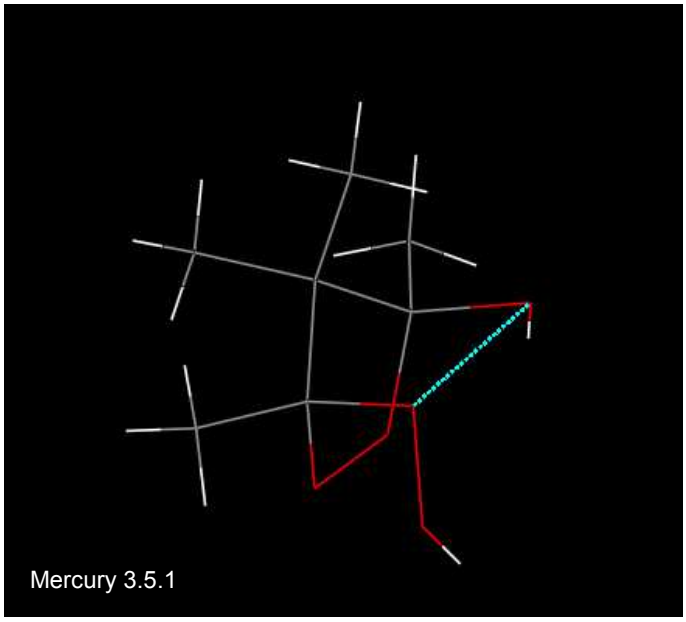

Figure 61. Intramolecular O–H···O hydrogen bond (blue) of **45**.

The multiple O···O, O···H, H···H, C···H, and/or C···O short contacts in the crystal structures of **39**–**43** and **45**–**48** are shorter or at the edge of their van der Waals radii (Tables 35–38).[120] The O···O short contact distances are in the range of 2.844–3.223 Å, and are present in the crystal structures of **39**, **40**, **47**, and **48**. The O···O short contacts are relatively less abundant in these cyclic hydroperoxy compounds with respect to the geminal hydroperoxides. There are O···H contacts (2.117–2.706 Å) in the cyclic dihydroperoxy compounds **39**–**43**. Short H···H contacts (2.373–2.387 Å) are present in the crystal structures of **39**, **40**, **45**, **47**, and **48**. The X-ray crystal structures of **42**, **43**, **45**, and **47** contain C···H contacts (2.733–2.900 Å). The weak C···O contacts (3.169–

2.199 Å) are the least abundant interactions in these X-ray crystal structures of cyclic hydroperoxy compounds, and are only present in **40**–**42**.

Molecular stacks are formed through hydrogen bonds and other short contacts except for **40** and **45**. In the crystal structures of **40** and **45**, pairs of molecules interact mainly through O–H···O hydrogen bonds (Figure 62), which are then interconnected via many short contacts. In order to separate the bulky methyl groups of **40** and **45**, the hydrogen bonded molecular pairs are separated creating void spaces in between, which can lead to high impact and friction sensitivities.

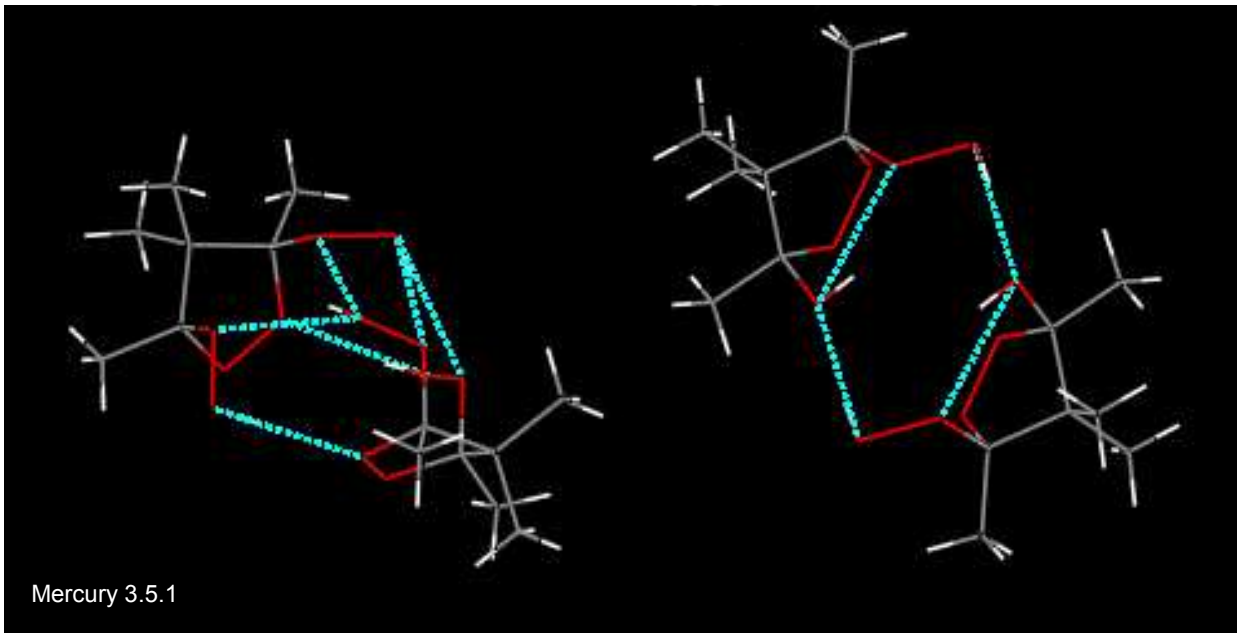

Figure 62. Pairs of molecules interacting mainly through O–H···O hydrogen bonds (blue) in the crystal structures of **40** (left) and **45** (right).

The molecular stacks of **39**, **41**, **42**, **47**, and **48** are interconnected with a large number of short contacts and thus, the relative movements of the stacks with respect to each other could be restricted. Figure 63 shows molecular stacks without and with

interstack short contacts of the crystal structure of **41**. Numerous short contacts might reduce the ability to dissipate energy upon initiation by impact and friction stimuli rendering the corresponding compounds more sensitive to stimuli. Compounds **43** and **46** contain molecular stacks that are not interacting with each other by intermolecular short contacts, which can help the energy dissipation upon stimulus. Figure 64 shows these non-interacting molecular stacks of **43**. All of the O–O trigger bonds in the X-ray crystal structures of **39**–**42** and **45**–**48** are involved in various intermolecular interactions, although the ring O–O bonds of **43** do not form any stabilizing interactions. Thus, **43** could still be highly sensitive despite the non-interacting molecular stacks that allow the energy dissipation when initiated.

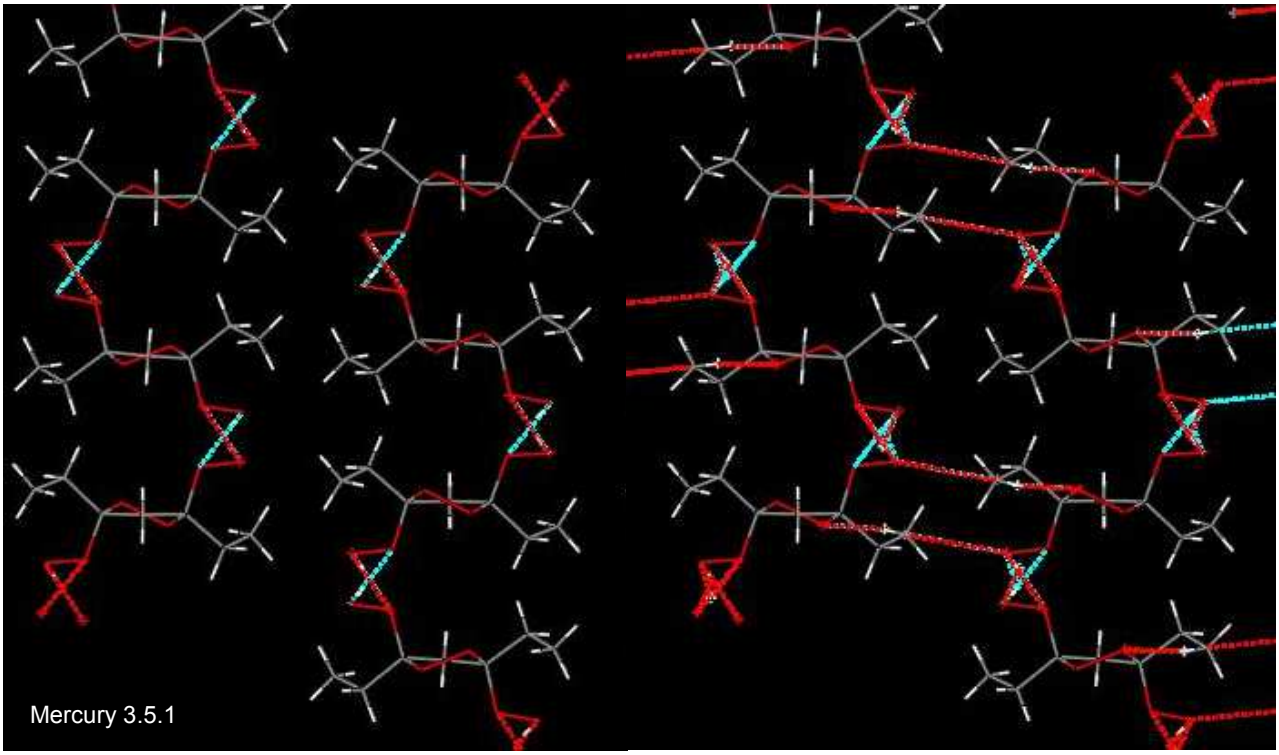

Figure 63. Molecular stacks of **41** without (left) and with (right) short contacts in between the stacks.

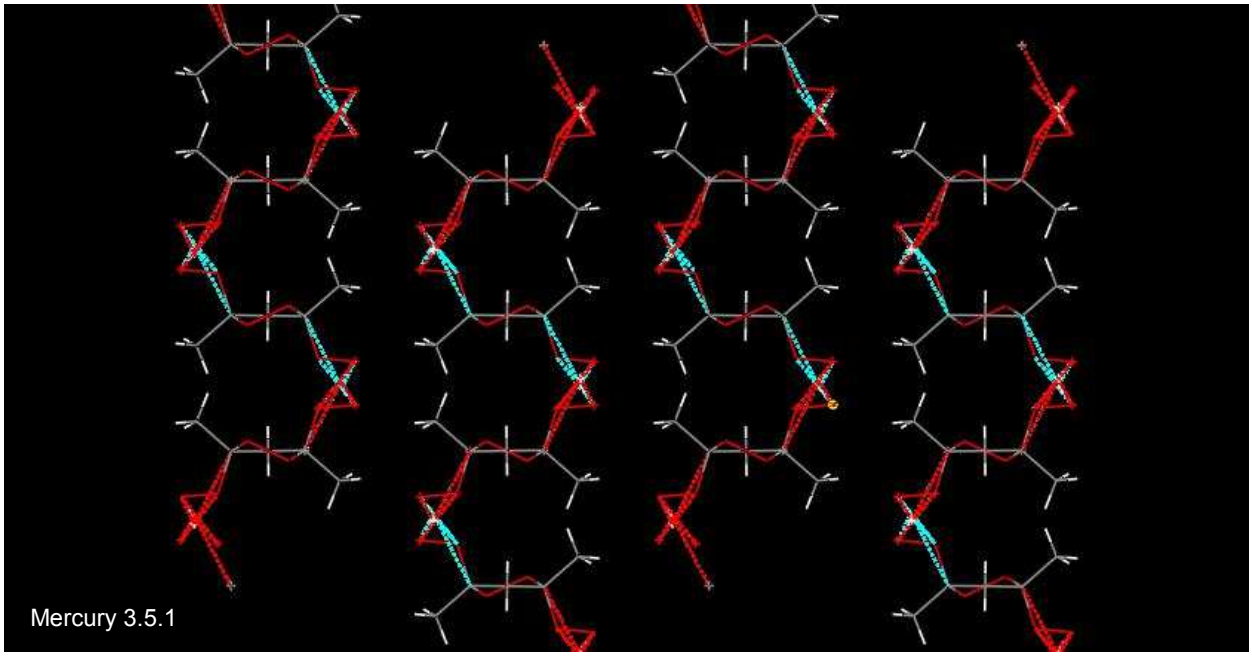

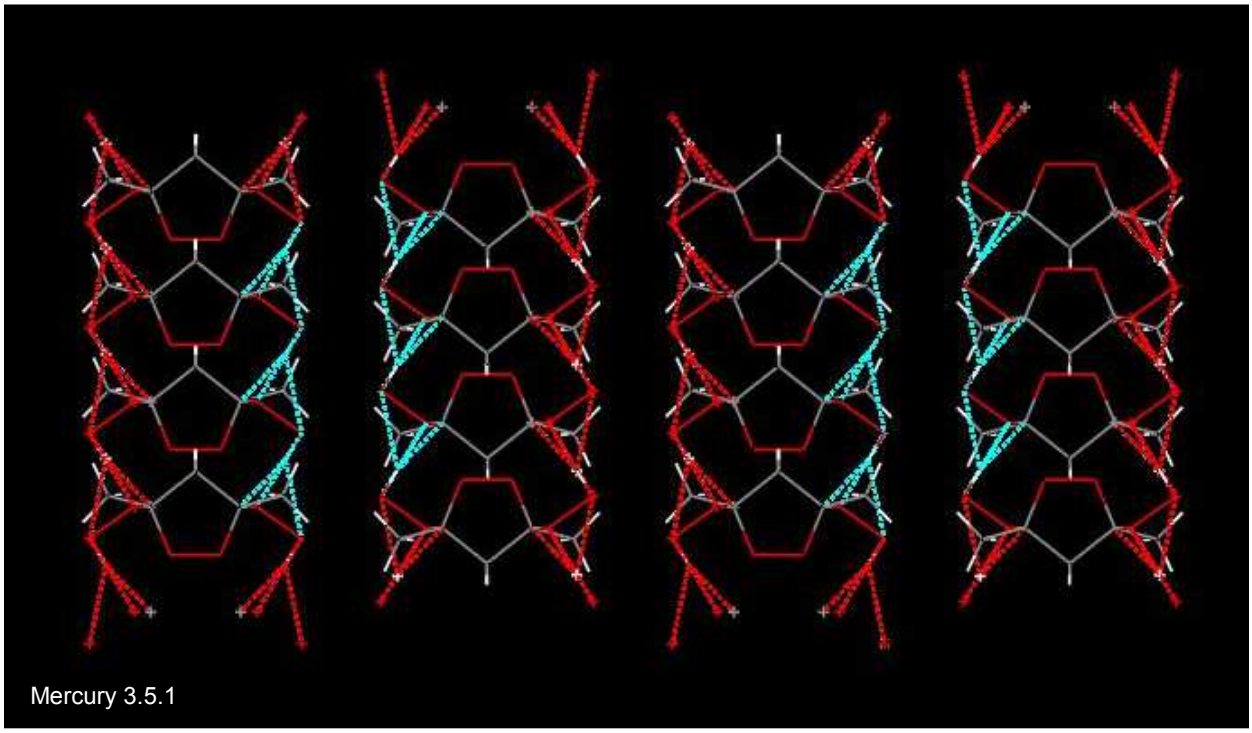

The intrastack hydrogen bonds and short contacts are shown in blue and red.

Figure 64. Non-interacting molecular stacks of **43** along a (top) and c (bottom) directions.

Although there are many stabilizing intermolecular interactions and non-interacting molecular stacks in **43** and **46**, the X-ray crystal structures of **39**–**43** and **45**–**48** all lack the large conjugated π-systems and slip planes of the low sensitivity HEDMs.[81,84] Thus, the cyclic hydroperoxy compounds can still be high sensitivity compounds. However, due to the multiple stabilizing interactions, they should have lower sensitivities than the extremely sensitive peroxide explosives TATP, DADP, HMTD, and MEKP.

5.2.4 Thermal Stability

Thermal stabilities of cyclic hydroperoxy compounds **39**–**43** and **44**–**48** were assessed using thermogravimetry (TGA/DTA). Their decomposition temperatures (T_{Dec}) were obtained from the thermograms. CBS-4M electronic enthalpies were calculated using the Gaussian09 software package to obtain heats of formation values ($\Delta_f H°$) by our collaborators in the Klapötke lab.[113] The T_{Dec} and $\Delta_f H°$ values of **39**–**43** and **44**–**48** are provided in Tables 39 and 40, respectively.

Table 39. Decomposition temperatures and heats of formation values of **39**–**43**.

Compound	T_{Dec} (°C)	$\Delta_f H°$ (kJ/mol)
39	124	–541.2
40	64	–542.7
41	129	–538.7
42	96	–529.6
43	118	–509.1

Table 40. Decomposition temperatures and heats of formation values of **44**–**48**.

Compound	T_{Dec} (°C)	$\Delta_f H°$ (kJ/mol)
44	131	–627.2
45	67	–646.5
46	95	–641.6
47	82	–615.4
48	133	–590.7

The cyclic hydroperoxy compounds **39**, **41**–**43**, **44**, and **46**–**48** are fairly thermally stable based on their decomposition temperatures. However, **40** and **45** have low thermal stabilities and thus, they are unsuitable for HEDM applications. These low thermal stabilities of **40** and **45** might be due to the high angle and torsional strain and arrangement of the molecules as hydrogen bonded pairs creating more voids in their crystal structures.

The $\Delta_f H°$ values for the cyclic dihydroperoxy compounds **39**–**43** are in the range of –542.7 to –509.1 kJ/mol. They are all low and negative, although the oxygen contents are high. The $\Delta_f H°$ values for the cyclic hydroperoxy compounds **44**–**48** are in the range of –646.5 to –590.7 kJ/mol. All the dihydroperoxy compounds **39**–**43** have more positive $\Delta_f H°$ values with respect to the corresponding hydroperoxy analogues. This indicates that the cyclic dihydroperoxy compounds **39**–**43** are more energetic than the hydroperoxy compounds **44**–**48**. The presence of the more stable hydroxy functional group in place of the hydroperoxy group has increased the overall stabilities of the cyclic hydroperoxy compounds **44**–**48** based on the $\Delta_f H°$ values.

5.2.5 Preliminary Qualitative Sensitivity Tests

Sensitivities of the cyclic hydroperoxy compounds **39**–**43** and **44**–**48** were studied using the flame, hammer impact, sand paper friction, and electrostatic discharge (Tesla coil) tests. For all the dihydroperoxy compounds **39**–**43**, sudden, large, and bright flames were obtained in the flame tests, and sudden flames appeared in the Tesla coil tests. These flame and Tesla coil test responses indicate that **39**–**43** are highly sensitive and energetic compounds. The most sensitive cyclic hydroperoxy compound was **40** based on the preliminary flame and the Tesla coil tests. This high sensitivity can be attributed to the high angle and torsional strain and arrangement of the molecules as hydrogen bonded pairs that create more voids in the crystalline lattice.

However, the sensitivity responses obtained for the cyclic hydroperoxy compounds **44**–**48**, which contain only one less oxygen atom than the corresponding dihydroperoxy compounds, were much less aggressive. For **44**–**48**, rapid and bright flames were observed in the flame tests and no positive responses were obtained in the Tesla coil tests. Thus, the cyclic hydroperoxy compounds **44**–**48** should be less sensitive to impact and friction stimuli than the dihydroperoxy compounds **39**–**43**. Compounds **45** and **48** were slightly more sensitive and energetic than the rest of the cyclic hydroperoxy compounds based on the flame and the Tesla coil tests. Compound **45** could be sensitive due to the high strain and poor crystal packing while **48** has the highest oxygen content among the cyclic hydroperoxy compounds **44**–**48**. Similar to the peroxo-based compounds of the previous Chapters, no positive responses were obtained in the hammer and sand paper tests of **39**–**43** and **44**–**48**.

5.2.6 Standard Sensitivity Tests

Impact, friction, and electrostatic discharge sensitivities of the cyclic hydroperoxy compounds **39**–**43** and **44**–**48** were determined with a BAM drop hammer, BAM friction tester, and an electrostatic spark sensitivity tester using standard experimental methods by our collaborators in the Klapötke lab.[29–34] Tables 41 and 42 include the impact, friction, and electrostatic discharge sensitivities of **39**–**43** and **44**–**48**, respectively.

Table 41. Impact, friction, and electrostatic discharge sensitivities of **39**–**43**.

Compound	IS (J)	FS (N)	ESDS (J)
39	< 1	< 5	0.15
40	< 1	< 5	0.065
41	2	< 5	0.15
42	< 1	< 5	0.1
43	< 1	< 5	0.5

Table 42. Impact, friction, and electrostatic discharge sensitivities of **44**–**48**.

Compound	IS (J)	FS (N)	ESDS (J)
44	1	5	NM*
45	2	6	0.1
46	3	14	0.2
47	1	40	0.2
48	3	40	0.15

*Not measurable since **44** is an oil

Based on the "UN Recommendations on the Transport of Dangerous Goods",[28] the cyclic hydroperoxy compounds **39**–**43** and **44**–**48** are "very sensitive" towards

impact. Compounds **39**–**45** are “extremely sensitive” and **44**–**48** are “very sensitive” towards friction. Thus, the cyclic hydroperoxy compounds **39**–**43** and **44**–**48** have appropriate impact and friction sensitivities to be categorized as primary explosives. Interestingly, there is a significant difference in the impact and friction sensitivities between the cyclic dihydroperoxy compounds **39**–**43** and hydroperoxy compounds **44**–**48**. The hydroperoxy compounds **44**–**48** have lower impact sensitivities than the dihydroperoxy compounds **39**–**43** that are useful for primary HEDMs. Most importantly, the optimum impact sensitivity values for primary explosives (≤ 3 J) were obtained for **46** and **48**. The friction sensitivities of the hydroperoxy compounds **44**–**48** are also lower than the dihydroperoxy compounds **39**–**43**. Especially, much lower friction sensitivities were obtained for **46**–**48**. Since the optimum friction sensitivity values for primary explosives are ≤ 10 N, **46**–**48** can be categorized as primary explosives that can be safely handled.

Impact sensitivities < 1 J and friction sensitivities < 5 N could not be measured in the Klapötke lab. Thus, the impact and friction sensitivities of the dihydroperoxy compounds **39**–**43** are comparable to the known peroxo-based explosives TATP, DADP, HMTD, and MEKP (Tables 3–6). Interestingly, the impact and friction sensitivities of the hydroperoxy compounds **44**–**48** are much less than TATP, DADP, HMTD, and MEKP (Tables 3–6). The lack of one O–O trigger bond in **44**–**48** with respect to **39**–**43** has led to peroxo-based compounds that are practically useful as primary HEDMs.

The cyclic hydroperoxy compounds **39**, **41**–**43**, and **44**–**48** show electrostatic discharge sensitivity values that are much higher than the electrical discharges that can

be created by the human body (≤ 0.02 J)[2] and they can be safely handled. However, **40** has a very high sensitivity towards electrostatic discharge and could be a hazardous compound for practical use.

The dihydroperoxy compounds **39**–**43** contain many O–H···O and C–H···O hydrogen bonds and multiple short contacts, including the stabilizing O···O contacts, although TATP and DADP lack any of these stabilizing intermolecular contacts.[59] Still, **39**–**43** demonstrate high sensitivities comparable to TATP and DADP. The O:C ratios of **39**–**43** are higher than TATP and DADP, which might have caused these high impact and friction sensitivities of **39**–**43**, regardless of the stabilizing interactions. The impact and friction sensitivities of **39**–**43** and **44**–**48** do not vary much with the nature of the organic framework due to the predominant effect of the number of O–O trigger bonds that initiate decomposition upon cleavage. However, the electrostatic discharge sensitivity of **40** was higher than the other compounds. The higher ring and torsional strain and the presence of void spaces might influence the high sensitivities of **40**. Compound **40** was the most sensitive cyclic hydroperoxy compound based on the preliminary sensitivity tests as well. The presence of stabilizing O···O contacts in the dihydroperoxy compounds **39** and **40** was not sufficient to reduce their high impact and friction sensitivities. However, the stabilizing O···O contacts in the hydroperoxy compounds **47** and **48** might have caused the lowest friction sensitivities (40 N) from the cyclic hydroperoxy compounds **45**–**48**. The non-interacting molecular stacks of **46** might have caused the low impact and friction sensitivities, although the similar non-interacting molecular stacks were not sufficient to reduce the impact and friction sensitivities of **43** due to the non-interacting O–O trigger bonds.

According to the above mentioned observations, the ability of the intermolecular interactions in the solid state to reduce the impact and friction sensitivities becomes less as the peroxy O:C ratio of the peroxo-based compounds reaches approximately 1.00. Thus, increasing the peroxy O:C ratio to increase the energy content of the peroxo-based compounds above 1.00 only will result in high sensitivity peroxides that are not practically useful. Hence, a better alternative to increase the oxygen contents on peroxo-based compounds would be the use of more stable functional groups like nitro groups, which were shown to be effective in Chapter 3, and hydroxy groups, which were important to reduce the sensitivities based on this Chapter.

5.2.7 Energetic Performance Calculations

The energetic properties of the cyclic hydroperoxy compounds **39**–**43** and **45**–**48** were calculated using the EXPLO5 V6.02 software (Table 43 and 44) by our collaborators in the Klapötke lab.[114] These calculated V_{Det} and P_{Det} values of **39**–**43** are in the range of 6350–6694 m/s and 124–154 kbar, respectively. They are high detonation velocities, which are useful for HEDM applications. Unfortunately, the high impact and friction sensitivities of **39**–**43** are highly disadvantageous for their practical use. The calculated V_{Det} and P_{Det} values of **45**–**48** are in the range of 6100–6461 m/s and 98–136 kbar, respectively. The energetic properties of **44** could not be calculated since it was an oil. The detonation velocities of **45**–**48** are slightly inferior to **39**–**43**, as expected, due to the lower oxygen contents of **45**–**48**. However, the detonation velocities of the cyclic hydroperoxy compounds **45**–**48** have not been reduced by a large magnitude. Additionally, **45**–**48** have much lower impact and friction sensitivities based on the standard sensitivity tests. Since **45** is too low in thermal stability for HEDM

applications, cyclic hydroperoxy compounds **46**–**48** can be summarized as practical safer peroxo-based compounds for primary HEDMs applications.

Table 43. Calculated energetic properties of **39**–**43**.

Property	39	40	41	42	43
Formula	$C_6H_{12}O_6$	$C_7H_{14}O_6$	$C_7H_{14}O_6$	$C_6H_{12}O_6$	$C_5H_{10}O_6$
FW (g/mol)	180.16	194.18	194.21	180.18	166.13
Ω[a] (%)	–106.57	–123.59	–123.59	–106.57	–86.68
ρ[b] (g/cm^3)	1.411	1.387	1.418	1.425	1.469
ρ[c] (g/cm^3)	1.37	1.35	1.38	1.38	1.43
EXPLO5 V6.02					
$\Delta_{Ex}U°$ (kJ/kg)	–4885	–4748	–4783	–4952	–5133
P_{Det} (kbar)	130	124	132	134	154
V_{Det} (m/s)	6350	6357	6501	6511	6694
V_o (L/kg)	853	871	869	853	840

[a]Oxygen balance for oxidation of carbon to CO_2
[b]Crystalline density at 100 K
[c]Crystalline densities at 298 K (for energetic calculations)
$\rho_{298K} = \rho_T / [1 + \alpha_v (298 - T)]$ (T = 100 K, ρ_T = Desnsity at 100 K, α_v = 1.5 x 10^{-4} K^{-1})

The most energetic cyclic dihydroperoxy compound is **43** due to the highest crystalline density and the highest oxygen content. However, the impact and friction sensitivities of **43** are too high for HEDM applications. The calculated detonation velocities of **39**–**43** are greater than the detonation velocities of the known peroxide explosives TATP, DADP, HMTD and MEKP (4,511–5,300 m/s).[6b,35]

Table 44. Calculated energetic properties of **45**–**48**.

Property	45	46	47	48
Formula	$C_7H_{14}O_5$	$C_7H_{14}O_5$	$C_6H_{12}O_5$	$C_5H_{10}O_5$
FW (g/mol)	178.18	178.18	164.18	150.13
Ω[a] (%)	–143.67	–143.67	–126.70	–106.57
ρ[b] (g/cm^3)	1.360	1.328	1.400	1.474
ρ[c] (g/cm^3)	1.32	1.29	1.36	1.43
EXPLO5 V6.02				
$\Delta_{Ex}U°$ (kJ/kg)	–3498	–3517	–3780	–4572
P_{Det} (kbar)	104	98	109	136
V_{Det} (m/s)	6100	5954	6103	6461
V_o (L/kg)	876	878	864	842

[a]Oxygen balance for oxidation of carbon to CO_2
[b]Crystalline density at 100 K
[c]Crystalline densities at 298 K (for energetic calculations)
$\rho_{298K} = \rho_T / [1 + \alpha_v (298 - T)]$ (T = 100 K, ρ_T = Desnsity at 100 K, α_v = 1.5 x 10^{-4} K^{-1})

The most energetic cyclic hydroperoxy compound is **48** due to the highest crystalline density and the highest oxygen content. Since the impact and friction sensitivities of **48** are in the optimum expected range, **48** is an excellent candidate as a safe primary HEDM. The detonation velocity of **48** is close to that of **43** due to the similar crystalline densities at 298 K. The calculated detonation velocities of **45**–**48** are also greater than the detonation velocities of the known peroxide explosives TATP, DADP, HMTD and MEKP (4,511–5,300 m/s).[6b,35]

The effect of ring strain on the detonation velocities can be assessed using the compound pair **39** and **42** with the same O:C ratios. The more strained cyclopentane ring-based compound **42** has a higher detonation velocity with respect to **39**. The effect of the steric strain on the detonation velocities can be assessed using the compound pair **40** and **41** along with **45** and **46**. The compounds **40** and **45** have the more strained structures than **41** and **46**, respectively. Based on the higher detonation velocity of **41** with respect to **40**, steric crowding was disadvantageous, since it caused a reduction in the crystalline density. However, the crystalline density of **46** was lower than **45** and thus, a lower detonation velocity was obtained for **46**. There is a predominant effect from crystalline densities on the detonation velocities, which renders the differences in steric strain negligible.

5.3 Conclusions

The series of oxygen-rich cyclic dihydroperoxy compounds **39**–**43** and hydroperoxy compounds **44**–**48** were synthesized to study their sensitivities and energetic properties. The solid cyclic hydroperoxy compounds were fully characterized by X-ray crystallography. The O:C ratios of these cyclic hydroperoxy compounds were in the range of 0.71–1.20.

Based on the low thermal stabilities and high sensitivities of **40**, it is not useful for HEDM applications. Compound **45** was also too low in thermal stability for HEDM applications. The dihydroperoxy compounds **39**–**43** have impressive calculated detonation velocities that are greater than the known peroxide explosives. However, their high sensitivities render them unsafe for HEDM applications. Interestingly, the hydroperoxy compounds **45**–**48** also have high detonation velocities even with the

slightly lower oxygen contents than the corresponding dihydroperoxy compounds **39**–**43**. The hydroperoxy compounds **46** and **48** with high detonation velocities and optimum impact and friction sensitivities are attractive candidates for use as primary HEDMs.

Higher oxygen contents lead to higher energetic compounds. However, when the peroxy O:C ratio is approximately 1.00, peroxo-based compounds tend to become highly sensitive. This was observed previously with geminal hydroperoxides as well. Thus, the oxygen content in peroxo-based compounds should be increased with more stable functional groups such as nitro (similar to the *tert*-butyl peroxy esters **21** and **22**) and hydroxy (similar to **46**–**48**) groups to obtain more energetic peroxo-based compounds. Ring strain was useful in increasing the detonation velocities, although steric strain was not very useful. Increasing the steric strain not only increased the sensitivity of **40** and **45**, but also reduced their thermal stabilities. Additionally, the lower crystalline density of **40** with respect to **41** decreased the detonation velocity.

According to this work with cyclic dihydroperoxy compounds **39**–**43** and hydroperoxy compounds **44**–**48** with many structural variations, we have understood that sensitivities and energetic properties of peroxo-based compounds could be tuned by careful structural manipulations of peroxo-based compounds to design peroxo-based HEDMs.

5.4 Experimental Section

General Considerations: The syntheses of all cyclic hydroperoxy compounds were carried out at room temperature under ambient atmosphere. Chemicals were purchased from Sigma-Aldrich, Acros Organics, EMD, or Alfa Aesar and were used without further purification. ACS grade solvents were obtained from EMD and Fisher

Scientific. The syntheses of **39**, **40**, **42**, and **45**–**47** were carried out using a modified published procedure for geminal hydroperoxides.[95] The synthetic procedure for **39** was different from the general synthetic procedure of **40**, **42**, and **45**–**47**. Compound **43** was synthesized using a modified published procedure.[126c] Compounds **44** and **48** were prepared based on a modified published procedure for compound **43**.[125a]

Silica gel 60, 230–400 mesh (EMD Chemicals) was used to perform silica gel column chromatography.[104] ASTM TLC plates precoated with silica gel 60 F_{254} (250 μm layer thickness) were used for thin-layer chromatography (TLC). TLC spots were observed using a UV lamp and/or a potassium permanganate solution as a stain (3 g $KMnO_4$, 20 g K_2CO_3, 5 mL 5% w/v aqueous NaOH, 300 mL H_2O). The spots on the stained TLC plates were visualized after heating with a heat gun.

^1H and $^{13}C\{^1H\}$ NMR spectra were obtained from the Varian Mercury 400 (400 MHz and 101 MHz) NMR spectrometer or MR 400 (400 MHz and 101 MHz) NMR spectrometer, in CD_3OD as indicated and were referenced to the residual proton and carbon resonances of the solvent (^1H δ 3.31, ^{13}C 49.00 ppm). Infrared spectra were obtained from a Shimadzu MIRacle 10 IRAffinity-1 equipped with a single reflection ATR accessory. Melting points were determined on an Electrothermal IA 9300 melting point apparatus and are uncorrected. Thermogravimetric (TGA/DTA) measurements to determine the decomposition temperatures of **39**–**43** and **44**–**48** were performed at a heating rate of 5 °C min^{-1} with an OZM Research DTA 552-Ex instrument.

Qualitative Sensitivity Tests: Qualitative sensitivities to heat, impact, and electrostatic discharge were determined to assess initial safety issues. Tests included burning about 3–5 mg of the compound in the Bunsen burner flame, striking 3–5 mg of

the compound on a metal plate with a hammer, and passing an electrostatic discharge through 3-5 mg of the compound on a metal plate using an Electro Technic BD 10 Tesla coil (120 V, 0.35 A).

Quantitative Sensitivity Tests: Quantitative sensitivity Tests include BAM drop hammer[31] impact tests carried out according to STANAG 4489[29] modified instructions[30] using approximately 0.4 mL of the compound, Friction tests with a BAM friction tester carried out according to STANAG 4487[32] modified instructions[33] using approximately 5 mg of the compound, and electrostatic spark tests with an ESD 2010 EN, OZM Electric Spark Tester according to STANAG 4515[34] instructions using 0.1 mL of the compound performed by the Klapötke group.

General Procedure for the Synthesis of 40, 42, and 45–47: A solution of I_2 (0.025 g, 0.100 mmol, 0.1 equivalents per ketone group) in CH_3CN (10 mL) was treated with a 50 wt.% aqueous solution of H_2O_2 (0.17 mL, 3.0 mmol, 3 equivalents per ketone group) while the reaction was stirred at room temperature (23 °C). Afterwards, the diketone starting material (0.5 mmol) was added and the reaction was stirred at room temperature (23 °C) for 5 h. Then, the reaction was concentrated under reduced pressure, redissolved in dichloromethane (10 mL), and anhydrous Na_2SO_4 was added to dry the solution. The dichloromethane solution was again concentrated and the product was purified by silica gel column chromatography.

General Procedure for the Synthesis of 44 and 48: A solution of the diketone starting material (2.0 mmol) in CH_3CN (10 mL) was treated with $SnCl_2{\cdot}2H_2O$ (0.090 g, 0.200 mmol) and the reaction was stirred at room temperature (23 °C) for about 5 min.

Then, H_2O_2, 50 wt. % in H_2O (0.6 mL, 10 mmol) was added and the reaction was allowed to stir at room temperature for 24 h. Afterwards, distilled water (30 mL) was added and the products were extracted to ethyl acetate (20 x 2 mL). The combined ethyl acetate layers were dried with anhydrous $MgSO_4$ and were concentrated. Then, the product was purified by silica gel column chromatography with 4:1 dichloromethane:ethyl acetate.

Preparation of 3,6-Dihydroperoxy-3,6-dimethyl-1,2-dioxane (39). A solution of I_2 (0.102 g, 0.400 mmol, 0.1 equivalents per ketone group) in CH_3CN (5 mL) was treated with a 50 wt. % aqueous solution of H_2O_2 (1.4 mL, 24 mmol, 6 equivalents per ketone group) while the reaction was stirred at room temperature (23 °C). Afterwards, 2,5-Hexanedione (0.24 mL, 2.0 mmol) was added and the reaction was stirred at room temperature (23 °C) for 24 h. At this point, the reaction mixture was concentrated under reduced pressure and was redissolved in dichloromethane (10 mL). Then, it was concentrated again and the aqueous layer was separated from the dichloromethane layer by decanting it. Afterwards, the aqueous layer was dissolved in methanol (10 mL) and was concentrated. Crystallization from the concentrated methanol solution at – 29 °C afforded 0.225 g (62%) of **39** as thick, colorless, plate-like single crystals: mp 128–130 °C (lit[126b] 131 °C); IR (ν, cm^{-1}): 3332 (broad, m), 3300 (broad, m), 3277 (broad, m), 3246 (broad, m), 2999 (w), 2947 (w), 1439 (m), 1377 (s), 1344 (m), 1272 (m), 1250 (w), 1157 (m), 1120 (s), 1062 (s), 1022 (w), 960 (w), 924 (w), 893 (w), 862 (s), 761 (w); ^{1}H NMR (400 MHz, CD_3OD, 23 °C, δ) OO*H* resonance not observed due to exchange with CD_3OD, 1.89-1.77 (m, 2H), 1.60-1.47 (m, 2H), 1.38 (s, 6H, C*H*$_3$); $^{13}C\{^1H\}$ NMR (101

MHz, CD_3OD, 23 °C, ppm) 109.29 (hydroperoxy-*C*), 27.97 (*C*H_2), 19.05 (*C*H_3); Anal. Calcd for $C_6H_{12}O_6$: C, 40.00; H, 6.71. Found: C, 40.35; H, 6.76.

Preparation of 3,5-Dihydroperoxy-3,4,4,5-tetramethyl-1,2-dioxolane (40). 3,3-Dimethylpentane-2,4-dione was treated with a 50 wt.% aqueous solution of H_2O_2 based on the general procedure of **40**, **42**, and **45**–**47** on a 4 times larger scale and the product was purified by silica gel column chromatography with 9:1 dichloromethane:ethyl acetate followed by 4:1 dichloromethane:ethyl acetate to obtain 0.129 g (33%) of **40** as a white solid: product crystals exploded at 84 °C in the melting point apparatus and a melting point could not be obtained; IR (ν, cm^{-1}): 3414 (broad, m) 3011 (w), 2956 (w), 2523 (m), 1456 (m), 1396 (m), 1377 (m), 1267 (w), 1221 (w), 1142 (m), 1098 (s), 1043 (w), 951 (w), 925 (w), 887 (s), 849 (m), 798 (w), 732 (w); ^{1}H NMR (400 MHz, CD_3OD, 23 °C, δ): OO*H* resonance not observed due to exchange with CD_3OD, 1.45 (s, 6H, C*H*$_3$), 1.16 (s, 3H, C*H*$_3$), 1.01 (s, 3H, C*H*$_3$); ^{13}C{^{1}H} NMR (101 MHz, CD_3OD, 23 °C, ppm): 113.62 (hydroperoxy-*C*), 60.69 (*C*), 24.06 (*C*H_3), 15.99 (*C*H_3), 15.33 (*C*H_3); Anal. Calcd for $C_7H_{14}O_6$: C, 43.30; H, 7.27. Found: C, 42.99; H, 7.10. Colorless, polygonal single crystals were grown by slow evaporation from diethyl ether.

Preparation of 3,5-Diethyl-3,5-dihydroperoxy-1,2-dioxolane (41). A solution of 50 wt. % H_2O_2 in H_2O (1.20 mL, 19.2 mmol) and concentrated H_2SO_4 (0.038 g or 2 drops, 0.400 mmol) was treated with 3,5-heptanedione (0.41 mL, 3.0 mmol) dropwise at 0 °C. Afterwards, the reaction was stirred for 1 h at 0 °C. The products were extracted with ethyl acetate (5 x 3 mL). Then, the combined ethyl acetate layers were dried to obtain a crude white solid that was crystallized by slow evaporation from diethyl ether to obtain 0.290 g (50%) of **41** as a colorless, thick, needle-like single crystals: mp 118–120

°C; IR (ν cm^{-1}): 3377 (m, broad), 2982 (w), 2947 (w), 2885 (w), 2511 (w), 1462 (m), 1443 (w), 1425 (w), 1383 (w), 1341 (m), 1321 (m), 1275 (w), 1219 (m), 1159 (s), 1121 (m), 1084 (m), 1020 (m), 1003 (m), 984 (w), 953 (s), 895 (w), 876 (w), 847 (w), 826 (w), 787 (s), 736 (w); ^{1}H NMR (400 MHz, CD_3OD, 23 °C, δ): OO*H* resonance not observed due to exchange with CD_3OD, 2.49 (s, 2H), 1.96–2.10 (m, 2H), 1.62–1.75 (m, 2H), 0.99 (t, 6H, *J* = 7.6 Hz, C*H*$_3$); ^{13}C NMR (101 MHz, CD_3OD, 23 °C, ppm): 115.61 (hydroperoxy-*C*), 48.43 (*C*), 24.92 (*C*H_2), 9.26 (*C*H_3); Anal. Calcd for $C_7H_{14}O_6$: C, 43.30; H, 7.27. Found: C, 43.40; H, 7.37.

Preparation of 3,5-Dihydroperoxy-3,4,5-trimethyl-1,2-dioxolane (42). 3-Methylpentane-2,4-dione was treated with a 50 wt.% aqueous solution of H_2O_2 based on the general procedure of **40**, **42**, and **45**–**47** on a 4 times larger scale and the product was purified by silica gel column chromatography with dichloromethane, 9:1 dichloromethane:ethyl acetate, followed by 4:1 dichloromethane:ethyl acetate to obtain 0.083 g (23 %) of **42** as a white solid: mp 59–61 °C; IR (ν cm^{-1}): 3603 (broad, w), 3410 (broad, m), 3364 (broad, m), 2999 (w), 2945 (w), 1713 (w), 1628 (w), 1464 (m), 1439 (m), 1377 (s), 1337 (m), 1263 (w), 1229 (w), 1165 (s), 1124 (m), 1086 (s), 1047 (m), 1009 (m), 947 (w), 874 (s), 802 (m), 754 (w); ^{1}H NMR (400 MHz, CD_3OD, 23 °C, δ): OO*H* resonance not observed due to exchange with CD_3OD, 2.70 (q, 1H, *J* = 8.0 Hz, C*H*), 1.50 (s, 3H, C*H*$_3$), 1.39 (s, 3H, C*H*$_3$), 1.06 (d, 6H, *J* = 8.0 Hz, C*H*$_3$); ^{13}C NMR (101 MHz, CD_3OD, 23 °C, ppm): 114.86 (hydroperoxy-*C*), 113.00 (hydroperoxy-*C*), 57.08 (*C*H), 16.69 (*C*H_3), 16.14 (*C*H_3), 9.18 (*C*H_3); Anal. Calcd for $C_6H_{12}O_6$: C, 40.00; H, 6.71. Found: C, 39.68; H, 6.63. Colorless, polygonal single crystals were grown from a solution of 2:1 toluene:dichloromethane at –29 °C.

Preparation of 3,5-Dihydroperoxy-3,5-dimethyl-1,2-dioxolane (43). A solution of 50 wt. % aqueous solution of H_2O_2 (0.60 mL, 9.6 mmol) and concentrated H_2SO_4 (0.019 g, 0.200 mmol) was cooled to 0 °C. This solution was treated with 2,4-pentanedione (0.32 mL, 3.0 mmol) dropwise at 0 °C. The mixture was then stirred for 1 h at 0 °C and was kept in the refrigerator (2–8 °C) for 24 h. Then, the reaction mixture was added to a separatory funnel, and was extracted with diethyl ether (3 x 5 mL). The combined ether layers were dried under reduced pressure to afford 0.295 g (59%) of **43** as a white solid. Crystallization of this crude solid from a solution of 20:1 dichloromethane:ethyl acetate at –29 °C afforded 0.209 g (42%) of **43** as colorless, polygonal single crystals: mp 98–100 °C (lit[125a] 98–100 °C); IR (ν, cm^{-1}): 3362 (m, broad), 3003 (w), 2953 (w), 1431 (m), 1379 (m), 1329 (m), 1225 (m), 1167 (s), 1088 (m), 1028 (w), 953 (w), 920 (w), 889 (w), 849 (m), 820 (w), 789 (m), 750 (w); ^{1}H NMR (400 MHz, CD_3OD, 23 °C, δ) OO*H* resonance not observed due to exchange with CD_3OD, 2.61 (s, 2H, C*H*$_3$), 1.52 (s, 6H, C*H*$_3$); $^{13}C\{^1H\}$ NMR (101 MHz, CD_3OD, 23 °C, ppm) 113.42 (hydroperoxy-*C*), 52.69 (*C*H_2), 18.14 (*C*H_3); Anal. Calcd for $C_5H_{10}O_6$: C, 36.15; H, 6.07. Found: C, 36.07; H, 5.98.

Preparation of 6-Hydroperoxy-3,6-dimethyl-1,2-dioxan-3-ol (44). Hexane-2,5-dione was treated with a 50 wt.% aqueous solution of H_2O_2 based on the general procedure of **44** and **48** to obtain 0.048 g (15%) of **44** as a colorless oil: IR (ν cm^{-1}): 3399 (broad, m), 2992 (w), 2972 (w), 2943 (w), 2870 (w), 1703 (w), 1634 (w), 1449 (m), 1400 (m), 1377 (m), 1337 (m), 1256 (m), 1231 (m), 1167 (m), 1148 (m), 1115 (s), 1070 (s), 1024 (w), 964 (m), 943 (m), 881 (w), 849 (s), 766 (w), 743 (w); ^{1}H NMR (400 MHz, CD_3OD, 23 °C, δ): OO*H* and O*H* resonances not observed due to exchange with

CD_3OD, 1.80–1.96 (m, 2H), 1.61–1.78 (m, 1H), 1.44–1.60 (m, 1H), 1.40 (s, 3H, C*H*$_3$), 1.30 (s, 3H, C*H*$_3$); $^{13}C\{^1H\}$ NMR (101 MHz, CD_3OD, 23 °C, ppm): 107.21 (hydroperoxy-*C*), 100.04 (hydroxy-*C*), 30.02 (*C*H_2), 26.99 (*C*H_2), 22.52 (*C*H_3), 18.08 (*C*H_3); Anal. Calcd for $C_6H_{12}O_5$: C, 43.90; H, 7.37. Found: C, 43.60; H, 7.35.

Preparation of 5-Hydroperoxy-3,4,4,5-tetramethyl-1,2-dioxolan-3-ol (45). 3,3-Dimethylpentane-2,4-dione was treated with a 50 wt.% aqueous solution of H_2O_2 based on the general procedure of **40**, **42**, and **45**–**47** on a 4 times larger scale and the product was purified by silica gel column chromatography with 9:1 dichloromethane:ethyl acetate followed by 4:1 dichloromethane:ethyl acetate to obtain 0.111 g (31%) of **45** as a white solid: mp 79–81 °C; IR (ν cm^{-1}): 3455 (m), 3260 (broad, m), 3005 (w), 2943 (w), 2874 (w), 2555 (w), 2419 (w), 1454 (m), 1396 (m), 1375 (m), 1279 (w), 1253 (w), 1213 (m), 1140 (s), 1115 (s), 1098 (s), 1063 (m), 943 (m), 916 (m), 880 (s), 851 (m), 810 (w), 791 (w), 734 (w); ^{1}H NMR (400 MHz, CD_3OD, 23 °C, δ): OO*H* and O*H* resonances not observed due to exchange with CD_3OD, 1.48 (s, 3H, C*H*$_3$), 1.31 (s, 3H, C*H*$_3$), 1.11 (s, 3H, C*H*$_3$), 1.09 (s, 3H, C*H*$_3$); ^{13}C NMR (101 MHz, CD_3OD, 23 °C, ppm): 114.86 (hydroperoxy-*C*), 108.05 (hydroxy-*C*), 59.73 (*C*), 23.41 (*C*H_3), 18.72 (*C*H_3), 16.94 (*C*H_3), 14.41 (*C*H_3); Anal. Calcd for $C_7H_{14}O_5$: C, 47.19; H, 7.92. Found: C, 47.20; H, 7.93. Colorless, polygonal single crystals were grown from a solution of 2:1 dichloromethane:methanol at –29 °C.

Preparation of 3,5-Diethyl-5-hydroperoxy-1,2-dioxolan-3-ol (46). Heptane-3,5-dione was treated with a 50 wt.% aqueous solution of H_2O_2 based on the general procedure of **40**, **42**, and **45**–**47** on a 4 times larger scale and the product was purified by silica gel column chromatography with dichloromethane followed by 4:1

dichloromethane:ethyl acetate to obtain 0.126 g (35 %) of **46** as a white solid: mp 79–81 °C; IR (ν cm^{-1}): 3410 (broad, m), 3333 (broad, m), 2982 (m), 2947 (w), 2887 (w), 2797 (w), 2359 (s), 2160 (w), 2023 (w), 1973 (w), 1742 (w), 1690 (m), 1647 (w), 1551 (m), 1526 (m), 1458 (m), 1406 (m), 1306 (m), 1260 (m), 1213 (w), 1163 (m), 1113 (m), 1072 (m), 1018 (m), 934 (m), 899 (m), 851 (m), 800 (m), 718 (m); ^{1}H NMR (400 MHz, CD_3OD, 23 °C, δ): OO*H* and O*H* resonances not observed due to exchange with CD_3OD, 2.47 (q, 2H, *J* = 10.0 Hz, C*H*$_2$), 2.05–2.17 (s, 1H), 1.66–1.81 (m, 3H), 1.00 (t, 6H, *J* = 7.6 Hz, C*H*$_3$); ^{13}C NMR (101 MHz, CD_3OD, 23 °C, ppm): 115.93 (hydroperoxy-*C*), 108.57 (hydroxy-*C*), 51.79 (*C*H$_2$), 30.07 (*C*H$_2$), 25.17 (*C*H$_2$), 9.40 (*C*H$_3$), 9.35 (*C*H$_3$); Anal. Calcd for $C_7H_{14}O_5$: C, 47.19; H, 7.92. Found: C, 46.98; H, 7.89. Colorless, plate-like single crystals were grown by slow evaporation from a solution of 10:1 toluene:diethyl ether.

Preparation of 5-Hydroperoxy-3,4,5-trimethyl-1,2-dioxolan-3-ol (47). 3-Methylpentane-2,4-dione was treated with a 50 wt.% aqueous solution of H_2O_2 based on the general procedure of **40**, **42**, and **45**–**47** on a 4 times larger scale and the product was purified by silica gel column chromatography with dichloromethane, 9:1 dichloromethane:ethyl acetate, followed by 4:1 dichloromethane:ethyl acetate to obtain 0.140 g (43 %) of **47** as a white solid: mp 71–73 °C; IR (ν cm^{-1}): 3445 (broad, m), 3296 (broad, m), 2995 (w), 2947 (w), 2888(w), 1649 (w), 1622 (w), 1558 (m), 1510 (w), 1467 (m), 1383 (s), 1342 (w), 1290 (w), 1263 (w), 1209 (m), 1171 (s), 1124 (s), 1084 (s), 1011 (m), 949 (s), 854 (s), 797 (m), 758 (m); ^{1}H NMR (400 MHz, CD_3OD, 23 °C, δ): OO*H* and O*H* resonances not observed due to exchange with CD_3OD, 2.48 (q, 1H, *J* = 7.6 Hz, C*H*), 1.42 (s, 3H, C*H*$_3$), 1.41 (s, 3H, C*H*$_3$), 1.06 (d, 6H, *J* = 7.2 Hz, C*H*$_3$); ^{13}C NMR (101 MHz, CD_3OD, 23 °C, ppm): 115.18 (hydroperoxy-*C*), 107.01 (hydroxy-*C*),

57.02 (*C*H), 21.63 (*C*H_3), 16.09 (*C*H_3), 10.24 (*C*H_3); Anal. Calcd for $C_6H_{12}O_5$: C, 43.90; H, 7.37. Found: C, 43.71; H, 7.45. Colorless, hexagonal single crystals were grown from a solution of 5:1 toluene:diethyl ether at –29 °C.

Preparation of 5-Hydroperoxy-3,5-dimethyl-1,2-dioxolan-3-ol (48). Pentane-2,4-dione was treated with a 50 wt.% aqueous solution of H_2O_2 based on the general procedure of **44** and **48** to obtain 0.137 g (46%) of **48** as a white solid: mp 110–112 °C (lit[126a] 110–112 °C); IR (ν cm^{-1}): 3439 (broad, m), 3260 (broad, m), 3005 (w), 2956 (w), 2835 (s), 1439 (m), 1381 (m), 1331 (m), 1308 (m), 1217 (m), 1173 (s), 1078 (m), 1057(m), 959 (m), 918 (w), 883 (w), 845 (s), 808 (s), 799 (s); ^{1}H NMR (400 MHz, CD_3OD, 23 °C, δ): OO*H* and O*H* resonances not observed due to exchange with CD_3OD, 2.58 (s, 2H, C*H*$_2$), 1.58 (s, 3H, C*H*$_3$), 1.47 (s, 3H, C*H*$_3$); ^{13}C NMR (101 MHz, CD_3OD, 23 °C, ppm): 113.69 (hydroperoxy-*C*), 106.53 (hydroxy-*C*), 56.11 (*C*H_2), 22.80 (*C*H_3), 18.54 (*C*H_3); Anal. Calcd for $C_5H_{10}O_5$: C, 40.00; H, 6.71. Found: C, 40.35; H, 6.66. Colorless, polygonal single crystals were grown by slow evaporation from diethyl ether.

CHAPTER 6

Synthesis, Characterization, and Study of Highly Energetic Peroxy Acids with Surprisingly Low Impact and Friction Sensitivities

6.1 Introduction

6.1.1 Peroxy Acids

Peroxy acids have the basic RC(O)OOH formula, where the R group can be an alkyl or aryl group. They form dimers in the solid state due to hydrogen bonding according to X-ray crystal structures, but are monomeric in solution and liquid state.[128] Increases in the effective molecular volumes from the carboxylic acids to peroxy acids (12–18 $Å^3$) lead to less efficient crystal packing and to lower melting temperatures than the corresponding carboxylic acids.[128] The pK_a values of peroxy acids are higher than the corresponding carboxylic acids and they are weaker acids due to the absence of resonance stabilization of the anion.[39] The average O–O bond dissociation energy reported for some simple peroxy acids is 48 kcal/mol.[40]

There are different methods to synthesize peroxy acids, but the most popular method is the acid catalyzed reaction of the parent carboxylic acid with hydrogen peroxide.[129] Instead of the parent carboxylic acid, acid chlorides or anhydrides can be reacted with hydrogen peroxide at low temperatures.[130] Peroxy acids are very powerful oxidizing organic peroxides and are used for oxidation reactions such as the epoxidation of olefins and Baeyer-Villiger oxidation of ketones in both academia and in industry.[128,131,132] Peroxy acids or peroxy acid precursors are also used as bleaching agents, disinfectants, and fungicides.[128]

Organic peroxy acids are not stable for long at room temperature in solution and tend to lose the active oxygen, decomposing into carboxylic acid and hydrogen peroxide starting materials.[39] This decomposition is accelerated by metals, metal ions, metal complexes, acids, and bases. As the molecular weight of the peroxy acid is increased the stability increases.[39] Pure peroxyformic acid and peroxyacetic acid are known to be explosive at higher temperatures.[130]

6.1.2 Use of Peroxy Acids as HEDMs

TATP, DADP, HMTD, and MEKP are the only well-studied peroxo-based compounds for which the energetic materials properties have been determined.[2,35] However, the extremely high sensitivities of these peroxo-based explosives render them unsafe to handle.[2,6b,35,64] Furthermore, low thermal stabilities (Tables 3–6), high volatilities (TATP and DADP),[2,35,64] and lower detonation velocities (Tables 3–6) with respect to the high nitrogen explosives such as RDX and HMX (Table 2) are highly disadvantageous for HEDM applications.[1e,6b,35] Thus, peroxo-based explosives TATP, DADP, HMTD, and MEKP have not found any civilian or military HEDM applications.

Peroxo-based compounds can serve as useful HEDMs if their high impact and friction sensitivities can be reduced to optimum levels for their applications and for safe handling. Attempts were made to reduce the high sensitivities of the known peroxo-based compounds using different strategies such as the use of desensitizing (water or WD-40 oil) or phlegmatizing (paraffin wax) agents without much success.[122] Recently, Landenberger has shown that cocrystals of DADP and TITNB have a reduced impact sensitivity compared to both the pure forms of DADP and TITNB due to the I···O close contacts in the DADP/TITNB cocrystals.[68b] Peroxy acids are generally not known to be

shock sensitive. Hence, they could be useful peroxo-based candidates for HEDM applications. Pure low molecular weight peroxy acids were reported to be explosive at elevated temperatures.[39,130] However, the energetic materials properties of these oxygen-rich peroxy acids have not been studied up to date.

In this Chapter, we report the synthesis, structure, and energetic materials properties of four oxygen-rich aromatic peroxy acids **49**–**52** (Figure 65). Compounds **49**–**52** were synthesized in high yields with minimal synthetic manipulations. They are oxygen rich, and contain O:C ratios in the range of 0.71–1.00. Interestingly, the peroxy acids **49**, **51**, and **52** have higher thermal stabilities when compared to other peroxo-based subclasses, low impact and friction sensitivities, and highly impressive detonation velocities. These properties render the peroxy acids **49**, **51**, and **52** appropriate for applications as secondary HEDMs. These peroxy acids **49**, **51**, and **52** are among the first peroxo-based oxygen-rich compounds that can be classified as secondary HEDMs. Through this research, we have demonstrated that the peroxo-based compounds can have impressive properties to be developed as HEDMs.

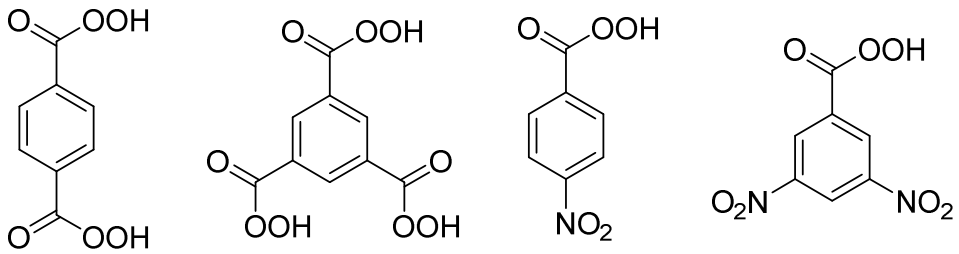

49, 94% O:C = 6:8 = 0.75 | **50**, 99% O:C = 9:9 = 1.00 | **51**, 94% O:C = 6:7 = 0.71 | **52**, 96% O:C = 7:7 = 1.00

Figure 65. Aromatic peroxy acids **49**–**52**.

6.2 Results and Discussion

A series of aromatic peroxy acids was chosen in this study since the π-interactions in their crystal structures may be useful to obtain low sensitivities and high crystalline densities. Compounds **49** and **50** contain only the peroxy acid functional groups while **51** and **52** contain peroxy acid and nitro functional groups. Nitro groups have been commonly used in energetic materials to increase the oxygen and nitrogen contents without excessively increasing the impact and friction sensitivities.[2] Compounds **49** and **50** are the corresponding peroxy acids of the *tert*-butyl peroxy esters **16** and **17** of Chapter 3, respectively. The highest O:C ratio that was safely obtained with peroxy acids **49**–**52** was 1.00.

6.2.1 Synthetic Aspects

Caution: High concentrations of aqueous H_2O_2 (84 wt.%) and oxygen-rich organic peroxy acids in this study are potentially explosive. These hazardous materials require handling with extreme care. Hence, reactions and other manipulations were performed in a fume hood behind a blast shield. Personal protective equipment was used whenever necessary: a face shield, leather gloves, and a leather apron. Interactions with strong acids, metals, metal salts, or easily oxidizable species were avoided to prevent hazardous decomposition reactions. All reactions were performed on small scales (≤ 350 mg) and the temperatures were not increased above 50 °C.

The peroxy acids **49**–**52** were prepared in high yields (≥ 94%) as shown in Figure 65. The synthesis of **49**–**52** was carried out according to Scheme 8. Compounds **51** and **52** were synthesized based on the published procedures for **51**[133] and **52**,[134] respectively. Compound **50** is a new peroxy acid obtained in this study.

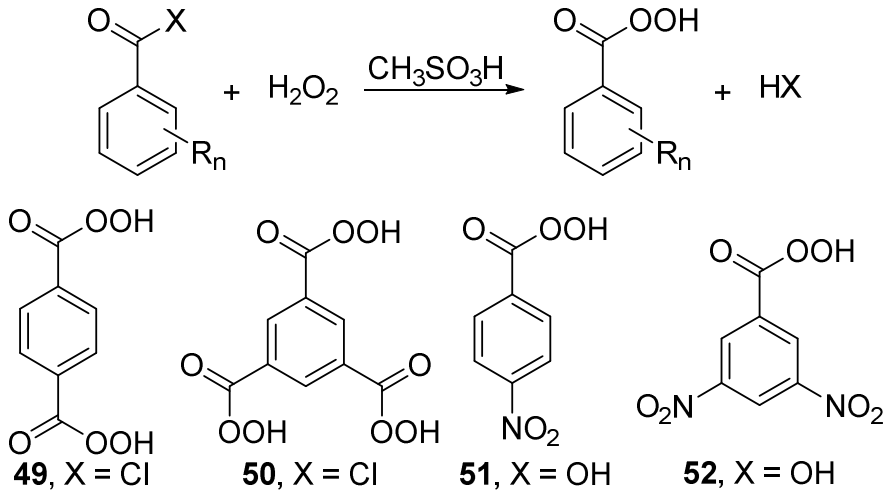

Scheme 9. Synthesis of peroxy acids.

Peroxy acids **49** and **50** were prepared by treatment of the corresponding acid chlorides with 84 wt.% H_2O_2 in the presence of methanesulfonic acid at 50 °C. The syntheses of **49** and **50** using the corresponding carboxylic acids under similar conditions only led to low yields of peroxy acids. However, **51** and **52** were prepared in high yields by treatment of the corresponding carboxylic acids with 84 wt.% H_2O_2 in the presence of methanesulfonic acid at 35 and 50 °C, respectively.[133,134] Compounds **49**–**52** were easily precipitated from the reaction solutions by cooling to 0 °C and the pure products were isolated by filtration, washing, and drying under reduced pressure.

Ease of the syntheses and minimal synthetic manipulations required in the preparation of **49**–**52** are great advantages in the design of HEDMs. The major byproducts in these reactions were the parent carboxylic acids, which cannot be easily separated from the peroxy acids. Hence, high concentrations of H_2O_2 and elevated temperatures were required to ensure high yields of product peroxy acids. The addition of 84 wt.% H_2O_2 also needed to be carried out slowly, along the walls of the reaction flasks, to avoid any violent reactions.

Attempts to prepare peroxy acids from the corresponding acid chlorides of 1,2,4,5-benzene tetracarboxylic acid and mellitic acid only resulted in violent reactions with the elimination of smoke upon the addition of 84 wt.% H_2O_2. Thus, the corresponding peroxy acids of the *tert*-butyl peroxy esters **18** and **19** of Chapter 3 were not obtained. Since the O:C ratio of 1.00 was reached with only three peroxy acid functional groups, substitution of the aromatic rings with more peroxy acid groups might not be safely achievable.

Peroxy acids **49** and **50** were isolated as white solids, while **51** and **52** were isolated as pale yellow solids. It was a challenging process to obtain single crystals of peroxy acids since they tend to decompose in to the parent carboxylic acids in solution. However, X-ray quality single crystals of **49**·DMF and **52** were grown by cooling the saturated solutions of DMF and 1:1 diethyl ether:pentane at –29 °C, respectively. Both single crystals of **49**·DMF and **52** were colorless. They were in the form of thin needles. The X-ray crystal structure of **51** was reported in the literature.[135] Compound **50** was highly unstable in solution and thus, single crystals of **50** were not obtained. Peroxy acids **49**–**52** were characterized by ^{1}H and ^{13}C NMR spectroscopy, melting point analysis, IR spectroscopy, and elemental analysis. X-ray crystal structures were obtained for complete characterization of **49**·DMF and **52**.

6.2.2 Spectroscopy

^{1}H NMR chemical shifts of the parent carboxylic acid and the product peroxy acid varied only slightly in CD_3OD. However, in $(CD_3)_2NCOD$, the OO*H* chemical shift of **49** was shifted downfield to δ 14.18 from δ 13.56 of terephthalic acid. ^{13}C NMR spectroscopy was also useful in the identification of the presence of peroxy acids, since

the carbonyl carbon chemical shift was changed in going from the parent carboxylic acid to the product peroxy acid. The chemical shifts of the carbonyl carbons of peroxy acids were shifted upfield by 1–3 ppm with respect to the corresponding carboxylic acids.

IR spectroscopy has mainly assisted in differentiating between the parent carboxylic acid and the product peroxy acid. The carbonyl stretching frequency of the peroxy acids were shifted towards higher frequencies with respect to the corresponding carboxylic acids by 20–40 cm^{-1}. These carbonyl stretching frequencies were in the range of 1715–1744 cm^{-1}. Also, the O–H stretching frequencies of peroxy acids were shifted towards higher frequencies by about 200–300 cm^{-1}. They were medium and broad peaks in the range of 3226–3447 cm^{-1}. These higher O–H stretching frequencies of peroxy acids might be due to lesser participation in hydrogen bonding with respect to the parent carboxylic acids. In the IR spectra of **49**–**52**, medium and/or strong peaks were present in the region of 1000–1300 cm^{-1} for C–O stretching modes. There were also medium to weak O–O stretching modes in the range of 800–1000 cm^{-1}.

6.2.3 X-ray Crystal Structures

X-ray crystal structures of **49**·DMF and **52** were obtained. There were no unusual interactions in the X-ray crystal structures. Experimental crystallographic data of the X-ray crystal structures of **49**·DMF and **52** are summarized in Table 45. Perspective views of the crystal structures of **49**·DMF and **52** are given in the Figures 66 and 67. Selected bond lengths and angles from the crystal structures are provided in Table 46. The list of hydrogen bonds and short contacts of **52** prepared by Mercury 3.5.1 software is provided in Table 47.

Table 45. Experimental crystallographic data of **49**·DMF and **52**.

	49·DMF	**52**
Formula	$C_6H_{10}N_2O_4$	$C_{14}H_9N_4O_{14}$
FW	174.16	457.25
Space group	P 1bar	P 2_1 2_1 2_1
a (Å)	5.8492(6)	6.4707(7)
b (Å)	7.6189(8)	10.8839(10)
c (Å)	9.8922(11)	24.673(2)
V (Å^3)	406.59(8)	1737.6(3)
Z	2	4
T (K)	100(2)	100(2)
λ (Å)	0.71073	0.71073
ρ_{calc} (g/cm^3)	1.423	1.748
μ (mm^{-1})	0.120	0.161
R(F)[a] (%)	3.78	3.62
R_w(F)[b] (%)	12.08	9.74

[a] $R(F) = \sum \| |F_o| - |F_c| \| / \sum |F_o|$; [b] $Rw(F) = [\sum w(F_o^2 - F_c^2)^2 / \sum w(F_o^2)^2]^{1/2}$

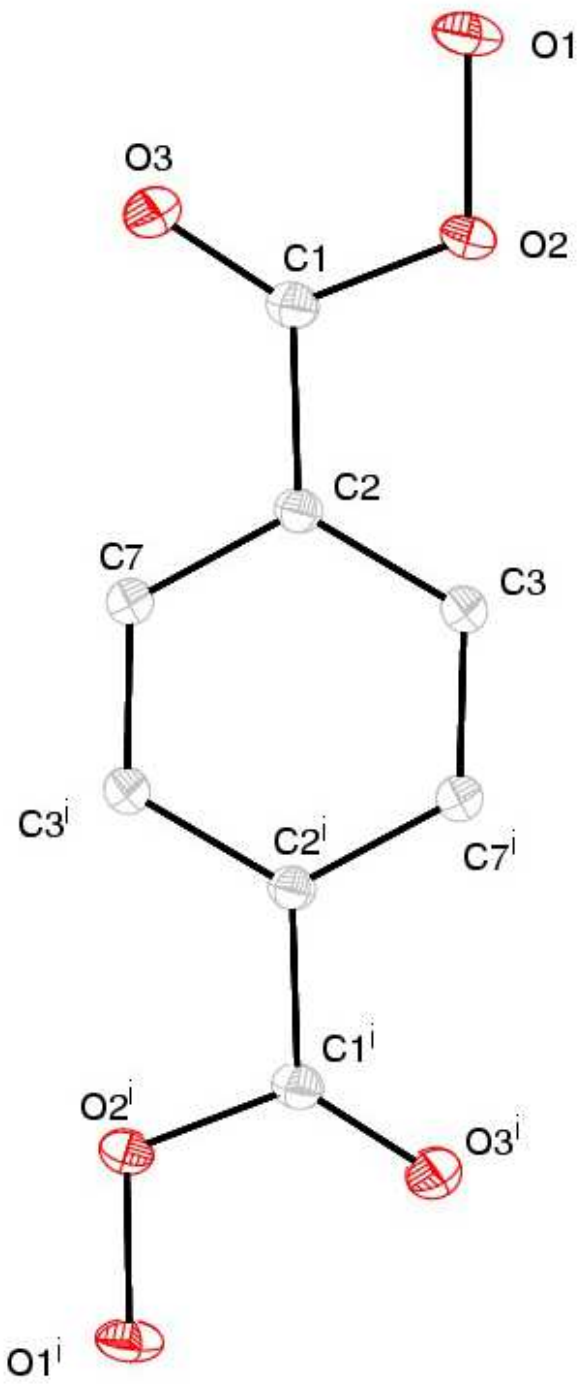

Figure 66. Perspective view of **49**·DMF with thermal ellipsoids at the 50% probability level.

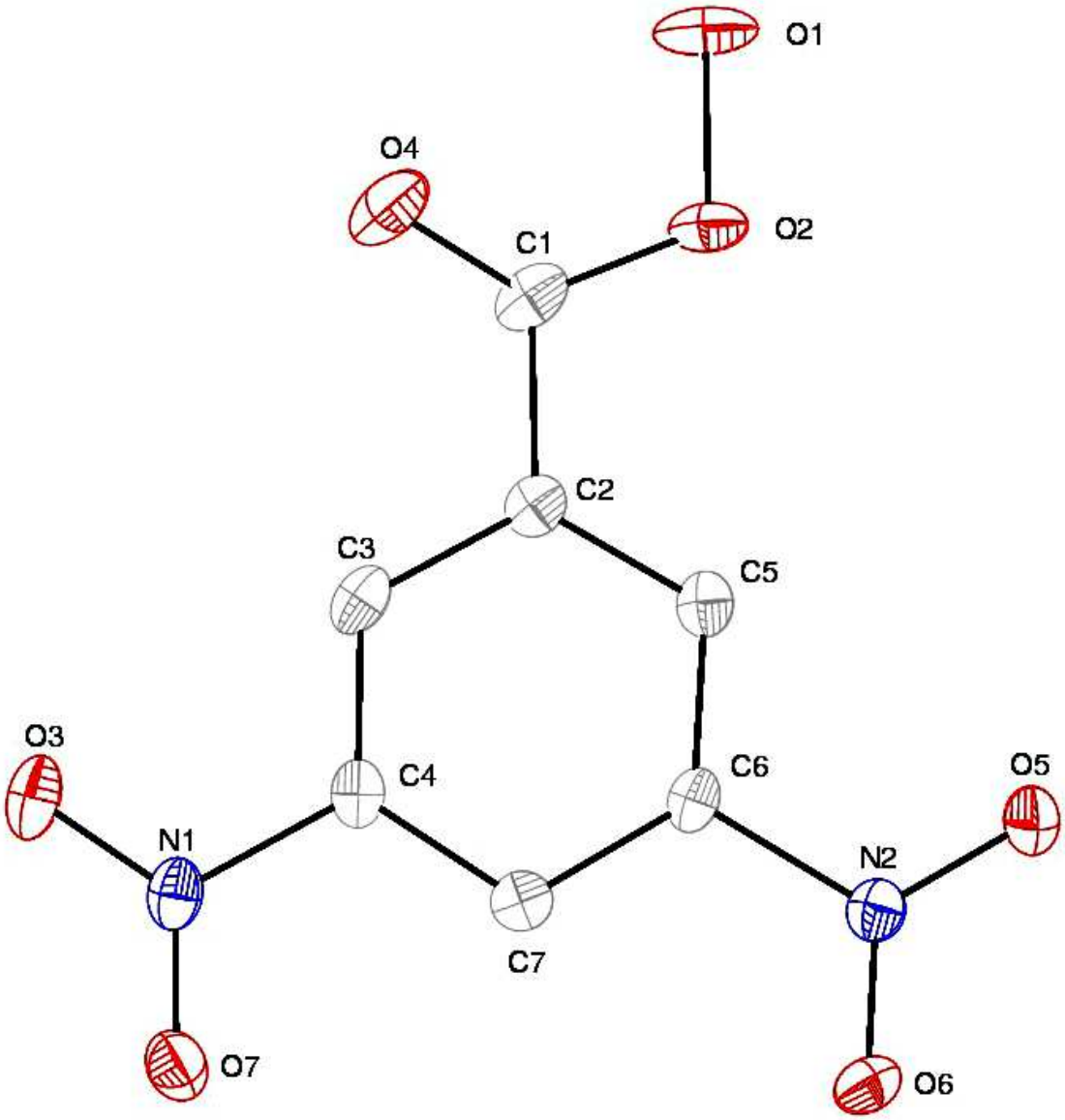

Figure 67. Perspective view of **52** with thermal ellipsoids at the 50% probability level.

Table 46. The selected bond lengths (Å) and angles (°) of **49**·DMF and **52**.

Bond/Angle	**49**·DMF	**52**
O–O	1.4559(5)	1.447(3)
C=O	1.2065(6)	1.196(4)
N–O		1.229(4)
		1.215(4)
		1.231(4)
		1.217(3)
C_{ring}–C(O)OOH	1.4957(6)	1.492(4)
N–C		1.473(4)
		1.470(4)
Angles:		
O=C–O	124.76(4)	125.7(3)
C–O–O	110.97(4)	111.5(2)
O–N–C_{ring}		117.4(3)
		117.9(3)
		118.9(3)
		117.5(3)
O–N–O		124.7(3)
		123.6(3)

Table 47. The list of hydrogen bonds and short contacts of **52**.

Compound	Number	Atom 1	Atom 2	Length (Å)	Length-VdW (Å)
52	1	O6	N1	3.001	–0.069
	2	N2	O3	3.054	–0.016
	3	O5	C7	3.055	–0.165
	4	O5	H5	2.712	–0.008
	5	O5	O1	2.887	–0.153
	6	H3	O1	2.343	–0.377
	7	O7	H7	2.435	–0.285
	8	N1	O8	2.993	–0.077
	9	H5	O11	2.431	–0.289
	10	O1	O10	3.017	–0.023
	11	O1	O11	2.749	–0.291
	12	H1	O10	2.365	–0.355
	13	H1	O11	1.884	–0.836
	14	H1	C11	2.747	–0.153
	15	O2	O10	3.021	–0.019
	16	O7	C12	3.048	–0.172
	17	O4	O9	3.029	–0.011
	18	O4	O10	2.67	–0.37
	19	O4	H6	1.74	–0.98
	20	C1	H6	2.758	–0.142
	21	O2	H6	2.45	–0.27
	22	C5	O13	3.142	–0.078
	23	O3	N4	3.053	–0.017
	24	O4	H8	2.534	–0.186
	25	N4	O8	3.006	–0.064
	26	C13	O8	3.215	–0.005
	27	O12	N3	3.032	–0.038
	28	O11	O14	2.978	–0.062
	29	C11	O14	3.043	–0.177

The O–O bond lengths of the peroxy acids **49**·DMF and **52** (Tables 24 and 25) are in the range of the O–O bond lengths reported for peroxy acids.[99] The crystalline densities of **49**·DMF, **51**,[135] and **52** are in the range of 1.423–1.748 g/cm^3. Compound **52** provided the highest crystalline density (1.748 g/cm^3) of all peroxo-based compounds in our study.

The X-ray crystal structure of **49**·DMF contains hydrogen bonds and many short contacts between molecules of **49** and DMF. These molecules of **49** and DMF are packed in wave-like layers assisted by intermolecular O–H···O hydrogen bonds (Figure 68). These are relatively strong O–H···O hydrogen bonds with distances of 2.580 Å. Based on the packing structure, there should be C–H···π interactions between methyl groups of DMF and the aromatic rings. These molecular layers interact via weak C–H···O hydrogen bonds, where H···O distances are in the range of 2.465–2.689 Å with short contacts such as C···O (2.978 Å) and C···H (2.614 Å). However, since **49** cannot be crystallized without DMF, it is hard to assess how the solid state interactions of solvent free **49** would influence the impact and friction sensitivities.

Compound **52** was obtained as solvent free crystals and the solid state structural features can be related to the impact and friction sensitivities. The X-ray crystal structure of **52** contains edge-to-face π-interactions (Figure 69). An oxygen atom of a nitro group from one molecule of **52** interacts with the aromatic ring of another molecule of **52**. This C_π···O short contact distance is 3.048 Å. There is a large number of stabilizing intermolecular interactions that involves the weak O–O bonds (Figure 70) as well as the oxygen atom of the carbonyl groups. These interactions can hold the oxygen atoms in place and stabilize the O–O trigger bonds in the crystalline lattice of **52**.

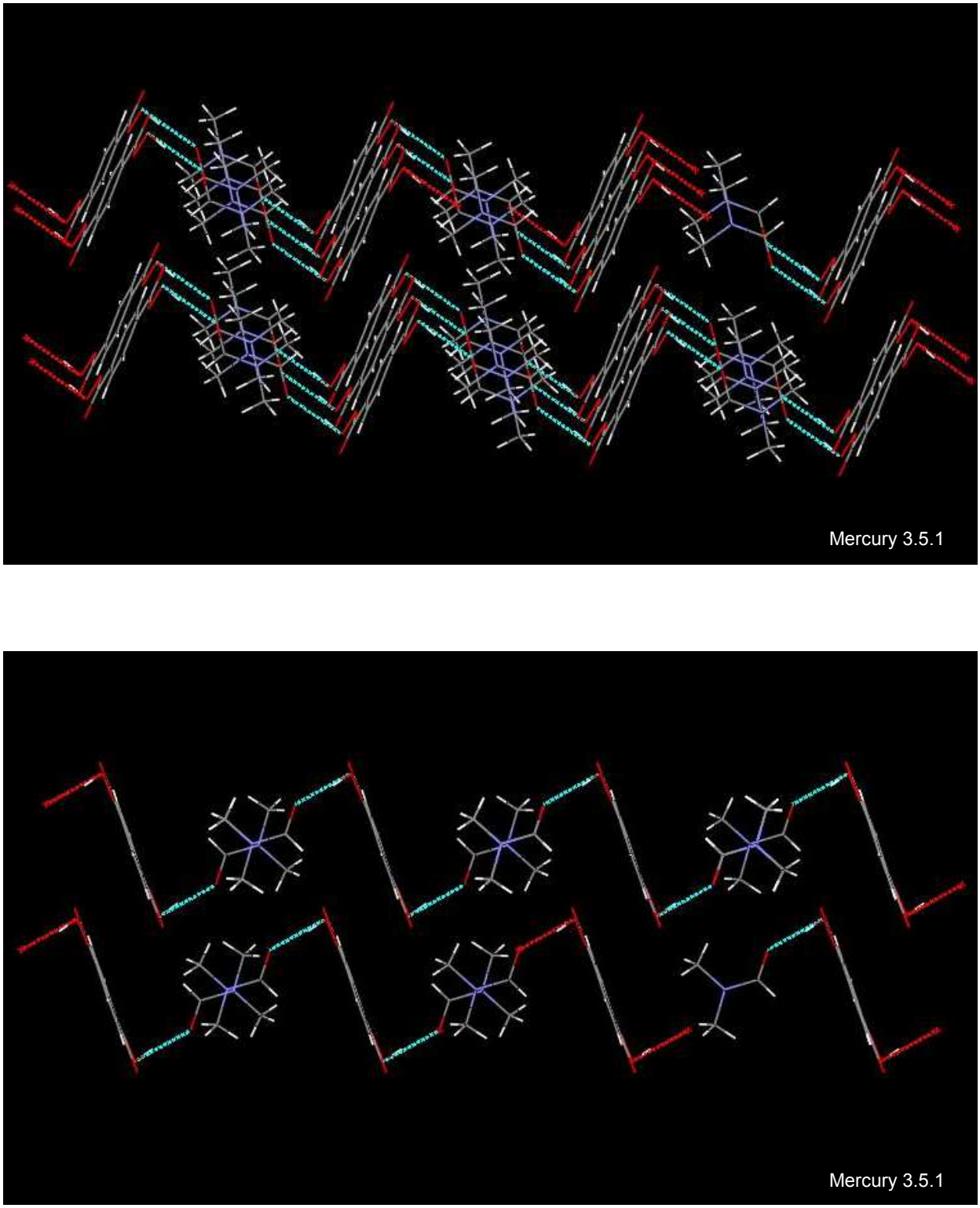

Figure 68. Wave-like layers of **49**·DMF assisted by intermolecular O–H···O hydrogen bonds (blue and red) between **49** and DMF.

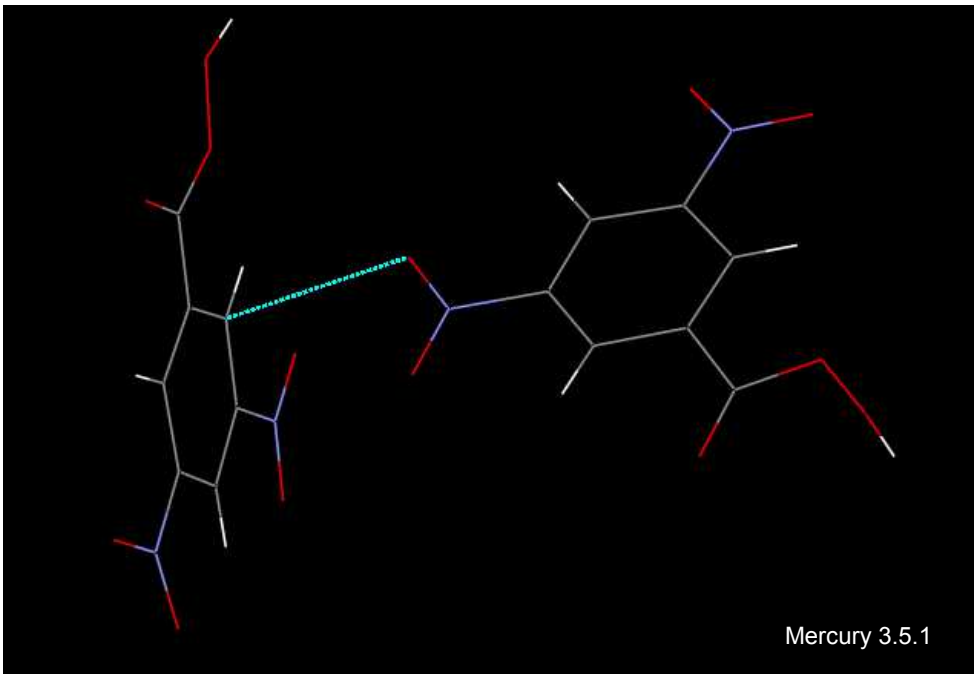

Figure 69. Edge-to-face π-interaction of **52**.

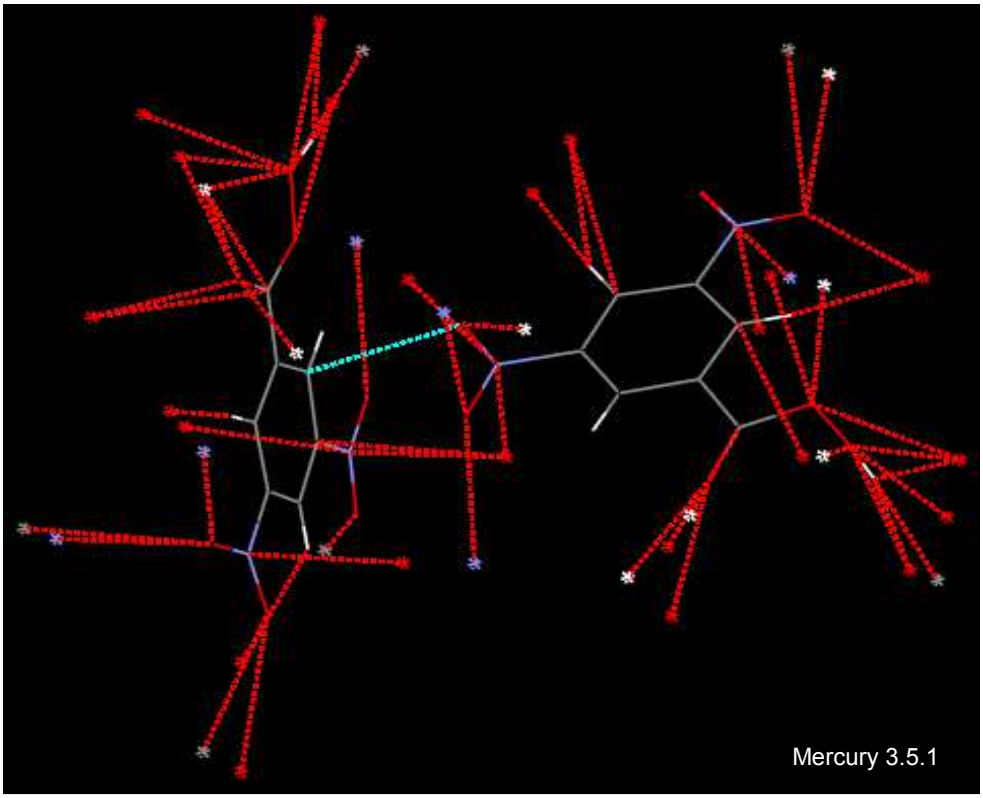

Grey, purple, white, and red asterisks indicate C, N, H, and O atoms, respectively

Figure 70. Stabilizing intermolecular interactions of **52**.

There are no molecular layers in the crystal structure of **52**. The aromatic rings are oriented in multiple directions (Figure 71) and a large number of hydrogen bonds and short contacts are present between these molecules. Thus, there are no slip planes that can move with respect to each other to reduce the impact and friction sensitivities.

In the crystal structure of **52**, there are moderate intermolecular O–H···O hydrogen bonds (2.670–2.749 Å) between the oxygen atom of the carbonyl groups and the –OOH groups. Many weak C–H···O hydrogen bonds are present where the H···O distances are in the range of 2.343–2.712 Å. There are six different types of O···O short contacts with distances in the range of 2.821–3.029 Å, which are less than the sum of the van der Waals radii for an O···O (3.04 Å) interaction (Table 47).[120] Interestingly, **52** contains the highest number of the stabilizing O···O short contacts from the peroxo-based crystal structures obtained. Both of the oxygen atoms of the O–O bonds form two O···O short contacts, and altogether there are four O···O short contacts for each O–O trigger bond. Each attractive O···O short contact can exert a stabilization energy of 3–13 kJ/mol.[81,83a,84a] The stabilizing effects of these interactions are cumulative in the solid state, and thus, these O···O short contacts, which cradle the O–O bonds, might assist in stabilizing the crystalline lattice as well as the weak O–O bonds of **52**.

The other two major types of short contacts of **52** are N···O and C···O interactions. The N···O interaction distances are in the range of 2.993–3.054 Å while the C···O interaction distances are in the range of 3.048–3.215 Å. These N···O and C···O short contacts are less than the sum of the van der Waals radii for N···O (3.07 Å) and C···O (3.22 Å) interactions, respectively.[120] There are also some C···H (2.747 and 2.758 Å) and O···H (2.365 and 2.450 Å) short contacts in the crystal structure of **52**.

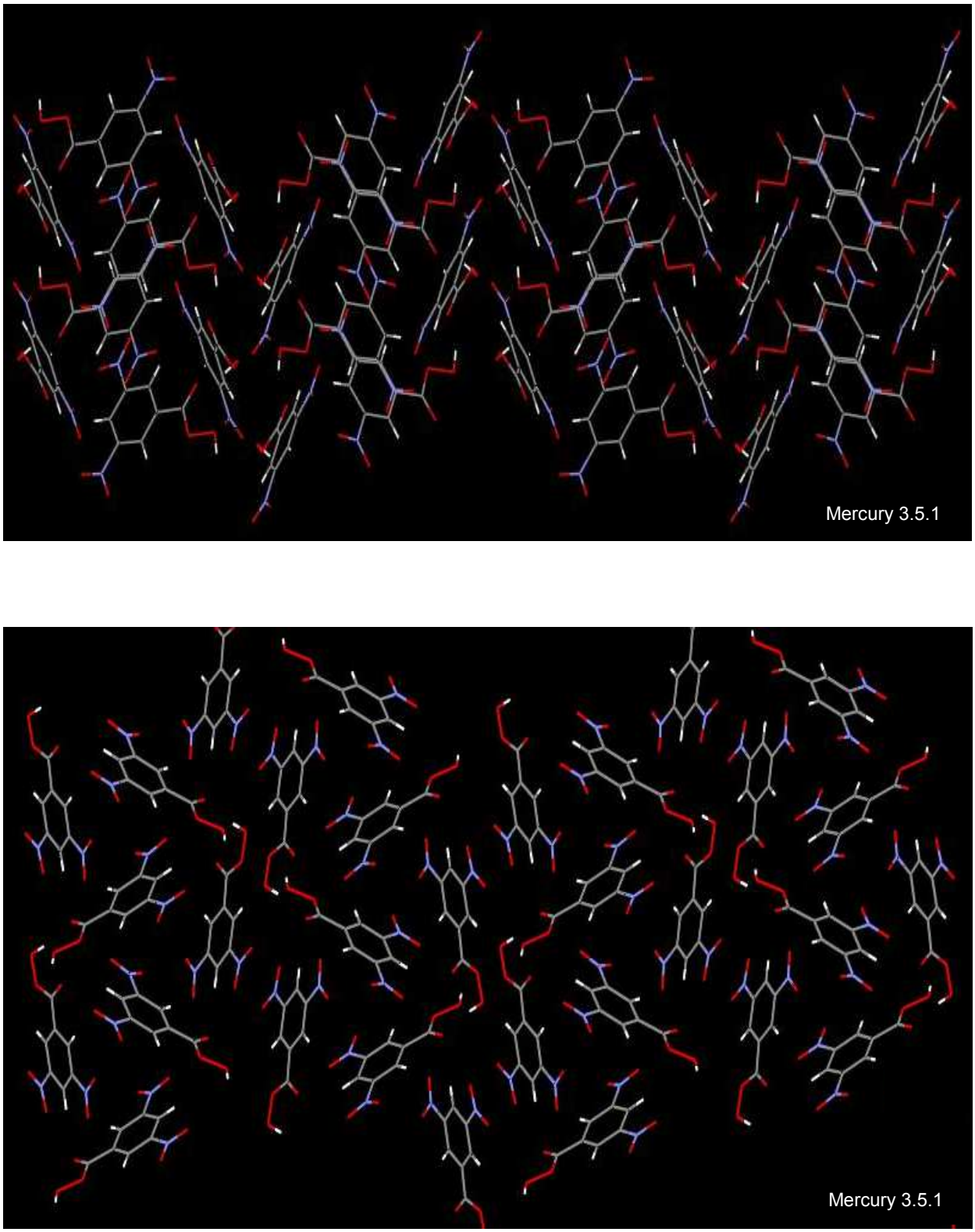

Figure 71. Crystal packing of molecules in the X-ray crystal structure of **52** without hydrogen bonds or short contacts.

The high crystalline density of **52** (1.748 g/cm^3 at 100 K) is useful in order to obtain a high detonation velocity. This crystalline density of **52** is higher than those of orthorhombic (1.704 g/cm^3 at 123 K) and monoclinic (1.713 g/cm^3 at 100 K) TNT.[119] The molecular weights of **52** and TNT (228.11 and 227.14 g/cm^3) are similar, and as a result the molecules of **52** pack more efficiently than TNT in the solid state.

Since the expected crystalline density goal for HEDMs is ≥ 1.8 g/cm^3, peroxo-based compounds with higher crystalline densities need to be obtained for higher detonation veloctities.[2] The secondary HEDMs with nitro groups have higher crystalline densities and hence, higher detonation velocities.[2,6b] By the addition of another nitro group onto **52**, the peroxy acid with the highest crystalline density (1.748 g/cm^3 at 100 K) in our study, we can obtain 2,4,6-trinitrobenzoperoxoic acid (**53**) shown in Figure 72.

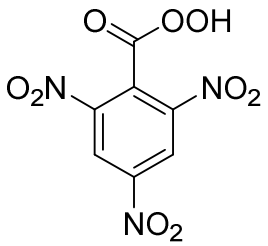

O:C = 9:7 = 1.29

Figure 72. 2,4,6-Trinitrobenzoperoxoic acid (**53**).

Unfortunately, the synthesis of **53** requires the known explosive TNT as the starting material, and the use of known explosives in academic laboratories is restricted. Thus, we have not attempted the synthesis of **53**. The crystalline density of **53** at 298 K was estimated to be 1.80 g/cm^3 by our collaborators from the Klapötke lab for the

energetic calculations. Since the crystalline density goal of ≥ 1.8 g/cm^3 can be approached with **53**, its energetic properties are of high interest.

6.2.4 Thermal Stability

Thermal stabilities of peroxy acids **49**–**52** were assessed using thermogravimetry (TGA/DTA). Their decomposition temperatures (T_{Dec}) were obtained from the thermograms. The decomposition temperature of **53** was estimated based on the functional groups present.[136] CBS-4M electronic enthalpies of **49**–**53** were calculated using the Gaussian09 software package to obtain heats of formation values ($\Delta_fH°$) by our collaborators from the Klapötke lab.[113] The T_{Dec} and $\Delta_fH°$ values of **49**–**53** are provided in Table 48.

Table 48. Decomposition temperatures and heats of formation values of **49**–**53**.

Compound	T_{Dec} (°C)	$\Delta_fH°$ (kJ/mol)
49	160	–584.1
50	167	–846.6
51	141	–324.3
52	132	–310.3
53	140[a]	–275.5

[a]Estimated decomposition temperature based on the functional groups present.[136]

The peroxy acids **49**–**53** are all fairly thermally stable. They have decomposition onsets ranging from 132–160 °C (Table 48). Their T_{Dec} values are relatively higher with respect to the other subclasses of organic peroxides. HEDM applications require T_{Dec} values ≥ 150 °C.[2,15] Compounds **49** and **50** have higher T_{Dec} values than 150 °C. However, the T_{Dec} values of peroxy acids **51**–**53** are also close to 150 °C for potential HEDM applications.

The $\Delta_f H°$ values of **49**–**53** are all negative, which indicates they are stable compounds that release energy upon formation. The nitro substituted peroxy acids have more positive $\Delta_f H°$ values in the range of –324.3 to –275.5 kJ/mol. These are the highest $\Delta_f H°$ values that were obtained for the peroxo-based compounds in our study. The higest $\Delta_f H°$ value was obtained for compound **53**, with the highest crystalline density and the highest oxygen and nitrogen content.

6.2.5 Preliminery Sensitivity Tests

The sensitivities of the peroxy acids **49**–**52** were studied using the flame, hammer impact, sand paper friction, and electrostatic discharge (Tesla coil) tests. Based on the flame and the Tesla coil tests, **50** appeared as a highly sensitive and energetic compound. It produced a sudden, large, and bright flame with a loud sound in the flame test and a sudden, large, and bright flame in the Tesla coil test. Compounds **49**, **51**, and **52** produced sensitive and energetic responses as well. However, the flame and Tesla coil test responses of **49**, **51**, and **52** were not as rapid as **50**. This indicates that **49**, **51**, and **52** are not highly sensitive, but are still energetic to produce positive responses.

Preliminary sensitivity test responses were also useful to confirm the formation of the peroxy acids by comparing with the corresponding carboxylic acids. The flame and Tesla coil test responses of the corresponding acids were significantly different from the peroxy acids. The acids only burned slowly in the flame tests and produced no responses in the Tesla coil tests. No sensitive responses were observed for the peroxy acids **49**–**52** in the hammer impact and sand paper friction tests.

6.2.6 Standard Sensitivity Tests

Impact, friction, and electrostatic discharge sensitivities of the peroxy acids **49**–**52** were determined with a BAM drop hammer, BAM friction tester, and an electrostatic spark sensitivity tester using standard experimental methods by our collaborators from Klapötke lab.[29–34] Table 49 includes the impact, friction, and electrostatic discharge sensitivities of **49**–**52**.

Table 49. Impact, friction, and electrostatic discharge sensitivities of **49**–**52**.

Compound	IS (J)	FS (N)	ESDS (J)
49	10	288	0.1
50	1	5	0.025
51	9	360	0.1
52	9	360	0.1

Based on the "UN Recommendations on the Transport of Dangerous Goods",[28] the peroxy acids **49**, **51**, and **52** are between "less sensitive" and "sensitive" while **50** is "very sensitive" towards impact. Compound **49** is "sensitive", **50** is "extremely sensitive", and **51** and **52** are "less sensitive" towards friction. The electrostatic discharge sensitivity value of **50** is only 0.025 J. This value is similar to the electrical discharges that can be generated by the human body (≤ 0.02 J).[2] Thus, **50** should only be handled with extreme care. The electrostatic discharge sensitivity values of **49**, **51**, and **52** are well above 0.02 J, and can be safely handled.

The sensitivities of the peroxy acids **49**, **51**, and **52** are much less than the known peroxo-based explosives TATP, DADP, HMTD, and MEKP. These sensitivities of **49**, **51**, and **52** are similar to the secondary explosive TNT (Table 2). Compounds **49**,

51, and **52** display the lowest sensitivity responses reported for the oxygen-rich peroxo-based compounds. When only peroxy acid groups were employed to increase the oxygen content and the energetic performance, the highly sensitive peroxy acid **50** was obtained. The attempts to increase the oxygen content further were also unsuccessful. However, when the oxygen and nitrogen contents were increased with nitro groups to increase the energetic performance, the sensitivities were not increased excessively. Compound **50** can be categorized as a primary explosive while **49**, **51**, and **52** can be categorized as secondary explosives. Peroxy acids **49**, **51**, and **52** are the first peroxo-based oxygen-rich compounds that are useful as secondary HEDMs.

Compound **51** contains a layered structure, packed in a wave-like orientation, with intralayer hydrogen bonding and only weak van der Waals forces in between the layers.[135] Thus, the solid state structure of **51** allows for some dissipation of energy upon initiation by movement of these layers with respect to each other.[84] However, the relative movement of the layers of **51** is restricted in certain directions since these layers are in a wave-like orientation.[84] The most insensitive crystals contain face-to-face stacked layers where sliding is unrestricted in all directions of the sliding plane.[84] Additionally, the short contacts and hydrogen bonds of **51**[135] may assist in stabilizing the O–O bonds in the crystalline lattice.

The X-ray crystal structure of **52** lacks face-to-face π-interactions, and has a layered structure assisted by intralayer hydrogen bonding with only weak van der Waals interactions in between the layers. Thus, slip planes are not present similar to the low sensitivity HEDMs.[84] According to the analysis of intermolecular short contacts, we discovered that **52** contains O–H···O and C–H···O hydrogen bonds and a large number

of O···O, N···O, and C···O short contacts. There are four stabilizing O···O short contacts and an O–H···O hydrogen bond that involve each O–O trigger bond. There are many N···O and C···O short contacts that can also stabilize the crystalline lattice of **52**. This network of weak interactions might facilitate energy dissipation in the crystalline lattice by disintegrating and reforming. The highly sensitive peroxo-based compounds TATP and DADP lack these strong O–H···O hydrogen bonds and stabilizing O···O, N···O, and C···O short contacts. Thus, the low sensitivity of **52** can be attributed to the stabilization of the O–O trigger bonds in the crystalline lattice by O–H···O hydrogen bonds and O···O short contacts as well as gaining an alternative means to dissipate energy without breaking covalent bonds with the weakly interacting network of O···O, N···O, and C···O short contacts. Still, more studies need to be carried out to understand the influence of these solid state interactions on the physical properties of materials more completely.

6.2.7 Energetic Performance Calculations

The energetic properties of the peroxy acids **49**–**53** were calculated using the EXPLO5 V6.02 software (Table 50) by our collaborators from the Klapötke lab.[114] The calculated V_{Det} and P_{Det} values of **49**–**53** are in the range of 5262–7885 m/s and 88–269 kbar, respectively. They are high detonation velocities, which are highly useful for HEDM applications.

Table 50. Calculated energetic properties of **49**–**53**.

Property	49	50	51	52	53
Formula	$C_8H_6O_6$	$C_9H_6O_9$	$C_7H_5NO_5$	$C_7H_4N_2O_7$	$C_7H_3N_3O_9$
FW (g/mol)	198.14	258.15	183.12	228.11	271.11
Ω[a] (%)	–105.0	–74.38	–100.5	–63.13	–38.08
ρ[b] (g/cm^3)	1.423	-	1.586[135]	1.748	-
ρ[c] (g/cm^3)	1.397	1.4[d]	1.557	1.716	1.8[d]
EXPLO5 V6.02					
$\Delta_{Ex}U°$ (kJ/kg)	–3373	–3590	–3934	–4660	–5243
P_{Det} (kbar)	88	105	133	213	269
V_{Det} (m/s)	5262	5588	6176	7217	7885
V_o (L/kg)	598	628	593	596	619

[a]Oxygen balance for oxidation of carbon to CO_2
[b]Crystalline density at 100 K
[c]Crystalline densities at 298 K (for energetic calculations)
$\rho_{298K} = \rho_T / [1 + \alpha_v (298 - T)]$ (T = 100 K, ρ_T = Desnsity at 100 K, α_v = 1.5 x 10^{-4} K^{-1})
[d]Estimated crystalline densities at 298 K (for energetic calculations)

The detonation velocities of peroxy acids **49**–**53** increase with the increasing crystalline densities. Since the higher crystalline densities were obtained with the nitro aromatic compounds **51**–**53**, the higher detonation velocities were obtained for **51**–**53**. The synthesized peroxy acid with the highest crystalline density, **52**, has the highest detonation velocity (7217 m/s) reported for peroxo-based compounds. This detonation velocity of **52** is greater than the detonation velocity (6900 m/s) of the common secondary explosive TNT. Compound **53** has the highest detonation velocity (7885 m/s)

of our whole study of the peroxo-based compounds. This detonation velocity of **53** is much higher than TNT and is even approaching the detonation velocity of the secondary high explosive RDX (8750 m/s). The oxygen balance of **53** (–38.08%) is also close to RDX (–21%). Since the impact and friction sensitivities of the peroxy acids **49**, **51**, and **52** are low, they are good candidates for secondary HEDMs with their impressive detonation velocities. Although impact and friction sensitivities of **53** were not measured, they should be sufficiently low for use as secondary HEDMs based on the organic framework that is similar to the low sensitivity explosive TNT. Thus, **53** could be an excellent candidate for secondary HEDMs with the highly impressive detonation velocity.

6.3 Conclusions

We have synthesized and characterized oxygen-rich peroxy acids **49**–**52** for potential use as HEDMs. The energetic properties of **53** were calculated since it could be a highly impressive candidate for HEDM applications. However, it cannot be synthesized in our laboratory, since the known high explosive TNT is required as a starting material.

The peroxy acids **49**, **51**, and **52** have surprisingly low impact and friction sensitivities and high detonation velocities, compared to the other peroxo-based subclasses studied and the known peroxo-based explosives TATP, DADP, HMTD, and MEKP. We propose that the stabilization of the O–O trigger bonds in the crystalline lattice through O–H···O and C–H···O hydrogen bonds and O···O, N···O, and C···O short contacts are the cause for the surprisingly low impact and friction sensitivities of **52**. The detonation velocity of **52** (7217 m/s) is the highest reported detonation velocity

for peroxo-based compounds. We can approach the detonation velocity of the secondary high explosive RDX (8750 m/s)[6b] with **53** (7885 m/s). The low sensitivities and high detonation velocities of peroxy acids **49**, **51**, and **52** are appropriate for applications as secondary HEDMs. The peroxy acids **49**, **51**, and **52** are the first peroxo-based oxygen-rich compounds that are useful as secondary HEDMs. Through this work, we have obtained peroxy acids with high detonation velocities and surprisingly low sensitivities for potential use as HEDMs.

Major issues with the known peroxo-based explosives are their high volatilities (TATP and DADP) and low thermal stabilities (HMTD), which are disadvantageous for HEDM applications. Compound **52** was reported as a storable reagent that could be useful for epoxidation and Baeyer-Villiger oxidation reactions.[133] It has been stored for periods up to 1 year in a freezer (< –10 °C) without an observable loss of activity. Thus, peroxy acids might be stored for long periods without a loss in their energetic performances in HEDM applications. Based on the thermogravimetric data, peroxy acids were also more thermally stable than the other subclasses.

Additionally, we have obtained the peroxy acids in high yields without much synthetic manipulations. All of these properties combined together render peroxy acids a highly suitable subclass of peroxo-based compounds that could be developed as HEDMs. This work also suggests that the peroxy acid functional group can be effectively used to increase the oxygen contents and thus, the energetic properties without excessively increasing the impact and friction sensitivities.

6.4 Experimental Section

General Considerations: Chemicals were purchased from Sigma-Aldrich, Acros Organics, or Alfa Aesar and were used without further purification. ACS grade solvents were obtained from EMD and Fisher Scientific. Syntheses of **51** and **52** were carried out using slightly modified published procedures.[133,134] Hydrogen peroxide solution (50 wt.% in H_2O) was evacuated on the Schlenk line (4–5 h per 5.0 mL) to obtain a concentrated hydrogen peroxide solution (84 wt.% in H_2O) for the syntheses of **49**–**52**. The final concentration of the hydrogen peroxide solution was analyzed by titrating with a solution of 0.176 M $KMnO_4$ under acidic conditions (H_2SO_4).

^1H and $^{13}C\{^1H\}$ NMR spectra were obtained from the Varian Mercury 400 (400 MHz and 101 MHz) NMR spectrometer or MR 400 (400 MHz and 101 MHz) NMR spectrometer, in $CDCl_3$, CD_3OD, or $(CD_3)_2NCOD$ as indicated and were referenced to the residual proton and carbon resonances of the solvents ($CDCl_3$, ^1H NMR δ 7.27; ^{13}C NMR 77.23 ppm. CD_3OD, ^1H NMR δ 3.31; ^{13}C NMR 49.00 ppm. $(CD_3)_2NCOD$, ^1H NMR δ 2.74; ^{13}C NMR 162.70 ppm). Infrared spectra were obtained with a Shimadzu MIRacle 10 IRAffinity-1 equipped with a single reflection ATR accessory. Melting points were determined on an Electrothermal IA 9300 melting point apparatus and are uncorrected. Thermogravimetric (TGA/DTA) measurements to determine the decomposition temperatures of compounds **49**–**52** were performed at a heating rate of 5 °C min^{-1} with an OZM Research DTA 552-Ex instrument.

Qualitative Sensitivity Tests: Qualitative sensitivities to heat, impact, and electrostatic discharge were determined to assess initial safety issues. Tests included burning about 3–5 mg of the compound in the Bunsen burner flame, striking 3–5 mg of

the compound on a metal plate with a hammer, and passing an electrostatic discharge through 3–5 mg of the compound on a metal plate using an Electro Technic BD 10 Tesla coil (120 V, 0.35 A).

Quantitative Sensitivity Tests: Quantitative sensitivity Tests include BAM drop hammer[31] impact tests carried out according to STANAG 4489[29] modified instructions[30] using approximately 0.4 mL of the compound, Friction tests with a BAM friction tester carried out according to STANAG 4487[32] modified instructions[33] using approximately 5 mg of the compound, and electrostatic spark tests with an ESD 2010 EN, OZM Electric Spark Tester according to STANAG 4515[34] instructions using 0.1 mL of the compound performed by Klapötke group.

Preparation of Benzene-1,4-bis(carboperoxoic) acid (49). A 100 mL round bottomed flask was charged with a magnetic stir bar and terphthaloyl chloride (0.105 g, 0.517 mmol). Then, methanesulfonic acid (0.4 mL, 5 mmol) was added and the reaction mixture was allowed to stir for 5–10 min at 50 °C. Afterwards, hydrogen peroxide solution (84 wt.% in H_2O, 0.25 mL, 4.0 mmol) was added drop by drop and the reaction mixture was stirred for 1 h at 50 °C. The product mixture was cooled to 0 °C in an ice bath, and then crushed ice (0.5 g) was added to the reaction mixture. The resultant white precipitate was collected by suction filtration and was dried under reduced pressure to afford 0.093 g (94%) of **49** as a white solid: mp 165 °C, dec. (explodes); IR (ν, cm^{-1}): 3240 (m, broad), 3125 (w), 3107 (w), 3063 (w), 1715 (m), 1504 (w), 1414 (m), 1393 (m), 1304 (w), 1267 (m), 1250 (m), 1092 (m), 1015 (m), 895 (m), 866 (m), 845 (m), 714 (s); ^{1}H NMR (400 MHz, $(CD_3)_2NCOD$, 23 °C, δ) 14.18 (broad s, 1H, OO*H*), 8.06 (s, 4H, C*H*); $^{13}C\{^1H\}$ NMR (101 MHz, $(CD_3)_2NCOD$, 23 °C, ppm) 164.93 (peroxy *C*), 132.50

(*C*), 130.04 (*C*H); Anal. Calcd for $C_8H_6O_6$: C, 48.49; H, 3.06. Found: C, 48.10; H, 3.36. Colorless needle-like single crystals were grown from DMF at –29 °C.

Preparation of Benzene-1,3,5-tris(carboxyloperoxoic) acid (50). A dry 100 mL Schlenk flask was charged with a magnetic stir bar and benzene-1,3,5-tricarbonyl trichloride (0.105 g, 0.396 mmol). Then, methanesulfonic acid (0.5 mL, 6 mmol) was added and the reaction mixture was allowed to stir for 5–10 min at 50 °C. Afterwards, hydrogen peroxide solution (84 wt.% in H_2O, 0.30 mL, 4.8 mmol) was added drop by drop and the reaction mixture was stirred for 30 min at 50 °C. The product mixture was cooled to 0 °C in an ice bath, and then crushed ice (0.5 g) was added into the reaction mixture. The white solid in the reaction mixture was collected by suction filtration and was dried under reduced pressure to afford 0.101 g (99%) of **50** as a white solid: mp not taken due to explosion hazard; IR (ν, cm^{-1}): 3226 (m, broad), 3087 (m), 1737 (s), 1608 (w), 1410 (m), 1326 (m), 1278 (m), 1224 (s), 1131 (m), 1115 (m), 1098 (m), 934 (w), 881 (m), 835 (w), 767 (w), 717 (s); ^{1}H NMR (400 MHz, CD_3OD, 23 °C, δ) CO_3H not observed due to exchange with CD_3OD, 8.65 (s, 4H, C*H*); $^{13}C\{^1H\}$ NMR (101 MHz, CD_3OD, 23 °C, ppm) 164.95 (peroxy *C*), 134.52 (*C*), 130.51 (*C*H); Anal. Calcd for $C_9H_6O_9$: C, 41.87; H, 2.35. Found: C, 41.98; H, 2.36.

Preparation of 4-Nitrobenzoperoxoic acid (51). Compound **51** was prepared in 94% yield as a pale yellow solid by a literature procedure[133] starting from 4-nitrobenzoic acid: mp 138–140 °C (lit[133] 139 °C); IR (ν, cm^{-1}): 3308 (broad, m), 3115 (w), 2986 (w), 1744 (m), 1718 (m), 1609 (m), 1541 (m), 1491 (w), 1414 (m), 1383 (m), 1348 (m), 1321 (m), 1302 (m), 1258 (m), 1242 (m), 1111 (w), 1074 (m), 1013 (w), 974 (w), 951 (w), 934 (w), 893 (m), 868 (m), 837 (s), 775 (w), 710 (s); ^{1}H NMR (400 MHz, $CDCl_3$, 23 °C, δ)

11.57 (broad s, 1H, OO*H*), 8.37 (dm, *J* = 8.4 Hz, 2H, C*H*), 8.21 (dm, *J* = 8.8 Hz, 2H, C*H*); $^{13}C\{^{1}H\}$ NMR (101 MHz, $CDCl_3$, 23 °C, ppm) 166.33 (peroxy *C*), 151.45 (*C*), 131.55 (*C*), 130.81 (*C*H), 124.26 (*C*H); Anal. Calcd for $C_7H_5NO_5$: C, 45.90; H, 2.76; N, 7.65. Found: C, 46.37; H, 3.00; N, 7.75.

Preparation of 3,5-Dinitrobenzoperoxoic acid (52). Compound **52** was prepared in 96% yield as a pale yellow solid by a literature procedure[134] starting from 3,5-dinitrobenzoic acid: mp 113–115 °C (lit[134] 113–115 °C); IR (ν cm^{-1}): 3447 (broad, m), 3088 (m), 2883 (w), 1734 (m), 1717 (m), 1701 (m), 1628 (m), 1597 (w), 1541 (s), 1489 (w), 1458 (m), 1420 (w), 1348 (s), 1269 (m), 1179 (m), 1152 (s), 1094 (m), 1043 (m), 916 (m), 881 (w), 781 (m), 764 (w), 714 (s); ^{1}H NMR (400 MHz, CD_3OD, 23 °C, δ) OO*H* resonance not observed due to exchange with CD_3OD, 9.22 (t, *J* = 2.4 Hz, 1H, C*H*), 9.03 (d, *J* = 2.4 Hz, 2H, C*H*); $^{13}C\{^{1}H\}$ NMR (101 MHz, CD_3OD, 23 °C, ppm) 163.62 (peroxy *C*), 150.17 (*C*), 131.98 (*C*), 129.73 (*C*H), 123.83 (*C*H); Anal. Calcd for $C_7H_4N_2O_7$: C, 36.86; H, 1.77; N, 12.27. Found: C, 36.89; H, 1.90; N, 11.95. Colorless, thin, needle-like single crystals were grown from 1:1 diethyl ether:pentane at –29 °C.

CHAPTER 7

Conclusions and Future Directions

The design of highly energetic and low sensitivity HEDMs is an extremely challenging process since the molecules tend to be unstable and sensitive to stimuli with higher energy contents. However, many highly energetic inorganic, organic, and polymeric HEDMs have been synthesized with appropriate sensitivities for the safe use as primary, secondary, and tertiary HEDMs. The field of organic HEDMs is dominated by compounds with high nitrogen contents, due to the ability of increasing the energy content without excessively increasing the sensitivities to stimuli. They are mainly nitrogen rich heterocycles or nitro compounds. The highest detonation velocity obtained for the organic HEDMs is 10,100 m/s for octanitrocubane (ONC).[1e,6b] There is still a constant effort to obtain low sensitivity HEDMs with high detonation velocities.

The other main aspect of HEDM design is the synthesis of compounds with environmentally friendly decomposition products. Primary explosives LA, LS, and MF contain heavy metals such as lead and mercury that cause heavy metal poisoning. The tertiary explosive NH_4ClO_4 has been widely used in propellant and explosive formulations. Leaching of NH_4ClO_4 into groundwater has resulted in accumulation of it causing groundwater plumes. Hence, people have been exposed to ClO_4^- ions. The ClO_4^- ion is similar in size to the iodide ion, which causes a competition in the thyroid gland. This could lead to disruptions of metabolic pathways and even thyroid cancer. Many research efforts are currently being carried out to find replacements for the toxic primary explosives and NH_4ClO_4 with only a little success.

Peroxo-based oxygen-rich compounds can be proposed as a potential new class of greener HEDMs due to the more environmentally friendly decomposition products CO_2 and/or CO, H_2O, and O_2. These peroxo-based compounds have been studied as a strategy to increase the oxygen contents in the design of HEDMs. However, increasing the oxygen contents with the peroxo-based compounds gained only a limited interest due to their extremely high sensitivities, low thermal and chemical stabilities, and low detonation velocities. Currently, TATP, DADP, MEKP, and HMTD are the only well-studied energetic peroxides. These peroxo-based compounds have not found any practical applications as civilian or military HEDMs due to their extreme sensitivities. Unfortunately, due to the ease of synthesis and wide availability of the starting materials TATP, DADP, MEKP, and HMTD have been used in multiple terrorist attacks.

For practical use as HEDMs, the extremely high impact and friction sensitivities of peroxo-based compounds need to be reduced. Also, new peroxo-based compounds with better detonation velocities, high thermal stabilities, and more chemical compatibilities need to be discovered. The peroxo-based compounds also need to be systematically studied to discover the highest possible oxygen contents that can be safely incorporated, their sensitivities and energetic properties, and paths to gear towards safer less sensitive peroxo-based compounds. This study also allows ensuring safety in numerous current applications of peroxo-based compounds by educating the industrial community about their sensitivities and energetic properties. Also, a wealth of fundamental information can be obtained about the structures and energetic properties of peroxo-based compounds for further development of peroxo-based HEDMs.

We have chosen four categories of peroxo-based compounds: *tert*-butyl peroxides, *tert*-butyl peroxy esters, hydroperoxides, and peroxy acids to study the sensitivities and energetic properties systematically for their potential use as greener HEDMs. Initially, more carbon rich *tert*-butyl peroxides and *tert*-butyl peroxy esters and then, more oxygen rich hydroperoxides and peroxy acids were synthesized and fully characterized. Preliminary sensitivity tests (flame, hammer impact, sand paper friction, and Tesla coil electrostatic discharge tests) were carried out to select the most sensitive and energetic compounds. The standard sensitivities and energetic properties of the selected highly energetic compounds were further studied in collaboration with Prof. Thomas M. Klapötke, Ludwig-Maximilians University, Munich, Germany. Standard impact, friction, and electrostatic discharge sensitivities of the more energetic peroxo-based compounds were studied with a BAM drop hammer, BAM friction tester, and an electrostatic spark sensitivity tester using standard experimental methods.[29–34] The influence of solid state interactions on the impact and friction sensitivities of peroxo-based compounds was analyzed to gain insights about controlling the solid state structural features to reduce their high sensitivities for safer practical applications. The energetic properties of the peroxo-based compounds with varying oxygen contents, crystalline densities, and ring and steric strain energies were obtained by theoretical calculations using the Explo5 V6.02 software.[114]

tert-Butyl peroxides **1**–**15** were synthesized in low to moderate yields and were fully characterized. X-ray crystal structures were obtained for **1**, **3**, **5**, **8**, **11**, **13**, and **15**. Their crystalline densities are in the range of 1.098–1.166 g/cm^3, which are too low for HEDM applications. *tert*-Butyl peroxides **1**–**15** are fairly thermally stable compounds

with decomposition temperatures in the range of 110–140 °C. Compounds **1**–**15** only deflagrated upon burning. They were not sensitive to impact, friction, or electrostatic spark according to the preliminary sensitivity tests. Only slight differences in the sensitivities and energetic properties were observed with the increasing oxygen content or ring strain. Hence, **1**–**15** can be described as low energetic and fairly safe peroxo-based compounds to handle. Thus, no standard energetic materials properties were obtained for *tert*-butyl peroxides **1**–**15**.

tert-Butyl peroxy esters **16**–**22** were synthesized in moderate to high yields and were all completely characterized along with X-ray crystal structures. Their crystalline densities are in the range of 1.161–1.487 g/cm^3, which are higher than *tert*-butyl peroxides, but are still low for HEDM applications. Except for **20**, the rest of the *tert*-butyl peroxy esters are fairly thermally stable compounds with the decomposition temperatures in the range of 86–123 °C. The heats of formation values of **16**–**22** are all negative, which indicates that they are fairly stable organic compounds. Nitro-substituted aromatic *tert*-butyl peroxy esters **21** and **22** have the more positive heats of formation values and thus, higher energy contents. The aromatic *tert*-butyl peroxy esters **16**–**18**, **21**, and **22** have much lower impact and friction sensitivities with respect to the peroxo-based explosives TATP, DADP, MEKP, and HMTD. There are numerous intermolecular interactions that involve the oxygen atoms of the peroxy ester groups, which could assist in reducing the impact and friction sensitivities of **16**–**18**, **21**, and **22**. Since there are weak O–O bonds that are not involved in any intermolecular contacts in the crystal structure of **19**, it was relatively high in sensitivity. Large voids in the crystal structure of the non-

aromatic *tert*-butyl peroxy ester **20** might have caused its high sensitivity. Compounds **16**–**22** were all surprisingly highly energetic despite the low oxygen and nitrogen contents. This highly energetic nature could be a result of the high O:C ratios (0.75–3.00) in the central cores of **16**–**22**. The calculated detonation velocities of **20**–**22** (5361–6003 m/s) are greater than the detonation velocities of TATP, DADP, MEKP, and HMTD (4,511–5,300 m/s).[6b,35] The highest detonation velocities were obtained for the nitro-substituted aromatic *tert*-butyl peroxy esters **21** and **22** due to the high crystalline densities. With their very low impact and friction sensitivities, they could be useful as secondary explosives. Compounds **21** and **22** are among the first highly energetic and low sensitivity peroxo-based compounds that can be categorized as secondary HEDMs. Through this work, we have obtained surprisingly highly energetic and low sensitivity *tert*-butyl peroxy esters with relatively low oxygen and nitrogen contents for potential use as HEDMs.

Geminal hydroperoxides **23**–**38** were synthesized in moderate to high yields and were fully characterized. These are more oxygen rich peroxo-based compounds and the O:C ratios are in the range of 0.40–1.33. Compounds with higher peroxy oxygen contents were not feasible with the mild synthetic method employed. X-ray crystal structures were obtained for the geminal hydroperoxides **24**, **26**, **27**, **29**, **30**, **34**, and **36** and the crystalline densities are in the range of 1.266–1.648 g/cm^3. These crystalline densities are higher than the *tert*-butyl peroxides and *tert*-butyl peroxy esters. Compounds **24**–**31** and **34**–**38** were fairly thermally stable geminal hydroperoxides and their decomposition temperatures are in the range of 90–130 °C. The heats of formation

values of **34**–**36** and **38** are all negative, which indicates that they are stable organic compounds. Compound **36** was the geminal hydroperoxide with the most positive heat of formation and thus, it is the geminal hydroperoxide with the highest energy content. The sensitivities and the energetic properties increase with the increasing oxygen contents and ring strain based on the preliminary sensitivity tests. According to the standard sensitivity tests, the impact and friction sensitivities of **34**–**36** and **38** are high, and they can be categorized as primary explosives. However, the sensitivities of **34**–**36** are less than the known peroxo-based explosives TATP, DADP, MEKP, and HMTD. This could be due to the involvement of the weak O–O bonds of **34**–**36** in numerous stabilizing intermolecular interactions including O–H···O hydrogen bonds and O···O contacts. These sensitivities of **34**–**36** are practically useful, although they are higher than the optimum sensitivities for primary explosives. Compound **38** has the highest O:C ratio (1.33), and has impact and friction sensitivities comparable to TATP, DADP, MEKP, and HMTD (Tables 3–6). This indicates that when the peroxy O:C ratio is above 1.00, sensitivity becomes high regardless of the stabilizing intermolecular short contacts. Thus, the maximum peroxy O:C ratio that could be safe to handle is about 1.00. Compounds **34**–**36** and **38** were the most energetic compounds and their detonation velocities are in the range of 6150–7130 m/s. These calculated detonation velocities are greater than the detonation velocities of TATP, DADP, MEKP, and HMTD (4,511–5,300 m/s).[6b,35] The highest detonation velocity was obtained for **36**, which has the highest crystalline density. The detonation velocity of **36** (7130 m/s) is greater than the secondary explosive TNT (6900 m/s).[11b] According to this work, we

have learned that through careful manipulation of organic peroxide structures, compounds with highly useful energetic materials properties can be obtained.

The series of oxygen-rich cyclic dihydroperoxy compounds **39**–**43** and hydroperoxy compounds **44**–**48** were synthesized and fully characterized with the X-ray crystal structures obtained for all the solid compounds **39**–**43** and **45**–**48**. Their crystalline densities are in the range of 1.328–1.474 g/cm^3. Except for **40** and **45**, the rest of the cyclic hydroperoxy compounds are fairly thermally stable. Their decomposition temperatures are in the range of 82–133 °C. The heats of formation values are all negative, which indicates that they are fairly stable organic compounds. More positive heats of formation values were obtained for the dihydroperoxy compounds **39**–**43** than the hydroperoxy compounds **44**–**48**. All of the cyclic dihydroperoxy compounds **39**–**43** were highly sensitive to impact and friction similar to the peroxo-based explosives TATP, DADP, MEKP, and HMTD regardless of the stabilizing intermolecular interactions including O–H···O and C–H···O hydrogen bonds and multiple short contacts. The higher O:C ratios (0.86–1.00) of **39**–**43** than TATP and DADP might have caused these high impact and friction sensitivities of **39**–**43**. The extremely high sensitivities of **40** can be attributed to the high angle and torsional strain and arrangement of the molecules as hydrogen bonded pairs that create more voids in the crystalline lattice. The hydroperoxy compounds **45**–**48** with one less O–O trigger bond than the corresponding dihydroperoxy compounds were less sensitive than **39**–**43**. All of the dihydroperoxy compounds **39**–**43** have impressive calculated detonation velocities in the range of 6350–6694 m/s. However, their extremely high sensitivities render them unsafe for HEDM applications. Interestingly, the hydroperoxy compounds

45–**48** also have high detonation performances in the range of 6100–6461 m/s even with the slightly lower oxygen contents. The detonation velocities were higher with higher crystalline densities and higher oxygen contents. Thus, compounds **43** and **48** were the most energetic from the cyclic dihydroperoxy and hydroperoxy compounds, respectively. Except for **45** with a low thermal stability, **46**–**48** with high detonation performances and low impact and friction sensitivities are attractive candidates for use as primary HEDMs. We observed that the ring strain was useful in increasing the detonation velocities, since it led to compounds with higher crystalline densities. However, increasing the steric strain using bulky groups led to lower crystalline densities and lower detonation velocities. Additionally, increasing the steric strain not only increased the sensitivity of **40** and **45** but also reduced their thermal stabilities. According to this work with cyclic dihydroperoxy compounds **39**–**43** and hydroperoxy compounds **44**–**48**, we have demonstrated that sensitivities and energetic performances of peroxo-based compounds could be tuned by careful structural manipulations of peroxo-based compounds.

We have synthesized oxygen-rich peroxy acids **49**–**52** in high yields with minimum synthetic manipulations and they were fully characterized for potential use as HEDMs. The X-ray crystal structures of **49** and **52** were obtained and the crystalline densities are in the range of 1.423–1.748 g/cm^3. Compound **52** provided the highest crystalline density (1.748 g/cm^3) of all the peroxo-based compounds in our study. Compound **53** with high oxygen and nitrogen contents and an estimated crystalline density of 1.8 g/cm^3 at 298 K could be a highly impressive candidate for HEDM applications, although it cannot be synthesized in our laboratory. The decomposition

temperatures of peroxy acids **49**–**52** are in the range of 132–167 °C and they are more thermally stable than the other categories of peroxo-based compounds studied. The peroxy acids **49**, **51**, and **52** have lower impact and friction sensitivities than all of the other peroxo-based subclasses studied and the known peroxo-based explosives TATP, DADP, HMTD, and MEKP. Compound **50**, with three peroxy acid groups and an O:C ratio of 1.00, was highly sensitive. Based on the crystal structure of **52**, there is no layered arrangement of molecules to provide slip planes to dissipate energy upon initiation by stimuli. Thus, the low sensitivity of **52** can be attributed to the stabilization of the weak O–O bonds in the crystalline lattice by O–H···O hydrogen bonds and O···O short contacts. The weakly interacting network of stabilizing intermolecular interactions might be providing an alternative mean to dissipate energy without breaking covalent bonds. The detonation velocity of **52** (7217 m/s) is the highest detonation velocity obtained for the peroxo-based compounds synthesized in our study. The calculated detonation velocity of **53** (7885 m/s) is close to the detonation velocity of the secondary high explosive RDX (8750 m/s).[6b] The low sensitivities and high detonation velocities of **49**, **51**, and **52** are appropriate for applications as secondary HEDMs. These peroxy acids **49**, **51**, and **52** are the first peroxo-based oxygen-rich compounds that are useful as secondary HEDMs. Through this work, we have obtained highly attractive peroxy acids with high detonation performances and surprisingly low sensitivities for potential use as HEDMs. The ease of synthesis in high yields with minimum synthetic manipulations, storability, and high thermal stabilities are all advantageous properties of peroxy acids for their use as HEDMs. This work also suggests that the peroxy acid functional group can be effectively used in the design of HEDMs to increase the oxygen

contents and thus, the energetic performances without excessively increasing the impact and friction sensitivities.

Based on the studies with *tert*-butyl peroxy esters, geminal hydroperoxides, cyclic hydroperoxy compounds, and peroxy acids we have learned invaluable ways to reduce the extremely high sensitivities of peroxo-based compounds while increasing their detonation velocities. They are the use of peroxy acid or hydroxy groups to increase the oxygen content, use of nitro groups to increase both the nitrogen and oxygen contents, and limiting the peroxy O:C ratio to 1.00. Using these strategies, more energetic and lower sensitivity peroxo-based compounds can be synthesized as future HEDMs.

Although we attempted to rationalize the physical behavior of peroxo-based compounds upon initiation by impact and friction stimuli based on the solid state intermolecular interactions, more theoretical studies are required to understand more about these complex phenomena. As recently suggested by Landenberger,[68] cocrystallization could be used as a novel method to use these solid state characteristics of peroxo-based compounds to reduce their sensitivities and improve the detonation velocities. Future peroxo-based HEDM design should aim to have large conjugated π-systems assisted by hydrogen bonding and face-to-face π-π interactions to create slip planes for low sensitivity HEDMs.

Another important issue for peroxo-based compounds is to increase their thermal stabilities. Based on our study, peroxy acids were the most thermally stable category of peroxo-based compounds. However, to reach decomposition temperatures above 150 °C, more research needs to be carried out. The energetic properties and thermal

stabilities of peroxo-based compounds need to be improved further to replace the hazardous tertiary explosive NH_4ClO_4 and primary explosives LA, LS, and MF.

Through this research, a wealth of information about the sensitivities and energetic materials properties of a large family of peroxo-based compounds was gathered to fill the void in the field of peroxo-based HEDMs. We were able to reach beyond the boundaries set by TATP, DADP, MEKP, and HMTD both with regards to sensitivities and energy content. We have discovered many attractive highly energetic and low sensitivity peroxo-based compounds that are much more impressive in the overall performance than the known peroxo-based explosives TATP, DADP, MEKP, and HMTD for the potential use as greener HEDMs.

REFERENCES

1. a) Badgujar, D. M.; Talawar, M. B.; Asthana, S. N.; Mahulikar, P. P. *J. Hazard. Mater.* **2008**, *151*, 289–305. b) Oxley, J. C.; Smith, J. L.; Higgins, C.; Bowden, P.; Moran, J.; Brady, J.; Aziz, C. E.; Cox, E. *J. Environ. Manage.* **2009**, *90*, 3629–3634. c) Oommen, C.; Jain, S. R. *J. Hazard. Mater.* **1999**, *A67*, 253–281. d) Seo, Y.-D.; Chung, S. H.; Yoh J. J. *Fuel* **2011**, *90*, 1395–1401. e) Agrawal, J. P. High Energy Materials. *Propellants, Explosives and Pyrotechniques*; WILEY-VCH Verlag GmbH & Co. KGaA: Weinheim, Germany, 2010.
2. Klapötke, T. M. *Chemistry of High-Energy Materials*, 2nd edn; Walter de Gruyter: Berlin/Boston, Germany/USA, 2012.
3. Fadala, S. *The Complete Black Powder Handbook, 5th edn*; Krause Publications: Wisconsin, USA, 2006.
4. Sastri, M. N. Chemical Explosives. *Weapons of Mass Destruction*; A. P. H. Publishing Corporation: New Delhi, India, 2004; pp 1–24.
5. Madigan, M. L. *The Responders Handbook, Responding with Knowledge*; Page Publishing Inc.: New York, USA, 2015.
6. a) Akhavan, J. Chapter 2. Classification of Explosive Materials. *The chemistry of Explosives*; Royal Society of Chemistry: Cambridge, United Kingdom, 2011; pp 27–59. b) Matyáš, R.; Pachman, J. Chapter 2. Explosive Properties of Primary Explosives. *Primary Explosives*; Springer-Verlag Berlin Heidelberg: Wiesbaden, Germany, 2013; pp 11–36.
7. Ilyushin, M. A.; Tselinsky, I. V.; Shugalei, I. V. *Cent. Eur. J. Energetic Mater.* **2012**, *9*, 293–327.

8. Matyáš, R.; Pachman, J. Chapter 1. Introduction to Initiating Substances. *Primary Explosives*; Springer-Verlag Berlin Heidelberg: Wiesbaden, Germany, 2013; pp 1–10.

9. Kuperman, R. G.; Checkai, R. T.; Johnson, M. S.; Robidoux, P. Y.; Lachance, B.; Thiboutot, S.; Ampleman, G. Chapter 12. Ecological Risk Assessment of Soil Contamination with Munition Constituents in North America. *Ecotoxicology of Explosives*; Sunahara, G. I.; Lotufo, G.; Kuperman, R. G.; Hawari, J. *Eds.*; CRC press, Taylor and Francis Group, LLC: Florida, USA, 2009; pp 277–308.

10. Buczkowski, D. *Cent. Eur. J. Energetic Mater.* **2011**, *8*, 99–106.

11. a) Krause, H. H. New Energetic Materials. *Energetic Materials*; Teipel, U. *Ed.*; WILEY-VCH Verlag GmbH & Co. KGaA: Weinheim, Germany, 2005; pp 1–25. b) Meyer, R.; Köhler J.; Homburg, A. *Explosives*, 6th *edn*; WILEY-VCH Verlag GmbH & Co. KGaA: Weinheim, Germany, 2007. c) Skinner, D.; Olson, D.; Block-Bolten, A. *Propellants Explos. Pyrotech.* **1998**, *23*, 34–42. d) Cooper, P. *Explosives Engineering*; John Wiley & Sons Inc.: New York, USA, 2015.

12. Sinditskii, V. P.; Chernyi A. N.; Marchenkov, D. A. *Combust. Explos. Shock Waves* **2014**, *50*, 158–167.

13. Urbanski, T.; Vasudeva, S. K. *J. Sci. Ind. Res.* **1981**, *40*, 512–519.

14. Shackelford, S. A. *J. Phys. IV France* **1995**, *05*, 485–499.

15. Göbel, M.; Klapötke, T. M. *Adv. Funct. Mater.* **2009**, *19*, 347–365.

16. Sikder, A. K.; Sikder, N. *J. Hazard. Mater.* **2004**, *A112*, 1–15.

17. a) Klapötke, T. M.; Petermayer, C.; Pierce, D. G.; Stierstorfer, J. *J. Am. Chem. Soc.* **2012**, *134*, 20827–20836. b) Singh, R. P.; Verma, R. D.; Meshri, D. T.;

Shreeve, J. M. *Angew. Chem. Int. Ed.* **2006**, *45*, 3584–3601. c) Fischer, N.; Fischer, D.; Klapötke, T. M.; Piercey, D. J.; Stierstorfer, J. *J. Mater. Chem.* **2012**, *22*, 20418–20422.

18. a) Klapötke, T. M.; Mayer, P.; Schulz, A.; Weigand, J. J. *J. Am. Chem. Soc.* **2005**, *127*, 2032–2033. b) Oyumi, Y.; Brill, T. B. *Combust. Flame* **1985**, *62*, 225–231. c) Klapötke, T. M.; Sabaté, C. M. *Chem. Mater.* **2008**, *20*, 1750–1763. c) Klapötke, T. M.; Mayer, P.; Sabaté, C. M.; Welch J. M.; Wiegand, N. *Inorg. Chem.* **2008**, *47*, 6014–6027.
19. Zarko, V. E. *Combust. Explos. Shock Waves* **2010**, *46*, 121–131.
20. Sikder, A. K.; Maddala, G.; Agrawal, J. P.; Singh, H. *J. Hazard. Mater.* **2011**, *A84*, 1–26.
21. Huynh, M.-H. V.; Hiskey, M. A.; Hartline, E. L.; Montoya, D. P.; Gilardi, R. *Angew. Chem. Int. Ed*. **2004**, *43*, 4924–4928.
22. a) Agrawal, J. P. *Cent. Eur. J. Energetic Mater.* **2012**, *9*, 273–290. b) Zhang J.; Parrish, D. A.; Shreeve, J. M. *Chem. Asian J.* **2014**, *9*, 2953–2960. c) Mousavi, S.; Esmaeilpour, K.; Keshavarz, M. H. *Cent. Eur. J. Energetic Mater.* **2013**, *10*, 455–465. d) Wu, B.; Yang, H.; Lin, Q.; Wang, Z.; Lu, C.; Cheng, G. *New J. Chem.* **2015**, *39*, 179–186.
23. a) Kumar, A. S.; Rao, V. B.; Sinha, R. K.; Rao, A. S. *Propellants Explos. Pyrotech.* **2010**, *35*, 359–364. b) Nair, U. R.; Sivabalan, R.; Gore, G. M.; Geetha, M.; Asthana, S. N.; Singh, H. *Combust. Explos. Shock Waves* **2005**, *41*, 121–132. c) Boddu, V. M.; Viswanath, D. S.; Ghosh, T. K.; Damavarapu, R. *J. Hazard. Mater.* **2010**, *181*, 1–8.

24. a) Wang, H.-B.; Wang, Y.-H.; Li, Y.-X.; Liu, Y.-C.; Tan, Y.-X. *Defense Tech.* **2014**, *10*, 343–348. b) Agrawal J. P.; *Hodgson, R. D. Organic Chemistry of Explosives*; John Wiley & Sons Ltd.: West Sessex, United Kingdom, 2007.

25. a) Charnley, G. *Food Chem. Toxicol.* **2008**, *46*, 2307–2315. b) Kucharzyk, K. H.; Crawford, R. L.; Cosens, B.; Hess, T. F. *J. Environ. Manage.* **2009**, *91*, 303–310.

26. Leung, A. M.; Pearce, E. N.; Braverman, L. E. *Best Pract. Res. Cl. En.* **2010**, *24*, 133–141.

27. a) Fronabarger, J. W.; Williams, M. D.; Sanborn, W. B.; Bragg, J. G.; Parrish, D. A.; Bichay, M. *Propellants Explos. Pyrotech.* **2012**, *37*, 320–328. b) Huynh, M. H. V.; Coburn, M. D.; Meyer, T. J.; Wetzler, M. *PNAS*, **2006**, *103*, 10322–10327. c) Fronabarger, J. W.; Williams, M. D.; Sanborn, W. B.; Parrish, D. A.; Bichay, M. *Propellants Explos. Pyrotech.* **2011**, *36*, 459–470. d) Fischer, D.; Klapötke, T. M.; Stierstorfer, J. *Angew. Chem. Int. Ed.* **2014**, *53*, 8172–8175. e) Oyler, K. D. Chapter 5. Green Primary Explosives. *Green Energetic Materials, 5th edn*; Brink, T. *Ed.*; John Wiley & Sons Ltd.: West Sussex, United Kingdom, 2014; pp 103–132.

28. a) Test Methods According to the UN Manual of Tests and Criteria, Recommendations on the Transport of Dangerous Goods, United Nations Publications, New York, Geneva, 4th revised edn, 2003. Impact: Insensitive > 40 J, less sensitive ≥ 35 J, sensitive ≥ 4 J, very sensitive ≤ 3 J; friction: Insensitive > 360 N, less sensitive = 360 N, sensitive < 360 N and > 80 N, very sensitive ≤ 80 N, extreme sensitive ≤ 10 N b) www.reichel-partner.de.

29. NATO standardization agreement (STANAG) on explosives, *Impact Sensitivity Tests*, no. 4489, 1st ed., Sept. 17, **1999**.

30. WIWEB-Standardarbeitsanweisung 4-5.1.02, Ermittlung der Explosionsgefährlichkeit, hier der Schlagempfindlichkeit mit dem Fallhammer, Nov. 8, **2002**.

31. http://www.bam.de (accessed January 29, **2013**).

32. NATO Standardization Agreement (STANAG) on Explosives, *Friction Sensitivity Tests*, no. 4487, 1st ed., Aug. 22, **2002**.

33. WIWEB-Standardarbeitsanweisung 4-5.1.03, Ermittlung der Explosionsgefährlichkeit oder der Reibeempfindlichkeit mit dem Reibeapparat, Nov. 8, **2002**.

34. a) http://www.ozm.cz (accessed January 29, **2013**). b) NATO Standardization Agreement 4515, August 23, **2002**.

35. Klapötke, T. M.; Wloka, T. Peroxide Explosives. *PATAI'S Chemistry of Functional Groups*; Patai S. *Ed.*; John Wiley & Sons Ltd.: 2014; pp 1–28.

36. a) Matyáš, R.; Šelešovský, J. *J. Haz. Mater.* **2009**, *165*, 95–99. b) Peterson, G. R.; Bassett, W. P.; Weeks B. L.; Hope-Weeks, L. J. *Cryst. Growth Des.* **2013**, *13*, 2307–2311. c) Derek, F.; Laine, I.; Cheng, F. *Microchem. J.* **2009**, *91*, 125–128. d) Kuzmin, V. V.; Solov`ev, M. Y.; Tuzkov, Y. B. *Cent. Eur. J. Energetic Mater.* **2008**, *5*, 77–85. e) Kozak, G. D.; Tsvigunov, A. N.; Akinin, N. I. *Cent. Eur. J. Energetic Mater.* **2011**, *8*, 249–260. f) Espinosa-Fuentes, E. A.; Peña-Quevedo, A. J.; Pacheco-Londoño, L. C.; Infante-Castillo, R.; Hernández-Rivera, S. P. A Review of Peroxide Based Homemade Explosives: Characterization and Detection. *Explosive Materials: Classification, Composition, and Properties*; Janssen, T. J. *Ed.*; Nova Science Publishers, Inc. New York, USA, 2011; pp 259–282.

37. a) Mamo, S. K.; Gonzalez-Rodriguez, J. *Sensors* **2014**, *14*, 23269–23282. b) Parajuli, S.; Miao, W. *Anal. Chem.* **2013**, *85*, 8008–8015. c) Amani, M.; Chu, Y.; Waterman, K. L.; Hurley, C. M.; Platek, M. J.; Gregory, O. J. *Sens. Actuators, B* **2012**, *162*, 7–13. d) Zhang, W.-H.; Zhang, W.-D.; Chen, L.-Y. *Nanotechnology* **2010**, *21*, 1–5. e) MacCrehan, W.; Moore, S.; Hancock, D. *Anal. Chem.* **2011**, *83*, 9054–9059. f) Lin, H.; Suslick, K. S. *J. Am. Chem. Soc.* **2010**, *132*, 15519–15521.

38. Mageli, O. L.; Sheppard, C. S. Chapter 1. Organic Peroxides and Peroxy Compounds—General Description. *Organic Peroxides.* Vol. 1; Swern, D. *Ed.*; John Wiley & Sons, Inc.: New York, USA, 1970; pp 1–104.

39. Sanchez, J.; Myers, T. N. Peroxides and Peroxide Compounds, Organic Peroxides. *Kirk-Othmer Encyclopedia of Chemical Technology,* John Wiley & Sons, Inc.: New York, USA, 2000; pp 1–86.

40. Bach, R. D.; Ayala, P. Y.; Schlegel, H. B. *J. Am. Chem. Soc.* **1996**, *118*, 12758–12765.

41. a) Hordijk, A. C.; De Groot, J. J. *Thermochim. Acta* **1986**, *101*, 45–63. b) Buback, M.; Kling, M.; Schmatz, S.; Schroeder, J. *Phys. Chem. Chem. Phys.* **2004**, *6*, 5441–5455.

42. a) Mukherjee, S.; Samanta, S.; Roy, B. C.; Bhaumik, A. *Appl. Catal., A* **2006**, *301*, 79–88. b) Pardieck, D. L.; Bouwer, E. J.; Stone, A. T. *J. Contam. Hydrol.* **1992**, *9*, 221–242. c) Brown, S. B.; Jones, P.; Suggett, A. Recent Developments in the Redox Chemistry of Peroxides. *Progress in Inorganic Chemistry: Inorganic Reaction Mechanisms*, Vol. 13, Edwards, J. O. ed.; John Wiley & Sons, Inc.: Hoboken, New Jersey, USA, 1970; pp 159–204.

43. a) United Nations Economic Commission of Europe. Dangerous Goods. http://www.unece.org/trans/danger/danger.html (accessed June 9, 2015) b) Occupational Safety & Health Administration. A Guide to the Globally Harmonized System of Classification and Labeling of Chemicals (GHS). https://www.osha.gov/dsg/hazcom/ghs.html (accessed June 9, 2015) c) Transportation Pictograms. http://www.qsdsconversion.com/pictograms-transport/ (accessed June 9, 2015).

44. Niki, E. Chapter 15. Peroxides in Biological Systems. *Organic Peroxides*; Ando, W. *Ed*.; John Wiley & Sons Ltd.: West Sussex, United Kingdom, 1992; pp 765–787.

45. a) Su, Y.-T.; Lin, H.-Y.; Putikam, R.; Matsui, H.; Lin, M. C.; Lee, Y.-P. *Nat. Chem.* **2014**, *6*, 477–483. b) Voukides, A. C.; Konrad, K. M.; Johnson, R. P. *J. Org. Chem.* **2009**, *74*, 2108–2113.

46. a) Redington, L. E. *J. Polym. Sci. Part A: Polym. Chem.* **1948**, *3*, 503–517. b) Walling, C.; Indictor, N. *J. Am. Chem. Soc.* **1958**, *80*, 5814–5818.

47. a) Keller, R. C. *Rubber Chem. Technol.* **1988**, *61*, 238−254. b) Dluzneski, P. R. *Rubber Chem. Technol.* **2001**, *74*, 451−492.

48. a) Kampouris, E. M.; Andreopoulos, A. J. *J. Appl. Polym. Sci.* **1987**, *34*, 1209−1216. b) Zhou, W.; Zhu, S. *Macromolecules,* **1998**, *31*, 4335–4341.

49. a) Basting, R. T.; Rodrigues Jr., A. L.; Serra, M. C. *JADA,* **2003**, *134*, 1335–1342. b) Wagner, M.; Brumelis, D.; Gehr, R. *Water. Environ. Res.* **2002**, *74*, 33−50.

50. a) Swern, D. *Chem. Rev.* **1949**, *45*, 1–68. b) Chidambaram, N.; Chandrasekaran, S. *J. Org. Chem.* **1987**, *52*, 5048–5051. c) Gelalcha, F. G.; Bitterlich, B.; Anilkumar, G.; Tse, M. K.; Beller, M. *Angew. Chem. Int. Ed.* **2007**, *74*, 7923−7926.

51. Campos-Martin, J. M.; Blanco-Brieva, G.; Fierro, J. L. G. *Angew. Chem. Int. Ed.* **2006**, *45*, 6962−6984.

52. Jones, C. W. *Applications of Hydrogen Peroxide and Derivatives;* Clark, J. H. *Ed.*; Royal Society of Chemistry: Cambridge, United Kingdom, 1999.

53. Oxley, J. C. Chapter 5. The Chemistry of Explosives. Explosive Effects and Applications. Zukas, J. A.; Walters, W. Eds.; Springer Science Business Media, New York, USA, 1998; pp 137–172.

54. a) Sorge, A. R.; Turco, M.; Pilme, G. Bagnasco, G. *J. Propul. Power* **2004**, *20*, 1069–1075. b) Pirault-Roy, L.; Kappenstein, C.; Guerin, M.; Eloirdy, R.; Pillet, N. *J. Propul. Power* **2002**, *18*, 1235–1241.

55. Wolffenstein, R. *Ber. Dtsch. Chem. Ges.* **1895**, *28*, 2265–2269.

56. a) Milas, N. A.; Golubovic, A. *J. Am. Chem. Soc.* **2004**, *81*, 6461–6462. b) Matyáš, R.; Chylkova, *J. Forensic Sci. Int.* **2013**, *228*, 170–173.

57. a) Oxley, J. C.; Smith, J. L.; Bowden, P. R.; Rettinger, R. C. *Propellants Explos. Pyrotech.* **2013**, *38*, 244–254. b) Oxley, J. C.; Smith, J. L.; Steinkamp, L.; Zhang, G. *Propellants Explos. Pyrotech.* **2013,** *38,* 841–851.

58. Groth, P. *Acta Chem. Scand.* **1969**, *23*, 1311–1329.

59. Dubnikova, F.; Kosloff, R.; Almog, J.; Zeiri, Y.; Boese, R.; Itzhaky, H.; Alt, A.; Keinan, E. *J. Am. Chem. Soc.* **2005**, *127*, 1146–1159.

60. a) Denkamp, C.; Gottlieb, L.; Tamiri, T.; Tsoglin, A.; Shilav, R.; Kapon, M. *Org. Lett.* **2005**, *7*, 2461–2464.

61. Reany, O.; Kapon, M.; Botoshansky, M.; Keinan, E. *Cryst. Growth and Des.* **2009**, *9*, 3661–3670.

62. Matyáš, R.; Zeman, S. *Propellants Explos. Pyrotech.* **2008**, *33*, 296–300.

63. a) Matyáš, R.; Šelešovsky, J.; Musil, T. *Cent. Eur. J. Energetic Mater.* **2013**, *10*, 263–275. b) Contini, A. E.; Bellamy, A. J.; Ahad, L. N. *Propellants Explos. Pyrotech.* **2012**, *37,* 320–328.

64. Matyáš, R.; Pachman, J. Chapter 10. Peroxides of Acetone. *Primary Explosives*; Springer-Verlag Berlin Heidelberg: Wiesbaden, Germany, 2013; pp 255–288.

65. Sinditskii, V. P.; Kolesov, V. I.; Egorshev, V. Y.; Patrikeev, D. I.; Dorofeeva, O. V. *Thermochim. Acta*, **2014**, *585*, 10–15.

66. Oxley, J. C.; Smith J. L.; Chen, H. *Propellants Explos. Pyrotech.* **2002**, *27*, 209–216.

67. Cafferta, L. F. R.; Lombardo, J. D. *Int. J. Chem. Kinet.* **1994**, *26*, 503–509.

68. a) Landenberger, K. B.; Bolton, O.; Matzger, A. J. *Angew. Chem. Int. Ed.* **2013**, *52*, 6468–6471. b) Landenberger, K. B.; Bolton, O.; Matzger, A. J. *J. Am. Chem. Soc.* **2015**, *137*, 5074–5079.

69. Kahnooji, M.; Pandas, H. M.; Mirzaei, M.; Peyghan, A. A. *Monatsh. Chem.* 2015, DOI 10.1007/s00706-015-1419-6.

70. Legler, L. *Ber. Dtsch. Chem. Ges.* **1885**, *18*, 3343–3351.

71. Schaefer, W. P.; Fourkas, J.; Tiemann, T. B. *J. Am. Chem. Soc.* **1985**, *107*, 2461–2463.

72. Wierzbicki, A.; Salter, E. A.; Cioffi, E. A.; Stevens, E. D. *J. Phys. Chem A*, **2001**, *105*, 8763–8768.

73. Oxley, J. C.; Smith, J. L.; Chen, H.; Cioffi, E. *Thermochim. Acta* **2002**, *388*, 215–225.

74. a) Milas, N. A.; Golubović, A. *J. Am. Chem. Soc.* **1959**, *81*, 5824–5826. b) Zhang, J.; Wu, W.; Qian, G.; Zhou X.-G. *J. Hazard. Mater.* **2010**, *181*, 1024–1030.

75. a) Wu, S. H.; Su, C. H.; Shu, C. M. *Int. J. Chem. Sci.* **2008**, *6*, 487–496. b) Yuan, M.-H.; Shu, C.-M.; Kossoy, A. A. *Thermochim. Acta* **2005**, *430*, 67–71.

76. Oxley, J.; Smith, J. Peroxide Explosives. *Detection and Disposal of Improvised Explosives;* Schubert, H.; Kuznetzov, A. *Eds*; Springer: Dordrecht, Netherlands, 2006; pp 113–122.

77. Wolff, S.; Boddenberg, A.; Thamm, J.; Turner, W. V.; Gäb, S. *Atmos. Environ.* **1997**, *31*, 2965–2969.

78. a) Rieche, A.; Hitz, F. *Ber. Dtsch. Chem. Ges.* **1929**, *62*, 2458–2474. b) Churakov, A. V.; Kuz'mina, L. G.; Prikhodchenko, P. V.; Howard, J. A. K. *Acta Cryst.* **2006**, *E62*, 2265–2267. c) Hamann, H.-J.; Bunge, A.; Liebscher, J. *Chem. Eur. J.* **2008**, *14*, 6849–6851.

79. a) Lee, K.-Y.; Chapman, L. B.; Cobura, M. D. *J. Energ. Mater.* **1987**, *5*, 27–33. b) Tremblay, M. *Can. J. Chem.* **1965**, *43*, 1227–1230. c) Zhang, Q.; He, C.; Yin, P.; Shreeve, J. M. *Chem. Asian J.* **2014**, *9*, 212–217. d) Sing, R.; Gao, H.; Meshri, D. T.; Shreeve, J. M. Nitrogen-Rich Heterocycles. *High Energy Density Materials, Structure and Bonding,* Vol. 125; Mingos, D. M. P.; Klapötke, T. M. *Eds.*; Springer-Verlag Berlin Heidelberg: Wiesbaden, Germany, 2007; pp 35–83.

80. Oxley, J. C. A Survey of Thermal Stability of Energetc Materials. *Energetic Materials: Part 2. Detonation, Combustion*, Politzer, P.; Murray, J. S. *Eds.*; Elsevier B. V.: Amsterdam, Netherlands, 2003, pp 5–48.

81. Ma, Y.; Zhang, A.; Xue, X.; Jiang, D.; Zhu, Y.; Zhang, C. *Cryst. Growth Des.* **2014**, *14*, 6101–6114.

82. a) Politzer, P.; Murray, J. S. Detonation Performance and Sensitivity: A Quest for Balance. *Advances in Quantum Chemistry, Energetic Materials*, Vol. 69; Sabin, J. R. *Ed.*; Elsevier Inc.: Oxford, United Kingdom, 2014; pp 1–30. b) Davidson, A. J.; Dias, R. P.; Dattelbaum, D. M.; Yoo, C.-S. *J. Chem. Phys.* **2011**, *135*, 174507-1–174507-5. c) Zeng, G.; Pang, W.; Zhou, J. *Procedia Eng.* **2015**, *102*, 610–614.

83. a) Eckhardt, C. J.; Gavezotti, A. J. *Phys. Chem. B* **2007**, *111*, 3430–3437. b) Pakiari, A. H.; Eskandari, K. *J. Mol. Struc.: THEOCHEM* **2007**, *806*, 1–7. c) Matta, C. F. Chapter 9. Hydrogen-Hydrogen Bonding: The Non-Electrostatic Limit of Closed-Shell Interaction between Two Hydrogen Atoms. A Critical Review. *Hydrogen Bonding—New insights*; Grabovski, S. J. *Ed.*; Springer: Dordrecht, Netherlands, 2006; pp 337–375.

84. a) Ma, Y.; Zhang, A.; Zhang, C.; Jiang, D.; Zhu, Y.; Zhang, C. *Cryst. Growth Des.* **2014**, *14*, 4703–4713. b) Zhang, J. Zhang, Q.; Vo, T. T.; Parrish, D. A.; Shreeve, J. M. *J. Am. Chem. Soc.* **2015**, *137*, 1697–1704.

85. Criegee, R. *Angew. Chem. Int. Ed.* **2003**, *14*, 745–752.

86. Sheldon, R. A. Chapter 6. Synthesis and use of alkyl hydroperoxides and dialkyl peroxides. *Peroxides,* Patai, S. *Ed.*; John Wiley & Sons, Ltd.: Chichester, United Kingdom 1983; pp 161–200.

87. Buback, M.; Fischer, B.; Hinrichs, S.; Jauer, S.; Meijer, J.; Sandmann, J. *Macromol. Chem. Phys.* **2007**, *208*, 772–783. b) Sheppard, C. S.; Kamath, V. R. *Polym. Eng. Sci.* **1979**, *19*, 597–606.

88. a) Handy, C. T.; Rothrock, H. S. *J. Am. Chem. Soc.* **1958**, *80*, 5306–5308. b) Hendry, D. J. Polymeric peroxides. *Encyclopedia of Polymer Science and Technology – Plastics, Resins, Rubbers, Fibers. Supplement Vol. 9*; John Wiley & Sons, Ltd.: 1968; pp 807–814.

89. a) Kosnikov, A. Y.; Antonovskii, V. L.; Lindeman, S. V.; Struchkov, Y. T.; Fedorova, E. V. *B. Acad. Sci. USSR* **1989**, *38*, 247–249. b) Pavlovskii, Y. P.; Kachurina, N. S.; Gerasimchuk, S. I.; Van-Chin-Syan, Y. Y. *Russ. J. Phys. Chem. A* **2013**, *87*, 1253–1258. c) Milas, N. A.; Plesnicar, B. *J. Am. Chem. Soc.* **1968**, *90*, 4450–4453. d) Terent'ev, A. O.; Kutkin, A. V.; Troizky, N. A.; Ogibin, Y. N.; Nikishin, G. I. *Synthesis* **2005**, *13*, 2215–2219. e) Dickey, F. H.; Raley, J. H.; Rust, F. F.; Treseder, R. S.; Vaughan, W. E. *Ind. Eng. Chem.* **1949**, *41*, 1673–1679.

90. a) Shelton, J. R.; Uzelmeier, W. *J. Org. Chem.* **1970**, *35*, 1576–1581. b) Peng, H.; Yu, J.-T.; Jiang, Y.; Yang, H.; Cheng, J. *J. Org. Chem.* **2014**, *79*, 9847–9853.

91. Pritchard, H. O.; Clothier, P. Q. E. *J. Chem. Soc., Chem. Commun.* **1986**, *20*, 1529–1530.

92. a) Jiayua, L.; Wanghuaa, C.; Lipinga, C.; Yingtaoa, T.; Xin, S. *Procedia Eng.* **2012**, *43*, 312–317. b) Yip, C. K.; Pritchard, H. O. *Can. J. Chem.* **1971**, *49*, 2290–2296.

93. (a) Žmitek, K.; Zupan, M.; Stavber, S.; Iskra, J. *Org. Lett.* **2006**, *8*, 2491–2494. (b) Žmitek, K.; Zupan, M.; Stavber, S.; Iskara, J. *J. Org. Chem.* **2007**, *72*, 6534–6540.

94. Anslyn, E. V.; Dougherty, D. A. Chapter 2. Strain and Stability. *Modern Physical Organic Chemistry*, University Science Books: California, USA, 2006; pp 65–91.

95. Chang, S.; McNally, D.; Shary-Tehrany, S.-T. Hickey, S. M. J.; Boyd, R. H. *J. Am. Chem. Soc.* **1970**, *92*, 3109–3118.

96. Oxley, J.; Smith, J.; Brady, J.; Dubnikova, F.; Kosloff, R.; Zeiri, L.; Zeiri, Y. *Appl. Spectrosc.* **2008**, *62*, 906–915.

97. Socrates, G. Peroxides and Hydroperoxides: O-O Group. *Infrared and Raman Characteristic Group Frequencies: Tables and Charts,* 3rd edition; John Wiley & Sons Ltd: Chichester, West Sussex, United Kingdom, 2004; pp 105–106.

98. Lin-Vien, D.; Clothup, N. B.; Fateley, W. G.; Grasselli, J. G. Chapter 5. Ethers and Peroxides. *The Handbook of Infrared and Raman Characteristic Frequencies of Organic Molecules,* Academic Press: San Diego, Calofornia, 1991; pp 61–72.

99. Hartung, J. Chapter 2. The Structural Chemistry of Acyclic Organic Peroxides. *The chemistry of peroxides.* Vol. 2; Rappoport, Z. *Ed.*; John Wiley & Sons, Ltd.: Chichester, United Kingdom, 2006; pp 93–144.

100. Braga, D.; Grepioni, F. C–H···O Hydrogen Bonds in Organometallic Crystals. *Intermolecular Interactions*; Gans, W.; Boeyen J. C. A. *Eds.*; Springer Science Business Media: New York, USA, 1998; pp 83–96.

101. Platts, J. A.; Howard, S. T.; Woźniak, K. *Chem. Commun.* **1996**, *1*, 63–64.

102. Bakhmutov, V. I. Intermolecular Dihydrogen Bonded Complexes: From Groups 1 A–4 A to Xenon Dihydrogen-Bonded Complexes. *Dihydrogen Bonds. Principles, Experiments, and Applications*; John Wiley & Sons, Inc. New Jersey, USA, 2008; pp 112–96.

103. Tsuzuki, S.; Honda, K.; Uchimaru, T.; Mikami, M.; Tanabe, K. *J. Am. Chem. Soc.* **2002**, *124*, 104–112.

104. Still, C. W.; Kahn, M.; Mitra, A. *J. Org. Chem.* **1978**, *43*, 2923–2925.

105. Terent'ev, A. O.; Kutkin, A. V.; Troizky, N. A.; Ogibin, Y. N.; Nikishin, G. I. *Synthesis* **2005**, *13*, 2215–2219.

106. a) Buback, M.; Fischer, B.; Hinrichs, S.; Jauer, S.; Meijer, J.; Sandmann, J. *Macromol. Chem. Phys.* **2007**, *208*, 772–783. b) Sheppard, C. S.; Kamath, V. R. *Polym. Eng. Sci.* **1979**, *19*, 597–606. c) Peroxy Esters Product Bulletin, LUPEROX® organic peroxides, www.arkema-inc.com or www.luperox.com.

107. a) Andrus M. B.; Chen, X. *Tetrahedron Lett.* **1997**, *53*, 16229–16240. b) Beckwith, A. L. J.; Zavitsas, A. A. *J. Am. Chem. Soc.* **1986**, *108*, 8230–8234. c) Denney, D. B.; Goodyear, W. F.; Goldstein B. *J. Am. Chem. Soc.* **1961**, *83*, 1726–1733.

108. a) Nishinaga, A.; Nakamura, K.; Matsuura, T. *J. Org. Chem.* **1983**, *48*, 3696–3700. b) Moulay, S. *Chem. Educ. Res. Pract.* **2002**, *3*, 33–64.

109. a) Sosnovsky, G.; Zaret, E. H.; Schmitt, K. D. *J. Org. Chem.* **1970**, *35*, 336–340. b) Sosnovsky , G.; Zaret, E. H.; Konieczny, M. *J. Org. Chem.* **1972**, *37*, 2267–2272.

110. Patnaik, P. Organic Peroxides. *A Comprehensive Guide to the Hazardous Properties of Chemical Substances*; John Wiley & Sons, Inc.: New Jersey, USA, 2007; pp 719–740.

111. (a) Dalapati, S.; Saha, R.; Jana, S.; Patra, A. K.; Bhaumik, A.; Kumar, S.; Guchhait, N. *Angew. Chem. Int. Ed.* **2012**, *51*, 12534–12537. (b) Ranganathan, S.; Muraleedharan, K. M.; Rao, C. H. C.; Vairamani, M.; Karle, I. L.; Gilardi, R. D.

Chem. Commun. **2001**, *51*, 2544–2545. (c) Zhang, A.; Han, Y.; Yamato, K.; Zeng, X. C.; Gong, B. *Org. Lett.* **2006**, *8*, 803–806.

112. (a) Dalia, A.; Asri Abd, G. M.; Cunningham, M. F. *Can. J. Chem.* **2004**, *82*, 1393–1402. (b) Bartlett, P. D.; Benzing, E. P.; Pincock, R. E. *J. Am. Chem. Soc.* **1960**, *82*, 1762–1768.

113. a) CBS-4M method:[2] The complete basis set (CBS) method by Petersson and coworkers is used to calculate the formation enthalpies of compounds. A Hartree–Fock geometry optimization, HF/3-21G(d), is the first step in the CBS-4 method. Calculation of the zero point energy is carried out at the same level. Then, a self-consistent field (SCF) calculation with a large basis set is performed to obtain the base energy. To correct the base energy through second order contributions, a Møller–Plesset perturbation theory calculation, MP2/6-31+G, with a CBS extrapolation is performed. Afterwards, the higher order contributions are approximated by a Møller–Plesset perturbation theory calculation, MP4(SDQ)/6-31+(d, p). The modified CBS-4M method, where M refers to the use of minimal population localization, is a re-parameterized version of the initial CBS-4 method. This modified CBS-4M method has additional empirical corrections to obtain more accurate energies. b) Gaussian 09, Revision A.1, Frisch et. al., Gaussian, Inc., Wallingford CT, 2009.

114. Sućeska, M. EXPLO5 V6.02 program, *Brodarski Institute,* Zagreb, Croatia, 2014.

115. a) Tropina, V. I.; Krivykh, O. V.; Sadchikova, N. P.; Terent'ev, A. O.; Krylov, I. B. *Pharm. Chem. J.* **2010**, *44*, 248–250. b) Wiesner, J.; Ortmann, R.; Jomaa, H.; Schlitzer, M. *Angew. Chem. Int. Ed.* **2003**, *42*, 5274–5293.

116. a) Terent'ev, A. O.; Platonov, M. M.; Kutkin, A. V. *Cent. Eur. J. Chem.* **2006**, *4*, 207–215. b) Azarifar, D.; Khosravi, K.; Soleimanei, F. *Molecules* **2010**, *15*, 1433–1441.

117. a) Sashidhara, K. V.; Avula, S. R.; Singh, L. R.; Palnati, G. R. *Tetrahedron Lett.* **2012**, *53*, 1433–1441. b) Das, B.; Krishnaiah, M.; Veeranjaneyulu, B.; Ravikanth, B. *Tetrahedron Lett.* **2007**, *48*, 6286–6289. c) Azarifar, D.; Najminejad, Z.; Khosravi, K. *Synth. Commun.* **2013**, *43*, 826–836. d) Khosravi, K. *Cogent Chem.* **2015**, *1*, 1–9. e) Bunge, A.; Hamann. H.-J.; Dietz, D.; Liebsher, J. *Tetrahedron Lett.* **2013**, *69*, 2446–2450. f) Ghorai, P.; Dussault, P. H. *Org. Lett.* **2008**, *10*, 4577–4579.

118. Remizova, A. B.; Kamalovab, D.I.; Skochilova, R.A.; Suvorovaa, I. A.; Batyrshina, N. N.; Kharlampidi, K. E. *J. Mol. Struct.* **2004**, *700*, 73–79.

119. Vreclj, R. M.; Sherwood, J. N.; Kennedy, A. R.; Gallagher H. G.; Gelbrich, T. *Cryst. Growth. Des.* **2003**, *3*, 1027–1032.

120. Mantina, M.; Chamberlain, A. C.; Valero, R.; Cramer, C. J.; Truhlar, D. G. *J. Phys. Chem. A* **2009**, *113*, 5806–5812.

121. Terent'ev, A. O.; Platonov, M. M.; Tursina, A. I.; Chernyshev, V. V.; Nikishin, G. I. *J. Org. Chem.* **2008**, *73*, 3169–3174.

122. a) Matyáš, R.; Šelešovsky, J.; Musil, T. *Cent. Eur. J. Energetic Mater.* **2013**, *10*, 263–275. b) Contini, A. E.; Bellamy, A. J.; Ahad, L. N. *Propellants Explos. Pyrotech.* **2012**, *37,* 320–328.

123. Terent'ev, A. O.; Borisov, D. A.; Vil', V. A.; Dembitsky, V. M. Beilstein *J. Org. Chem.* **2014**, *10*, 34–114.

124. a) Korshin, E. E.; Bachi, M. D. Chapter 5. Synthesis of Cyclic Peroxides. *The Chemistry of Peroxides*, Vol. 2; Rappoport, Z. *Ed.*; John Wiley & Sons Ltd: Chichester, United Kingdom, 2006; pp 189–305. b) Jefford, C. W. *Curr. Top. Med. Chem.* **2012**, *12*, 373–399. c) McCullough, K. J.; Nojima, M. *Curr. Org. Chem.* **2001**, *5*, 601–636. d) Azarifar, D.; Khosravi, K. *Eur J. Chem. Soc.* **2010**, *1*, 15–19.

125. a) Azarifar, D.; Khosravi, K. *Eur J. Chem. Soc.* **2010,** *1,* 15–19. b) Bunge, A.; Hamann, H.-J.; Dietz, D.; Liebscher, J. *Tetrahedron* **2013**, *69*, 2446–2450.

126. a) Rieche, A. *Angew. Chem.* **1961**, *73*, 57–58. b) Milas, N. A.; Golubovic, A. *J. Org. Chem.* **1962**, *27*, 4319–4323. c) Milas, N. A.; Mageli, O. L.; Golubović, A.; Arndt, R. W.; Ho, J. C. J. *J. Am. Chem. Soc.* **1963,** *85*, 222–226. d) Novikov, V. L.; Shestak, O. P. *Russ. Chem. Bull. Int. Ed.* **2013**, *62*, 2171–2190. e) Cocker, W.; Grayson, D. H. *J. Chem. Soc. Perkin Trans.* **1975**, *1*, 1347–1352.

127. Steiner, T. *Angew. Chem. Int. Ed.* **2002**, *41*, 48–76.

128. Gougoutas, J. Z. Chapter 12. Structural aspects of organic peroxides. *Peroxides,* Patai, S., Ed.; John Wiley & Sons, Ltd.: Chichester, 1983, pp 375–415.

129. Phillips, B.; Starcher, P. S.; Ash, B. D. *J. Org. Chem.* **1958**, *23*, 1823–1826.

130. a) Swern, D. Chapter V. *Organic peroxides.* Vol. II; Wiley-Interscience: New York, USA, 1971; pp 355–533. b) Swern, D. Chapter VI. *Organic peroxides.* Vol. I; Wiley-Interscience: New York, USA, 1970; pp 313–474.

131. a) Bach, R. D.; Canepa, C.; Winter, J. E.; Blanchette, P. E. *J. Org. Chem.* **1997**, *62*, 5191–5197. b) Bach , R. D.; Owensby , A. L.; Gonzalez , C.; Schlegel, H. B.; McDouall, J. J. W. *J. Am. Chem. Soc.* **1991**, *113*, 2338–2339. c) Okovytyy, S.; Gorb, L.; Leszczynski, J. *Tetrahedron. Lett.* **2002**, *43*, 4215–4219. d)

Freccero, M.; Gandolfi, R.; Sarzi-Amadè, M.; Rastelli, A. *J. Org. Chem.* **2005**, *70*, 9573–9583.

132. a) Baeyer, A.; Villiger, V. *Ber. Dtsch. Chem. Ges.* **1899**, *32*, 3625–3633. b) Baeyer, A.; Villiger, V. *Ber. Dtsch. Chem. Ges*. **1900**, *33*, 858–864. c) Canan Koch S. S.; Chamberlin, A. R. *Synth. Commun.* **1989**, *19*, 829–833. d) Renz, M.; Meunier, B. *Eur. J. Org. Chem.* **1999**, *1999*, 737–750.
133. Rastetter, W. H.; Richard T. J.; Lewis, M. D. *J. Org. Chem.* **1978**, *43*, 3163–3166.
134. Harman, D. G.; Ramachandran, A.; Gracanin, M.; Blanksby, S. *J. Org. Chem.* **2006**, *71*, 7996–8005.
135. Kim, H. S.; Chu, S.-C.; Jeffrey, G. A. *Acta Crystallogr. Sect. B: Struct. Sci.* **1970**, *26*, 896–900.
136. Chervin, S.; Bodman, G. T. *Process Saf. Prog.* **2003**, *22*, 241–243.

ABSTRACT

SYNTHESIS, CHARACTERIZATION, AND PROPERTIES OF PEROXO-BASED OXYGEN-RICH COMPOUNDS FOR POTENTIAL USE AS GREENER HIGH ENERGY DENSITY MATERIALS

by

NIPUNI-DHANESHA HORADUGODA GAMAGE

December 2015

Advisor: Professor Charles H. Winter

Major: Chemistry (Inorganic)

Degree: Doctor of Philosophy

One main aspect of high energy density material (HEDM) design is to obtain greener alternatives for HEDMs that produce toxic byproducts. Primary explosives lead azide, lead styphnate, and mercury fulminate contain heavy metals that cause heavy metal poisoning. Leaching of the widely used tertiary explosive NH_4ClO_4 into groundwater has resulted in human exposure to ClO_4^- ions, which cause disruptions of thyroid related metabolic pathways and even thyroid cancer. Many research efforts to find replacements have gained little success. Thus, there is a need for greener HEDMs. Peroxo-based oxygen-rich compounds are proposed as a potential new class of greener HEDMs due to the evolution of CO_2 and/or CO, H_2O, and O_2 as the main decomposition products. Currently, triacetone triperoxide (TATP), diacetone diperoxide (DADP), hexamethylene triperoxide diamine (HMTD), and methyl ethyl ketone peroxide (MEKP) are the only well-studied highly energetic peroxides. However, due to their high impact and friction sensitivities, low thermal stabilities, and low detonation velocities they have not found any civil or military HEDM applications.

In this dissertation research, we have synthesized and fully characterized four categories of peroxo-based compounds: *tert*-butyl peroxides, *tert*-butyl peroxy esters, hydroperoxides, and peroxy acids to perform a systematic study of their sensitivities and the energetic properties for potential use as greener HEDMs.

tert-Butyl peroxides were not sensitive to impact, friction, or electrostatic spark. Hence, *tert*-butyl peroxides can be described as fairly safe peroxo-based compounds to handle. *tert*-Butyl peroxy esters were all surprisingly energetic (4896–6003 m/s), despite the low oxygen and nitrogen contents. Aromatic *tert*-butyl peroxy esters were much lower in impact and friction sensitivities with respect to the known peroxo-based explosives. These are among the first low sensitivity peroxo-based compounds that can be categorized as secondary HEDMs.

Oxygen-rich (0.80–1.00) geminal hydroperoxides have detonation velocities in the range of 6150–7130 m/s. These impressive detonation velocities are greater than the detonation velocities of the known peroxo-based explosives. The highest detonation velocity (7130 m/s) was obtained for 1,4-bis(dihydroperoxymethyl)benzene, which has the highest crystalline density (1.648 g/cm^3). This detonation velocity is greater than the secondary explosive 2,4,6-trinitrotoluene (TNT). The sensitivities of these oxygen-rich geminal hydroperoxides are lower than the known peroxo-based explosives due to the O–H···O hydrogen bonds and O···O contacts, which stabilize the weak O–O bonds in the crystalline lattice. They could be useful as primary HEDMs.

Dihydroperoxy dioxane and dioxolanes have impressive detonation velocities in the range of 6350–6694 m/s. However, their extremely high sensitivities render them unsafe for HEDM applications. Interestingly, hydroperoxy dioxanol and dioxolanols also

have high detonation velocities in the range of 6100–6461 m/s even with the lower oxygen contents. The hydroperoxy compounds with one less O–O bond were much less sensitive than the dihydroperoxy compounds. These hydroperoxy compounds could be useful as primary HEDMs. We observed that the ring strain was useful in increasing the detonation velocities, since it led to compounds with higher crystalline densities. However, increasing the steric strain using bulky groups led to lower crystalline densities and lower detonation velocities. Higher steric strain not only resulted in higher sensitivities but also lower thermal stabilities.

Peroxy acids have high detonation velocities in the range of 5262–7885 m/s. The detonation velocity of 3,5-dinitrobenzoperoxoic acid (7217 m/s) was the highest detonation velocity obtained for the peroxo-based compounds synthesized in our study, which is greater than the detonation velocity of TNT. The detonation velocity of 2,4,6-trinitrobenzoperoxoic acid (7885 m/s) is close to the detonation velocity of the secondary high explosive 1,3,5-trinitroperhydro-1,3,5-triazine (RDX). Peroxy acids have surprisingly low impact and friction sensitivities that are well below the known peroxo-based explosives TATP, DADP, HMTD, and MEKP. Based on the crystal structure of 3,5-dinitrobenzoperoxoic acid, the low sensitivities can be attributed to the stabilization of the weak O–O bonds in the crystalline lattice by O–H···O hydrogen bonds and O···O short contacts. These are the first peroxo-based oxygen-rich compounds that can be useful as secondary HEDMs. The ease of synthesis in high yields with minimum synthetic manipulations, storability, and high thermal stabilities are all advantageous properties of peroxy acids for their use as HEDMs.

Through this work, we have gained a wealth of fundamental information about the structures and energetic materials properties of a large family of peroxo-based compounds. Solid state intermolecular interactions were useful to understand the impact and friction sensitivities. The safe peroxy O:C ratio was found to be approximately 1.00. However, the oxygen contents could be further increased with more stable nitro and hydroxy groups. Highly attractive low sensitivity peroxo-based compounds were obtained with impressive detonation performances for potential use as greener primary and secondary HEDMs.

AUTOBIOGRAPHICAL STATEMENT

NIPUNI-DHANESHA HORADUGODA GAMAGE

Education **Ph.D.**, Inorganic Chemistry, Wayne State University, Detroit, MI, USA, 2013−2015 (GPA: 4.00/4.00). Advisor: Professor Charles H. Winter
M.S., Inorganic Chemistry, Wayne State University, Detroit, MI, USA, 2007−2011 (GPA: 4.00/4.00). Advisor: Professor Matthew J. Allen
B.S., Special Degree in Chemistry with First Class Honors, University of Colombo, Colombo-3, Sri Lanka, 2002−2006 (GPA: 3.60/4.00).

Honors and Awards

1. Knoller Fellowship (2014–2015), Department of Chemistry, Wayne State University
2. Graduate Student Professional Travel Awards (2010, 2013–2014), Department of Chemistry, Wayne State University
3. Honor Citation for Excellence in Teaching Service (2010–2011), Department of Chemistry, Wayne State University
4. Bhikaji Framji Khan Gold Medal for Highest Competence in Chemistry (2002–2003), University of Colombo
5. Professor Pearlyn Pereira Memorial Gold Medal for Physical Chemistry 2002–2003), University of Colombo

Publications

1. **Gamage, N.-D. H**.; Stiasny, B.; Stierstorfer, J.; Martin, P. D.; Klapötke, T. M.; Winter C. H. “Less Sensitive Oxygen-Rich Organic Peroxides Containing Geminal Hydroperoxy Groups.” *Chem. Comm.* **2015**, *51*, 13298–13300.
2. **Gamage, N.-D. H.**; Stiasny, B.; Stierstorfer, J.; Martin, P. D.; Klapötke, T. M.; Winter C. H. “Highly Energetic, Low Sensitivity Aromatic Peroxy Acids.” *Chem. A Eur. J.* 2015, in press.
3. **Gamage, N.-D. H.**; Stiasny, B.; Stierstorfer, J.; Martin, P. D.; Klapötke, T. M.; Winter C. H. “Surprisingly High Energetic and Low Sensitivity *tert*-Butyl Peroxy Esters with Low Oxygen and Nitrogen Contents.” manuscript in preparation.
4. **Gamage, N.-D. H.**; Stiasny, B.; Stierstorfer, J.; Martin, P. D.; Klapötke, T. M.; Winter C. H. “Tuning Impact and Friction Sensitivities and Energetic Performances of a Series of Cyclic Hydroperoxy Compounds.” manuscript in preparation.
5. **Gamage, N.-D. H.**; Mei, Y.; Garcia, J.; Allen, M. J. “Oxidatively Stable, Aqueous Europium(II) Complexes through Steric and Electronic Manipulation of Cryptand Coordination Chemistry.” *Angew. Chem. Int. Ed.* 2010, *49,* 8923–8925.

Patents

1. Formation of Cryptands Imparting Oxidative Stability to Europium(II); by Allen, Matthew J.; **Gamage, Nipuni-Dhanesha H.**; Garcia, Joel; Moore, Jeremiah; from PCT Int. Appl. (2011), WO 2011090977 A1 20110728.